

**ROLES OF SENESENCE ESCAPE AND EPIGENETIC
MODIFICATIONS IN LIVER CANCER**

**A THESIS SUBMITTED TO
THE DEPARTMENT OF MOLECULAR BIOLOGY AND GENETICS
AND THE GRADUATE SCHOOL OF ENGINEERING AND SCIENCE
OF BILKENT UNIVERSITY
IN PARTIAL FULFILLMENT OF THE REQUIREMENTS FOR
THE DEGREE OF DOCTOR OF PHILOSOPHY**

**BY
GÖKHAN YILDIZ
AUGUST 2013**

I certify that I have read this thesis and that in my opinion it is fully adequate, in scope and in quality, as a thesis for the degree of Doctor of Philosophy.

Prof. Dr. Mehmet ÖZTÜRK (Advisor)

I certify that I have read this thesis and that in my opinion it is fully adequate, in scope and in quality, as a thesis for the degree of Doctor of Philosophy.

Prof. Dr. Hilal ÖZDAĞ

I certify that I have read this thesis and that in my opinion it is fully adequate, in scope and in quality, as a thesis for the degree of Doctor of Philosophy.

Assoc. Prof. Dr. Rengül ÇETİN-ATALAY

I certify that I have read this thesis and that in my opinion it is fully adequate, in scope and in quality, as a thesis for the degree of Doctor of Philosophy.

Assoc. Prof. Dr. Hakan FERHATOSMANOĞLU

I certify that I have read this thesis and that in my opinion it is fully adequate, in scope and in quality, as a thesis for the degree of Doctor of Philosophy.

Assist. Prof. Dr. Özlen KONU

Approved for The Graduate School of Engineering and Science

Director of Graduate School of Engineering and Science
Prof. Dr. Levent ONURAL

ABSTRACT

ROLES OF SENESENCE ESCAPE AND EPIGENETIC MODIFICATIONS IN LIVER CANCER

Gökhan YILDIZ

Ph.D. in Molecular Biology and Genetics

Supervisor: Prof. Dr. Mehmet ÖZTÜRK

August 2013, 126 Pages

Development of hepatocellular carcinoma (HCC) is a multi-step progressive process in which a healthy liver transforms into cancerous tissue. Senescence is a permanent proliferation arrest in response to cell stress such as DNA damage, serving as a major barrier against tumor development. Most tumor cells are believed to bypass the senescence barrier (become “immortal”) by inactivating growth control genes and reactivating telomerase reverse transcriptase gene. Senescence-to-immortality transition is accompanied by major phenotypic and biochemical changes mediated by genome-wide transcriptional modifications. This appears to happen during HCC development in patients with liver cirrhosis; however, the accompanying transcriptional changes are virtually unknown. This study describes genome-wide transcriptional changes related to the senescence-to-immortality switch during hepatocellular carcinogenesis. Starting with a strong support of the hypothesis that *in vitro* senescent HCC clones are alike *in vivo* cirrhosis cells, and *in vitro* immortal HCC cells are alike *in vivo* HCC hepatocytes using microarray data analysis methods;

we determined differentially expressed genes and deregulated biological mechanisms during senescence escape and immortalization. Gene set enrichment analysis revealed that cirrhosis/senescence-associated genes were preferentially expressed in non-tumor tissues, less malignant tumors, and differentiated or senescent cells. In contrast, HCC/immortality genes were up-regulated in tumor tissues, or more malignant tumors and progenitor cells. In HCC tumors and immortal cells genes involved in DNA repair, cell cycle, telomere extension and branched chain amino acid metabolism were up-regulated, whereas genes involved in cell signaling, as well as in drug, lipid, retinoid and glycolytic metabolism were down-regulated. Through the analysis of senescence-related gene expression in different liver tissues we showed that cirrhosis and HCC display expression patterns compatible with senescent and immortal phenotypes, respectively; dysplasia being a transitional state. Based on these distinctive gene expression features we developed a 15-gene hepatocellular immortality signature test that discriminated HCC from cirrhosis with high accuracy. Since an epigenetic player gene, ATAD2, came forward as one of the hepatocellular immortality signature test genes in senescence escape processes, we also investigated roles of epigenetic regulatory genes in hepatocellular carcinogenesis. Bioinformatics analyzes on cirrhosis and HCC as well as dysplasia and normal liver samples using a comprehensive list of epigenetic regulatory genes revealed several transcriptionally deregulated epigenetic regulatory mechanisms during liver carcinogenesis. However, we could not detect any mutational differences in N-terminal tail encoding DNA sequences of histone variants. Our findings demonstrate that senescence bypass plays a central role in hepatocellular carcinogenesis engendering systematic changes in the transcription of genes regulating DNA repair, proliferation, differentiation and metabolism.

ÖZET

KARACİĞER KANSERİNDE SENESENSTEN KAÇIŞ VE HİSTONE MODİFİKASYONLARININ ROLLERİ

Gökhan YILDIZ
Moleküler Biyoloji ve Genetik Doktorası
Tez Danışmanı: Prof. Dr. Mehmet ÖZTÜRK
Ağustos 2013, 126 Sayfa

Hepatosellüler karsinom (HSK) oluşumu, sağlıklı bir karaciğerin kanserli bir dokuya dönüşümüyle sonuçlanan çok aşamalı bir süreçtir. Senesens DNA hasarı gibi hücrel streslere karşı yanıt olarak ortaya çıkan ve tümör gelişimi önünde engel işlevi gören, hücre çoğalmasının kalıcı olarak durdurulması olayıdır. Çoğu tümör hücresinin hücre çoğalmasını kontrol eden genleri etkisizleştirerek ve telomeraz ters transkriptaz genini yeniden etkinleştirerek senesens engelini aştıkları (“ölümsüz” oldukları) düşünülmektedir. Senesensten ölümsüzlüğe geçiş genom çapında gen ifadesi değişikliklerin yönettiği önemli fenotipik ve biyokimyasal değişikliklerle birlikte gerçekleşmektedir. Bu durum, geçiş sırasında gerçekleşen gen ifade değişiklikleri neredeyse hiç bilinmese de, sirozlu hastalarda HSK gelişimi sırasında da gerçekleşiyor görünmektedir. Bu çalışmada HSK gelişimi sırasında senesensten ölümsüzlüğe geçişte tüm genom çapında gerçekleşen gen ifade değişikliklerini tanımlanmaktadır. *In vitro* senesensli HSK hücrelerinin *in vivo* sirozlu hepatositlere ve *in vitro* ölümsüz HSK hücrelerinin *in vivo* HSK hücrelerine benzediği hipotezini mikrodizin veri analizi yöntemleriyle kanıtlanmasıyla başladıktan sonra; senesensten

kaçış ve ölümsüzlük sırasında değişikliğe uğrayan biyolojik mekanizmaları ve farklı düzeyde ifade edilen genleri belirledik. Gen seti zenginleştirme analizleri siroz/senesens ilişkili genlerin özellikle tümörlü olmayan dokularda, daha az malign tümörlerde ve farklılaşmış veya senesensli hücrelerde ifade edildiklerini ortaya koydu. Buna karşılık HSK/ölümsüzlük genlerinin ifadelerinin tümörlü dokularda ve ilerlemiş malign tümörlerde arttığı belirlendi. HSK tümörlerinde ve ölümsüz hücrelerde DNA onarımı, hücre döngüsü, telomere uzaması ve amino asit metabolizması genlerinin ifadesi artarken; hücre sinyali, ilaç metabolizması, lipid metabolizması ve glikolitik metabolizma genlerinin ifadeleri de azalmaktadır. Farklı dokular üzerinde senesens ile ilişkili genlerin ifadelerinin incelenmesi ile de displazi aşamasının bir geçiş aşaması olduğu yanında siroz ve HSK örneklerinin sırasıyla senesensli ve ölümsüz hücrelere benzer gen ifade profilleri sergiledikleri belirlenmiştir. Bu belirgin gen ifadesi farklılıklarından yararlanarak HSK örneklerinin siroz örneklerinden ayrımını yüksek hassasiyetle sağlayan 15 genlik bir karaciğer hücresi ölümsüzlük imza testi geliştirdik. Karaciğer hücresi ölümsüzlük imza testi genleri arasında öne çıkan ATAD2 geninin bir epigenetic düzenleyici gen olması sebebiyle epigenetik düzenleyici genlerin karaciğer kanserinin gelişimindeki rollerini de araştırdık. Siroz, HSK, displazi ve normal karaciğer doku örnekleri verileriyle ve kapsamlı bir epigenetic düzenleyici genler listesiyle yaptığımız biyoinformatik analizler sonucunda karaciğer kanseri gelişimi sırasında gen ifadesi değişikliklerine uğrayan bir çok epigenetic düzenleyici mekanizmayı da belirledik. Ancak histon varyantlarının N-terminal uçlarını kodlayan DNA dizilerinde mutasyon farklılığı bulamadık. Elde ettiğimiz bulgular senesensin DNA onarımı, hücre çoğalması, hücre farklılaşması ve hücre metabolizması üzerinde gen ifade farklılıklarına sebep olarak HSK gelişiminde merkezi bir rol oynadığını ortaya koymaktadır.

Aileme...

ACKNOWLEDGEMENTS

It is of great pleasure for me to thank many people who have made this thesis possible.

First and foremost, I wish to express my greatest thanks to my thesis advisor and mentor Prof. Dr. Mehmet ÖZTÜRK for his invaluable supervision and guidance throughout this study. I am grateful for his endless patience, motivation, enthusiasm, inspiring comments and immense knowledge in molecular biology and encouragement for personal development in this research field.

I would like to thank the entire MBG faculty. I am especially grateful to Assoc. Prof. Özlen KONU, Assoc. Prof. Rengül ÇETİN-ATALAY for their efforts and help in providing me with experimental support and inspiration.

Many thanks will go to all the members of the Öztürk lab, especially to the past members I worked with: Şerif ŞENTÜRK, Eylül HARPUTLUGİL, Ayça ARSLAN-ERGÜL, Ceyhan CERAN, Mine MUMCUOĞLU, Sevgi BAĞIŞLAR, Haluk YÜZÜGÜLLÜ, Özge Şehriban GÜR SOY-YÜZÜGÜLLÜ, Mustafa YILMAZ, Hande TOPEL; and current members who have always been so much more than just lab colleagues: Emre YURDUSEV, Engin DEMİRDİZEN, Umur KELEŞ, Ayşegül ÖRS, Dilek ÇEVİK, Çiğdem ÖZEN, Merve Deniz ABDÜSSELAMOĞLU, Yusuf İsmail ERTUNA, Derya SONER.

I would also like to thank all the members of the MBG lab, especially to İbrahim Fırat TAŞ, Hani ALOTAIBI, Pelin TELKOPARAN, Mehmet ŞAHİN, İhsan DERELİ, Ender AVCI, Sıla ÖZDEMİR, Tamer KAHRAMAN, Şükrü ATAKAN, Verda BİTİRİM, Tülin ERŞAHİN, Nilüfer SAYAR and Gurbet KARAHAN for their friendship and support.

I was delighted to interact with Bilge KILIÇ, Füsun ELVAN, Sevim BARAN, Abdullah ÜNNÜ, Turan DAŞTANDIR and Yavuz CEYLAN during my research period at Bilkent University. I am indebted to them for their help in or outside the lab.

Last but not the least, my deepest gratitude goes to my family for their unconditional love and support throughout my life; I would like to dedicate this dissertation to them.

I would like to thank to TÜBİTAK for financially supporting me during my Ph.D. education with BİDEB-2211 and BİDEB-2214 programs.

TABLE OF CONTENTS

ABSTRACT.....	iii
ÖZET	v
ACKNOWLEDGEMENTS.....	viii
TABLE OF CONTENTS.....	x
LIST OF TABLES	xiii
LIST OF FIGURES	xiv
ABBREVIATIONS.....	xv
CHAPTER 1	1
INTRODUCTION	1
1.1 Hepatocellular carcinogenesis	1
1.2 Tumor-free chronic liver diseases.....	2
1.2.1 Characteristic properties, functions and homeostasis of the liver.....	2
1.2.1.1 Carbohydrate metabolism	3
1.2.1.2 Fat metabolism.....	3
1.2.2 Fibrosis of the liver	4
1.2.3 Non-alcoholic fatty liver disease	5
1.2.4 Cirrhosis.....	6
1.3 CLD and liver cancer inducing major factors.....	8
1.3.1 Hepatitis B virus (HBV) and hepatitis C virus (HCV) infections	8
1.3.2 Obesity and insulin resistance.....	9
1.3.3 Chronic alcohol consumption and aflatoxin exposure.....	9
1.4 Hepatocellular carcinoma (HCC)	10
1.4.1 Etiology of liver cancer.....	10
1.4.2 Deregulated molecular signaling pathways in HCC.....	12
1.4.2.1 NF- κ B, JAK-STAT, IL-6 pathway axis in HCC	12
1.4.2.2 Mitogen activated protein kinases (JNK, p38, ERK), and Akt pathways in HCC	14
1.4.2.3 TGF- β pathway	16
1.4.2.4 Wnt pathway	17
1.4.2.5 c-Met Pathway	17
1.4.3 Genetic abnormalities in HCC.....	18
1.4.3.1 Genetic instability events observed in HCC	18
1.4.3.2 Recurrent somatic mutations of HCC	19
1.4.4 Epigenetics and HCC.....	21
1.4.4.1 DNA methylation alterations in HCC.....	21
1.4.4.2 Roles of microRNAs in HCC	22
1.4.4.3 Histone code related alterations in HCC.....	22
1.4.4.5 Roles of histone variants in HCC.....	24
1.5 Cellular senescence.....	25
1.5.1 Mechanisms of cellular senescence	25

1.5.1.1 The replicative senescence.....	27
1.5.1.2 Oncogene-induced senescence (OIS)	28
1.5.1.3 PTEN loss induced senescence (PICS).....	28
1.5.1.4 Other senescence mechanisms.....	29
1.5.2 Senescence in chronic liver diseases.....	29
1.5.3 Epigenetic players of the cellular senescence.....	30
CHAPTER 2	33
OBJECTIVES AND RATIONALE	33
CHAPTER 3	36
MATERIALS AND METHODS.....	36
3.1 Cell culturing materials and methods	36
3.1.1 Standart cell culture materials and solutions of our laboratory	36
3.1.2 Cryopreservation of stock cells.....	37
3.1.3 Thawing of frozen cells	37
3.1.4 Parental cell lines and human hepatocytes.....	37
3.1.5 Senescent and immortal Huh7 clones.....	38
3.1.6 Small interfering RNA (siRNA) transfection materials and methods	38
3.1.7 Adriamycin treatment of Huh7 cells.....	39
3.2 Senescence-associated beta-galactosidase (SA-β-Gal) staining materials and method.....	39
3.3 RNA extraction, cDNA synthesis and polymerase chain reaction (PCR) materials and methods.....	40
3.3.1 RNA extraction and cDNA synthesis	40
3.3.2 Polymerase chain reaction (PCR) materials and methods	40
3.3.2.1 Semi-quantitative and quantitative real-time RT PCR assays of ATAD2 experiments.....	40
3.3.2.2 Agarose gel electrophoresis materials and methods	41
3.3.2.3 Agarose gel electrophoresis of DNA	42
3.4 Western blotting materials and methods.....	42
3.4.1 Western blotting materials and solutions.....	42
3.4.2 Western blotting.....	43
3.5 Cirrhosis and HCC tissue samples.....	43
3.6 Genome-wide gene expression profiling of samples.....	44
3.7 Other Microarray Datasets	45
3.8 Gene Set Enrichment Analyzes (GSEA)	45
3.8.1 Basic GSEA materials and methods	45
3.8.2 Interpretation of GSEA results of <i>in vitro</i> and <i>in vivo</i> datasets	46
3.8.3 Integration and analyzes of the GSEA data to determine 74 commonly enriched gene sets of the two datasets	46
3.8.4 Leading Edge Analysis (LEA).....	49
3.9 Cluster Analysis	49
3.10 Generation and Validation of a Senescence-based Genomic Classifier	52
3.11 Generating Epigenetic Regulatory (EpiReg) Gene lists	52
3.12 Histone Mutation Analyzes.....	53
3.12.1 Samples of the histone mutation search experiments	53
3.12.2 PCR experiments of the Histone mutation study	53
3.12.3 Agarose Gel Electrophoresis and Sequencing	54
3.12.4 Restriction Enzyme Digestion	55
3.12.5 Analyzing Sequencing Data.....	55
CHAPTER 4	56

RESULTS	56
4.1 Genome-Wide Transcriptional Reorganization Associated with Senescence-to-Immortality Switch during Human Hepatocellular Carcinogenesis	56
4.1.1 Top 100 deregulated genes of <i>in vitro</i> and <i>in vivo</i> datasets	56
4.1.2 Gene Set Enrichment Analyses (GSEA) of <i>in vitro</i> and <i>in vivo</i> datasets using the C2_ALL curated gene sets list	59
4.1.3 Senescence and Immortality Gene Set Enrichments of <i>in vitro</i> and <i>in vivo</i> datasets	62
4.1.4 Senescence-related gene networks in cirrhosis and hepatocellular carcinoma	65
4.1.5 A senescence to immortality switch between dysplasia and HCC	71
4.1.6 Fifteen-gene hepatocellular-immortality signature	76
4.1.7 Association of ATAD2 RNA and protein levels with HCC and cellular immortality	78
4.2 Differential Expression of Epigenetic Regulatory Genes During Liver Carcinogenesis	81
4.2.1 Creating the epigenetic regulatory genes (EpiReg) list	81
4.2.2 Differentially expressed EpiReg gene sets during cirrhosis to HCC transition	82
4.2.3 Differential expression of epigenetic regulatory genes in different stages of hepatocellular carcinogenesis	83
4.2.4 Common core-enriched EpiReg genes of Wurmbach and Yildiz datasets	85
4.3 N-Terminal tail coding sequences of H2A and H3 histone variants have no mutation in HCC	90
CHAPTER 5	94
DISCUSSION	94
5.1 Genome-Wide Transcriptional Reorganization Associated with Senescence-to-Immortality Switch during Human Hepatocellular Carcinogenesis	94
5.2 Differential Expression of Epigenetic Regulatory Genes During Liver Carcinogenesis	104
5.3 Future perspectives	107
REFERENCES	109
APPENDIX	131

LIST OF TABLES

Table 1.1: Histone lysine modifications of histone H3 and H4.....	23
Table 1.2: Known mammalian replacement histone variants.....	25
Table 3.1: Patient samples (<i>in vivo</i> dataset) used in this study.....	44
Table 3.2: Pseudocode of the method used during Matlab analyzes.....	51
Table 3.3: Genomic DNA samples of the histone variant sequencing experiments.....	55
Table 4.1: Significantly enriched senescence and immortality related gene sets in <i>in vitro</i> and <i>in vivo</i> datasets.....	60
Table 4.2: 74 senescence escape oriented deregulated gene networks of hepatocellular carcinogenesis.....	66
Table 4.3: Detailed information on the “hepatocellular immortality signature set” containing 16 probe sets.....	72
Table 4.4: EpiReg gene sets and number of genes in each gene set used in GSEA studies	80
Table 4.5: Significantly enriched EpiReg gene sets in Wurnbach and Yildiz microarray datasets.....	80
Table 4.6: Differentially expressed EpiReg gene sets during different stages of human hepatocellular carcinogenesis.....	81
Table 5.1: Table of 15 genes hepatocellular immortality signature testlist.....	100

LIST OF FIGURES

Figure 1.1: Steps of the hepatocellular carcinogenesis.....	2
Figure 1.2: Major molecular units and mechanisms of the liver fibrosis.....	7
Figure 1.3: Multi-step progressive treat and molecular mechanisms of hepatocellular carcinogenesis.....	11
Figure 1.4: Different senescence response mechanisms.....	26
Figure 2.1: The basic study design to achieve the objectives of the thesis.....	35
Figure 3.1: Summarized GSEA results of <i>in vitro</i> and <i>in vivo</i> datasets.....	47
Figure 3.2: Examples of detailed outputs of GSEA experiments.....	48
Figure 3.3: Steps of the method used for identification of 74 commonly enriched gene sets.....	50
Figure 4.1: Heat map representation of the top 100 deregulated genes of <i>in vitro</i> and <i>in vivo</i> datasets	55
Figure 4.2: Statistically significantly enriched senescence or immortalization gene sets of <i>in vitro</i> and <i>in vivo</i> datasest.....	57
Figure 4.3: Comparative analysis of gene sets enriched in Huh7 clones and diseased liver tissues associated cirrhosis with senescence and HCC with immortality phenotypes, respectively	63
Figure 4.4: DNA repair and cell cycle gene sets of the 74 gene sets list display the major gene expression based similarities and differences of the two datasets regarding to DNA repair and cell cycle mechanisms.....	67
Figure 4.5: Retinol metabolism is deregulated in senescence to immortality switch.....	70
Figure 4.6: Hierarchical clustering of 75 non-malignant and malignant liver tissue samples using 1813 senescence-associated gene probe sets.....	71
Figure 4.7: Relative gene expression profiles of 18 probe sets.....	73
Figure 4.8: Nearest template prediction (NTP) of 15 gene hepatocellular signature test.....	75
Figure 4.9: Association of ATAD2 RNA and protein expressions with HCC and cellular immortality.....	77
Figure 4.10: Commonly core enriched genes of the three significantly enriched EpiReg group gene sets in Wurmbach and Yildiz datasets.....	84
Figure 4.11: Commonly core enriched genes of the three significantly enriched EpiReg domain gene sets in Wurmbach and Yildiz datasets.....	85
Figure 4.12: Core enriched genes of the six significantly enriched EpiReg group gene sets in early HCC and dysplasia comparison of the Wurmbach dataset.....	86
Figure 4.13: Core enriched genes of the Histone EpiReg gene set in Wurmbach and Yildiz datasets.....	88
Figure 4.14: Cirrhosis <i>versus</i> HCC gene expression level comparisons of seven histone variants in Wurmbach and Yildiz datasets.....	89
Figure 4.15: A possible amino acid substitution leading mutation in histone N-terminal encoding DNA sequences of Histone H3F3B.....	90
Figure 5.1: Genes core enriched at least five times in different common DNA repair and cell cycle gene sets of immortal or HCC samples.....	97

ABBREVIATIONS

3'-UTR	3' UnTranslated Regions
5hmC	5-methylcytosines to 5-hydroxy-methyl-cytosines
54K	54,000
A	Adenine
A2AR	Adenosine 2A Receptor
Ac	Acetylation
acetyl-CoA	Acetylcoenzyme A
ADH	Alcohol Dehydrogenase
ADP	Adenosine Diphosphate
AFB1	Aflatoxin B1
AKT	v-akt murine thymoma viral oncogene homolog
APC	Adenomatous Polyposis Coli
ARID1	AT Rich Interactive Domain 1 (SWI-like)
ARID2	AT Rich Interactive Domain 2 (ARID, RFX-like)
ATAD2	ATPase family, AAA Domain containing 2
AT1R	Angiotensin 1 Receptor
ATM	Ataxia Telangiectasia Mutated
ATR	Ataxia Telangiectasia and Rad3 related
BER	Base Excision Repair
BCMO1	β -carotene 15,15'-monooxygenase 1
BH	Benjamini-Hochberg
bp	Base pair
BrdU	Bromodeoxyuridine
C	Cytosine
c-Myc	v-myc myelocytomatosis viral oncogene homolog
cDNA	Complementary DNA

CpG	Poly cytosine and Guanine containing sequence
CBR1	Cannabinoid Receptor 1
CCLE	Cancer Cell Line Encyclopedia
CCNE2	Cyclin E2
CDKN2A	Cyclin-Dependent Kinase Inhibitor 2A
CK1	Casein Kinase 1
CLD	Chronic Liver Disease
CRNDE	Colorectal Neoplasia Differentially Expressed
CTNNB1	β -catenin
CYP	Cytochrome P-450
DAXX	Death-domain Associated Protein
DCP	Des-gamma-carboxy thrombin
ddH ₂ O	Double Distilled Water
DDR	DNA Damage Response
DEN	Diethylnitrosamine
DHRS4	Dehydrogenase/reductase (SDR family) member 4
DMEM	Dulbecco's Modified Eagle's Medium
DMSO	Dimethyl Sulphoxide
DNA	Deoxyribonucleic Acid
DNMT	DNA Methyltransferase
dNTP	Deoxyribonucleotide Triphosphate
DSB	Double Strand Break
DSH	Dishevelled
E	Glutamine
ECM	Extracellular matrix
EDTA	Ethylenediaminetetraacetic Acid
EGF	Epidermal Growth Factor
EpiReg	Epigenetic Regulatory Genes
ERK	Extracellular Signal Regulated Kinase
ET-1	Endothelin-1
ETAR	Endothelin A Receptor
EtBr	Ethidium Bromide
ETS	E-twenty-six
EZH2	Enhancer of zeste homolog 2 (Drosophila)

FAM83D	Family with sequence similarity 83, member D
FBS	Fetal Bovine Serum
FDR	False Discovery Rate
FXR	Farnesoid X receptor
g	Gram
G	Guanine
G-418	Neomycin
GAPDH	Glyceraldehyde-3-phosphate Dehydrogenase
GEO	Gene Expression Omnibus
GSEA	Gene Set Enrichment Analyses
GSK3 β	Glycogen Synthase Kinase 3-beta
HAT	Histone acetyltransferase
HBV	Hepatitis B Virus
HBX	Hepatitis B virus X protein
HBXAg	Hepatitis B virus X antigen
HCC	Hepatocellular Carcinoma
HCV	Hepatitis C Virus
HDV	Hepatitis D Virus
HDAC	Histone Deacetylase
HDM	Histone Demethylase
HGF	Hepatocyte Growth Factor
Hh(R)	Hedgehog (Receptor)
HMT	Histone Methyltransferase
HPV	Human Papilloma Virus
HR	Homologous Recombination
HRP	Horse Radish Peroxidase
HSC	Hepatic Stellate Cell
hTERC	Human Telomerase RNA Component
IGF	Insulin Like Growth Factor
IFN	Interferon
I κ B	Inhibitor of kappa B
IL	Interleukin
Int	Integrin
IRF2	Interferon Regulatory Factor 2

JAK	Janus kinase
JMJ	Jumonji
JNK	Jun N-terminal Kinase
JP	Japanese
K	Lysine
KCl	Potassium chloride
KDM	Lysine specific demethylase
kg	Kilo gram
KMT	Lysine specific methylase
LEA	Leading Edge Analysis
lncRNA	Large noncoding RNA
LRAT	Lecithin:retinol acyltransferase
LSEC	Liver sinusoidal endothelial cells
Log	Logarithmic scale
LOH	Loss of Heterozygosity
LPA1R	Lysophosphatidic acid Receptor 1
LTBP	Latent TGF- β binding protein
MAPK	Mitogen Activated Protein Kinase
MBP	Methyl-CpG binding proteins
MD	Moderately Differentiated
Me	Methylation
mg	Milligram
μ g	Microgram
MgSO ₄	Magnesium Sulfate
Min	Minute
miRNA (miR)	microRNA
ml	Milliliter
MLL	Myeloid/lymphoid or mixed-lineage leukemia
mM	Mili Molar
MMR	Mismatch Repair
MND1	Meiotic nuclear divisions 1 homolog (<i>S. cerevisiae</i>)
mRNA	Messenger RNA
μ l	Microliter
MS	Metabolic Syndrome

MsigDB	Molecular Signature Database
mTOR	Mechanistic Target of rapamycin
mTORC	mTOR Complex
N.A.	Not Available
NaCl	Sodium Chloride
NADPH	Nicotinamide Adenine Dinucleotide Phosphate
NaF	Sodium Fluoride
NAFLD	Nonalcoholic Fatty Liver Disease
NaOH	Sodium Hydroxide
Na ₃ VO ₄	Sodium Ortho-vanadate
NEAA	Non-essential Amino Acid
NFE2L2	Nuclear factor (erythroid-derived 2)-like 2
NF- κ B	Nuclear factor kappa B
ng	Nanogram
NGFR	Nerve Growth Factor Receptor
NGS	Next Generation Sequencing
NK	Natural Killer Cell
NKT	Natural Killer T Cell
nm	Nanometer
nM	Nanomolar
NOX4	NADPH oxidase 4
N-terminus	Amino Terminus
NS	Non-structural proteins
NUSE	Normalized Unscaled Standard Error
NTP	Nearest Template Prediction
OIS	Oncogene Induced Senescence
PBS	Phosphate Buffered Saline
PBS-T	Phosphate Buffered Saline with Tween-20
PCR	Polymearase Chain Reaction
PD	Population Doubling
PDGF	Platelet-Derived Growth Factor
PHD	Pleckstrin Homology Domain
PI3K	Phosphoinositide-3-kinase
PICS	PTEN Loss Induced Senescence

PIK3CA	Phosphatidylinositol-4,5-bisphosphate 3-kinase, catalytic subunit alpha
PIP2	Phosphatidylinositol 4,5-biphosphate
PNPLA4	Patatin-like Phospholipase-4
pRb	Retinoblastoma Protein
PRC	Polycomb Repressive Complex
PTEN	Phosphatase and Tensin Homolog
PTM	Post-translational Modification
PTX2	Pentraxin 2
PWWP	Proline-Tryptophan-Tryptophan-Proline motif
qRT-PCR	Quantitative Reverse Transcription PCR
r	Regression
R	Arginine
RAF	v-raf-1 murine leukemia viral oncogene homolog
RAS	v-Ki-ras2 Kirsten rat sarcoma viral oncogene homolog
RDH	Retinol dehydrogenase
RIN	RNA integrity number
RIPA	Radio-Immunoprecipitation Assay
RLE	Relative Log Expression
RMA	Robust Multichip Analysis
RNA	Ribonucleic Acid
ROS	Reactive Oxygen Species
rpm	Revolutions per Minute
RPMI	Roswell Park Memorial Institute
RPS6KA3	Ribosomal protein S6 kinase, 90kDa, polypeptide 3
RT-PCR	Reverse Transcription PCR
SA β G	Senescence Associated beta Galactosidase
S	Serine
S phase	Synthesis phase
SAHF	Senescence Associated Heterochromatin Foci
SAM	S-adenosylmethyonine
SASP	Senescence Associated Secretory Phenotype
SDF	Senescence-Associated DNA Damage Foci
SDS	Sodium Dodecyl Sulfate

SDS-PAGE	SDS- Polyacrylamide Gel Electrophoresis
Sec	Second
shRNA	Short Hairpin RNA
siRNA	Small Interfering RNA
SIRT	Sirtuin
SKP2	S phase Kinase-associated Protein 2
SMAD	Small Mothers Against Decapentapepic
SMYD	SET and MYND Domain Containing
SSB	Single Strand Break
STAT	Signal Transducer and Activator of Transcription
SUV39H2	Suppressor of variegation 3-9 homolog 2 (Drosophila)
SWI/SNF	SWItch/Sucrose NonFermentable
T	Thymidine
TAE	Tris-Acetate-EDTA Buffer
TBS	Tris Buffered Saline
TBS-T	Tris Buffered Saline with Tween-20
(h)TERT	(human) Telomerase Reverse Transcriptase
TGF- β	Transforming Growth Factor Beta
T _m	Melting Temperature
TMEM27	Transmembrane protein 27
TNF	Tumor Necrosis Factor
TOP2A	Topoisomerase 2A
TR	Turkish
TP53	Tumor suppressor protein 53
TRAILR	TNF-related Apoptosis-inducing Ligand Receptor
Tris	Tris (hydroxymethyl)-methylamine
UDP	Uridine Diphosphate
UGT	UDP Glucuronosyltransferase
UV	Ultraviolet
V	Valine
v/v	Volume/volume
VEGF	Vascular Endothelial Growth Factor
VHL	Von Hippel-Lindau
w/v	Weight/volume

WD	Well-Differentiated
WNT	Wingless-type MMTV integration site family
X-Gal	5-bromo-4-chloro-3-indolyl-b-D-galactoside
YB-1	Y-box Binding Protein

CHAPTER 1

INTRODUCTION

1.1 Hepatocellular carcinogenesis

Hepatocellular carcinogenesis is a multi-step progressive process, which comprise of tumor free liver disease steps (mainly fibrosis, non-alcoholic fatty liver disease and cirrhosis) and liver cancer (mainly hepatocellular carcinoma) [1-3]. During the hepatocellular carcinogenesis a normal healthy liver suffers impact of several metabolic changes, infections, inflammation events, chromatin abnormalities and molecular biological changes that finally cause generation of the HCC [3-9].

Hepatocellular Carcinogenesis

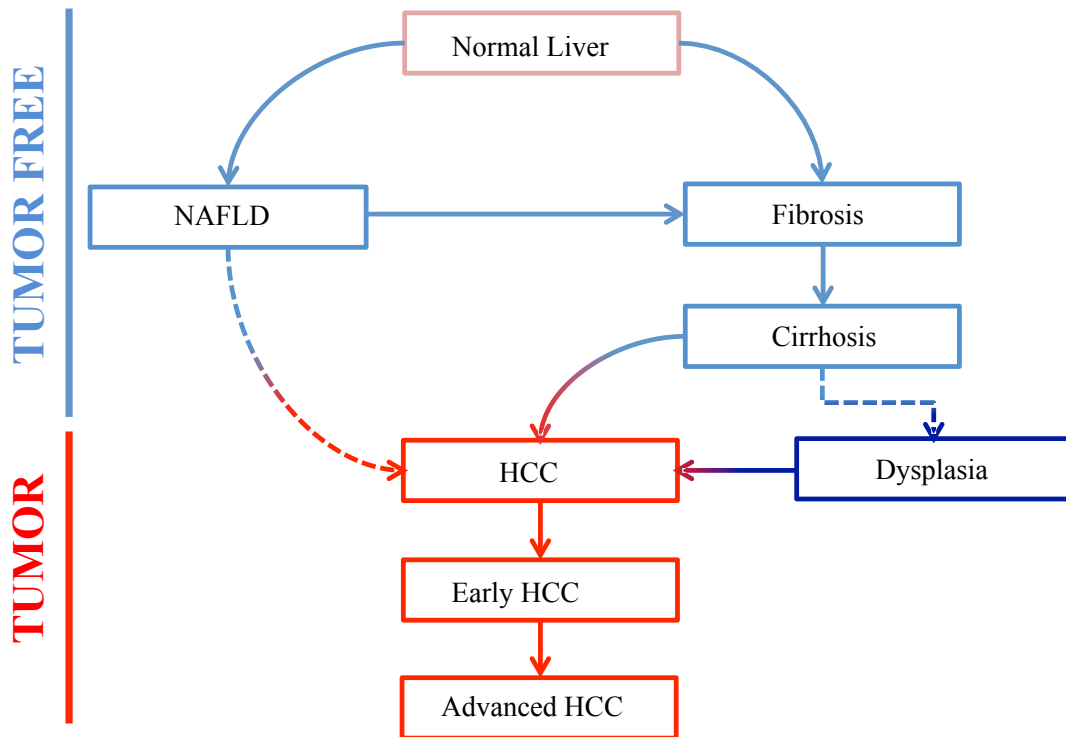


Figure 1.1: Steps of the hepatocellular carcinogenesis: A normal healthy liver can transform into non-alcohol induced liver disease (NAFLD) or fibrosis. Next step of the NAFLD can be fibrosis or hepatocellular carcinoma (HCC) if the disease is worsened. Cirrhosis may occur as a result of continued fibrosis and it might transform to HCC or generate dysplastic nodules become the HCC step. HCC can also progress from the early HCC to advanced HCC.

1.2 Tumor-free chronic liver diseases

1.2.1 Characteristic properties, functions and homeostasis of the liver

The human liver is the largest internal organ of the body, weighing 1.44–1.66 kg, with a triangular shape in reddish brown color containing four lobes of unequal size. The liver is connected to two blood vessels called hepatic artery and portal vein. The hepatic artery is responsible for carrying blood from the aorta. The portal vein carries blood containing digested nutrients. These blood vessels subdivide into capillaries leading to a lobule. Lobules are the functional units of the liver. A human liver contains 50,000 to 100,000 lobules and each lobule is composed of millions of hepatic cells, which are the fundamental metabolic cells of the liver. 80%

of the liver volume is occupied by hepatocytes whereas other cell types such as sinusoidal hepatic endothelial cells, Kupffer cells, and hepatic stellate cells constitute 6.5% of the total volume [10].

In addition to being a storage and filtration organ for blood, and being a secretory and excretory organ by forming the bile, the liver is mainly responsible for the majority of the metabolic systems of the body. Major metabolism events taking place in the liver are listed below [10-12]:

1.2.1.1 Carbohydrate metabolism

Specific functions performed by liver in terms of carbohydrate metabolism are: glycogen storage, conversion of glucose, gluconeogenesis, and generation of several chemical compounds of carbohydrate metabolism. By performing these functions the liver has a *glucose buffer function* to maintain a normal blood glucose concentration in the body (the excess amount of glucose can be stored in the liver as glycogen, or triglycerides can be converted to glucose by gluconeogenesis to increase the glucose amount in the blood when it is needed) [11].

1.2.1.2 Fat metabolism

Nearly all the events of synthesis of the fat in the body from carbohydrates and proteins occur in the liver. Following the synthesis of fat in the liver, it is stored in the adipose tissue after transportation of fat in the form of lipoproteins in the liver. Energy from the neutral fats is derived by first splitting the fat into glycerol and the fatty acids, then splitting the fatty acids into two-carbon acetyl radicals by beta oxidation and finally forming acetylcoenzyme A (acetyl-CoA). Acetyl-CoA can enter the citric acid cycle and be oxidized to achieve high amounts of energy. This event, the β -oxidation, can take place in any other cell of the body, but it occurs extremely rapidly in the hepatocytes. The excess amount of acetyl-CoA produced by hepatocytes is converted to acetoacetic acid and transferred to other tissues to be used to produce energy by the β -oxidation [1].

Almost all the cholesterol synthesized in the liver is converted into the bile salts, but the rest is transported in the lipoproteins. After that, the lipoproteins are carried to other tissue cells in the body by the blood. Phospholipids are also synthesized in the same method in the liver and transported in the lipoproteins [12].

In summary, specific functions of the liver in fat metabolism are: high rate of oxidation of fatty acids to supply energy for other bodily functions, formation of most of the lipoproteins, synthesis of large quantities of cholesterol and phospholipids, and conversion of large quantities of carbohydrates and proteins into fat [11, 12].

1.2.2 Fibrosis of the liver

The liver fibrosis is a diseased state of a liver with excess accumulation of extracellular matrix (ECM), as an intrinsic response to chronic injury, resulting from chronic inflammation. The inflammation in liver causes cell death of cells of the liver via necrosis or apoptosis and triggers wound-healing process leading to scar tissue formation. Major factors causing liver fibrosis are chronic hepatitis B or C virus infections, autoimmune and biliary diseases, alcoholic and non-alcoholic steatohepatitis [1, 13].

Cellular effectors of the liver fibrosis, which produce excess amount of ECM, are activated myofibroblasts that mainly derive from hepatic stellate cells and portal fibroblasts (Figure 1.2). In addition to that, there are three major multicellular functional units of the liver fibrosis, which have role in the fibrogenic pathways: (a) hepatic stellate cells, liver sinusoidal endothelial cells (LSECs), macrophages/Kupffer cells, and hepatocytes; (b) stromal inflammatory myofibroblasts, T cells, and macrophages; and (c) portal/peri-portal cholangiocytes/ductular cells, portal fibroblasts, and various inflammatory cells [4] (Figure 1.2).

The mild liver fibrosis is mainly asymptomatic and it usually reverses within a few weeks following the resolution of tissue damage, as demonstrated in less advanced rodent and human liver fibrosis [1, 13]. However, continued scar tissue formation and inflammation during fibrosis progresses towards cirrhosis, which

usually leads to hepatocellular carcinoma (HCC). In addition to that, advanced fibrosis or cirrhosis diseases are largely irreversible, even though they do not progress towards the HCC [13, 14].

Potential mechanisms of fibrosis-dependent hepatocellular carcinogenesis are:

i) Deregulated integrin signaling by the fibrotic matrix: Over-expressions of ECM components integrin 1b or integrin b3 may trigger apoptosis or cell cycle arrest via up-regulation of p21 and p27 in HCC cell lines) [1].

ii) Paracrine signaling of hepatic stellate cells (HSCs) and hepatocytes: During the liver fibrosis, HSCs produce growth factors such as hepatocyte growth factor, IL-6, and Wnt ligands creating a microenvironment supporting hepatocyte proliferation. In addition to that, activated myofibroblasts can both induce hepatocyte cell proliferation and metastasis by through PDGF and TGF- β mediated cross-talk mechanisms [15].

iii) Increased stromal stiffness: The ECM is more rigid in liver fibrosis, and this situation causes cell proliferation and HSC activation in liver [16].

iv) Growth factor sequestration by ECM: The TGF- β signaling, which is highly dependent on ECM interactions, is down-regulated in liver fibrosis via sequestration of TGF- β by latent TGF- β binding proteins (LTBPs) [17].

v) Reduced tumor surveillance by natural killer (NK) and natural killer T cells (NKT): NK cells have ability to induce cell death of tumor cells and activated hepatic stellate cells. However, because of the structure of the microenvironment created during the liver fibrosis, NK cells may remain in the stroma without making cell-cell contact to kill tumor cells [18, 19].

1.2.3 Non-alcoholic fatty liver disease

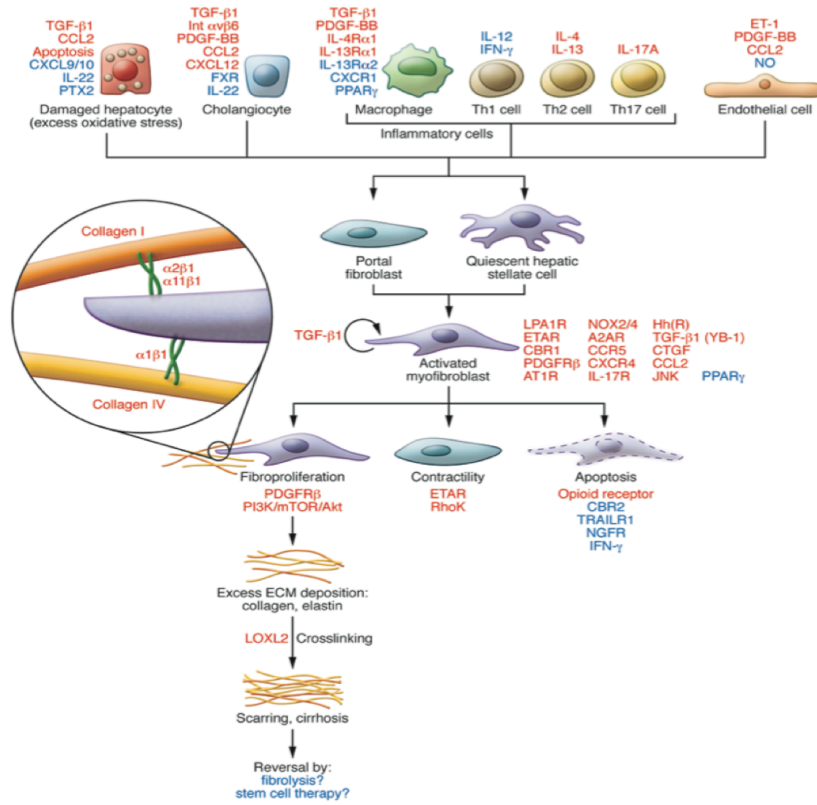
Nonalcoholic fatty liver disease (NAFLD), which is characterized by hepatocellular injury and inflammation with or without fibrosis, is a spectrum of disorders that are characterized by steatosis of the liver; it occurs in people who do

not consume significant amounts of alcohol [5]. The simple steatosis, abnormal accumulation of lipids in cells, is the only histological finding of the NAFLD. NAFLD is a “silent liver disease” because it is usually diagnosed in asymptomatic patients after accidental discovery of elevated liver enzymes or ultrasound [5,20]. Prolonged NAFLD can progress to cirrhosis and finally become HCC [21]. It is believed that NAFLD occurs as a result of metabolic syndrome (MS) in the liver [22].

1.2.4 Cirrhosis

Cirrhosis is known as the most crucial risk factor for development of HCC. Known risk factors for development of HCC in virus-related cirrhosis are age, male gender, ferocity of the liver disease, active viral replication during follow-up, viral genotype, alcohol intake, and aflatoxin exposure [6]. Earlier acquisition of HBV infection and longer duration of disease are also additional risk factors of HCC development in cirrhosis patients [23]. Cirrhosis is the final stage of the non-tumor chronic liver diseases manifested with replacement of liver tissue with fibrosis, generation of regenerative cirrhotic nodules and ascites (abdominal fluid accumulation) [24].

a



b

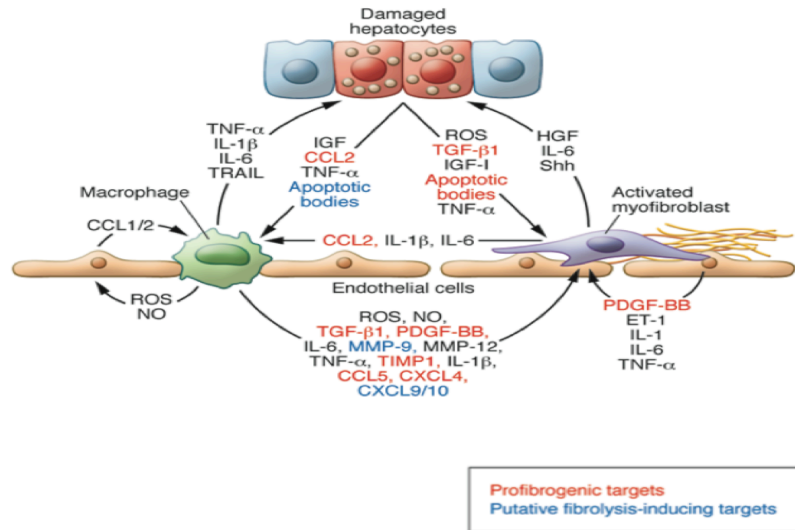


Figure 1.2: Major molecular units and mechanisms of the liver fibrosis: a) Fibrogenic activation mechanism of myofibroblasts. b) Major cellular functional unit affecting hepatocytes during liver fibrosis. TGF- β 1, Transforming growth factor 1; IL, interleukin; IFN, interferon; A2AR, adenosine 2A receptor; AT1R, angiotensin 1 receptor; CBR1, cannabinoid receptor 1; ET-1, endothelin-1; ETAR, endothelin A receptor; FXR, farnesoid X receptor; Hh(R), hedgehog (receptor); Int, integrin; LPA1R, lysophosphatidic acid receptor 1; NGFR, nerve growth factor receptor; PTX2, pentraxin 2; TRAILR, TNF-related apoptosis-inducing ligand receptor; YB-1, Y-box binding protein. Permission granted for reuse of figures by Copy Right Clearance Center (see Appendix).

1.3 CLD and liver cancer inducing major factors

1.3.1 Hepatitis B virus (HBV) and hepatitis C virus (HCV) infections

There are two major types of viruses, hepatitis B virus (HBV) and hepatitis C virus (HCV), able to replicate in hepatocytes and cause non-tumorigenic chronic liver diseases (CLD) and hepatocellular carcinoma (HCC) [25]. These viruses have high heterogeneity in their genome. There are eight different genotypes (A-H) of HBV and four major genotypes (G1-G4) of HCV characterized [26].

It is estimated that around 2 billion individuals are infected with HBV. Most of the HBV infections take place at birth and most of them (more than 90%) become chronic [7]. Regarding to HCV infections, almost 85% of the HCV infections become chronic. In Africa and Asia HBV is endemic and 60% of HCC is associated with HBV infection whereas, in the United States of America, Europe, Egypt and Japan 60% of HCC is associated with HCV infection [8]. Nearly half of people with chronic HBV or HCV infections develop CLD. In 5-20 years 5-20% of the infected people progress to cirrhosis. However, 1-2% of them progress to HCC each year, but it takes nearly 30 years from the original infection [26]. Each year more than 250.000 new HCC cases emerge and 500.000-600.000 people die because of the HCC [27].

The inflammation and regeneration events during the chronic liver damage create a suitable environment for HBV and HCV viruses. HBV and HCV generate proteins that make NK cells and NKT cells of the liver incapable of killing infected cells [28].

The HBV contributes to the development of HCC mainly by producing hepatitis B x (HBx) protein and, pre-S and S polypeptides, whereas non-structural proteins (NS) NS3 and NS5A are the main players of the HCV mediated oncogenic transformation to HCC [29, 30]. Both HBx and pre-S or S polypeptides of these viruses provide advantageous traits to hepatocytes for oncogenic transformation such as growth-factor independent proliferation and resistance to growth inhibition [8].

The oncogenic transformation events after chronic HBV and HCV infections trigger cellular senescence response in hepatocytes. However, both HBV and HCV viruses by-pass the cellular senescence mechanisms by inactivating tumor suppressors of the senescence mechanisms via different mechanisms such as up-regulating of DNA methyltransferases (DNMTs) to prevent gene expression of DNA repair genes and cyclin dependent kinase (CDK) inhibitors INK4A and p21, expressing microRNA (miRNA) miR-221 to prevent the gene expression of CDK inhibitor p27 [31-34].

1.3.2 Obesity and insulin resistance

Obesity is the major factor causing NAFLD and finally HCC. The prevalence of NAFLD is 80–90% in obese adults and steatosis is 4.6-fold higher than in normal weight people [5]. Leptin, an adipokine secreted by adipocytes to the blood stream with circadian rhythm, is the major player of the obesity mediated liver diseases. Since Leptin is functioning in lipid and carbohydrate metabolisms, it is demonstrated that deregulated gene expressions of Leptin and its receptor are associated with deregulated energy metabolism in NAFLD and HCC [35, 36]. Obesity is also associated with the insulin resistance, which is another factor causing NAFLD together with oxidative stress and inflammation [37, 38].

1.3.3 Chronic alcohol consumption and aflatoxin exposure

It is known for long-time that chronic intake of alcohol can cause cirrhosis and HCC in the liver [39]. Major mechanisms of alcohol-induced CLD and HCC are related to deregulated metabolic events, oxidative stress induction, and inflammation induction in the liver.

Liver is the main organ that alcohol-metabolism events take place in the body. The first major impact of the chronic alcohol intake on liver is excess production of acetaldehyde, produced by alcohol dehydrogenase (ADH) during the alcohol-metabolism events; which causes DNA damage in the liver [40]. Chronic alcohol consumption also causes production of isoprostane, a lipid peroxidation marker, in the liver [41], which is an indicator of oxidative stress that causes liver fibrosis and

cirrhosis in the liver. These, alterations in the alcohol-metabolism induce secretion of pro-inflammatory cytokines, such as TNF- α , Interleukin-1 β , and Interleukin 6, from Kupffer cells, which cause chronic destruction of hepatocytes, cirrhosis, and finally HCC [42].

Aflatoxin B1 (AFB1) is the most common type of the aflatoxins produced by fungus *Aspergillus flavus*. AFB1 is a very potent mutagene, which causes a very specific AGG to AGT mutation at codon 249 of the tumor suppressor p53 protein, which causes activation of several oncogenes and finally induction of HCC in the liver [9]. In addition to that, AFB1 infection usually coexists with HBV infection, but the molecular mechanism of this association is not known yet [43].

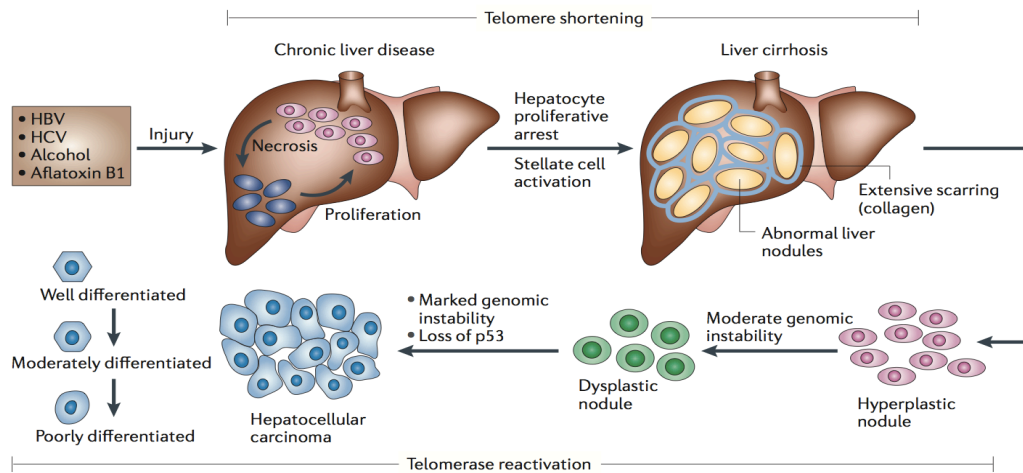
1.4 Hepatocellular carcinoma (HCC)

HCC is a multi-step progressive disease (Figure 1.3a) arises from accumulation of multiple genetic aberrations, epigenetic alterations, deregulated molecular signaling events and environmental factors (Figure 1.3b) detailed below.

1.4.1 Etiology of liver cancer

Liver cancer is the fifth most common cancer in men and seventh in female with more than 500.000 new cases and almost the same number of deaths in each year. 85% of the liver cancer cases occur in countries being developed. The most common type of the liver cancer is HCC (80% of the cases), while there are other types of liver cancers, such as cholangiocarcinoma and hepatocellular adenoma. Nearly 90% of the HCC cases are related to HBV or HCV infections; whereas there are other major HCC inducing factors, such as chronic alcohol consumption and aflatoxin exposure. Variations of HCC incidences in terms of age, sex or geographic distribution are mostly related to variations of virus infections. Geographically, HCC mostly (80%) occur in Sub-Saharan Africa and eastern Asia. In recent years, HCC cases started to decrease in these regions; while increasing in North America. HCC is mostly diagnosed at 55-65 years of life; and rarely seen in a person less than 40 years old [3].

a



b

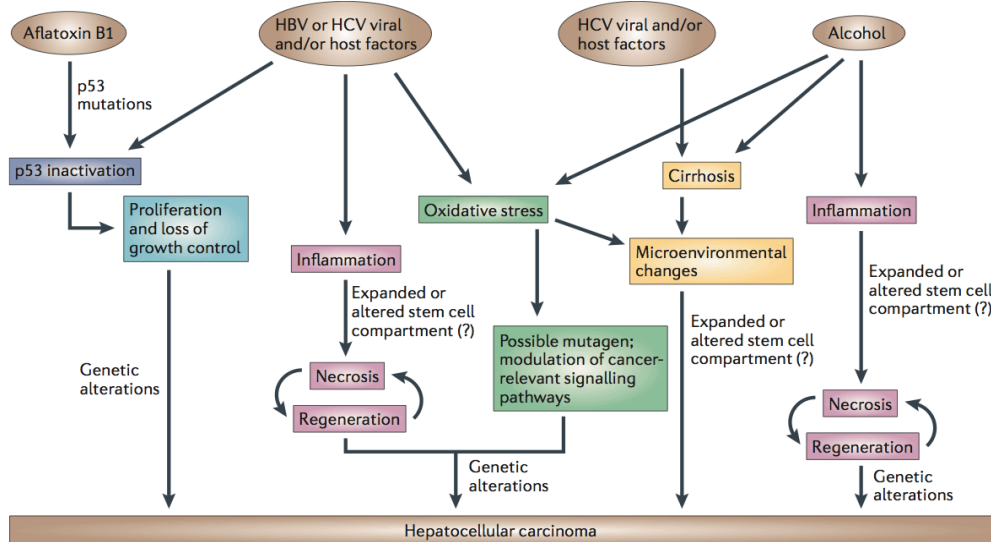


Figure 1.3: Multi-step progressive treat and molecular mechanisms of hepatocellular carcinogenesis: a) Different factors, such as viral infection and chronic alcohol consumption induce injury in hepatocytes. Injured hepatocytes die and new hepatocytes are produced to compensate the absence. However, continued injury causes destruction of hepatocytes. This situation triggers repetitive cycles of hepatocyte death and regeneration, which causes generation of chronic liver diseases; and cirrhosis. Progression of the diseases is characterized with conversion of cirrhotic nodules to hyperplastic nodules and dysplastic nodules, and finally HCC, in sequence. HCC can also be classified into early and advanced HCC. Telomere shortening is a feature of CLD and cirrhosis. Telomerase reactivation is associated with hepatocellular carcinogenesis. Loss and mutation of p53 with genomic instability are characterized with hepatocellular carcinogenesis as well. b) Mechanisms of hepatocellular carcinogenesis. Details of these mechanisms are provided in the text. Permission granted for reuse of figures by Nature Publishing Group (see Appendix).

1.4.2 Deregulated molecular signaling pathways in HCC

Hepatocellular carcinogenesis is a multi-step progressive event as a result of accumulations of different genetic abnormalities, epigenetic changes, impaired metabolic processes and deregulated signaling pathways of different cell types of the liver [44-46]. As described above, during the progression from healthy liver to non-tumorigenic chronic diseased liver to the HCC, chronic inflammation events and associated changes in the molecular signaling pathways in the liver play major role in hepatocellular carcinogenesis. Thus, understanding the major deregulated molecular signaling pathways during the hepatocellular carcinogenesis is a key step to understand molecular basis of the HCC.

1.4.2.1 NF- κ B, JAK-STAT, IL-6 pathway axis in HCC

The nuclear factor kappa B (NF- κ B) signaling generally functions as a regulator pathway of cell survival, immunity, and inflammation in cells [47, 48]. NF- κ B proteins function as protein dimers, composed by seven different proteins. p105, p50 (together form NF- κ B1), p100, p52 (together form NF- κ B2), RelA (p65), RelB, and c-Rel. When there is no stimulation, I κ B proteins bind to NF- κ B dimers and keep them inactive in the cytoplasm. However, I κ B cannot function on dimers of p105 and p100. NF- κ B dimers are released from I κ B kinases, become activated, and translocate into nucleus to induce transcription of several genes when a proinflammatory signal, such as tumor necrosis factor (TNF) or interleukin 1 β (IL-1 β) stimulus arrives to a cell [49, 50].

NF- κ B pathway has anti-apoptotic roles in early liver development. Both RelA/p65 deficient mice and IKK β deficient mice are embryonically lethal because of liver apoptosis and degeneration [51, 52]. In addition to those, NF- κ Bs cause gene expression of several reactive oxygen species (ROS) scavenging proteins, such as ferritin heavy chain and manganese-dependent super-oxide dismutase, to maintain anti-oxidant defense in hepatocytes [53].

However, the anti-apoptotic functions of the NF- κ B in the liver work as a major tumor promoter mechanism in case of inflammation. Using a non-degradable I κ B α mutant expressing mouse model Pikarsky et al. showed that continuous NF- κ B activation in hepatocytes causes survival of malignant cells by TNF- α production and paracrine TNF- α signaling in the liver [54].

Another NF- κ B associated tumor promoting signaling mechanism occurs through communications of NF- κ B, IL-6 and (signal transducer and activator of transcription 3) STAT3 in diethylnitrosamine (DEN) mouse model. NF- κ B and STAT3 transcription factors have common target genes and they communicate in both positive and negative crosstalk mechanisms [47, 48]. In mouse DEN model, a chemically induced HCC mouse model that displays a similar gene expression and histology profile of human HCC samples, DEN-induced hepatocyte death causes release of IL-1 α from hepatocytes. IL-1 α activates NF- κ B signaling in Kupffer cells, which release several cytokines and growth factors to the environment. IL-6, released by Kupffer cells with this mechanism, activates STAT3 in hepatocytes and cause transcription of several hepatocyte proliferation inducing genes [55, 56].

STAT3, which is normally inactive in cells, is phosphorylated and activated by Janus kinases (JAKs) in response to different cytokines and growth factors such as IL-6, and hepatocyte growth factor (HGF) [57, 58]. The active STAT3 found to be present almost 60% of human HCC samples, and especially in aggressive ones, but not in surrounding non-tumor tissue or in normal liver [59]. The main reason of elevated numbers of active STAT3 must be related to the increased expression of IL-6 in the tumor microenvironment, because active NF- κ B positive samples do not overlap with active STAT3 positive samples. In addition to that, hepatocyte specific IL-6 receptor transgenic mice spontaneously develop HCC, and gain of function mutations of human gp130 protein (another IL-6 receptor protein) [60] were found in 60% of hepatocellular adenomas like the percentage of active STAT3s in HCC samples.

In conclusion, inflammation related NF- κ B, JAK-STAT, IL-6 pathway axis seems as an important mechanism of the hepatocellular carcinogenesis.

1.4.2.2 Mitogen activated protein kinases (JNK, p38, ERK), and Akt pathways in HCC

Mitogen activated protein kinases (MAPKs) consist of at least four sub-families including Jun N-terminal kinase (JNK), p38 MAPKs, extracellular signal regulated kinases (ERKs) [61].

Jun N-terminal kinase (JNK) proteins (JNK1, JNK2, and JNK3) are encoded by MAPK8, MAPK9, and MAPK10 genes, respectively. JNKs are activated by MKK4 and MKK7, mainly by TNF- α or IL-1; and de-activated by different DUSP family members. Main activities of JNK pathway are favoring proliferation, survival and motility of hepatocytes, mostly through the activation of c-Jun [62]. JNK also functions in the processes of activation of mitochondrial apoptotic pathways [63].

JNK pathway is especially important in HBV-associated HCC, because elevated JNK activation is correlated with HBsAg positivity of cells [64]. Hyperphosphorylated JNK1 is found in more than 50% of both European and Chinese HCC samples [65, 66]. In addition to that, JNK activation increase is positively related to increased transcription of different histone methyltransferases, such as EZH2, SUV39H2, MLL3, SMYD3, and SMYD5 [66]. JNK1 $-/-$ mice show decreased hepatocellular carcinogenesis after DEN treatment, mainly due to increase expression of p21 and decreased expression of c-Myc due to the lack of JNK1 expression [65].

Despite the fact that JNK pathway is one of the activated pathways in the HCC, JNK pathway usually antagonizes with other activated pathways, such as NF- κ B, p38, and ERK pathways. NF- κ B negatively regulates JNK activation processes [67, 68]. However, JNK is activated in absence of active NF- κ B in hepatocytes, mainly due to increased ROS in hepatocytes. The increase of inflammatory cytokines and ROS accumulation in the liver, as results of metabolic syndrome related mechanisms, such as obesity and insulin resistance induce JNK activation, but not the NF- κ B pathway [69]. Thus, NF- κ B and JNK pathways play separate and independent roles during hepatocyte death and proliferation cycle events of the inflammation-related events in the liver.

The p38 family consists of p38 α , p38 β , p38 γ , and p38 δ isoforms; and activated by MKK3, MKK4, and MKK6 kinases [70, 71]. p38 α is one of the critical proteins in initiation of HCC from viral infection associated hepatitis. HBx protein, produced by HBV, increases activation of p38 that increase assembly of virus particles in the hepatocytes. However, HCV activates p38 pathway to produce pro-inflammatory chemokine IL-8 [72, 73].

In addition to positive contributions of p38 to hepatocellular carcinogenesis, p38 can negatively regulate hepatocellular carcinogenesis; because p38 antagonizes with JNK pathway and causes decrease of the proliferation of advanced liver tumor cells [74].

Extracellular signaling-regulated kinase (ERK) is activated by Ras proteins, which are bound to growth factor receptors. After receptor activation, the signal is transmitted to Ras, Raf, MEK, and ERK, in sequence. Main functions of this signaling pathway are to regulate cell growth, resistance to apoptosis, extracellular matrix production, and angiogenesis in a cell [75-77].

Raf-1 is hyperactivated in many cancers, including HCC [78, 79]. In an immunohistochemical study using HCC patient samples it is found that MEK1/2 are overexpressed in 100% (46/46) of samples, ERK1/2 are overexpressed in 91% (42/46) of samples, and ERK1/2 are phosphorylated in 69% (32/46) of samples; suggesting that the ERK signaling is highly active in many HCC cases [80]. Despite the fact that, studies using ELK1/2 knock out mice for hepatocellular carcinogenesis are missing to understand *in vivo* roles of the ERK pathway in hepatocellular carcinogenesis, extensive *in vitro* studies have been done on different ERK pathway components. Generally, *in vitro* experiments on ERK pathway indicate that knock down of ERK members cause attenuation of liver tumor cell proliferation, and DNA replication, and tumorigenesis (using xenograft tumors) [81, 82].

As it happens with JNK and p38, there is a negative communication between JNK and ERK pathways, as well as p38 and ERK pathways. Sustained JNK activation by TNF- α stimulation inhibits ERK activation in hepatocytes; and inhibition of p38

pathway by an inhibitor (SB203580) activates ERK in primary human hepatocyte cultures [83].

The PI3K/Akt/mTOR pathway is complex pathway that generally regulates growth, survival, cellular metabolism, and anti-apoptosis events of a cell. In this pathway phosphatidylinositol 3-kinase (PI3K) phosphorylates phosphatidylinositol 4,5-biphosphate (PIP2) and converts it to PIP3, which activates the Akt protein. The PTEN protein is antagonistic to activities of PI3K to inhibit Akt activation [84]. The other component of this pathway that regulates Akt is the mTOR. mTOR can be found in two different complexes: mTORC1, which activates Akt as an upstream regulator, and mTORC2, which is downstream of Akt protein [85].

The expression of Akt was found as a poor prognostic factor for survival for HCC, with a study using more than 500 HCC patient samples [86]. In addition to that, it is found that activation of mTOR is related with recurrence of HCC after excision of early HCC [84].

1.4.2.3 TGF- β pathway

Transforming growth factor beta (TGF- β) is a secreted protein that activates the TGF- β pathway by binding to TGF receptors and activating the canonical small mothers against decapentapegic (SMAD) pathway, which translocate to nucleus to induce transcription of various genes, or DAXX pathway [87]. The TGF- β pathway may have both tumor blocking or tumor promoting functions with a context dependent manner [88]. It is known that TGF- β is functioning for generation of liver fibrogenesis in non-tumorigenic CLD. TGF- β is produced and released from non-parenchymal cells, such as HSCs; used by hepatocytes and induces wound healing mechanisms in the hepatocytes during fibrogenesis of the liver [89]. On the other hand, different groups including ours showed that TGF- β is able to induce cellular senescence on *in vitro* HCC cells [90]. Senturk et al. showed that TGF- β treatment down-regulates c-Myc expression, but upregulates p21 and p15 proteins and cause G1 arrest through accumulation of ROS and down-regulation of NOX4 protein in HCC cells [90].

1.4.2.4 Wnt pathway

Main components of the Wnt signaling is composed of the ligand protein Wnt, Frizzled family transmembrane receptors, which binds to Wnt, and intracellular effector proteins, dishevelled (DSH), adenomatous polyposis coli (APC), casein kinase 1 (CK1), glycogen synthase kinase 3 β (GSK3 β), and β -catenin. β -catenin is normally inactive in the cytoplasm in a complex with APC, CK1, and GSK3 β . Binding of Wnt ligand to the Frizzled receptor causes activation of DSH, which in turn prevents ubiquitination of β -catenin. The free and active β -catenin protein in the cytoplasm translocates to the nucleus to achieve its gene expression modulation activities [91].

The Wnt pathway is an important mechanism in liver development, but this pathway is inactive in adult liver. However, this pathway is reactivated in regenerating adult liver, hepatoblastoma, and HCC. Studies using β -catenin transgenic mice indicate that abnormally active Wnt signaling is not enough for hepatocellular carcinogenesis [92]. On the other hand, one of the most frequently seen genetic events in HCC seen in 20-40% of the HCC patients is point mutations on the CTNNB1 gene, which encodes the β -catenin protein, that cause aberrant activation of the Wnt/ β -catenin pathway [93-95].

1.4.2.5 c-Met Pathway

c-Met is a receptor tyrosine kinase usually activated by hepatocyte growth factor (HGF) ligands. Following the activation, c-Met can activate different signaling mechanisms, such as JAK-STAT pathway and ERK pathway [96]. c-Met can also be activated by other ligands such as Des-gamma-carboxy thrombin (DCP), a prothrombin secreted from HCC cells that induces HGF independent c-Met pathway, epidermal growth factor (EGF), IL-1, IL-6, and TNF- α , and HBx. c-Met might also be activated in response to attachment of cells without a ligand [97].

It is found that c-Met is over-expressed in 20-48% of the human HCC samples [98, 99]. The increased gene expression is considered as a prognostic factor for HCC. c-Met transcription is elevated in invasive or poorly differentiated HCCs, as well as HCC samples with high proliferative index [98, 100]. It is also found that patients with c-Met transcription in elevated levels have decreased 5-year survival rates after surgical resection [100, 101]. Finally, based on the c-Met gene expression signatures, HCC patients able to be classified into good prognosis or bad prognosis in 83-95% accuracy with a predictive model [102]. Thus, the c-Met signaling emerges as a good target for targeted anti-HCC therapies in the future.

In addition to these pathways other pathways such as insulin like growth factor (IGF) [103], epidermal growth factor (EGF) [84], vascular endothelial growth factor (VEGF) [104], platelet derived growth factor (PDGF) [105], Sonic-Hedgehog [106], and Hippo pathways [106] are also deregulated in HCC, but less than the pathways described above.

1.4.3 Genetic abnormalities in HCC

The hepatocellular carcinogenesis is a multi-step progressive disease with accumulation of different abnormalities at different stages of the progression events, as described in the previous sections. Throughout these multistep processes different genetic abnormalities in the genome of the hepatocytes also accumulate and constitute one of the important factors of the hepatocellular carcinogenesis. Genetic abnormalities observed in hepatocellular carcinogenesis can be investigated in three different titles: *i*. Genomic instability events, *ii*. Somatic mutations.

1.4.3.1 Genetic instability events observed in HCC

The term “genetic instability” refers to abnormalities in structure of the chromosome (e.g., amplifications, deletions, and rearrangements), chromosomal copy number abnormalities (e.g., aneuploidy and polyploidy), and microsatellite instability [107]. Recurrent chromosomal abnormalities identified in HCC cases include allelic

deletion of 1p, 4q, 6q, 8p, 9p, 10q, 13q, 16q, and 17p; as well as amplification of 1q, 5, 6p, 7, 8q, 17q, and 20q [107, 108].

It is logical to assume deregulated gene expression profiles of genes located in these abnormal chromosomal locations in HCC. Over-expression of c-Myc gene located in chromosome 8q24 in virus and alcohol related HCCs is long been considered with a correlation of c-Myc's genomic location [109]. In addition to that, events of gain of 6p and loss of 6q are also considered as a possible early event in liver tumorigenesis of glycogen storage disease type I [110].

Some specific genetic instability events are considered as causative events of different stages of HCC as well. Gain of 1q and loss of 1p and 17p were only observed in early HCCs but not in CLDs; and gain of 5q, 6p, 8q and loss of 4q, 8p are seen mostly in advanced HCCs [107].

1.4.3.2 Recurrent somatic mutations of HCC

Genetic studies of the pre-next generation sequencing (NGS) era identified that genes encoding tumor suppressor protein 53 (TP53), and β -catenin (CTNNB1) are the most frequently mutated genes in HCC. TP53 mutations are found in 10-61% of HCCs most of the time specifically at codon 249 (R249S), since it is related to AFB1 contamination [9, 111]. β -catenin was found to be mutated at 20-40% of HCC samples, especially in HCC related ones [93, 94, 95, 112]. c-MET was found to be mutated in 30% of HCCs arising during childhood [113].

With use of the NGS techniques, in the last two years we learned previously uncharacterized recurrent mutations in HCC. Guichard et al. used exome sequencing method and mostly alcohol induced HCC patients [114]; whereas Fujimoto et al. used whole genome sequencing method and HBV or HCV infection related HCC samples [115]. Using the exome sequencing method Guichard et al. identified four new mutated genes in HCC: ARID1A, RPS6KA3, NFE2L2, and IRF2. They also identified 5 different pathways containing recurrently mutated genes: *i.* Beta-catenin pathway (CTNNB1: 32.8%, AXIN1: 15.2%, APC: 1.6%), *ii.* P53 pathway (TP53:

20.8%, IRF2: 4.8%, CDKN2A: 7.2%), *iii*. Chromatin remodeling pathway (ARID1A: 16.8%, ARID2: 5.6%), *iv*. PI3K/Ras pathway: (KRAS: 1.6%, PIK3CA: 1.6%, RPS6KA3: 9.6%), *v*. Oxidative and endoplasmic reticulum stress pathway: (NFE2L2: 6.4%) [114].

Using the whole genome sequencing method Fujimoto et al. also identified new mutated genes in HCC. Interestingly, they also identified recurrently mutated chromatin regulator genes, such as ARID1A, ARID1B, ARID2, MLL, and MLL3, suggesting that mutations of epigenetic regulator encoding genes are important factors for HCC [115].

In addition to identification of previously unidentified mutated genes in HCC using the NGS techniques, most frequently seen mutations of HCC have been identified in the core promoter region of the human telomerase reverse transcriptase (TERT) gene this year [116-118].

Two independent groups identified two highly recurrent mutations (chromosome 5 1,295,228 C>T, and 1,295,250 C>T) in core promoter sequences of the TERT gene in 71-85% of the melanomas examined [116, 117]. In addition to that, both groups also claimed that these mutations create a binding site for the E-twenty-six (ETS) transcription factors, which constitutes a new hypothesis for the mechanism of the TERT activation in cancer cells [116, 117].

Huang et al. searched these mutations in different type of cancers including HCC as well using the *in vitro* cell lines of the cancer cell line encyclopedia (CCLE). For HCC, they observed C228T mutations in 4 cell lines out of 6 [117]. However, a more comprehensive study for TERT promoter mutations of HCC samples came from the work of Killela et al. They identified C228T and/or C250T mutations in 44.2% of the HCC patient samples investigated (27/61). More interestingly, the TERT mutations identified mostly in early stage HCC samples, indicating that these mutations might be an early event for initiation of the HCC [118]. Thus, the TERT gene locus became the most frequently mutated gene yet identified in HCC.

1.4.4 Epigenetics and HCC

Deregulated epigenetic mechanisms of HCC will be summarized in: *i)* DNA methylation alterations in HCC, *ii)* Roles of microRNAs in HCC, *iii)* Histone code related alterations in HCC, *iv)* Roles of histone variants in HCC.

1.4.4.1 DNA methylation alterations in HCC

DNA hypermethylation and hypomethylation events occur in the CpG islands of gene promoters are frequent epigenetic disruptions in HCC. Nearly 50-60% of all genes have a CpG island, multiple cytosines and guanines containing DNA sequences, in the 5' area of their promoters [119]. Inappropriate methylation of the cytosine bases from C-5 with methyl provided from S-adenosylmethyonine (SAM) in CpG islands interferes with promoter function of the gene. Hypermethylation of a gene promoter attenuates and finally blocks the gene expression; whereas hypomethylation activates transcription; thus promoter CpG island methylation is generally related with gene silencing. Two major groups of proteins regulate these events: DNA methyl transferases (DNMTs), which enzymatically add methyl groups; and methyl-CpG binding proteins (MBPs), which recognize methylated CpG sequences and recruit other epigenetic players, such as histone modifying enzymes and chromatin remodelers to specific sites [119]. Although another group of genes called TET proteins, which catalyze enzymatic conversion of 5-methylcytosines to 5-hydroxy-methyl-cytosines (5hmC), were also identified, further studies are needed to uncover their roles on DNA methylation processes [120].

There are five DNMT proteins identified in mammals: DNMT1, DNMT2, DNMT3A, DNMT3B, DNMT3L. Among them only DNMT3A and DNMT3B are *de novo* methyltransferases. DNMT1 maintains DNA previous methylation patterns during DNA replication [121]. All these three enzymes over-expressed in HCC compared to non-tumor samples [122, 123]. DNA methylation seems an important epigenetic mechanism for liver homeostasis; because an old experiment with rats fed with methionine deficient diet for 9 weeks generated HCC due to loss of 40% global loss of DNA methylation on DNA [124]. In addition to that, DNA hyper-methylation

of promoters of tumor suppressors such as, p14, p15, and p16 are well known in HCC [124]. Frequencies of hyper-methylated promoter sequences of different genes in HCC are determined [108]. However, the mechanistic events of contribution of DNA methylation aberration to hepatocellular carcinogenesis are still ill-known.

1.4.4.2 Roles of microRNAs in HCC

MicroRNAs (miRNAs) are approximately 22 nucleotide long RNA molecules able to post-transcriptionally down-regulate gene expression of target genes by binding to complementary sequences of 3' untranslated regions (3'-UTRs). miRNAs are expressed in tissue specific manner [125].

There are several differentially expressed miRNAs identified in HCC. It was demonstrated by Zhou et al. that expression levels of some miRNAs are powerful for detecting early stages of HCC [126]. Some examples of miRNAs functioning as oncogene in HCC are miR-221, which inhibits apoptosis, and miR-9, which promotes cell invasion [127]. miR-101, miR-195, miR-122, let-7c, and miR-338 are some of the miRNAs function as tumor suppressors for HCC [127].

1.4.4.3 Histone code related alterations in HCC

Histones are important players of the epigenetic events. The fundamental unit of the chromatin structure is the nucleosome that consists of 147 base pairs of DNA wrapped around conventional H2A, H2B, H3, and H4 histones. In addition to these histone proteins, the H1 histone protein is another member of the nucleosome structure on the outer part of the nucleosome and it basically stabilizes this nucleosome structure. The N-terminal tails of the histones (especially H3 and H4) are subjected to post-translational modifications (PTMs), which functions as specific signals (histone codes). Types of these known small covalent modifications are: methylation, acetylation, phosphorylation, ubiquitination, sumoylation, deamination, ADP ribosylation. The most studied modifications among them are methylations and acetylations of histones H3 and H4. Histone proteins can be methylated on lysine

(mono, di, or tri) or arginine (mono or di) residues by specific enzymes called histone methyltransferases (HMTs). In addition to that, there are methyl removing enzymes called histone demethylases (HDMs) removing methyl molecules with different specificities. Generally histone methylations are considered as gene transcription permissive and heterochromatin permissive marks, although there are well known exceptions [119]. Functions of specific histone methylations and enzymes catalyzing these reactions are listed in Table 1.1.

Table 1.1: Histone lysine modifications of histone H3 and H4: Histone lysine methylation sites, their known transcriptional activities, code writers and erasers are listed in separate columns. R, Arginine; K, Lysine; Me, Methylation; HMT, histone methyltransferase; HDM. Histone demethylase.

Histone Modification	Activity	HMT	HDM
H3R2Me1	Unknown	PRMT6	Unknown
H3R2Me2	Regulation	PRMT6	JMJD6, PADI4
H3K4Me1	Activation	WDR5, SETD7, MLL5, ASH2L, SMYD1	KDM1A, KDM1B, C14ORF169, KDM5B
H3K4Me2	Activation	WDR5, MLL5, SMYD3, ASH2L, SETD3, SMYD1, WHSC1L1	KDM1A, KDM1B, KDM5A, KDM5B, KDM5C, KDM5D
H3K4Me3	Activation	PRDM9, SMYD3, SETD1A, SETD1B, MLL, MLL2, MLL3, MLL4, SMYD1	KDM2B, C14ORF169, KDM5A, KDM5B, KDM5C, KDM5D
H3R8Me1	Activation	PRMT5	Unknown
H3R8Me2	Unknown	Unknown	PADI4
H3K9Me1	Activation	EHMT1, EHMT2	KDM1A, KDM3A, KDM3B, PHF8
H3K9Me2	Repression	SUV39H1, SUV39H2, EHMT1, EHMT2, PRDM2	KDM1A, KDM3A, KDM3B, JHDM1D, PHF2, PHF8, KDM4D
H3K9Me3	Repression	SUV39H1, SUV39H2, SETDB2	KDM4A, KDM4B, KDM4C, KDM4D
H3R17Me1	Activation	CARM1	Unknown
H3R17Me2	Unknown	CARM2	PADI4
H3K27Me1	Activation	EZH1, EZH2	Unknown
H3K27Me2	Repression	EZH1, EZH2, WHSC1L1	JHDM1D, KDM6A, KDM6B, PHF8, UTY
H3K27Me3	Repression	EZH1, EZH2, WHSC1L1	KDM6A, KDM6B, UTY
H3K36Me1	Activation	ASH1L	Unknown
H3K36Me2	Repression	SETD3, SMYD2, ASH1L, NSD1, SETMAR	KDM2A, KDM2B, C14ORF169, JMJD5
H3K36Me3	Activation	SETD2, WHSC1	KDM4A, KDM4C
H3K79Me1	Activation	Unknown	Unknown
H3K79Me2	Activation	DOT1L	Unknown
H3K79Me3	Activation	SETDB1, DOT1L	Unknown
H4R3Me1	Repression	PRMT1, PRMT5	Unknown
H4R3Me2	Regulation	PRMT1, PRMT7, PRMT5	JMJD6
H4K20Me1	Activation	SETD8, WHSC1	PHF8
H4K20Me2	Repression	NSD1	Unknown
H4K20Me3	Repression	SUV420H1, SUV420H2, PRDM6, WHSC1	Unknown

Recent studies on histone modifications indicate that Histone H3 trimethylated lysine (H3K27Me3) modification is significantly increased in HCC compared to non-tumor tissue; and this aberration is significantly correlated with poor differentiation, large tumor size, and shortened survival time of HCC patients [128]. The H3K27Me3 mark putting HMT called enhancer of zeste homolog 2 (EZH2 or KMT6), the catalytical component of the Polycomb Repressive Complex 2 (PRC2), is also over-expressed in HCC; and mostly associated with aggressiveness of HCC like the H3K27Me3 mark [128, 129]. More specifically, EZH2 causes constitutive activation of the Wnt/beta-catenin pathway by silencing transcription of Wnt pathway

antagonists [130]; and prevents gene expression of several tumor suppressor miRNAs in HCC [131]. The other HMTs and HDMs deregulated in HCC are SMYD3 (a histone H3K4 and H3K5 methylating enzyme), which is up-regulated by HBx in HepG2 cells [132], and JHDM1D (KDM7A, a HDM removing methyl residues from histone H3K9Me2, H3K27Me2, and H3K4Me1), which is up-regulated after nutrient starvation in HepG2 cells [133].

Histone acetyltransferases (HATs) and histone deacetylases (HDACs) catalyze acetylations of histone proteins. HATs are categorized in two groups (A-type HATs, functioning in nucleus; and B-type HATs functioning in the cytoplasm); whereas HDACs are categorized in four classes [119].

HDAC1, HDAC2, and HDAC3 are found being over-expressed in HCC. HDAC3 seems more important than the other class I HDACs, since it is a candidate prognostic and cancer proliferating factor for HCC [134]. SIRT1 is another HDAC over-expressed in HCC and this expression was associated with advanced stages of HCC [135]. HDAC2 and SIRT1 are critical epigenetic factors in regulation of transcription of NF- κ B target genes in alcohol induced liver diseases [121].

1.4.4.5 Roles of histone variants in HCC

In addition to the canonical histone proteins, there are another type of histone proteins called “replacement histone variants” able to take place in the nucleosomes of the chromatin structure (Table 1.2). Despite they have high similarity in protein sequences and basic function; these two groups of proteins have several differences. Replacement histone variants and conventional histones are encoded by separate genes. Canonical histones are mainly expressed in the synthesis (S) phase of the cell cycle and incorporated to the DNA during the DNA replication; whereas replacement histone variants are synthesized independently of S phase and they are usually incorporated to the DNA independently to the DNA replication. Genome-wide distributions of these two types of histones also differ. The typical example of this difference is incorporation of the histone H3 variant CENP-A to solely the kinetochore region of a chromosome; whereas canonical histone H3 does not have

such specificities. Functional nucleosome deposition machineries of the two groups of histones are also differing [136].

In HCC, CENPA and MacroH2A1 are over-expressed in HCC; MacroH2A2 is over-expressed in liver steatosis [136-138].

Table 1.2: Known mammalian replacement histone variants:

H1 VARIANTS	H2A VARIANTS	H2B VARIANTS	H3 VARIANTS
H1FO	H2A.X	TSH2B	H3.1
H1FOO	H2A.Z1 (H2AFZ)	H2BWT	H3.2
H1FX	H2A.Z2 (H2AFV)		H3.3
	MacroH2A.1-1 (H2AFY)		CENPA
	MacroH2A.1-2		H3T
	MacroH2A.2 (H2AFY2)		H3.X
	H2AL1		H3.Y
	H2AL2		H3.5
	H2ABbd		

1.5 Cellular senescence

1.5.1 Mechanisms of cellular senescence

Cellular senescence is a state of a cell, which permanently stops dividing with continued metabolic activity. Typical senescent cells are characterized with having an enlarged and flattened morphology, presence of vacuoles and multi-nuclei, and positive staining with senescence associated beta-galactosidase (SA- β -Gal) at pH 6.0 *in vitro* [139-141]. The cellular senescence is classified into two main types: Replicative senescence and stress induced premature senescence, which is also sub-categorized into oncogene induced senescence (OIS), PTEN loss induced senescence (PICS), and senescence induced by other molecular factors (e.g., TGF-beta, or oxidative stress) (Figure 1.4).

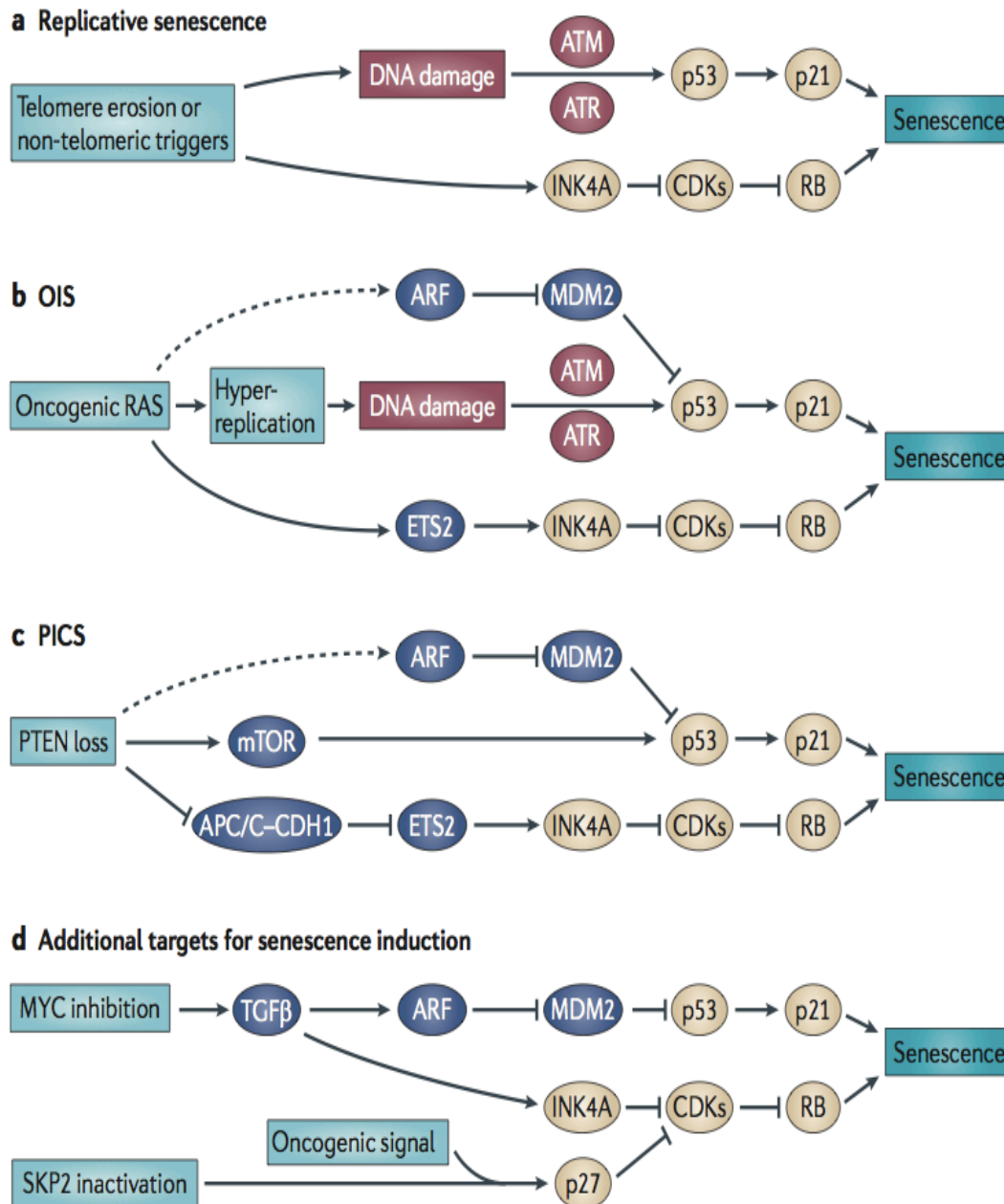


Figure 1.4: Different senescence response mechanisms: a) Replicative senescence, mainly driven by shortening of telomere, activates p16^{INK4A} expression and activates DNA damage pathways causing in p53 induction. b) P53 activation during OIS is mediated by two mechanisms. *i*) p53 is stabilized via phosphorylation by the DNA damage response (DDR), *ii*) ARF mediates stabilization of p53 via inhibiting MDM2. The dashed arrows indicate that there are contradictory data on importance of ARF in human and mouse. c) p53 up-regulation in PICS is mainly mediated by mTOR, but the ETS2–INK4A pathway can also induce senescence. d) MYC inactivation (inhibiting an inhibitor of senescence) can cause the restoration of TGF-β signaling pathway that may induce senescence. Inhibition of S phase kinase-associated protein 2 (SKP2) with additional oncogenic events can induce senescence as well. CDK, cyclin-dependent kinase. Permission granted for reuse of figures by Nature Publishing Group (see Appendix).

1.5.1.1 The replicative senescence

The phenomenon of senescence was first discovered at 1965 in the form of replicative senescence by Hayflick and Moorhead. They observed that primary fibroblast were unable to divide more than 50 population doublings and finally became senescent [142]. The molecular mechanism of the replicative senescence is regulated by a cascade of molecular events strictly dependent to the biology of telomeres. The telomeres are ends of the eukaryotic chromosomes. The main components of the telomeres are; repetitive DNA sequences (several TTAGGG repeats for vertebrates including humans), and a protein complex called “shelterin complex”, which covers and protects the telomeric DNA repeat sequences [143, 144]. Because of the inability of the eukaryotic replication machinery to properly replicate the ends of the linear chromosomes, telomeres of eukaryotic animals are shortened at each DNA replication. The shortened telomeric DNA sequences lose their ability to bind to the shelterin complex, which protects telomeres as ends of the chromosomes and chromosomal instability events [145]. However, after rounds of DNA replications telomeres are shortened to a critical stage and signal to the DNA damage response (DDR) mechanism of a cell and the cell become senescent via the mechanisms described below. However, the shortening of telomeres can be prevented by the natural activities of an enzyme complex called telomerase. A telomerase reverse transcriptase consists of a protein subunit (hTERT) and an RNA subunit (hTERC); and adds telomeric repeats to the ends of the chromosomes to prevent their shortening [146, 147]. Normally, only certain stem cell populations and activated lymphocytes have the active telomerase in adults [143, 148].

The replicative senescence, triggered by erosion of the telomeres, is achieved by p53-dependent or pRb-dependent pathways. In the p53-dependent replicative senescence pathway, the shortening of the telomere is first sensed by the cells as double strand breaks (DSB) or single strand breaks (SSB), causing the formation of γ -H2AX-positive senescence-associated DNA damage foci (SDF). The SDF cause activation of ATR in DSBs, and ATM in SSBs that activate p53 protein. The activated p53 induces transcription of the p21^{Cip1} protein, which causes p53-dependent senescence [149]. In the mechanism of the Rb-dependent senescence pathway, the erosion of the telomeres directly triggers activation of the p16^{INK4A}

protein, which binds to cyclin dependent kinases (CDKs) CDK4/6 to inhibit their suppressive function of Rb and induces senescence [150].

1.5.1.2 Oncogene-induced senescence (OIS)

Oncogene-induced senescence (OIS), a cellular response mechanism to oncogenic transformation events, was first observed by Serrano et al. on *in vitro* primary human or rodent cells after over-expression of activated Ras mutant (HRAS^{G12V}) [151]. The OIS events were also observed with ectopic expressions of other oncogenes, such as RAF, MEK, and BRAF^{V600E}, E2F1 [152-155]. In the OIS mechanism the hyper-replication of DNA triggered by active oncogenes activates S phase specific DDR mechanisms. The DDR and SDF, as well as DDR-unrelated activation of the ARF protein can activate the p53-p21 senescence pathway in the OIS [156]. As it happens in the replicative senescence mechanism, the DNA damage unrelated activation of the Rb-dependent senescence also occurs [157, 158]. Thus, the OIS serves as a barrier mechanism against the oncogenic transformation events in a cell.

1.5.1.3 PTEN loss induced senescence (PICS)

The PICS mechanism of senescence is an OIS-like mechanism with the role of hyper-proliferative activities and lack of DDR or SDF in the initiative events. In the PICS, again the p53 and pRb-dependent mechanisms have role; but mTOR-mediated but not DDR mediated activation of the p53-dependent pathway, and CDH1-containing anaphase-promoting complex (APC/C-CDH1)-mediated activation of the pRb-dependent pathway are the main differences of the PICS from OIS or replicative senescence [159-161].

1.5.1.4 Other senescence mechanisms

i) Increase of the ROS by activated oncogenes, but not related to the OIS, causes a senescence response [162].

ii) p63 and p73 proteins, members of the p53 protein family, can induce cellular senescence by activating the p21 in absence of the p53 [163, 164].

iii) Tumor suppressor protein von Hippel-Lindau (VHL) can induce cellular senescence *in vitro* and *in vivo* via pRb activation and p400 reduction [165].

iv) Inactivation of S-phase kinase-associated protein 2 (SKP2), an E3 ligase, together with an additional oncogenic event, such as activation of RAS or loss of PTEN, can trigger senescence by activating the pRb via p21 and p27 [166].

v) The inhibition of the c-Myc oncogene activates TGF- β -induced senescence via the p53 and pRb-dependent mechanisms [160].

1.5.2 Senescence in chronic liver diseases

During the chronic liver diseases (CLD) injury of the liver causes activation and differentiation of the hepatic stellate cells into myofibroblasts, which secrete extracellular matrix components. In case of presences of intact senescence mechanism players in the liver, active myofibroblasts are cleared by the NK cells when they become senescent as a contributor mechanism of the wound healing processes of the liver [167]. However, inability of conversion of the active myofibroblasts to the senescent fibroblasts because of inactive senescent mechanisms cause accumulation of myofibroblasts and their ECM in the liver causing fibrosis and cirrhosis [168].

It is found by several different studies that the telomere lengths of the hepatocytes are longer in normal liver than chronic hepatitis, fibrotic, and cirrhotic liver. Even the HCC cells have shortened telomeres, but it is also known that HCC cells can activate telomerase to become immortal [169]. p16, p27, p21, p53, which are

critical components of the cellular senescence mechanism, are among the genes usually inactivated in HCC [168].

Although the cellular senescence is considered as a protective mechanism of a cell, some of the features of a senescent cell are in favor of malignant transformation of a cell. The senescent hepatocytes can secrete different cytokines, such as Interleukin-1 α , leptin, MCP1, and RANTES; as an event called senescence associated secretory phenotype (SASP) [168]. The SASP activates CD4⁺ T cell mediated clearance of the senescent cells. However, studies on CD4^{-/-} mice showed a defective immune response causing promotion of tumor development [170]. In addition to that the cytokines released via SASP can induce proliferation of the other cells in the microenvironment [168]. It is also known death senescent cells may exhibit resistance to cell death induced by apoptosis [171-173].

1.5.3 Epigenetic players of the cellular senescence

Epigenetic events play fundamental roles in regulation of cellular senescence processes. The best example of the roles of epigenetic players in cellular senescence is regulation of transcriptional repression and activation of the INK4-ARF locus by interplay of several epigenetic players. This locus encodes crucial players of the cellular senescence mechanisms: p16^{INK4a}, p15^{INK4b} and p19^{ARF} proteins. p19^{ARF} stabilizes p53 protein to sustain cell cycle arrest and apoptosis; whereas p16^{INK4a}, p15^{INK4b} proteins together block phosphorylation of pRb [174]. In normal conditions, when senescence is not induced, this locus is epigenetically repressed by different epigenetic players. EZH2, catalytic component of the PRC2, puts transcription repressive H3K27Me3 marks on this gene. This mark is recognized by PRC1 complex containing RING1b and BMI1 proteins, which put H2AK119Ub mark to further, prevent gene transcription. HDAC3, HDAC4, and histone H3K36 demethylase JHDM1B also recruited to this region to prevent transcription. Finally, a stable transcription block is put on the INK4-ARF locus DNA sequences by DNMTs following these events [175]. Although gene expression of this locus is prevented by

several different players of the epigenetic mechanisms, activation of transcription from this locus is initiated with removal of one large noncoding RNA (lncRNA) called ANRIL during induction processes of the cellular senescence. When ANRIL, which recruits PRC2 members to this region, is down-regulated PRC2 complex leaves this chromatin region, which induces recruitment of the SWI/SNF complex to this region. These changes cause acetylation of H4K16, demethylation of H3K27Me3 mark by JMJD3, and demethylation of CpG islands of the INK4-ARF locus; which finally allow production of the effective proteins [174].

In addition to the specific epigenetic events affecting certain genes, global epigenetic modifications also happen during cellular senescence. Human fibroblasts have decreased levels of histones during senescence. Generally cells have decreased H3K56ac, H3K9me2, H3K9Me3 and H4K20Me3 levels, whereas increased H3K9me1 and H4K20me2 levels while they are undergoing senescence [176]. These differences may explain gene expression alterations and increased genomic instability events during senescence. For example, telomere region, which is normally surrounded with heterochromatin marks, has decreased CpG methylation, H3K9Me3 and H4K20Me3 mark, H3 and H4 histone levels [176].

Senescent cells can acquire major alterations in their chromatin structures called senescence associated heterochromatin foci (SAHF) formation. These foci are highly compact chromatin regions with highly methylated DNA sequences and heterochromatin protein HP1, hypoacetylated histones, increased H3K9Me3 and H4K20Me3 marks, and enrichment of a specific histone variant MacroH2A (both H2AFY and H2AFY2) [176, 177]. The other critical components of the SAHF are histone chaperones ASF1 and HIRA [177]. Although the SAHF is not formed in all cases of cellular senescence events, it is thought that SAHF contributes to senescence processes mainly by maintaining senescence [178].

In addition to the INK4-ARF locus, many genes epigenetically activated during the senescence, including the genes favoring increase inflammatory signaling. Senescence associated secretory phenotype (SASP) is characterized with secretion of pro-inflammatory cytokines, such as IL-6 and IL-8 from senescent cells. It is found that during oncogene induced senescence RAS protein can cause proteosomal

degradation of KMT1C (G9a) and KMT1D (GLP) enzymes, which catalyze formation of transcription repressive H3K9Me1 and H3K9Me2 marks, respectively. Degradations of these epigenetic proteins activate transcription of cytokines, such as IL-6 and IL-8 during senescence [179, 180].

HDACs are important separate group of epigenetic players family regulating several events during senescence. HDAC1 HDAC5 and HDAC6 are down-regulated in senescent hematopoietic stem cells [181]. However, roles of HDAC1 in senescent seem context dependent, since over-expression of HDAC1 in HeLa cells cause induces senescence by activating p300/Sp1 interaction to induces transcription of senescence inducing genes such as p16 [182]. Over-expression of HDAC1 is associated with decreased liver regeneration capacity of old mice [183]. SIRT1, another HDAC using NAD^+ as cofactor that normally regulates many lipid metabolism events in the liver, is associated with regulation of lifespan [184]. SIRT1 level decrease during cell replication and its deficiency is associated with replicative senescence in human fibroblast cells [185]. In liver, over-expression of HDAC1 or SIRT1 causes hepatic steatosis [175, 186].

In addition to the protein components, there are also non-coding RNAs (miRNAs and lncRNAs) being produced by both tumor suppressors and oncogenes. Active p53 induces transcription of miR-34a, miR-34b, and miR-34c to down-regulate production of several proliferation-inducing proteins, such as E2F3, bcl-2, Met, CDK6, for induction of cellular senescence [187-189]. p53, p63, and p73 proteins can induce transcription of let-7, miR-143, miR-107, miR-16, miR-145, miR-134, miR-449a, miR-503, and miR-21 [190, 191]. c-myc try to evade the cellular senescence response by reducing gene expression of some miRNAs induced by p53 (e.g., miR-34a, let-7) and by inducing gene expression of miRNAs targeting mRNAs of some tumor suppressors (e.g., miR-17-92) [192, 193].

CHAPTER 2

OBJECTIVES AND RATIONALE

Liver cancer is ranked as the fifth most common cancer in men and seventh in female with more than 500.000 new cases and nearly the same number of deaths in each year [3]. The most common type of the liver cancer is HCC, 80% of the cases [3]. Hepatocellular carcinogenesis is a multi-step progressive disease [3, 44]. Main steps of the hepatocellular carcinogenesis are transition of the normal liver to fibrotic liver, generation of fatty liver, cirrhosis, dysplastic liver and cancerous liver (mainly hepatocellular carcinoma). Cancerous liver also progress from early HCC to advanced HCC, or well-differentiated HCC to poorly differentiated HCC [3].

The most important risk factor for HCC is cirrhosis that is present in 80 to 90% of patients with HCC [3]. During chronic hepatitis, the development of cirrhosis is associated with accelerated telomere shortening. Moreover, cirrhotic tissues exhibit strong senescence-associated β -galactosidase (SA- β -Gal) activity, suggesting that most hepatocytes in a cirrhotic liver display a senescent phenotype [44].

In most human HCC tumors TERT expression is positive, telomerase activity is high and telomere length is short, but stabilized. Thus, it appears that human HCC cells, as opposed to cirrhotic hepatocytes, acquire an immortal phenotype, although this has not yet been fully demonstrated. In favor of this suggestion, the genes encoding p53 and p16^{INK4A}, two major players in senescence control, are known to be inactivated by mutation and/or epigenetic silencing in nearly 50% of HCCs [169].

However, several important questions remain unanswered with regard to the relevance of senescence escape or immortality in human HCC.

- i)* a comprehensive list of genes associated with hepatocellular senescence and immortality is lacking;
- ii)* cellular processes associated with senescence-related changes in cirrhosis and HCC are not well-documented;
- iii)* timing of senescence-to-immortality transition during HCC development is unknown;
- iv)* the potential value of senescence-related gene signatures for the diagnosis and/or prognosis of HCC has not yet been assessed;
- v)* although several epigenetic alterations have been identified for HCC, a comprehensive study identifying transcriptionally deregulated epigenetic regulatory mechanisms as well as genetically altered epigenetic players of human hepatocellular carcinogenesis are still unknown.

A better understanding of these mechanisms could contribute significantly to the discovery of novel molecular targets for diagnosis and treatment of cirrhosis and

HCC diseases. Thus, in order to find answers of these remaining questions we prepared a study design (Figure 2.1). Details are explained in the materials and methods and results sections.

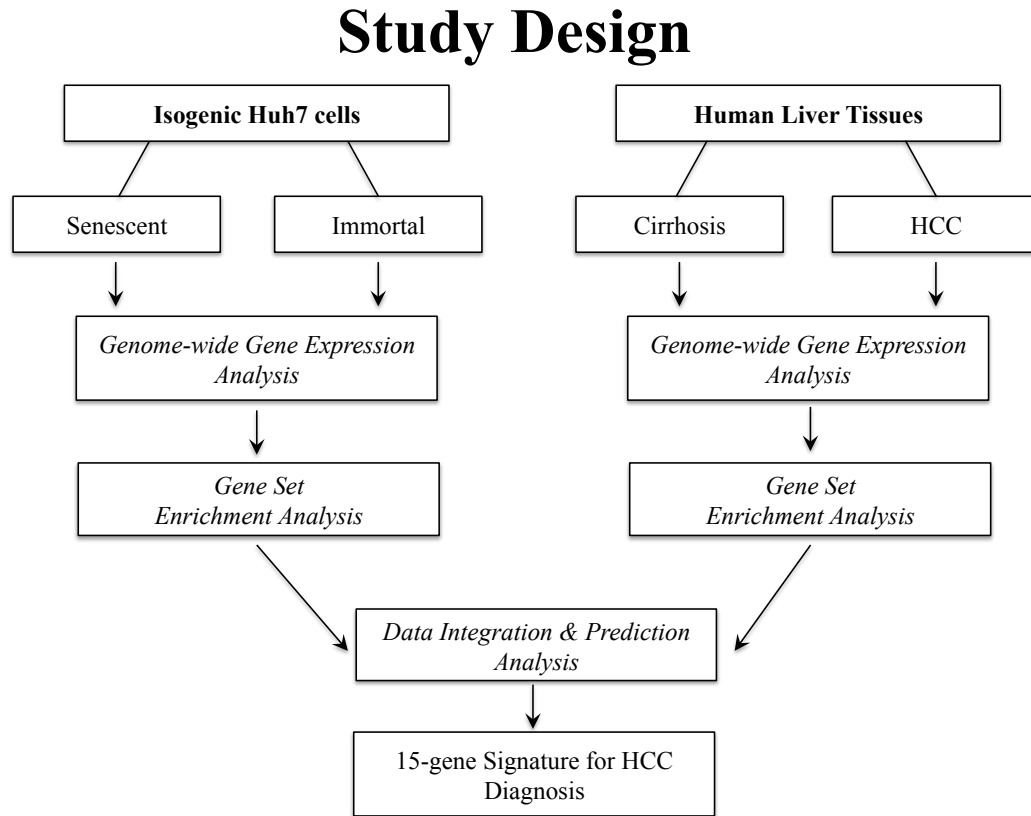


Figure 2.1: The basic study design to achieve the objectives of the thesis: Genome-wide transcriptional profiles of senescent and immortal clones generated from parental Huh7 cell line were determined with use of the microarray technology. These *in silico* samples were called as “the *in vitro* data set”. Same microarray gene expression profiling experiments were done to patient cirrhosis and HCC samples and collection of these samples were called as “the *in vivo* dataset”. Both *in vitro* and *in vivo* datasets were analyzed separately and in combination with different bioinformatics method, mainly via gene set enrichment analysis methods. Details are provided in materials and methods and results sections.

CHAPTER 3

MATERIALS AND METHODS

3.1 Cell culturing materials and methods

3.1.1 Standart cell culture materials and solutions of our laboratory

Dulbecco's modified Eagle's medium (DMEM), Roswell Park Memorial Institute (RPMI) 1640 medium, Opti-MEM medium, penicillin/streptomycin, trypsin-EDTA, fetal calf serum (FCS), and G-418 (neomycin) were from GIBCO (Invitrogen, Carlsbad, CA, USA). Tissue culture flasks, petri dishes, plates, cryotubes were purchased from Corning Life Sciences Inc. (USA). Serological pipettes were purchased from Costar Corp. (Cambridge, UK). Transfection reagent Oligofectamine was purchased from Invitrogen. Standard tissue culture solutions were prepared as follow:

- i) Complete DMEM/RPMI working medium: 10% FBS/FCS, 1% penicillin/streptomycin, 1% non-essential amino acid. Store at 4°C.
- ii) 10X Phosphate-buffered saline (PBS): 80 g NaCl, 2 g KCl, 14.4 g Na₂HPO₄, 2.4 g KH₂PO₄, pH 7.4. Store at 4°C.

3.1.2 Cryopreservation of stock cells

Cells were collected by 5 ml of complete medium following trypsin treatment and centrifuged at 1500 rpm for 3 min. After washing with 5 ml 1X PBS, cells were centrifuged at 1500 rpm for 3 min. The pellet was re-suspended in 1 ml of freezing medium, which contains complete growth medium supplemented with 10% DMSO, and transferred to cryotubes. Cells were kept at -20°C for 1 hour and transferred to -80°C for overnight and transferred to nitrogen tank for long-term storage.

3.1.3 Thawing of frozen cells

The vial of the frozen cell line was taken from the nitrogen tank, put into ice immediately, then placed into water bath at 37°C. The cells were re-suspended using a pipette, transferred to 15 ml falcon tube with 5 ml of medium, centrifuged at 1500 rpm for 3 min. to get rid of the DMSO. The pellet was then re-suspended in complete culture medium to be plated into suitable culture flask or plate. Cells were kept overnight in culture and culture medium was refreshed in the next day.

3.1.4 Parental cell lines and human hepatocytes

All cell lines were cultured at 37°C and 5% CO₂ conditions in suitable media supplemented with 10% FCS, 1% non-essential amino acids, 100 mg/ml penicillin/streptomycin. Huh7, HepG2, Hep3B, Hep3B-TR, Hep40, PLC/PRF-5, Mahlavu, Focus, SkHep1, FLC4 and MRC5 cell lines were cultured in complete

DMEM, whereas SNU182, SNU387, SNU398, SNU423, SNU449, SNU475 were cultivated in complete RPMI 1640 growing media. Freshly isolated human hepatocytes were obtained commercially (hNHEPS™- Human Hepatocytes, Lonza Group, Basel, Switzerland). The fibrolamellar HCC FLC4 cell line was provided by E. Galun (Hadassah), MRC-5 human embryonic lung fibroblast cells (at population doubling 45) were provided by R. Pedeux (Grenoble, France) and maintained in culture as previously described [194].

3.1.5 Senescent and immortal Huh7 clones

The establishment and culture conditions of senescence-programmed C3 and G12, and immortal C1 and G11 clones have been described previously [195]. Briefly, HCC-derived Huh7 cells were transfected with pcDNA3.1 (Invitrogen) or pEGFP-N2 (Clontech) vectors to obtain C1 and C3, and G11 and G12 clones, respectively. Following transfection, single cell-derived colonies were selected by G-418 sulfate (500 µg/ml; Gibco) treatment under low-density clonogenic conditions.

Senescence-programmed C3 and G12 clones proliferated stably until population doubling 80 (PD80) and PD90, respectively. Then, they entered senescence arrest as manifested by characteristic morphological changes, abundant senescence-associated beta-galactosidase (SA-β-Gal) staining and <5% 5-bromo-2'-deoxyuridine (BrdU) positivity after mitotic stimulation. Immortal C1 and G11 clones proliferated stably beyond PD140. For genome-wide expression studies, senescence-arrested C3 and G12 clones and immortal C1 and G11 clones were plated in triplicate onto 15-cm diameter petri dishes, left in culture for three days and collected for RNA extraction.

3.1.6 Small interfering RNA (siRNA) transfection materials and methods

Hep3B cells were transfected with specific ATAD2-siRNA1 (ACUAACACUGCUGAAGCUG), purchased from Eurogentec (Seraing, Belgium) using the method described by Caron et al. [196]. Briefly, 10⁵ cells were plated into

each well of a six-well plate, cultured for 24 h at 37°C and transfected twice (with 24 h intervals) with 10 µl of 0.02 mM ATAD2 siRNA1 using oligofectamine reagent (Invitrogen, Carlsbad, CA, USA). Cells were incubated with 200µM of siRNA and 4ul of oligofectamine transfection reagent for 6 hours without serum and antibiotics for transfection. Following 6 hours of incubation, 3X serum containing media were added to the media. Cells were maintained in standard culturing conditions for 72 hours. After 72h cells were subjected to protein extraction and western blotting experiments as described below.

3.1.7 Adriamycin treatment of Huh7 cells

Senescence was induced in Huh7 cells by Adriamycin (0.1 µM) treatment for three days as previously described [197]. Briefly, Adriamycin (Doxorubicin)- and DMSO vehicle control-treated cells were maintained in culture for three days. After three days cells were fixed by incubating with 4% formaldehyde for 15 min. in room temperature, subjected to SA-β-Gal staining as described below, counter stained with nuclear fast red (N3020, Sigma-Aldrich) and morphologically analyzed. After confirming the senescence induction by morphological examination and SA-β-Gal staining, cell lysates were subjected to western blotting analysis.

3.2 Senescence-associated beta-galactosidase (SA-β-Gal) staining materials and method

SA-β-Gal buffer contains: 40 mM citric acid/sodium phosphate buffer (pH 6.0), 5 mM potassium ferrocyanide, 5 mM potassium ferricyanide, 150 mM NaCl, 2 mM MgCl₂, 1 mg/ml X-gal (from 40 mg/ml stock solution) in ddH₂O. The pH of the solution was adjust to 6.0, and filtered before use.

For the SA-β-Gal staining cells were first rinsed twice using 1X PBS then fixed via keeping in 4% formaldehyde solution for 10 min. at room temperature. Following washing with 1X PBS for twice, cells were kept in SA-β-Gal buffer for

staining. Positive staining (presence of the blue colour) was observed using the light microscope after incubation of cells at 37°C in CO₂-free incubator for 12-16 hours.

3.3 RNA extraction, cDNA synthesis and polymerase chain reaction (PCR) materials and methods

3.3.1 RNA extraction and cDNA synthesis

NucleoSpin RNA II Kit (Macherey-Nagel) was used for isolation of the total RNA from cultured cells using the protocol provided by the manufacturer. RevertAid First Strand cDNA synthesis kit (Fermentas; Leon-Rot, Germany) was used for first-strand cDNA synthesis using 2 µg of DNase I-treated total RNA of each sample. cDNAs were stored at -20°C. cDNAs were subjected to semi-quantitative and quantitative reverse transcriptase PCR amplifications using specific primers. PCR reagents were obtained from Fermentas. DyNAmo HS SYBR Green qPCR Kit F-410L, master mix solution for qPCR reactions, was ordered from Finnzymes (Finland).

3.3.2 Polymerase chain reaction (PCR) materials and methods

3.3.2.1 Semi-quantitative and quantitative real-time RT PCR assays of ATAD2 experiments

Thermal cycler conditions of the PCR experiments were: 95°C for 5 min; 45 cycles of 95°C for 30 sec, at 60°C for 30 sec, at 72°C for 30sec; and a final extension at 72°C for 5 min.

Quantitative expression analyses were performed using DyNAmo HS SYBR Green qPCR Kit F-410 (Finnzymes) on Mx 3005P real-time RT-PCR machine (Stratagene).

For PCR experiments of ATAD2 transcript 5'-AGG CTC ATT GGA AAA ACC T-3' sequences were used as forwards primer; and 5'-CCT GCG GAA GAT AAT CGG TA-3' sequences were used as reverse primer. GAPDH was tested as a housekeeping control gene using the following primers: forward: 5'-GGC TGA GAA CGG GAA GCT TGT CAT-3'; reverse: 5'-CAG CCT TCT CCA TGG TGG TGA AGA-3'. All primers were purchased from IONTEK (Istanbul, Turkey).

2 µl cDNA for each sample were used in 20 ul final volume of PCR mixture. Expression levels were calculated using the following formula:

$R = (E_{\text{target}})^{\Delta C_{\text{t}}_{\text{target}}(\text{control-sample})} / (E_{\text{ref}})^{\Delta C_{\text{t}}_{\text{ref}}(\text{control-sample})}$. In the above formula E_{target} and E_{ref} represent the primer efficiencies for target and reference genes, respectively. PCR efficiency values of the indicated primers were 2.0. All experiments were performed in triplicates. GAPDH was used as internal control in qRT-PCR experiments.

3.3.2.2 Agarose gel electrophoresis materials and methods

Electrophoresis solutions were prepared and used as follow:

- i)* 50X Tris-acetic acid-EDTA (TAE): 2 M Tris-acetate, 50 mM EDTA pH 8.5. 50X solutions were diluted to 1X for working solution.
- ii)* Ethidium bromide (EtBr): 10 mg/mL in water solutions were used as stock solution; 30 ng/mL solutions were used as working solution for EtBr.
- iii)* 6X Gel loading dye solution: 10 mM Tris-HCl (pH 7.6), 0.03% bromophenol blue, 0.03% xylene cyanol, 60% glycerol, 60mM EDTA (0.5M pH 8.0).

3.3.2.3 Agarose gel electrophoresis of DNA

DNA fragments were separated with 2.0% agarose gel by horizontal electrophoresis. Agarose gels were prepared by heating agarose diluted with 1X TAE buffer in microwave. EtBr was added to a final concentration of 30 mg/mL. The DNA samples were mixed with 6X bromo-phenol blue loading buffer and loaded onto gels. The gels were run at 100-120 V at room temperature until the fragments were adequately separated. Nucleic acids were visualized under ultraviolet light.

3.4 Western blotting materials and methods

3.4.1 Western blotting materials and solutions

NuPAGE pre-cast 3-8% Tris-Acetate gels, running and transfer buffers were purchased from Invitrogen. 4X sample loading buffer, 10X denaturing agent used in immunoblotting were also from Invitrogen. Solutions used in western blotting experiments were prepared as following:

- i)* RIPA lysis buffer: 10 mM Tris-HCl (pH 7.6), 5 mM EDTA, 50 mM NaCl, 30 mM sodium pyrophosphate, 50 mM sodium fluoride, 100 mM sodium orthovanadate, 1% TritonX-100 and 1X protease inhibitor complex in double-distilled water.
- ii)* 10X Tris buffered saline (TBS): 12.2 g Trisma base, 87.8 g NaCl in 1 liter ddH₂O, pH 7.8.
- iii)* TBS-tween (TBS-T): 0.2% Tween-20 was dissolved in 1x TBS.
- iv)* Ponceau S: 0.1% (w/v) Ponceau, 5 % (v/v) acetic acid in double-distilled water.
- v)* Blocking solution: 5% (w/v) non-fat dry milk/bovine serum albumin in 0.2% TBS-T.

3.4.2 Western blotting

ATAD2 protein expression was compared by western blot analysis of cell lysates. Cells were lysed with Radio-Immunoprecipitation Assay (RIPA) Buffer (10 mM Tris-HCl, pH 7.6, 5 mM EDTA, 50 mM NaCl, 30 mM sodium pyrophosphate, 50 mM sodium fluoride, 100 mM sodium orthovanadate, 1% TritonX-100 and 1X protease inhibitor complex (Roche, Indianapolis, USA). Concentrations of protein lysates were measured by the conventional Bradford assay utilizing spectrophotometer at 595 nm. Sample protein concentrations were normalized in accordance with bovine serum albumin (BSA) protein of a known concentration. 30 µg of total proteins were subjected to gel electrophoresis using NuPAGE system with 3-8% Tris-Acetate gels and buffers. Proteins were wet-transferred onto HyBond ECL nitrocellulose membranes. The blocking was performed for 1 hr at room temperature with 5% dry milk in TBS-T solution. Membranes were incubated with the primary antibodies overnight at +4°C. Following primary antibody incubations and extensive washing with TBS-T, secondary antibodies conjugated with horse-radish peroxidase (HRP) were incubated 1 hour at room temperature. After an additional wash of half an hour, chemiluminescent reaction was detected using ECL+ western blot detection kit (Amersham, UK), according to the manufacturer's protocols. X-ray films were exposed to the emitted chemiluminescence, duration depends on the specific antibody. An anti-ATAD2 rabbit polyclonal antibody (Sigma; cat. no: HPA019860) was used at 1:500 dilution as the primary antibody. Anti-calnexin rabbit polyclonal antibody (Sigma; cat. no: C4731) was used at 1:10000 dilution for the loading control.

3.5 Cirrhosis and HCC tissue samples

Liver cirrhosis and HCC samples were collected from two medical centers in Turkey (Table 3.1). Ethical study protocols of Ankara and Dokuz Eylul Universities were followed and approved by these universities after taking written consents from each patient before experiments. Tissue samples were snap frozen in liquid nitrogen and stored at -80°C until use. Frozen tissues were cut into 20 µm thick slices, and scraped into microtubes for RNA extraction. Two 6 µm tissue slices were also cut for

pathological examination. Total RNAs from each sample were isolated using the materials and methods described above. RNA samples were analyzed using Agilent Bioanalyzer, as performed to cell line samples. Samples with RNA integrity number (RIN) > 6.5 were used for gene expression profiling studies.

Table 3.1: Patient samples (*in vivo* dataset) used in this study: The *in vivo* cirrhosis and HCC dataset was deposited to GEO and publically available with accession number of GSE17548. HBV: Hepatitis B virus. HCV: Hepatitis C virus. N.a: Not available. WD HCC: Well differentiated hepatocellular carcinoma. MD HCC: Moderately differentiated hepatocellular carcinoma.

Dataset	Country	Sample ID	Array Code	Age	Gender	Etiology	Diagnosis
GEO: GSE17548	Turkey	GSM437492	TR-1N	45	male	HBV	cirrhosis
GEO: GSE17548	Turkey	GSM437493	TR-1T	45	male	HBV	WD HCC
GEO: GSE17548	Turkey	GSM437466	TR-2N	52	male	HBV	Cirrhosis
GEO: GSE17548	Turkey	SM437467	TR-2T	52	male	HBV	HCC
GEO: GSE17548	Turkey	GSM437461	TR-3T	62	male	HCV	HCC
GEO: GSE17548	Turkey	GSM437473	TR-4N	60	male	HBV	Cirrhosis
GEO: GSE17548	Turkey	GSM437474	TR-4T	60	male	HBV	HCC
GEO: GSE17548	Turkey	GSM437483	TR-5T	n.a.	male	n.a.	HCC
GEO: GSE17548	Turkey	GSM437457	TR-6N	50	male	HBV	Cirrhosis
GEO: GSE17548	Turkey	GSM437458	TR-6T	50	male	HBV	HCC
GEO: GSE17548	Turkey	GSM437463	TR-21N	56	male	HBV	Cirrhosis
GEO: GSE17548	Turkey	GSM437464	TR-21T	56	male	HBV	Focal HCC
GEO: GSE17548	Turkey	GSM437469	TR-22N	44	female	n.a.	MD HCC
GEO: GSE17548	Turkey	GSM437491	TR-23T	65	male	HBV	WD HCC
GEO: GSE17548	Turkey	GSM437488	TR-24N	52	female	HCV	Cirrhosis
GEO: GSE17548	Turkey	GSM437489	TR-24T	52	female	HCV	MD HCC
GEO: GSE17548	Turkey	GSM437484	TR-25N	n.a.	male	n.a.	Cirrhosis
GEO: GSE17548	Turkey	GSM437471	TR-26N	64	male	HCV	Cirrhosis
GEO: GSE17548	Turkey	GSM437477	TR-27N	41	male	HBV+HDV	Cirrhosis
GEO: GSE17548	Turkey	GSM437487	TR-7T	69	male	HBV	MD HCC
GEO: GSE17548	Turkey	GSM437486	TR-28N	48	female	HBV	Cirrhosis
GEO: GSE17548	Turkey	GSM437481	TR-29N	52	male	HBV	Cirrhosis
GEO: GSE17548	Turkey	GSM437480	TR-210N	48	male	HBV	Cirrhosis
GEO: GSE17548	Turkey	GSM437479	TR-211N	50	male	HBV	Cirrhosis
GEO: GSE17548	Turkey	GSM437472	TR-212N	n.a.	female	n.a.	Cirrhosis
GEO: GSE17548	Turkey	GSM437476	TR-9T	62	male	HCV	MD HCC
GEO: GSE17548	Turkey	GSM437478	TR-10T	n.a.	male	HBV	MD HCC
GEO: GSE17548	Turkey	GSM437465	TR-11T	n.a.	male	n.a.	HCC
GEO: GSE17548	Turkey	GSM437459	TR-210T	49	male	HBV	MD HCC
GEO: GSE17548	Turkey	GSM437468	TR-211T	59	male	HBV	MD HCC

3.6 Genome-wide gene expression profiling of samples

Affymetrix platform with GeneChip Human Genome U133 Plus 2.0 arrays were used for microarray analysis of both cell and tissue RNA samples, following manufacturer instructions. GeneChip Operating Software (Affymetrix) was used to collect and store the microarray data. CEL files were uploaded to RMAExpress software to assess the quality of the arrays at the image level (<http://rmaexpress.bmbolstad.com>). Quality assessment of the Affymetrix datasets

was performed using affyPLM (<http://www.bioconductor.org>). NUSE and RLE plots were drawn and outliers with high deviation from the average probe intensity value were excluded from further analyses.

The microarray data reported in this thesis have been deposited in the Gene Expression Omnibus (GEO) database under accession numbers of GSE17546 (Huh7 clones) and GSE17548 (cirrhosis and HCC tumor samples). All cell line clones, 15 cirrhosis and 15 HCC tumor samples passed RNA quality control (RNA Integrity Number, RIN>6.5) and microarray quality control tests.

RMA normalization and class comparison analyses were performed using BRB-ArrayTools developed by Dr. Richard Simon and BRB-ArrayTools Development Team (<http://linus.nci.nih.gov/BRB-ArrayTools.html>; Version 4.2.0).

3.7 Other Microarray Datasets

Two independent microarray datasets (GSE6764 and GSE19665) were downloaded from Gene Expression Omnibus (GEO) database (<http://www.ncbi.nlm.nih.gov/geo>) and analyzed by BRB ArrayTools after normalization with RMA method.

3.8 Gene Set Enrichment Analyzes (GSEA)

3.8.1 Basic GSEA materials and methods

Gene set enrichment analyses (GSEA) were performed using GSEA program of the Broad Institute [198]. Whole genome gene expression data of each sample was used for GSEA experiments. C2_ALL curated gene list of Molecular Signature Database (MSigDB), which contains gene lists from online pathway databases, such as Reactome (www.reactome.org) and Biocarta (www.biocarta.com), genetic perturbation study gene lists of publications in PubMed

(<http://www.ncbi.nlm.nih.gov/pubmed/>), was used in GSEA studies.

3.8.2 Interpretation of GSEA results of *in vitro* and *in vivo* datasets

As results of the GSEA analyzes, GSEA program provided both summarized (Figure 3.1) and detailed results of the analyzes. The summarized results of the analyzes provided us the total number of enriched and significantly enriched ($p < 0.01$, $p < 0.05$ or False Discovery Rate < 0.25) gene sets of each phenotype. The detail enrichment results tables of each dataset (Figure 3.2a) provided detailed scores of each gene set analyzed (3263 gene sets for each dataset in total). The further detailed results of each gene sets were also provided by the program via enrichment plot figures (Figure 3.2b).

3.8.3 Integration and analyzes of the GSEA data to determine 74 commonly enriched gene sets of the two datasets

The total lists of enriched gene sets of each phenotype (2165 gene sets for senescent, 1098 gene sets for immortal, 2017 gene sets for cirrhosis, and 1246 gene sets for HCC) were integrated in four possible combinations and analyzed using the Matlab© in order to determine commonly enriched gene sets of the phenotypes (Figure 3.3). In order to that, enrichment result tables of each phenotype were integrated using the method described in table 3.2 and GSEA data of the commonly enriched gene sets of the four possible combinations (lists of commonly enriched gene sets in both senescence and cirrhosis samples, both immortal and cirrhosis samples, both senescence and HCC samples, and both immortal and HCC samples) were determined. The list of the 74 gene sets that significantly ($p < 0.05$) enriched were identified by sorting these results. Pearson's correlation coefficients of these correlations were calculated using Matlab© and Fisher's exact test was performed using VassarStats (Vassarstats.net).

a

Enrichment in phenotype: Immortal (6 samples)

- 1098 / 3263 gene sets are upregulated in phenotype **Immortal**
- 0 gene sets are significant at FDR < 25%
- 39 gene sets are significantly enriched at nominal pvalue < 1%
- 113 gene sets are significantly enriched at nominal pvalue < 5%
- [Snapshot](#) of enrichment results
- Detailed [enrichment results in html](#) format
- Detailed [enrichment results in excel](#) format (tab delimited text)
- [Guide to](#) interpret results

Enrichment in phenotype: Senescent (6 samples)

- 2165 / 3263 gene sets are upregulated in phenotype **Senescent**
- 22 gene sets are significant at FDR < 25%
- 213 gene sets are significantly enriched at nominal pvalue < 1%
- 598 gene sets are significantly enriched at nominal pvalue < 5%
- [Snapshot](#) of enrichment results
- Detailed [enrichment results in html](#) format
- Detailed [enrichment results in excel](#) format (tab delimited text)
- [Guide to](#) interpret results

b

Enrichment in phenotype: HCC (15 samples)

- 1246 / 3263 gene sets are upregulated in phenotype **HCC**
- 57 gene sets are significant at FDR < 25%
- 53 gene sets are significantly enriched at nominal pvalue < 1%
- 189 gene sets are significantly enriched at nominal pvalue < 5%
- [Snapshot](#) of enrichment results
- Detailed [enrichment results in html](#) format
- Detailed [enrichment results in excel](#) format (tab delimited text)
- [Guide to](#) interpret results

Enrichment in phenotype: CIRRHOSIS (15 samples)

- 2017 / 3263 gene sets are upregulated in phenotype **CIRRHOSIS**
- 0 gene sets are significantly enriched at FDR < 25%
- 21 gene sets are significantly enriched at nominal pvalue < 1%
- 161 gene sets are significantly enriched at nominal pvalue < 5%
- [Snapshot](#) of enrichment results
- Detailed [enrichment results in html](#) format
- Detailed [enrichment results in excel](#) format (tab delimited text)
- [Guide to](#) interpret results

Figure 3.1: Summarized GSEA results of *in vitro* and *in vivo* datasets: a) GSEA experiment of the samples of the *in vitro* dataset (immortal and senescence samples) resulted with enrichment of 1098 gene sets in the immortal phenotype and 2165 gene sets in the senescent phenotype. 113 of 1098 gene sets and 598 of 2165 gene sets were enriched significantly ($p < 0.05$) in the *in vitro* dataset. b) GSEA experiment of the samples of the *in vivo* dataset (HCC and cirrhosis samples) resulted with enrichment of 1246 gene sets in the immortal phenotype and 2017 gene sets in the senescent phenotype. 189 of 1246 gene sets and 161 of 2017 gene sets were enriched significantly ($p < 0.05$) in the *in vivo* dataset.

a

	GS follow link to MSigDB	GS DETAILS	SIZE	ES	NES	NOM p-val	FDR q-val	FWER p-val	RANK AT MAX	LEADING EDGE
1	REACTOME_RNA_POLYMERASE_III_TRANSCRIPTION_INITIATION	Details ...	29	0.55	1.79	0.012	0.946	0.521	7297	tags=69%, list=35%, signal=107%
2	REACTOME_RNA_POLYMERASE_I_CHAIN_ELONGATION	Details ...	31	0.63	1.76	0.002	0.707	0.633	3838	tags=52%, list=19%, signal=63%
3	REACTOME_RNA_POLYMERASE_III_TRANSCRIPTION	Details ...	34	0.50	1.74	0.015	0.619	0.705	7297	tags=62%, list=35%, signal=95%
4	ELLWOOD_MYC_TARGETS_UP	Details ...	11	0.71	1.74	0.000	0.479	0.717	601	tags=36%, list=3%, signal=37%
5	KAUFFMANN_DNA_REPAIR_GENES	Details ...	203	0.60	1.73	0.004	0.447	0.765	4990	tags=54%, list=24%, signal=70%
6	KEGG_NON_HOMOLOGOUS_END_JOINING	Details ...	13	0.72	1.72	0.004	0.414	0.790	767	tags=23%, list=4%, signal=24%
7	REACTOME_BASE_EXCISION_REPAIR	Details ...	17	0.64	1.71	0.014	0.384	0.807	4664	tags=59%, list=23%, signal=76%
8	KEGG_VALINE_LEUCINE_AND_ISOLEUCINE_BIOSYNTHESIS	Details ...	10	0.75	1.70	0.006	0.391	0.832	3391	tags=60%, list=16%, signal=72%
9	IVANOVA_HEMATOPOIESIS_STEM_CELL_SHORT_TERM	Details ...	7	0.71	1.70	0.010	0.369	0.848	2957	tags=43%, list=14%, signal=50%
10	WANG_RECURRENT_LIVER_CANCER_UP	Details ...	16	0.70	1.69	0.000	0.348	0.858	3956	tags=50%, list=19%, signal=62%

b

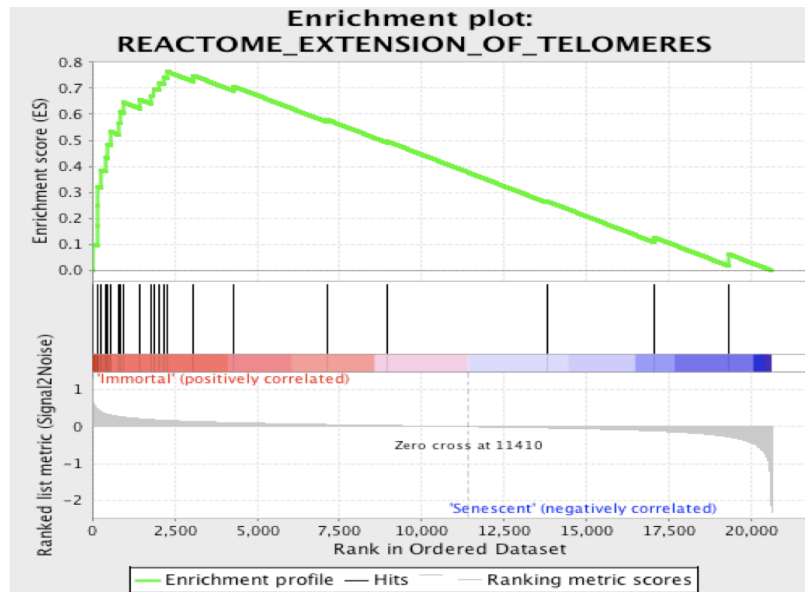


Figure 3.2: Examples of detailed outputs of GSEA experiments: a) Part of the detailed enrichment results table of the HCC phenotype: List of the top ten enriched gene sets based on their normalized enrichment scores (NES) are seen in the enrichment results table. GS Details (link of the details of the enrichment score of the gene set, where enrichment plot figure can be found), Size (number of genes in the gene set), ES (enrichment score of the gene set), NES (normalized enrichment score of the gene set), NOM p-val (nominal p-value score of the gene set), FDR q-val (false discovery rate value of the gene set), FWER p-value (family-wise error rate, which represents score of a more stringent FDR value), Rank at max (rank of the gene set among other gene sets analyzed based on its NES score), Leading Edge (percentage values of the genes contributing the enrichment score of a

gene set) results of each enriched gene set are provided in this table. b) Enrichment plot of a typical significantly enriched gene set: Enrichment plots (EP) are one of the results of GSEA experiments, which provide detailed information on different aspects. The y-axis of an EP graphic shows enrichment scores (ES), while x-axis shows distributions of individual genes of the gene set on the two phenotypes analyzed. Thus, black bars represent a gene and green line shows enrichment profile of genes of the gene set. Accumulation of the green line to one of the phenotypes determines both number and the sign (positive or negative) of the ES of a gene set. The ranked list metric score at the bottom of the enrichment plot figure shows rank of each gene among the whole genes in the total analysis. This rank is one of the criteria that determine if a gene is a core-enriched gene, or not.

3.8.4 Leading Edge Analysis (LEA)

Leading Edge Analyses (LEA) were performed on selected DNA repair and cell cycle gene sets using GSEA results and GSEA desktop software. Similarities of DNA repair and cell cycle gene sets were determined based on number of common core enriched genes in each gene set in the analysis.

3.9 Cluster Analysis

Cluster 3.0 software [199] was used to assess unsupervised clustering of datasets. First, data were adjusted by centering genes and arrays separately based on mean values, and then the average linkage clustering was applied to genes and arrays using a correlation (uncentered) similarity metric. Cluster files were visualized by Java Treeview [200].

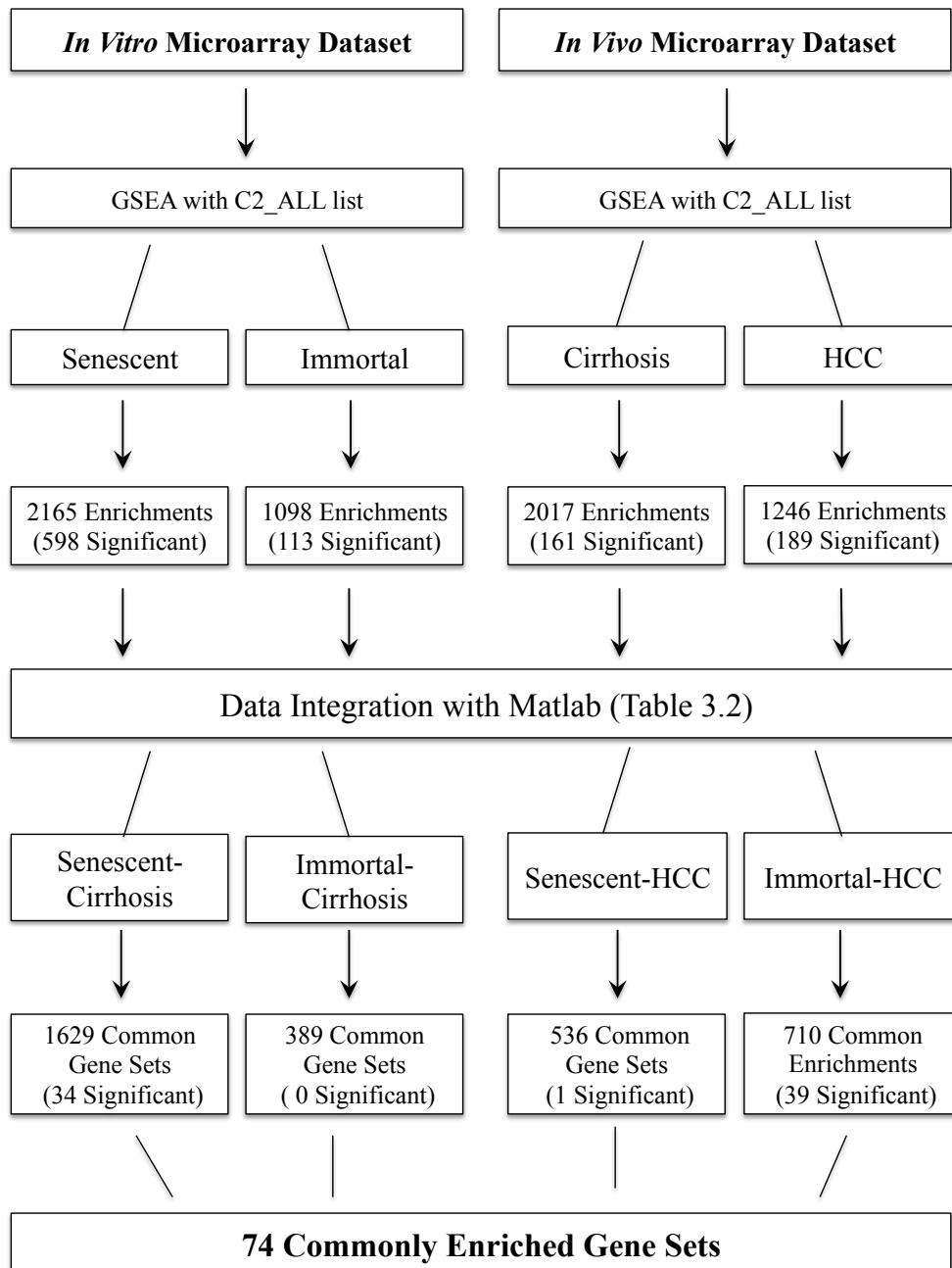


Figure 3.3: Steps of the method used for identification of 74 commonly enriched gene sets: In order to identify 74 significantly ($p < 0.05$) and commonly enriched gene sets in samples of the *in vitro* and *in vivo* datasets, we first obtained GSEA results of the *in vitro* (senescent and immortal samples) and *in vivo* (cirrhosis and HCC samples) microarray datasets. Results of the GSEA experiments were integrated using Matlab functions (details in Table 3.2). Results of the analyzes using Matlab provided a list of 74 (34 gene sets in both senescent and cirrhosis samples, 39 gene sets in both immortal and HCC samples, 1 gene set in both senescent and HCC samples) significantly enriched gene sets. Significance value of this result was calculated with the Fisher exact test method.

Table 3.2: Pseudocode of the method used during Matlab analyzes: Enrichment results of the each phenotype (senescent, immortal, cirrhosis and HCC) were used as inputs for the analyzes. Common gene sets were identified using the *intersect* command of the Matlab. Enrichment result tables of shared enriched gene sets of the phenotypes were determined using the *xls write* command. $p < 0.05$ filter was applied to determine the final list of 74 gene sets. Correlation value was determined using the enrichment scores of the dataset. Fisher exact test was also performed to test the result.

Data Integration of GSEA Results of <i>In Vitro</i> and <i>In Vivo</i> Datasets in Matlab and Fischer's Exact Test of these Results
<i>Input:</i> GSEA enrichment result tables of Senescent, Immortal, Cirrhosis, HCC phenotypes
<i>Intersect</i> (based on GSEA ids): Senescent with Cirrhosis
<i>xls write:</i> columns ES, NES, NOM p-val, FDR q-val
<i>Intersect</i> (based on GSEA ids): Immortal with Cirrhosis
<i>xls write:</i> columns ES, NES, NOM p-val, FDR q-val
<i>Intersect</i> (based on GSEA ids): Senescent with HCC
<i>xls write:</i> columns ES, NES, NOM p-val, FDR q-val
<i>Intersect</i> (based on GSEA ids): Immortal with HCC
<i>xls write:</i> columns ES, NES, NOM p-val, FDR q-val
<i>Filter</i> (based on significant p values)
Perform Fisher's exact test
Calculate correlation

3.10 Generation and Validation of a Senescence-based Genomic Classifier

A senescence-based genomic classifier associated with differential diagnosis of HCC from cirrhosis was generated in BRB Array Tools by Prediction Analysis of Microarrays [201] using data reported by Wurmbach et al. [202] as a “training set”. The resulting classifier was tested using the nearest template prediction (NTP) method [203] on a validation set constructed by combining data reported here for Turkish patients with data from Deng et al. [204] for Japanese patients. Nearest template prediction was performed using NTP module [203] of GenePattern program (<http://www.broadinstitute.org/cancer/software/genepattern/>) using default parameters of the module. The final image was generated using HeatMapImage module of the GenePattern and the output of the NTP.

3.11 Generating Epigenetic Regulatory (EpiReg) Gene lists

In order to create the total EpiReg gene list, which contains already identified histones, histone chaperones, chromatin remodelers, histone code readers and/or writers epigenetic regulatory genes, as well as putative epigenetic regulatory genes bearing well-characterized epigenetic regulatory protein domain sequences such as SET, JMJC, and PHD, I used QuickGO (<http://www.ebi.ac.uk/QuickGO/>) gene ontology website, GeneCards website (<http://www.genecards.org/>), MsigDB (Molecular Signature Database) (<http://www.broadinstitute.org/gsea/msigdb/>) and the current literature [205, 206]. Affymetrix Human GeneChip U133 plus 2.0 probe set ids, which were taken from the NetAffx website (<http://www.affymetrix.com/analysis/index.affx>) were also included for each gene in the total EpiReg list.

Members of the total EpiReg gene list were used either individually or in different combinations during the rest of analyzes. EpiReg gene sets used during Gene Set Enrichment Analysis (GSEA) analyzes were generated from the total EpiReg gene list. These gene sets comprise of two major gene set classes: EpiReg group gene sets, which include gene lists of certain epigenetic regulatory functions such as histone methyltransferases (HMTs), histone deacetylases (HDACs), and the EpiReg Domain gene sets, which include genes having well-characterized epigenetic regulatory protein domain sequences such as SET, JMJC, PHD, Ankyrin repeat in different gene sets. Both group and domain EpiReg gene sets also contain uncharacterized, putative EpiReg genes based on their conserved epigenetic regulatory domains.

3.12 Histone Mutation Analyzes

3.12.1 Samples of the histone mutation search experiments

32 samples used during histone N-terminal tail encoding mutation investigations were part of the samples used in another study [207].

3.12.2 PCR experiments of the Histone mutation study

AccuPrime GC-Rich DNA Polymerase (Cat No: 12337-016, Invitrogen Life Technologies Corp.) was used for PCR reactions. PCR ingredients for one sample: 10 ul of 5X AccuPrime GC-Rich Buffer A, 5 ul of 5X Q-Solution (Qiagen), 2 ul of forward and reverse primers, 0.4 ul of AccuPrime Taq, 27.6 ul of ddH₂O, 3 ul of DNA (50 ng/ul). PCR reaction: (3 min. at 95°C) 1 cycle, (30 sec. at 95°C, 1 min. at 58°C, 2 min. at 72°C) 32 cycle, (10 min. at 72°C) 1 cycle.

Primers used for mutation analyses of histone variants were:

CENPA Forward: 5'-CCCAGAAGCCAGCCTTTC-3'

CENPA Reverse: 5'-GCCTCGGTTTTCTCCTCTTC-3'

H3F3A Forward: 5'-TTGATTTTTCAATGCTGGTAGG-3'

H3F3A Reverse: 5'-CAAGAGAGACTTTGTCCCATTTTT-3'

H3F3B Forward: 5'-GGGGCGTCTTTCTTAGGTG-3'

H3F3B Reverse: 5'-AGCAGGGGAGGAGTGAGC-3'

H2AFZ Forward: 5'-CGCCGCCTTGGTAATTCTAT-3'

H2AFZ Reverse: 5'-GGAAATGCAAAGAAAACATCA-3'

H2AFV Forward: 5'-GGGATCACCTACATATTGTAACTACC-3'

H2AFV Reverse: 5'-AATAATGTAATGACAGCATGGATTC-3'

H2AFY Forward: 5'-CTCGCCTTCACAGTGTGCT-3'

H2AFY Reverse: 5'-TGGTGTCTGGGTTGACTGAG-3'

H2AFY2 Forward: 5'-AGGCCACTGTGTCAGCAAG-3'

H2AFY2 Reverse: 5'-CCTGCCAGGTACTCAATGAC-3'

3.12.3 Agarose Gel Electrophoresis and Sequencing

5 ul of PCR product loaded to 2% agarose gel (standard DNA grade agarose Cat. No: D5-E, Euromedex in 1X TAE buffer) with 5 ul of 1kb Plus Ladder (Cat. No: 10787-018, Invitrogen Life Technologies Corp.). Rest of the PCR products were sequenced by GATC Biotech (GATC Biotech. Konstanz, Germany) with Sanger sequencing method.

Table 3.3: Genomic DNA samples of the histone variant sequencing experiments:

SEQUENCING CODE	ORIGINAL NAME	COUNTRY
1	J8T	JAPAN
3	T37	MOZAMBIQUE
4	C14	CHINA
5	T80	GERMANY
6	C4	CHINA
7	T51	MOZAMBIQUE
8	K9T	MOZAMBIQUE
9	J5T	JAPAN
11	C11	CHINA
14	T70	FRANCE
17	J2T	JAPAN
18	J1T	JAPAN
19	J9T	JAPAN
20	C5	CHINA
21	J3T	JAPAN
22	T75	GERMANY
23	J7T	JAPAN
24	I2T	ISRAEL
26	C8	CHINA
27	T76	GERMANY
28	C1	CHINA
29	C2	CHINA
30	J10T	JAPAN
31	T69	FRANCE
32	T39	SWAZILAND
33	C9	CHINA
34	G3	GERMANY
35	J6T	JAPAN
36	T67	JAPAN
37	I3T	ISRAEL
48	C7	CHINA
49	T9	MOZAMBIQUE

3.12.4 Restriction Enzyme Digestion

PCR products of selected samples were digested with EarI (Cat. No: R0528S, New England Biolabs Inc.) and MboII (Cat. No: R0148S, New England Biolabs Inc.) restriction enzymes at 37°C according to instructions of the manufacturer and run at 2% agarose gel.

3.12.5 Analyzing Sequencing Data

Sequencing results were batch analyzed with ClustalW2 multiple sequence alignment tool (<http://www.ebi.ac.uk/Tools/msa/clustalw2/>), and manually if necessary. Wild type sequences were retrieved from UCSC genome browser database (<http://genome.ucsc.edu/>).

CHAPTER 4

RESULTS

4.1 Genome-Wide Transcriptional Reorganization Associated with Senescence-to-Immortality Switch during Human Hepatocellular Carcinogenesis

4.1.1 Top 100 deregulated genes of *in vitro* and *in vivo* datasets

We determined whole-genome gene expression profiles of four independently established Huh7 clones (two different senescent clones and two different immortal clones) with three independent biological replicates from each clone. Thus, a total of 12 different whole-genome gene expression signatures were obtained in the *in vitro* dataset. In order to obtain whole-genome gene expression profiles of *in vivo* cirrhosis

and HCC samples, we used tissue samples of 15 cirrhosis and 15 HCC samples as our *in vivo* dataset (Table 3.1).

As a first step of our analyses, we first determined list of the genes with the highest gene expression differences in each phenotype of the two datasets. In order to do that, first the signal intensities of 54.675 (54K) probe sets were collapsed to gene symbols to be able to work with genes instead of probe sets for the rest of the analyses. After collapsing the 54K probe sets to 20.606 genes, genes were rank ordered based on their average gene expression values in each phenotype. Heatmap figures of the 100 genes in the rank ordered lists (50 for each phenotype of a dataset) were generated for each datasets (Fig. 4.1a).

The heatmap figures indicate that samples of the *in vitro* data are highly homogenous for each phenotype, which is plausible since replicate samples of the each phenotype were obtained from certain clones of the Huh7 cell line. On the other hand, samples of the *in vivo* dataset, especially HCC samples, have heterogenous gene expression profiles based on gene expression profiles of the top 100 genes. This situation might also be expected, since the samples of the *in vivo* dataset have different etiologies, such as presence of HBV or HCV induced samples in the HCC phenotype.

The lists of the 100 genes for each dataset do not display high similarity, either. Among the list of nearly 200 genes in total only two genes, MND1 and TMEM27, are common in both datasets (Fig. 4.1). In addition to that, even though the TERT gene, which encode the protein part of the telomerase enzyme as a critical

player of the cellular immortalization processes, is among the highly expressed genes in the immortal samples as indicative of a molecular proof of our samples; the TERT gene is not among the 100 genes of the *in vivo* dataset. Thus, the results of the list of the highly deregulated genes indicate that, understanding the mechanisms of the senescence escape related processes needs extensive analyses, since it is not possible via the list of the genes with highly deregulated gene expressions.

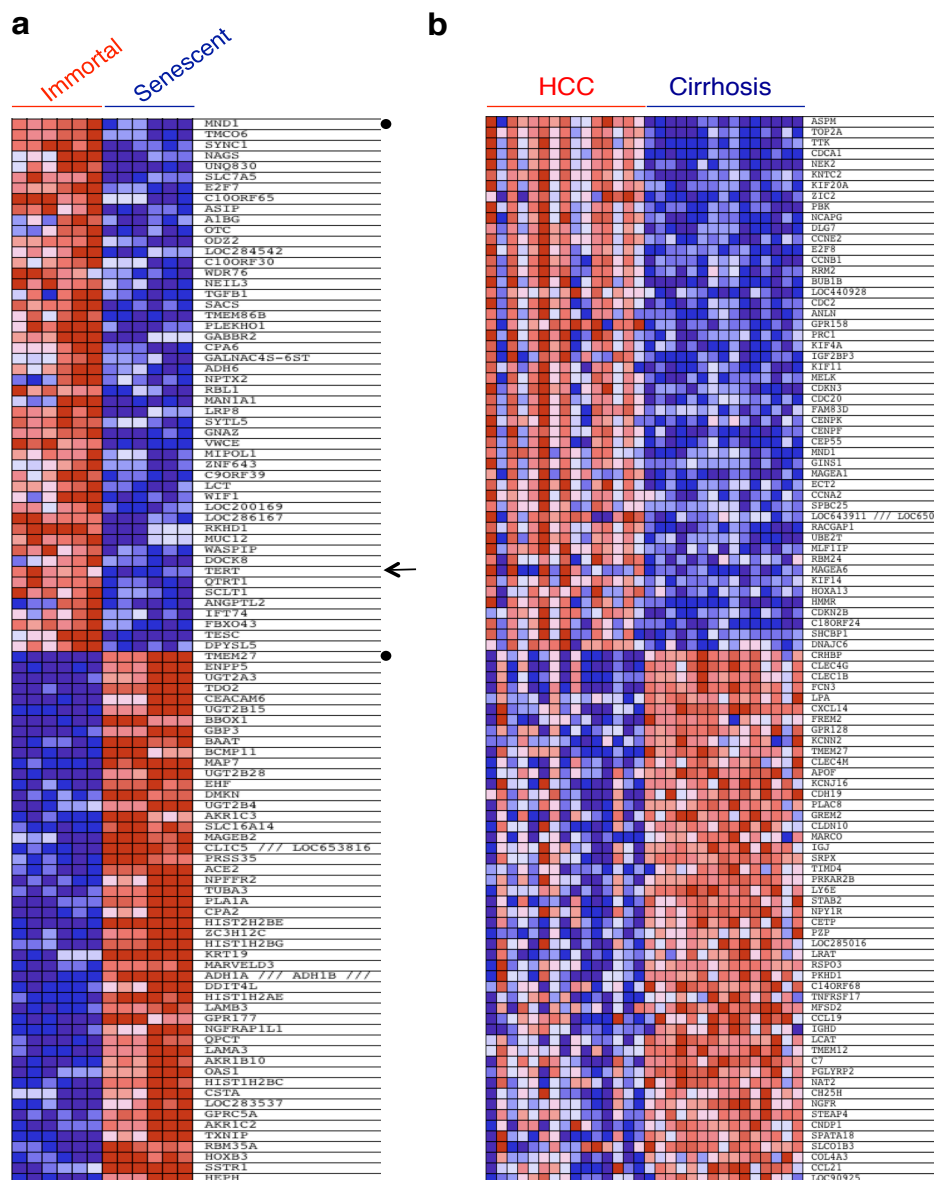


Figure 4.1: Heat map representation of the top 100 deregulated genes of *in vitro* and *in vivo* datasets: a) Heat map representation of the top 100 (50 genes for each phenotype) deregulated genes in immortal Huh7 clones (Immortal) versus senescent Huh7 (Senescent) clones. The arrow shows the TERT gene, one of the genes with highest expression values in immortal samples and

lowest expression values in senescent samples. Three biological replicates from each clone were analyzed for genome-wide gene expression using Affymetrix 54 K microarrays and normalized data were used for gene set enrichment analysis (GSEA). b) Heat map representation of the top 100 (50 genes for each phenotype) deregulated genes in immortal HCC samples versus cirrhosis samples. Fifteen cirrhosis and fifteen HCC samples were analyzed for genome-wide gene expression using Affymetrix 54K microarrays and normalized data were used for GSEA. Red: up-regulated; blue: down-regulated. Black dots indicate common genes of the two 100 gene lists.

4.1.2 Gene Set Enrichment Analyses (GSEA) of *in vitro* and *in vivo* datasets using the C2_ALL curated gene sets list

In order to identify gene expression-based biological differences of senescent and immortal samples, as well as cirrhosis and HCC samples we first performed Gene Set Enrichment Analysis (GSEA) on *in vitro* and *in vivo* datasets. The GSEA method performs pairwise analysis of microarray data and determines enrichment of a certain biological process in a certain phenotype by calculating the significance values of certain groups of genes (gene sets). The gene sets used in these analyses can vary according to the question being asked, such as genes of a molecular pathway, a metabolic process, genes containing a common DNA motif in their promoter, a list of genes affected by a chemical treatment, etc. The Molecular Signature Database (MSigDB) of the Broad Institute contains different curated gene lists ready-to use for GSEA experiments, C1 list to C7 lists. Among these lists, I used C2_ALL list, which contains gene sets of different ontology databases (Biocarta, KEGG, Reactome) as well as gene lists determined with research articles as results of different chemical and genetic perturbations (e.g., lists of down-regulated and up-regulated genes following treatments with different chemicals or small interfering RNAs, siRNAs). The C2_ALL curated list, which contains 3263 different gene sets, was a great tool to determine differentially regulated biological processes of samples of the *in vitro* and *in vivo* datasets.

IN VITRO

IN VIVO

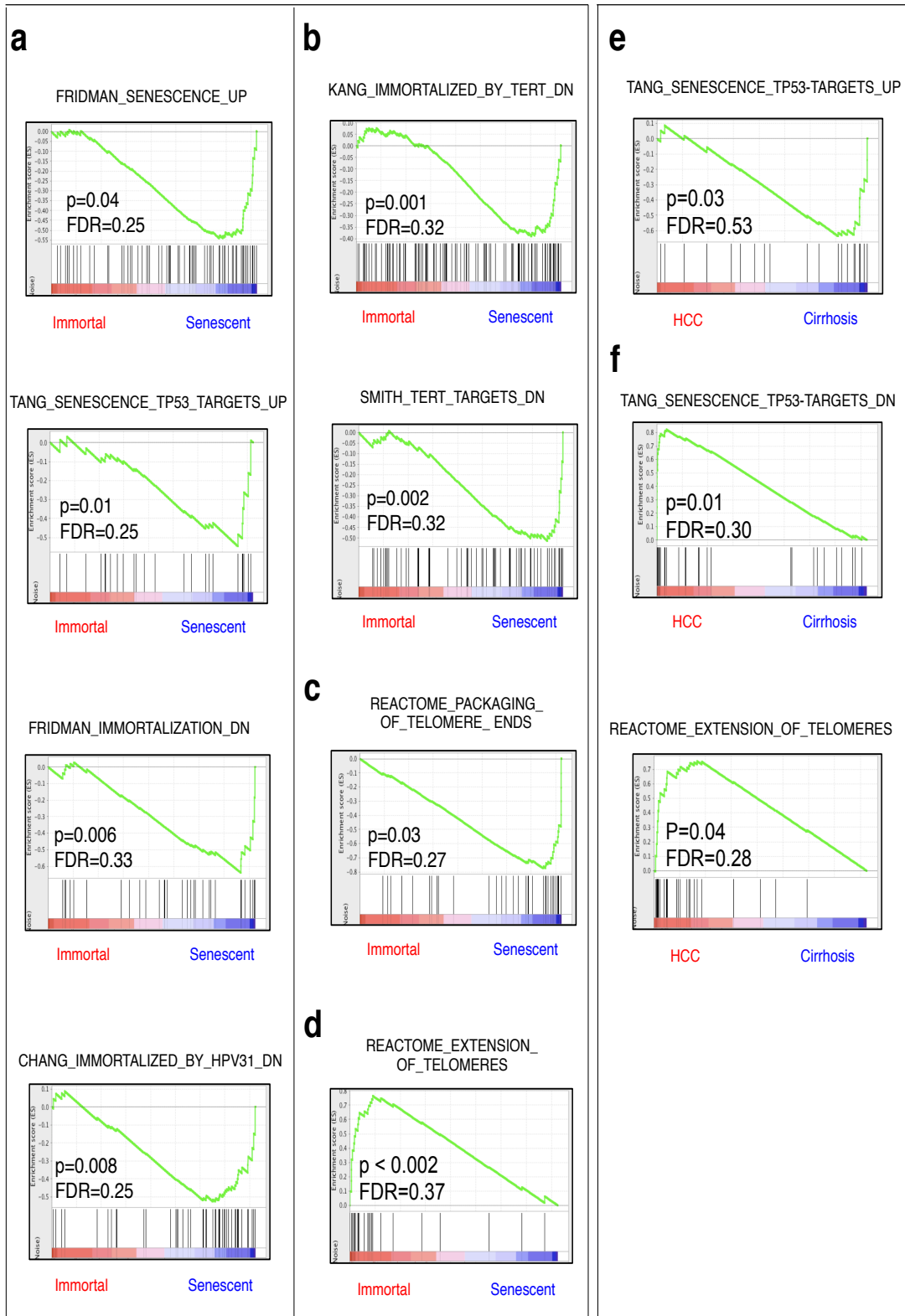


Figure 4.2: Statistically significantly enriched senescence or immortalization gene sets of *in vitro* and *in vivo* datasets: Previously identified gene sets (available at molecular signature database (MSigDB; www.broadinstitute.org/gsea/) were screened to identify those that are up-regulated in *in vitro* and *in vivo* datasets by the analysis of their relative expression levels using GSEA method. a) Gene set enrichment plots showing the up-regulated expression of two previously known senescence-associated gene sets in senescent Huh7 clones, including genes that are commonly up-regulated in senescent cells (“FRIDMAN_SENESCENCE_UP”) [208] and p53-responsive genes up-regulated during replicative senescence arrest (“TANG_SENESCENCE_TP53_TARGERTS_UP”) [209]. In addition, genes known to be down-regulated during immortalization in general (“FRIDMAN_IMMORTALIZATION_DN”) [208], and by human papillomavirus 31 (“CHANG_IMMORTALIZED_BY_HP_V_DN”) [210] were also up-regulated in senescent Huh7 clones. b) Genes known to be down-regulated by TERT-mediated immortalization (“KANG_IMMORTALIZED_BY_TERT_DN”) [211] and TERT-repressed target genes (“SMITH_TERT_TAR-GETS_DN”) [212] were also enriched in senescent Huh7 clones. c) Genes involved in telomere end packaging (“REACTOME_PACKAGING_OF_TELOMERE_ENDS”; www.reactome.org) were up-regulated in senescent Huh7 clones. d) In contrast, genes involved in telomere extension (“REACTOME_EXTENSION_OF_TELOMERES”; www.reactome.org) were enriched in immortal Huh7 clones. e) Enrichment plot of p53-responsive genes up-regulated during replicative senescence arrest (“TANG_SENESCENCE_TP53_TARGERTS_UP”) [209] showing over-expression in cirrhosis. f) In contrast, p53-responsive genes down-regulated during replicative senescence arrest (“TANG_SENESCENCE_TP53_TARGERTS_DN”) [209] and those involved in telomere extension (“REACTOME_EXTENSION_OF_TELOMERES”; www.reactome.org) were overexpressed in HCC tumors. Enrichment scores (ES) are shown on the y-axis. Positive and negative ES indicate enrichment in immortal and senescent Huh7 clones, respectively. X-axis bars represent individual genes of the indicated gene sets. FDR: False discovery rate, p: nominal p-value. Three biological replicates from each clone were analyzed for genome-wide gene expression using Affymetrix 54K microarrays and normalized data were used for GSEA.

The GSEAs of immortal versus senescent samples using the C2_ALL determined 113 gene sets significantly enriched ($p < 0.05$) in immortal samples, and 598 gene sets significantly enriched ($p < 0.05$) in senescent samples. The same analyses using the *in vivo* dataset identified 189 genes sets significantly enriched ($p < 0.05$) in HCC samples and 161 gene set significantly enriched ($p < 0.05$) in cirrhosis samples. Thus, we continued with further investigating these significantly enriched gene sets of the two datasets for the rest of the analyses.

4.1.3 Senescence and Immortality Gene Set Enrichments of *in vitro* and *in vivo* datasets

Among the results of significantly enriched gene sets, we first analyzed results of senescence and immortality related gene sets of the two datasets starting with the *in vitro* dataset; since these gene sets can prove whether our senescent and immortal microarray data are reliable, or not.

There were eight different senescence or immortality related gene sets among significantly enriched gene sets of the *in vitro* GSEA results (Table 4.1; Figure 4.2a-d). Commonly up-regulated genes during senescence, identified by Fridman et al. (“FRIDMAN_SENESCENCE_UP”) [208] were significantly enriched in senescent Huh7 cells. In addition to that, p53-responsive genes up-regulated during replicative senescence arrest, determined by Tang et al. [209] (“TANG_SENESCENCE_TP53_TARGERTS_UP”) were also enriched in senescent samples. Since our senescent Huh7 clones were generated with replicative senescent (see materials and methods), this enrichment is especially meaningful. In addition to these gene sets, the list of the genes down-regulated during immortalization in general (“FRIDMAN_IMMORTALIZATION_DN”) [208], as well as genes down-regulated by human papilloma virus (HPV) 31 (“CHANG_IMMORTALIZED_BY_HPVDN”) [210] were also enriched in senescent samples (Table 4.1; Figure 4.2a).

Table 4.1 : Significantly enriched senescence and immortality related gene sets in *in vitro* and *in vivo* datasets:

GENE SET NAME	# GENES	ENRICHED PHENOTYPE	BRIEF DESCRIPTION
FRIDMAN_SENESCENCE_UP	74	Senescent	Genes up-regulated in senescent cells [Fridman, 2008]
FRIDMAN_IMMORTALIZATION_DN	31	Senescent/ Cirrhosis	Genes down-regulated in immortalized cell lines [Fridman, 2008]
TANG_SENESCENCE_TP53_TARGETS_UP	24	Senescent	Genes up-regulated in WI-38 cells (senescent primary fibroblasts) after inactivation of TP53 by GSE56 polypeptide [Tang, 2007]
TANG_SENESCENCE_TP53_TARGETS_DN	39	HCC	Genes down-regulated in WI-38 cells (senescent primary fibroblasts) after inactivation of TP53 by GSE56 polypeptide [Tang, 2007]
CHANG_IMMORTALIZED_BY_HP131_DN	46	Senescent	Genes down-regulated in normal keratinocytes immortalized by infection with the high risk HPV31 (human papilloma virus) strain [Chang, 2000]
KANG_IMMORTALIZED_BY_TERT_DN	101	Senescent	Down-regulated genes in the signature of adipose stromal cells (ADSC) immortalized by forced expression of TERT [Kang, 2004]
SMITH_TERT_TARGETS_DN	65	Senescent	Genes consistently down-regulated in HMEC cells (primary mammary epithelium) upon expression of TERT off a retroviral vector [Smith, 2003]
REACTOME_PACKAGING_OF_TELOMERE_ENDS	40	Senescent	Genes involved in Packaging Of Telomere Ends [http://www.reactome.org]
REACTOME_EXTENSION_OF_TELOMERES	24	Immortal/HCC	Genes involved in Extension of Telomeres [http://www.reactome.org]

The other four senescence-immortality related gene sets enriched in *in vitro* dataset are related to either TERT or telomeres (Table 4.1; Figure 4.2b-d). “KANG_IMMORTALIZED_BY_- TERT_DN” gene set [211], containing genes down-regulated by TERT-mediated immortalization, “SMITH_TERT_TARGETS_DN” gene set [212], containing TERT-repressed target genes, and “REACTOME_PACKAGING_OF_- TELOMERE_ENDS” gene set, containing genes involved in telomere end packaging, were all significantly enriched in senescent Huh7 clones (Table 4.1; Fig. 4.2b,c). The remaining gene set (“REACTOME_EXTENSION_OF_TELOMERES”), containing genes involved in telomere extension is enriched in immortal Huh7 cells (Table 4.1; Fig. 4.2d).

Although eight senescence-immortality gene sets were enriched in the *in vitro* samples, only three senescence-immortality gene sets of the C2_ALL list were enriched in the *in vivo* dataset. The gene set “TANG_SENESCENCE_TP53_TARGETS_UP” [209] are enriched in cirrhosis samples as happened in senescent cells (Table 4.1; Fig. 4.2e). In contrast, HCC phenotype was enriched in “TANG_SENESCENCE_TP53_TARGETS_DN” [209] gene set, containing p53-responsive genes down-regulated during replicative senescence arrest; as well as the “REACTOME_EXTENSION_OF_TELOMERES” gene set, which was also enriched in immortal cells (Table 4.1; Fig. 4.2f).

4.1.4 Senescence-related gene networks in cirrhosis and hepatocellular carcinoma

In order to test the hypothesis that, gene expression profiles of *in vitro* senescent cells are similar to those of *in vivo* cirrhosis samples; and *in vitro* immortal cells are similar to those of *in vivo* HCC samples, we first analyzed the whole lists of significantly enriched gene sets of the both datasets. The significantly enriched gene set lists of the two datasets were analyzed pairwise (senescent-cirrhosis, immortal-cirrhosis, senescent-HCC, and immortal-HCC) to observe the overall percentage of the similarities of the four phenotypes.

Among the whole list of 1629 common gene sets in senescence and cirrhosis samples 328 (20%) of them were significant ($p < 0.05$) in at least one phenotype. However, among 388 gene sets commonly enriched both in immortal and cirrhosis samples only 25 of them (6.4%) were significantly enriched in any of the classes. A similar analysis between immortal and HCC samples resulted with 35% common enrichment (249 of 710) in at least one phenotype. Finally, senescence and HCC samples shared 7.8% of their commonly enriched genes. Thus, these first data analyses with overall gene expression pattern based differentially enriched molecular mechanisms of the four phenotypes suggested that *in vitro* senescent cells are like *in vivo* cirrhosis samples, and *in vitro* immortal cells are like *in vivo* HCC samples [213].

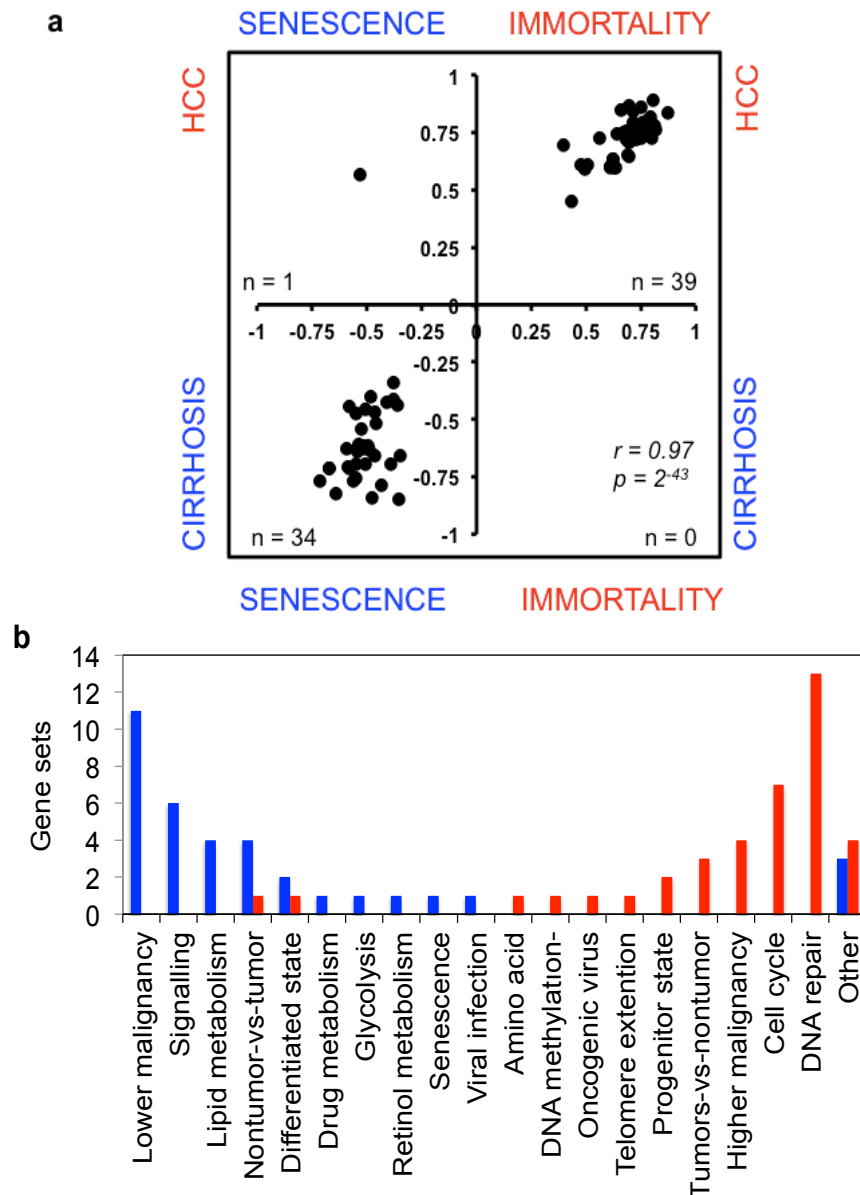


Figure 4.3: Comparative analysis of gene sets enriched in Huh7 clones and diseased liver tissues associated cirrhosis with senescence and HCC with immortality phenotypes, respectively: a) Scatter plot compares enrichment scores of 74 gene sets commonly enriched in Huh7 clones (senescent or immortal) and diseased liver tissues (cirrhosis or HCC) with a p value less than 0.05. Thirty-nine gene sets (53%) were significantly enriched in both HCC and immortal samples whereas 34 (46%) gene sets were significantly enriched in both cirrhosis and senescent samples (correlation value $r=0.97$, $p=2 \times 10^{-43}$). Only one gene set (1%) was enriched in both HCC and senescent clones. b) Distribution of biological features defined by different gene sets in cirrhosis/senescence (blue columns) and HCC/immortality (red columns) phenotypes, respectively. These analyses also revealed that cirrhosis/senescence- and HCC/immortality-associated gene sets implicated distinct biological features specific to each phenotype. Red color: immortal and/or HCC; blue color: senescent and/or cirrhosis.

To identify the driver senescence and immortality related gene networks we applied a more stringent criterion and determined lists of gene sets significantly enriched ($p < 0.05$) in both samples of the four pairs. This analysis revealed a list of 74 gene sets with 98.6% of them distributed to either senescence-cirrhosis pair (34 gene sets, 46%) or immortal-HCC pair (39 gene sets, 52.7%), whereas only one gene set was significantly enriched in both senescence and HCC classes (Figure 4.3a). The two-tailed Fisher exact test, ($p = 2.6 \times 10^{-20}$) and Pearson correlation values of co-enrichment scores ($r=0.97$, $p = 2 \times 10^{-43}$) resulted with highly significant results; indicating that *in vitro* senescent cells are like *in vivo* cirrhosis samples, and *in vitro* immortal cells are like *in vivo* HCC samples (Figure 4.3a).

The list of 74 senescence escape oriented deregulated gene networks of hepatocellular carcinogenesis is presented in the Table 3.2 and the distributions of the 73 common gene sets according to their cellular functional mechanisms in senescent-cirrhosis and immortal-HCC samples are depicted in the Figure 4.3b. Gene sets up-regulated in cirrhosis/ senescence group were also up-regulated in non-tumor tissues as opposed to those with tumors (four gene sets), or in less malignant tumors versus more malignant tumors (11 gene sets). In contrast, genes up-regulated in HCC/immortality group were associated with tumors as opposed to non-tumor tissues (four out of five gene sets), or in more malignant tumors as compared to less malignant tumors (four gene sets). The HCC/immortality state was characterized by an up-regulation of genes involved in DNA repair (13 gene sets), cell cycle (seven gene sets), progenitor state (two gene sets), telomere extension, DNA methylation and branched chain amino acid metabolism. In contrast, genes involved in cell signaling (six gene sets), lipid metabolism (four gene sets), drug metabolism, retinol

metabolism and glycolysis were down-regulated (Figure 4.3b, Table 4.2; see discussion).

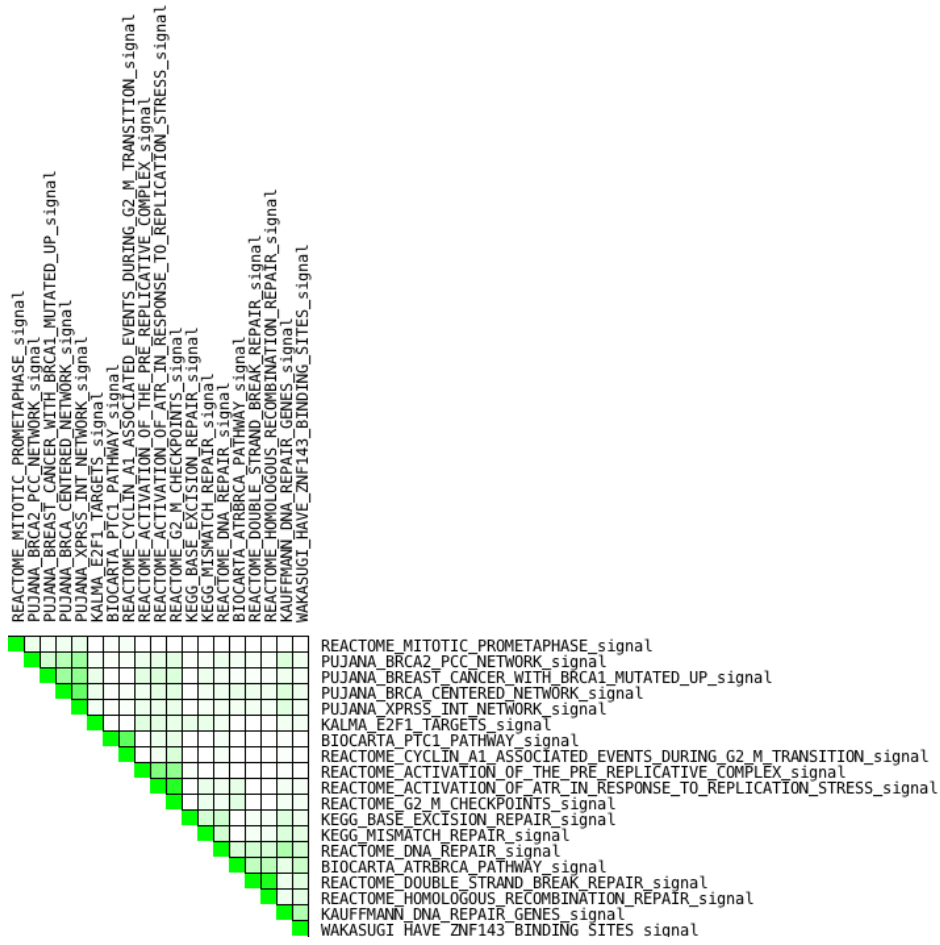
The shared significant enrichments of 20 DNA repair and cell cycle gene sets were further analyzed. Figure 4.4a shows gene name similarities of these separate gene sets indicative of presence of repetitively enriched genes in different gene sets (Figure 4.4a). Thus, the core enriched genes, the genes making the major contribution to the enrichment score of a gene set, of these gene sets were determined separately in immortal and HCC samples. Figure 4.4b indicates that immortal and HCC samples have both common recurrently core enriched and differentially core enriched genes in common DNA repair and cell cycle genes; suggesting mostly common, but also slightly differing active DNA repair and cell cycle mechanisms in immortal and HCC samples (see discussion) (Figure 4.4b).

Detailed analysis of genes involved in retinoid metabolism revealed that the expression of several genes encoding critical enzymes catalyzing the synthesis of retinoic acid (the active form of retinoids) was down-regulated in HCC tumors as compared to cirrhotic liver tissue. There was also down-regulated expression of genes involved in the storage of retinoids in tumors. Down-regulated genes included two members of retinol dehydrogenases, four members of alcohol dehydrogenases, NADP(H)-dependent retinol dehydrogenase/reductase (DHRS4) and β -carotene 15,15'-monooxygenase 1 (BCMO1), which are all involved in the synthesis of retinal, the immediate precursor of retinoic acid. Two genes involved in the synthesis of storage retinyl esters, namely lecithin:retinol acyltransferase (LRAT) and patatin-like phospholipase-4 (PNPLA4) were also down-regulated in HCC cells (Figure 4.5).

Table 4.2: 74 senescence escape oriented deregulated gene networks of hepatocellular carcinogenesis:

GENE SET NAME	Class	Associations
KALMA_E2F1_TARGETS	IMM-HCC	Cell cycle
REACTOME_MITOTIC_PROMETAPHASE	IMM-HCC	Cell cycle
REACTOME_ACTIVATION_OF_THE_PRE_REPLICATIVE_COMPLEX	IMM-HCC	Cell cycle
REACTOME_G2_M_CHECKPOINTS	IMM-HCC	Cell cycle
REACTOME_CYCLIN_A1_ASSOCIATED_EVENTS_DURING_G2_M_TRANSITION	IMM-HCC	Cell cycle
MANALO_HYPOXIA_DN	IMM-HCC	Cell cycle
BIOCARTA_PTC1_PATHWAY	IMM-HCC	Cell cycle
RIZ_ERYTHROID_DIFFERENTIATION	IMM-HCC	Differentiated state
MISSIAGLIA_REGULATED_BY_METHYLATION_DN	IMM-HCC	DNA methylation-activated
REACTOME_DNA_REPAIR	IMM-HCC	DNA repair
KAUFFMANN_DNA_REPAIR_GENES	IMM-HCC	DNA repair
WAKASUGI_HAVE_ZNF143_BINDING_SITES	IMM-HCC	DNA repair
REACTOME_DOUBLE_STRAND_BREAK_REPAIR	IMM-HCC	DNA repair
REACTOME_HOMOLOGOUS_RECOMBINATION_REPAIR	IMM-HCC	DNA repair
REACTOME_ACTIVATION_OF_ATR_IN_RESPONSE_TO_REPLICATION_STRESS	IMM-HCC	DNA repair
BIOCARTA_ATRBRCA_PATHWAY	IMM-HCC	DNA repair
KEGG_MISMATCH_REPAIR	IMM-HCC	DNA repair
KEGG_BASE_EXCISION_REPAIR	IMM-HCC	DNA repair
PUJANA_BRCA_CENTERED_NETWORK	IMM-HCC	DNA repair
PUJANA_BREAST_CANCER_WITH_BRCA1_MUTATED_UP	IMM-HCC	DNA repair
PUJANA_BRCA2_PCC_NETWORK	IMM-HCC	DNA repair
PUJANA_XPRSS_INT_NETWORK	IMM-HCC	DNA repair
KEGG_VALINE_LEUCINE_AND_ISOLEUCINE_BIOSYNTHESIS	IMM-HCC	Amino acid metabolism
RAMASWAMY_METASTASIS_UP	IMM-HCC	Higher malignancy
LOPEZ_MESOTELIOMA_SURVIVAL_TIME_UP	IMM-HCC	Higher malignancy
SMID_BREAST_CANCER_LUMINAL_A_DN	IMM-HCC	Higher malignancy
WEST_ADRENOCORTICAL_CARCINOMA_VS_ADENOMA_UP	IMM-HCC	Higher malignancy
MUNSHI_MULTIPLE_MYELOMA_DN	IMM-HCC	Nontumor-vs-Tumor
PYEON_HP_V_POSITIVE_TUMORS_UP	IMM-HCC	Oncogenic virus
KOKKINAKIS_METHIONINE_DEPRIVATION_48HR_DN	IMM-HCC	Other
PENG_Glutamine_DEPRIVATION_UP	IMM-HCC	Other
NAKAMURA_CANCER_MICROENVIRONMENT_DN	IMM-HCC	Other
CROONQUIST_STROMAL_STIMULATION_DN	IMM-HCC	Other
FOURNIER_ACINAR_DEVELOPMENT_LATE_DN	IMM-HCC	Progenitor state
FOURNIER_ACINAR_DEVELOPMENT_LATE_2	IMM-HCC	Progenitor state
REACTOME_EXTENSION_OF_TELOMERES	IMM-HCC	Telomere extention
WHITEFORD_PEDIATRIC_CANCER_MARKERS	IMM-HCC	Tumors-vs-Nontumor
VECCHI_GASTRIC_CANCER_EARLY_UP	IMM-HCC	Tumors-vs-Nontumor
WEST_ADRENOCORTICAL_TUMOR_MARKERS_UP	IMM-HCC	Tumors-vs-Nontumor
EBAUER_TARGETS_OF_PAX3_FOXO1_FUSION_UP	SEN-CIRR	Differentiated state
TARTE_PLASMA_CELL_VS_PLASMABLAST_UP	SEN-CIRR	Differentiated state
KEGG_DRUG_METABOLISM_CYTOCHROME_P450	SEN-CIRR	Drug Metabolism
REACTOME_GLYCOLYSIS	SEN-CIRR	Glycolysis
KEGG_LINOLEIC_ACID_METABOLISM	SEN-CIRR	Lipid metabolism
KEGG_ARACHIDONIC_ACID_METABOLISM	SEN-CIRR	Lipid metabolism
KEGG_GLYCOSPHINGOLIPID_BIOSYNTHESIS_LACTO_AND_NEOLACTO_SERIES	SEN-CIRR	Lipid metabolism
UZONYI_RESPONSE_TO_LEUKOTRIENE_AND_THROMBIN	SEN-CIRR	Lipid metabolism
NAKAYAMA_SOFT_TISSUE_TUMORS_PCA2_DN	SEN-CIRR	Lower malignancy
HOSHIDA_LIVER_CANCER_SUBCLASS_S3	SEN-CIRR	Lower malignancy
BOYALT_LIVER_CANCER_SUBCLASS_G123_DN	SEN-CIRR	Lower malignancy
CAIRO_HEPATOBLASTOMA_CLASSES_DN	SEN-CIRR	Lower malignancy
DOANE_BREAST_CANCER_ESR1_UP	SEN-CIRR	Lower malignancy
VANTVEER_BREAST_CANCER_ESR1_UP	SEN-CIRR	Lower malignancy
SMID_BREAST_CANCER_BASAL_DN	SEN-CIRR	Lower malignancy
MOREAUX_MULTIPLE_MYELOMA_BY_TACI_UP	SEN-CIRR	Lower malignancy
BOYLAN_MULTIPLE_MYELOMA_PCA1_UP	SEN-CIRR	Lower malignancy
LIEN_BREAST_CARCINOMA_METAPLASTIC_VS_DUCTAL_DN	SEN-CIRR	Lower malignancy
MOREAUX_B_LYMPHOCYTE_MATURATION_BY_TACI_UP	SEN-CIRR	Lower malignancy
CAIRO_HEPATOBLASTOMA_DN	SEN-CIRR	Nontumor-vs-Tumor
VECCHI_GASTRIC_CANCER_EARLY_DN	SEN-CIRR	Nontumor-vs-Tumor
DELYS_THYROID_CANCER_DN	SEN-CIRR	Nontumor-vs-Tumor
SABATES_COLORECTAL_ADENOMA_DN	SEN-CIRR	Nontumor-vs-Tumor
EHRLICH_ICF_SYNDROM_DN	SEN-CIRR	Other
LEE_LIVER_CANCER_MYC_DN	SEN-CIRR	Other
VALK_AML_CLUSTER_1	SEN-CIRR	Other
KEGG_RETINOL_METABOLISM	SEN-CIRR	Retinol Metabolism
TANG_SENESCENCE_TP53_TARGETS_UP	SEN-CIRR	Senescence
AMIT_EGF_RESPONSE_120_HELA	SEN-CIRR	Signaling-EGF
NAGASHIMA_EGF_SIGNALING_UP	SEN-CIRR	Signaling-EGF
REACTOME_G_ALPHA_Q_SIGNALLING_EVENTS	SEN-CIRR	Signalling-other
BASSO_CD40_SIGNALING_DN	SEN-CIRR	Signalling-other
ODONNELL_TFRC_TARGETS_UP	SEN-CIRR	Signalling-other
BROWNE_HCMV_INFECTION_2HR_UP	SEN-CIRR	Viral infection
REACTOME_RNA_POLYMERASE_I_III_AND_MITOCHONDRIAL_TRANSCRIPTION	SEN-HCC	Mitochondrial transcription

a



b

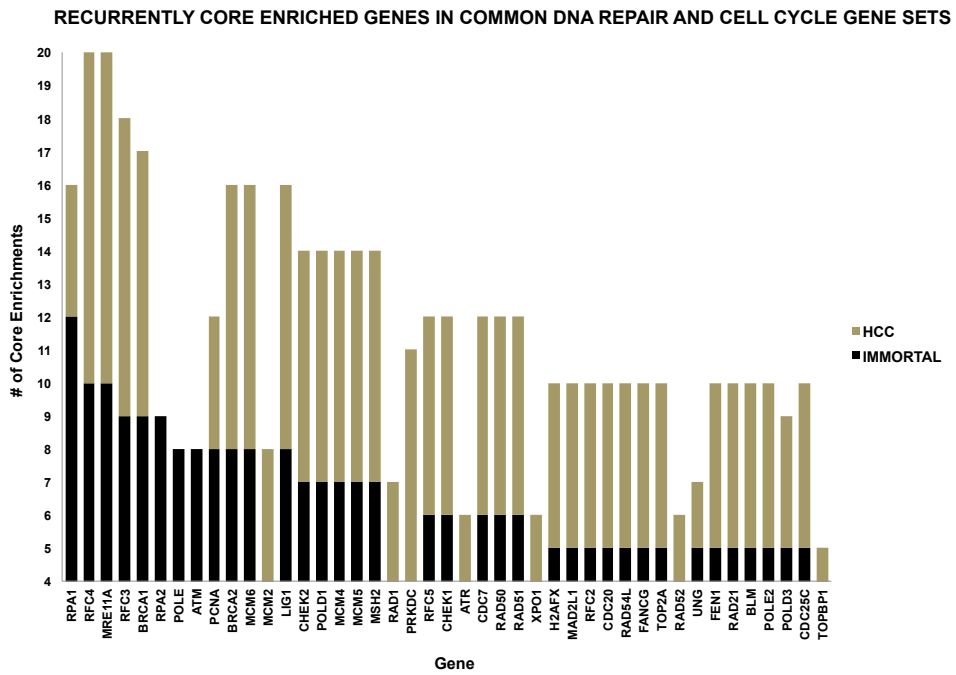


Figure 4.4: DNA repair and cell cycle gene sets of the 74 gene sets list display the major gene expression based similarities and differences of the two datasets regarding to DNA repair and cell cycle mechanisms:

DNA repair and cell cycle gene sets among the 74 gene sets were further analyzed using the leading edge analysis (LEA) method. a) Set-to-set analysis of the selected gene sets display degrees of pair-wise similarities among gene sets. Number of shared genes increase in darker green boxes compared to lighter ones. White color represents absence of common genes in the sets. b) Numbers of core enrichments of each gene were determined in two datasets. Genes core enriched more than five times at least in one phenotype were included in the chart. The chart shows both commonly enriched and differentially enriched genes of the selected DNA repair and cell cycle gene sets; providing clues for common and different DNA repair and cell cycle mechanisms in *in vitro* and *in vivo* HCC samples.

4.1.5 A senescence to immortality switch between dysplasia and HCC

Our GSEA results of *in vitro* and *in vivo* datasets demonstrated high similarities between senescence and cirrhosis, as well as immortal cells with HCC tissues. As described in the introduction, presence of cellular senescence is one of the characteristic traits of the cirrhotic liver tissue, and by-pass of the cellular senescence is the critical step of immortalization towards generation of HCC in a cirrhotic liver. Thus, after determining common deregulated molecular pathways, metabolic events, and critical genes of these mechanisms, we determined differentially expressed genes during senescence-immortality switch in our *in vitro* datasets and tested gene expression differences of these genes on *in vivo* liver cancer datasets to identify critical individual genes of the senescence-immortality switch process.

The list of significantly (>2.0 fold change with p values less than 10^{-7} between senescent and immortal clones) differentially expressed 1813 probe sets (corresponding to 1220 genes) was determined by class comparison analysis (data not shown). In order to determine the timing of the senescence-immortality switch during the multistep progression of the HCC, we used raw data of a publically available dataset containing samples of five different stages of the hepatocellular carcinogenesis [202]. The dataset of the Wurmbach et al. contains 10 normal liver

samples, 13 cirrhotic tissues, 17 dysplastic lesions (originally described low-grade and high-grade dysplasia cases combined), 17 early HCCs (originally described very early and early HCC cases combined) and 18 advanced HCCs (originally described advanced and very advanced cases combined). The unsupervised clustering analysis using gene expression values of the 1813 probe sets in the Wurmbach dataset (containing 75 samples in total) generated two main clusters. Cluster 1 grouped together 39 out of the 40 non-HCC samples (97.5%) and 1 out of the 35 (3%) HCC samples. Conversely, cluster 2 was composed of 34 out of the 35 HCCs (97%) and one of 40 (2.5%) of the non-HCC samples (Fig. 4.6) suggesting that gene expression values of the senescence-immortality genes can identify non-tumor and tumor liver disease samples.

The other result of this analysis was formation of a homogenous subgroup of dysplastic and cirrhotic samples in the cluster 1, while normal liver samples shared similarities with either cirrhotic or dysplastic tissue. Thus, dysplastic liver samples were clustered with cirrhotic samples, rather than HCC samples; suggesting that dysplasia is a more senescence-like state instead of being an immortal-like state. In addition to that, HCC samples formed several minor clusters, with a tendency of early and advanced tumors to form distinct sub-clusters in this analysis (Fig. 4.6).

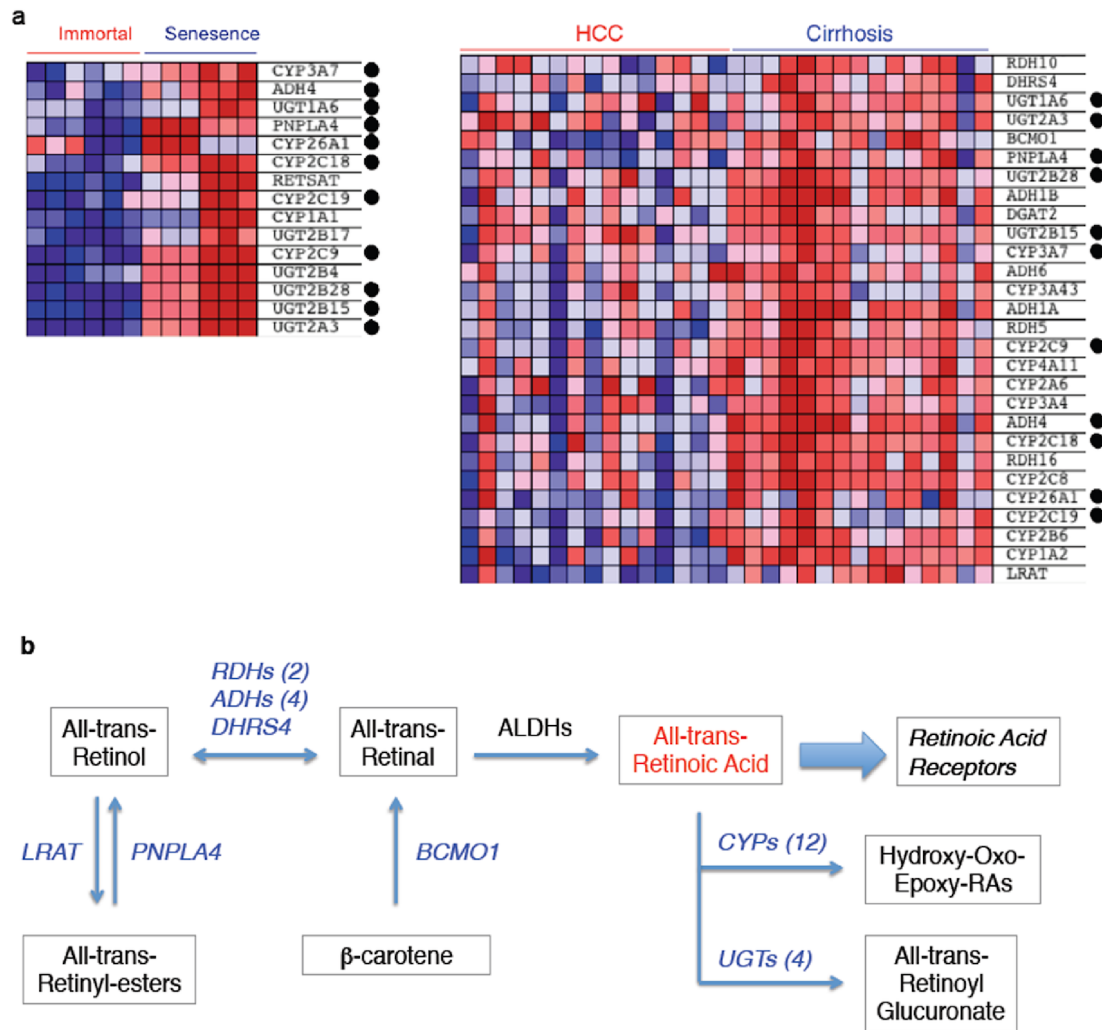


Figure 4.5: Retinol metabolism is deregulated in senescence to immortality switch: Comparative analysis of core enriched gene sets in Huh7 clones (senescent versus immortal) and diseased liver tissues (cirrhosis versus HCC) indicated that retinol metabolism genes (“KEGG_RETINOL_METABOLISM”) undergo systematic changes in immortal cells and HCC, when compared to senescent cells and cirrhosis, respectively. a) Heat map of core enriched retinol metabolism genes in Huh7 clones (left) and diseased liver tissues (right). Red: up-regulated; blue: down-regulated. Genes commonly deregulated in both Huh7 clones and diseased liver tissues are indicated with a dot. b) A simplified view of retinol metabolism. Enzyme-encoding genes down-regulated in HCC are shown in blue. LRAT: lecithin retinol acetyl transferase, PNPLA4: patatin-like phospholipase domain containing-4; RDHs: retinol dehydrogenases; ADHs: alcohol dehydrogenases; DHRS4: dehydrogenase/reductase (SDR family) member-4; BCMO1: beta-carotene 15,159-monooxygenase-1; CYPs: Cytochrome P-450 family proteins; UGTs: UDP glucuronosyltransferases.

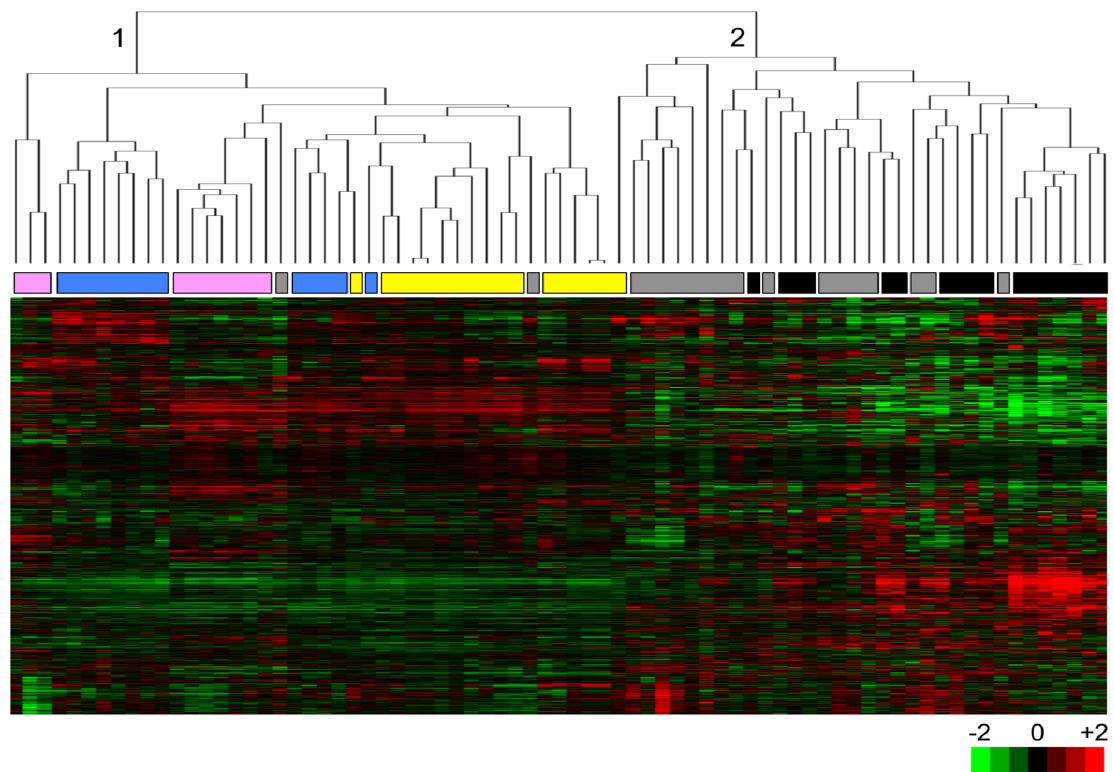


Figure 4.6: Hierarchical clustering of 75 non-malignant and malignant liver tissue samples using 1813 senescence-associated gene probe sets: Hepatocellular carcinoma and non-tumor liver tissues formed two distinct clusters (1 and 2) with the exception of one dysplasia and two early HCC samples. The rows and columns represent genes and samples, respectively on the cluster map. Tissue samples are normal liver (pink), cirrhosis (blue), dysplasia (yellow), early HCC (gray), and advanced HCC (black). Red: over-expressed, green: under-expressed probe set in the heat map.

Table 4.3: Detailed information on the “hepatocellular immortality signature set”, containing 16 probesets:

ProbeSet ID	Symbol	Gene Name	Chromosomal Location	Mean Immortal Cell Expression Value (log2)	Mean Senescent Cell Expression Value (log2)	Immortal to Senescence Ratio (log2)	Mean HCC Expression Value (log2)	Mean Cirrhosis Expression Value (log2)	HCC to Cirrhosis Ratio (log2)
225687_at	FAM83D	family with sequence similarity 83, member D	20q11.22-q12	9.58	8.50	1.08	7.17	5.29	1.88
222740_at	ATAD2	ATPase family, AAA domain containing 2	8q24.13	8.94	7.66	1.27	8.04	6.66	1.38
228401_at	ATAD2	ATPase family, AAA domain containing 2	8q24.13	7.39	6.30	1.10	7.64	6.26	1.38
201292_at	TOP2A	topoisomerase (DNA) II alpha 170kDa	17q21-q22	9.80	8.82	0.98	7.23	4.44	2.80
205034_at	CCNE2	cyclin E2	8q22.1	6.24	5.22	1.02	6.69	4.73	1.96
238021_s_at	CRNDE	colorectal neoplasia differentially expressed (non-protein coding)	16q12.2	8.43	7.05	1.38	7.25	5.22	2.03
201839_s_at	EPCAM	epithelial cell adhesion molecule	2p21	9.65	11.62	-1.96	6.88	9.26	-2.38
223784_at	TMEM27	transmembrane protein 27	Xp22	3.19	8.68	-5.49	6.33	8.76	-2.43
209278_s_at	TFPI2	tissue factor pathway inhibitor 2	7q22	8.08	10.63	-2.56	6.15	7.86	-1.71
209189_at	FOS	FBJ murine osteosarcoma viral oncogene homolog	14q24.3	4.17	5.27	-1.10	8.78	10.15	-1.37
206797_at	NAT2	N-acetyltransferase 2 (arylamine N-acetyltransferase)	8p22	6.00	7.68	-1.68	8.21	10.32	-2.10
1553296_at	GPR128	G protein-coupled receptor 128	3q12.2	5.24	6.76	-1.52	5.61	7.62	-2.01
220432_s_at	CYP39A1	cytochrome P450, family 39, subfamily A, polypeptide 1	6p21.1-p11.2	4.57	5.81	-1.25	7.20	9.26	-2.06
218532_s_at	FAM134B	family with sequence similarity 134, member B	5p15.1	3.48	6.24	-2.76	7.12	8.41	-1.29
233565_s_at	SDCBP2	syndecan binding protein (syntenin) 2	20p13	5.72	6.72	-1.00	7.50	8.25	-0.75
229160_at	MUM1L1	melanoma associated antigen (mutated) 1-like 1	Xq22.3	7.03	8.42	-1.39	5.53	6.84	-1.31

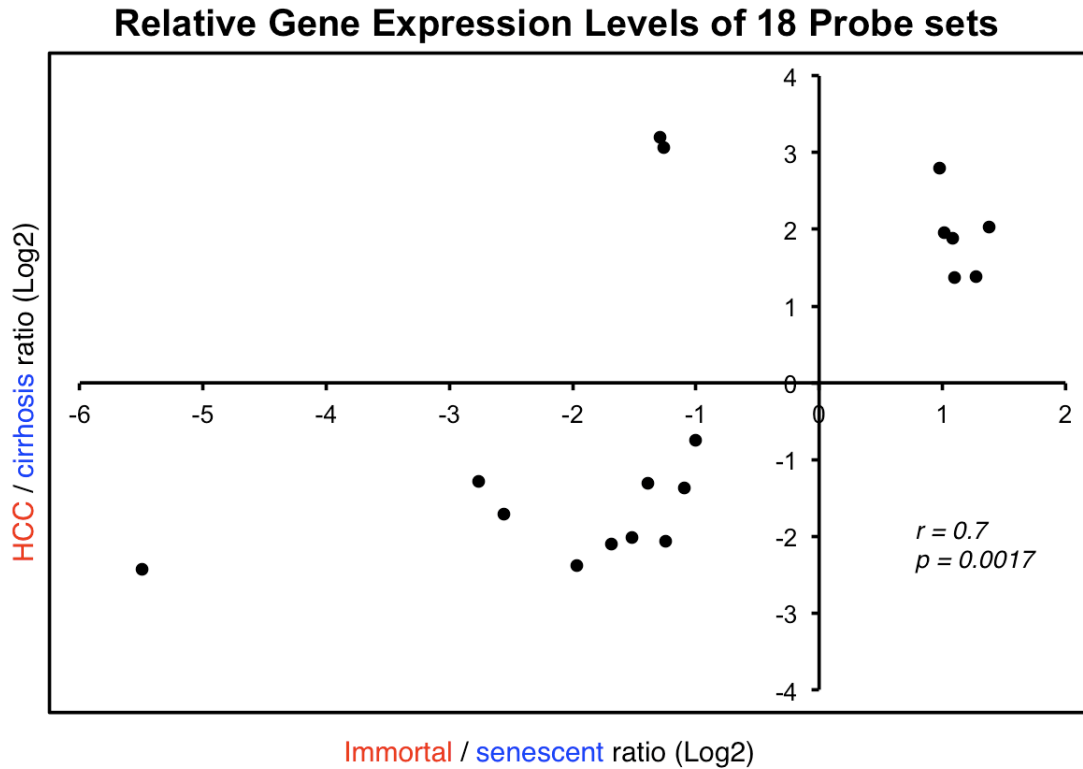


Figure 4.7: Relative gene expression profiles of 18 probe sets: Scatter plot graphic compares relative expression levels (Log₂ ratios) of 18 classifier probe sets representing 17 genes in Huh7 clones (immortal versus senescent) and diseased liver tissues (HCC versus cirrhosis). Expression ratios of classifier genes showed a linear correlation (correlation value $r=0.7$, $p=0.0017$) with ratios observed in Huh7 clones (immortal/senescent) and diseased liver tissues (HCC/cirrhosis). The classifier set was identified by PAM analysis of 1813 senescence-associated probe sets using a training tissue set composed of cirrhosis ($n=13$) and HCC ($n=35$) samples described by Wurmbach et al. [202]. Two probe sets which did not show expression patterns compatible with our *in vivo* senescence model were discarded to define a final signature set composed of 16 probe sets representing 15 genes.

4.1.6 Fifteen-gene hepatocellular-immortality signature

Based on remarkable clustering of tumor and non-tumor tissues by the 1220 senescence-related genes, we then asked whether we could select a smaller subset of genes for discrimination of HCC from cirrhosis. We used expression data from 35 HCC and 13 cirrhosis samples from Wurmbach et al. [202] as a “training set”. The PAM analysis using “nearest shrunken centroid method” identified a list of 18 probe sets able to predict all 13 cirrhosis samples and 33 out of 35 HCC samples (96% accuracy) of the Wurmbach dataset with specificity of 0.943 and sensitivity of 1 for cirrhosis phenotype; specificity of 1 and sensitivity of 0.943 for HCC phenotype. The

list of 18 classifiers, composed of six immortality-associated probe sets (representing five genes) up-regulated in HCC tissues, ten senescence-associated probe sets up-regulated in cirrhosis samples, and two senescence-associated probe sets up-regulated in HCC (Fig. 4.7). Fisher's exact test demonstrated a strong association of cirrhosis with senescence and HCC with immortal phenotypes ($p=0.0015$). Then, we selected ten "cirrhosis- and senescence-associated" and five "HCC- and immortality-associated" genes (16 probe sets in total) to construct a "hepatocellular immortality signature set" (Table 4.3).

After that, we tested the diagnostic value of the signature genes using a "test set" composed of 45 tissue samples, including 30 Turkish patient samples reported here and 15 Japanese patient samples with publicly available expression data [204]. Based on Nearest Template Prediction method [203], the signature set was able to predict 100% (20/20) of cirrhotic tissues with high confidence ($FDR < 0.05$). Five of 25 HCC samples (20%) were unpredictable ($FDR > 0.05$). Of the remaining 20 HCC samples, 19 (95%) were predicted correctly (Fig. 4.8). Overall, the signature set provided high confidence prediction ($FDR < 0.05$) in 89% (40/45) of patients with 97.5% (39/40) accuracy.

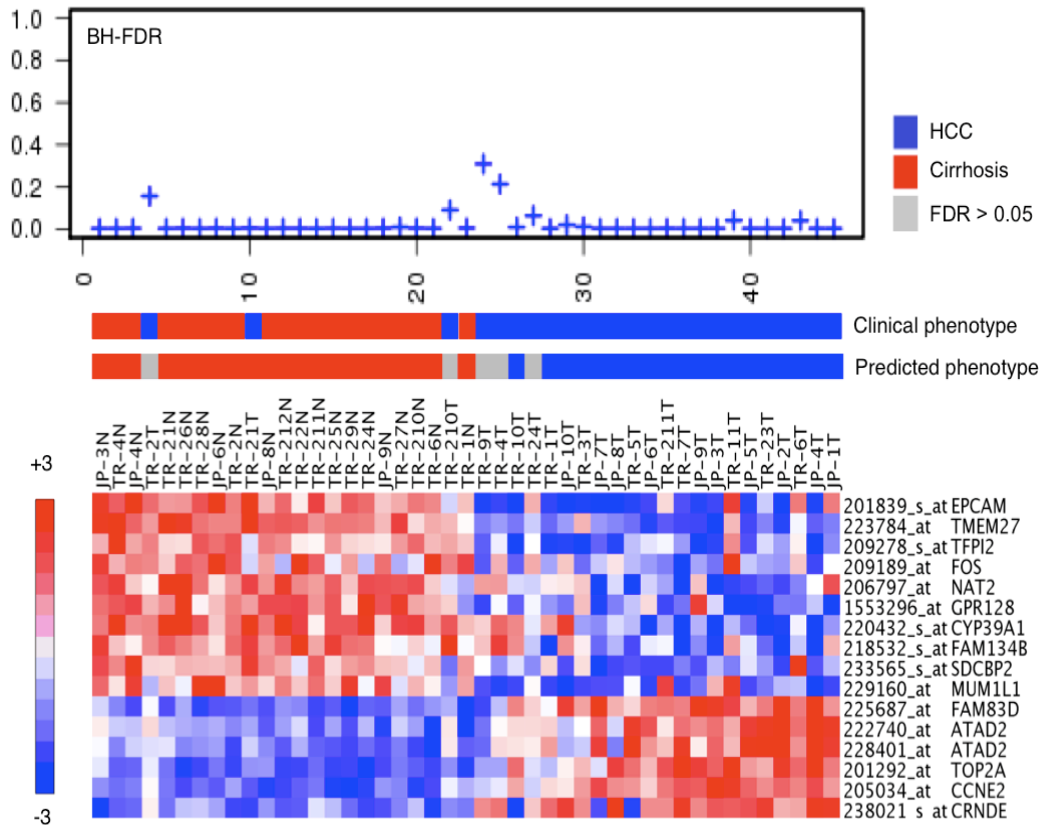


Figure 4.8: Nearest template prediction (NTP) of 15 gene hepatocellular signature test: Validation of molecular prediction of HCC and cirrhosis by 15-classifier genes. Using the nearest template prediction method [200], we compared expression levels of sixteen probe sets representing 15 classifier genes in a test tissue set composed of 20 cirrhosis and 25 HCC samples originating from Turkish (TR) patients described in this report, and Japanese (JP) patients described elsewhere [204]. BH FDR (Benjamini-Hochberg false discovery rates) values (top), clinical versus predicted phenotypes (middle) and heatmaps of classifier gene expression levels (bottom) are shown. The test provided a diagnostic result for 40 out of 45 samples (89%) with 97.5% (39/40) accuracy.

4.1.7 Association of ATAD2 RNA and protein levels with HCC and cellular immortality

ATAD2, one of the fifteen hepatocellular immortality signature genes, was of particular interest warranting further investigation. The ATAD2 gene is mapped to chromosome 8q24 and codes for a predicted protein of 1,391 amino acids that contains a double AAA ATPase domain and a bromodomain [214]. The 8q24 locus displays frequent copy number gains in HCC [215], and many other cancers [216]. Therefore, we selected ATAD2 as a representative of our hepatocellular immortality

signature to validate its immortality- and HCC-associated expression by additional experiments (Fig. 4.9). Freshly isolated normal adult human hepatocytes and MRC-5 normal human fetal lung fibroblasts (at PD44) were used as non-immortal control cells that enter replicative senescence at around PD65 [194]. When compared to normal hepatocytes, most HCC cell lines (n=12/14; 86%) displayed between two- and 20-fold higher ATAD2 mRNA expression. ATAD2 expression was less in MRC-5 cells than hepatocytes (Fig. 4.9a). In order to further investigate ATAD2 expression, we tested its protein levels using a polyclonal rabbit anti-ATAD2 antibody that recognized a single major band in Hep3B HCC cells (Fig. 4.9b line Hep3B). The knock-down of ATAD2 by siRNA1 in these cells resulted in the loss of an anti-ATAD2 immunoreactive band (Fig. 4.9b line Hep3B-si), demonstrating the specificity of this antibody. ATAD2 protein was undetectable in normal hepatocytes, but highly abundant in six out of nine HCC cell lines, and easily detectable in the remaining three (Fig. 4.9b). In order to further investigate immortality-associated expression of ATAD2 in HCC cells, we induced senescence arrest in Huh7 cells by 0.1 mM Adriamycin treatment (Fig. 4.9c) as previously described [197], and compared ATAD2 expression between Adriamycin-treated and control Huh7 cells by western blot assay. We observed a drop in the levels of ATAD2 proteins in senescence-arrested cells, as compared to immortal Huh7 cells (Fig. 4.9d).

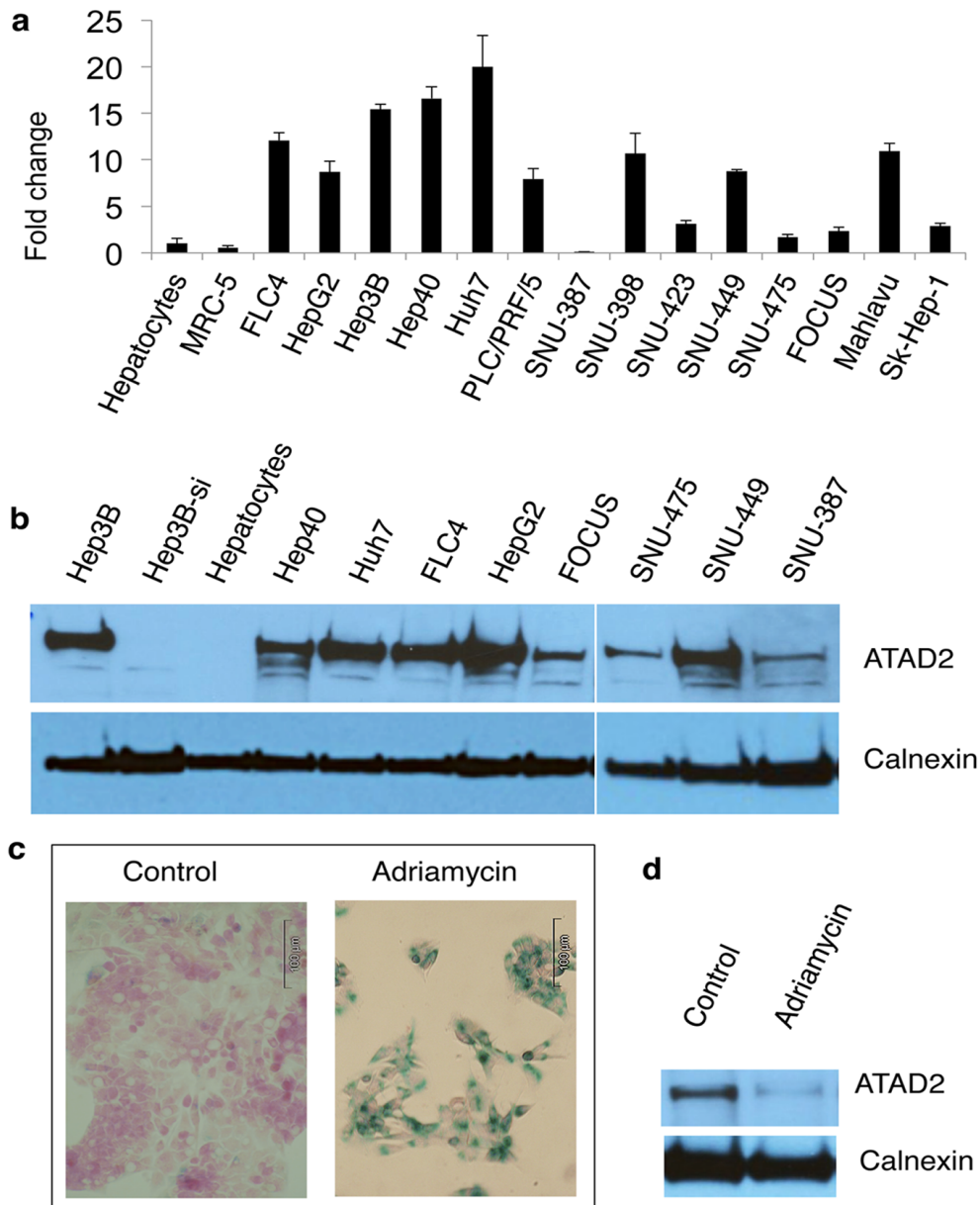


Figure 4.9: Association of ATAD2 RNA and protein expressions with HCC and cellular immortality: a) Amplified expression of ATAD2 RNA in HCC cell lines, as compared to normal hepatocytes and MRC-5 fibroblasts. Total RNAs were extracted from freshly isolated adult human hepatocytes (Hepatocytes), MRC-5 human embryonic lung fibroblast cells (PD44) and 14 HCC cell lines; reverse transcribed into cDNA; and ATAD2 RNA was quantified by quantitative real-time PCR using specific primers. ATAD2 expression values for each sample were normalized with housekeeping gene GAPDH RNA values. Relative expression of ATAD2 in MRC-5 and HCC cell lines was expressed in reference to its expression in hepatocytes. Averages of three measurements. Error bars: SD. b) Amplified expression of ATAD2 protein in HCC cells, as compared to normal hepatocytes. Total proteins were extracted from freshly isolated adult human hepatocytes (Hepatocytes), untreated (Hep3B) and ATAD2 siRNA1- treated (Hep3B-si) Hep3B and eight other HCC cell lines, and ATAD2 protein levels were tested by western blot analysis using a specific anti-ATAD2 antibody (ATAD2). Western blot analysis of calnexin protein from the same blots was used for loading control (Calnexin). c, d) Comparative analysis by western blotting demonstrated that ATAD2 protein is overexpressed in immortal Huh7 cells as compared to senescence-arrested Huh7 cells. c) Huh7 cells were treated with Adriamycin (0.1 mM) or DMSO (Control) for three days and subjected to senescence assay by SA-b-Gal staining (blue). Cells were counterstained with fast red (red). d) Total protein was extracted from control and Adriamycin-treated Huh7 cells, and ATAD2 and Calnexin proteins were tested as described in (b). Figures were adapted from reference 217.

4.2 Differential Expression of Epigenetic Regulatory Genes During Liver Carcinogenesis

4.2.1 Creating the epigenetic regulatory genes (EpiReg) list

As described in the introduction different epigenetic alterations have been observed during process of hepatocellular carcinogenesis. Although identification of these epigenetic alterations in HCC suggests that deregulation of epigenetic mechanisms is an important event of hepatocellular carcinogenesis, a comprehensive study is still lacking. Thus, in order to determine genome-wide expressional changes of different epigenetic players during liver carcinogenesis, we first generated a comprehensive list of epigenetic regulatory genes (EpiReg) as described in the materials and methods section.

To prepare the total EpiReg list, containing 1990 probe sets corresponding to 872 genes, we first included known histone and DNA code writer proteins (Histone methyltransferases, HMTs, Histone demethylases, HDMs, Histone acetyltransferases, HATs, Histone deacetylases, HDACs, DNA methyltransferases, DNMTs, and other histone modifier proteins such as histone ubiquitinating, histone phosphorylating proteins, etc.), histone and DNA code reader proteins (such as methylated CpG DNA binding proteins, and TUDOR domain containing reader proteins), histones (conventional and variant histones), histone chaperones, and other proteins with known chromatin regulatory functions (such as ARID1A, ARID2, SMARCD1). After that I included uncharacterized, conserved epigenetic regulatory function related protein domain containing putative genes to the EpiReg list to complete the list. Some examples of these genes are JMJC domain containing JMJD6, JMJD7, JMJD8 genes,

ankyrin repeat domain containing ANKS6, ACAP1, ANKFY1 genes, and pleckstrin homology domain (PHD) containing SHPRH, ZMYND8, ZMYND11 genes.

4.2.2 Differentially expressed EpiReg gene sets during cirrhosis to HCC transition

In order to determine significantly deregulated groups of epigenetic regulatory mechanisms in a critical step of liver carcinogenesis (cirrhosis to HCC transition), we first created EpiReg gene sets using the EpiReg gene list to be able to analyze the list via GSEA method (Table 4.4). Differential expressions of the gene sets were determined with separate analyzes of cirrhosis and HCC samples of two microarray datasets, Wurmbach [202] and Yildiz [213]. GSEA studies determined three group gene sets (Histone chaperones, HMTs and other modifiers) and four domain gene sets (SET, BROMO, SANT, and TUDOR domain) significantly enriched in both datasets according to their p values ($p < 0.05$) and false discovery rates ($FDR < 0.25$). All seven gene sets were enriched in HCC phenotype compared to cirrhosis phenotype in both datasets (Table 4.5).

Table 4.4. EpiReg gene sets and number of genes in each gene set used in GSEA studies:

EPIREG Domain Genesets	Size	EPIREG Group Genesets	Size
BROMO	40	Chaperone	16
CHROMO	33	Code Reader	482
PHD	181	Histone	83
SANT	53	HMT	60
TUDOR	25	Other Modifier	49
WD40	17	Other	55
SET	51	DNADEM	6
Histone Domain	87	DNMT	6
AcTrfase	13	HAT	18
Ankyrin_rpt	222	HDAC	19
DNA Mtfase	5	HDEM	34
His_deacetylase	19	Me CpG DNA Binding	5
JMJ	7		
MBT	8		
Me CpG DNA Bnd	5		
MeTrfase	14		
PWWP	22		
Znf_CW	8		

Table 4.5. Significantly enriched EpiReg gene sets in cirrhosis and HCC samples of Wurmbach and Yildiz microarray datasets:

EPIREG Group Genesets	Size	Wurmbach HCC Vs. Cirrhosis		Yildiz HCC Vs. Cirrhosis	
		p-value	FDR value	p-value	FDR value
Histone chaperone	15	0.006	0.051	0.01	0.15
HMT	59	0.006	0.041	0.02	0.087
Other Modifier	47	0.008	0.029	0.029	0.083
EPIREG Domain Genesets					
SET	50	0.004	0.036	0.034	0.083
BROMO	34	0.04	0.107	0.045	0.089
SANT	42	0.043	0.108	0.047	0.104
TUDOR	20	<0.002	0.07	0.004	0.074

4.2.3 Differential expression of epigenetic regulatory genes in different stages of hepatocellular carcinogenesis

To determine whether certain epigenetic player groups are significantly deregulated as sets during different stages of liver carcinogenesis, we used lists of EpiReg gene sets and performed GSEA using Wurmbach et al.'s whole-genome gene expression microarray dataset [202], which includes normal liver, cirrhotic liver, dysplastic liver, early HCC, and advanced HCC samples. GSEA experiments revealed that generally EpiReg genes are differentially expressed as sets at each step during step-wise progression of liver carcinogenesis

Table:4.6: Differentially expressed EpiReg gene sets during different stages of human hepatocellular carcinogenesis: Significantly enriched ($p < 0.05$ and $FDR < 0.25$) and not significantly (N.S.) enriched gene sets were listed. Asterisks indicate enrichment in opposite direction (enriched in cirrhosis samples compared to dysplasia samples). Red color indicates significantly enriched gene sets among gene sets list of the Table 3.5.

Gene Sets	Size	N.I.L.	Cirrhosis	Cirrhosis	Dysplasia*	Early HCC	Early HCC	Advanced HCC
EPIREG Domain Gene sets	# of Genes	p/FDR values	p/FDR values	p/FDR values	p/FDR values	p/FDR values	p/FDR values	p/FDR values
SET	50	N.S.	N.S./0.23	N.S.	0.002/0.05		N.S.	
BROMO	34	N.S.	N.S.	N.S.	0.023/0.091		N.S.	
SANT	42	N.S.	N.S.	N.S.	0.002/0.082		N.S.	
CHROMO	27	N.S.	N.S.	N.S.	0.006/0.061		N.S./0.183	
PHD	143	N.S.	N.S.	N.S.	0.033/0.096		N.S.	
Ankyrin_rpt	169	N.S.	0.031/0.235		0.015/0.136		N.S.	
WD40	15	N.S.	0.029/0.219		N.S./0.129		N.S.	
PWWP	15	N.S.	0.032/0.242		N.S.		N.S.	
AcTrfase	8	N.S.	N.S./0.224		N.S.		N.S./0.238	
TUDOR	20	N.S.	N.S.		N.S./0.146		N.S.	
Histone Domain	80	N.S.	N.S.		N.S.		N.S./0.224	
MeTrfase	13	N.S.	N.S.		N.S.		N.S./0.244	
DNA Mtfase	4	N.S.	N.S.		N.S.		N.S./0.249	
MBT	8	N.S.	N.S.		N.S.		N.S.	
Znf_CW	6	N.S.	N.S.		N.S.		N.S.	
His_deacetylase	18	N.S.	N.S.		N.S.		N.S.	
JMJ	11	N.S.	N.S.		N.S.		N.S.	
Me CpG DNA Bnd	7	N.S.	N.S.		N.S.		N.S.	
EPIREG Group Gene sets								
Histone Chaperone	15	N.S.	N.S.		0.015/0.077		N.S./0.222	
Other Modifier	47	N.S.	N.S.		0.008/0.058		N.S.	
HMT	59	N.S.	N.S.		0.004/0.059		N.S.	
Code Reader	386	N.S.	N.S.		0.002/0.053		N.S.	
HAT	11	N.S.	N.S.		0.066/0.133		N.S.	
Other	49	N.S.	N.S.		N.S./0.124		N.S.	
Histone	76	N.S.	N.S.		N.S.		N.S./0.219	
DNADEM	3	N.S.	N.S.		N.S.		N.S.	
DNMT	5	N.S.	N.S.		N.S.		N.S.	
HDAC	18	N.S.	N.S.		N.S.		N.S.	
HDM	11	N.S.	N.S.		N.S.		N.S.	
Me CpG DNA Binding	5	N.S.	N.S.		N.S.		N.S.	

starting from cirrhotic liver till the advanced HCC, without a change during normal liver to cirrhotic liver transition (Table 4.6). These analyzes also revealed that EpiReg gene sets were up-regulated at each step of liver carcinogenesis from dysplasia to advanced HCC progression. Six of the seven common significantly deregulated gene sets between cirrhosis and HCC (Table 4.5) were also significantly enriched during dysplasia to early HCC transition step of the hepatocellular carcinogenesis (Table 4.6). The other significantly enriched genes sets were enriched generally in either cirrhosis to dysplasia transition or dysplasia to early HCC transition steps. Ankyrin_rpt, WD40 and PWWP domain gene sets were down-regulated as sets during cirrhosis to dysplasia transition (indicated with asterisk in Table 4.6); whereas CHROMO, PHD, Ankyrin_rpt, HMT and HAT gene sets were enriched in early HCC samples during dysplasia to early HCC transition.

4.2.4 Common core-enriched EpiReg genes of Wurmbach and Yildiz datasets

In order to investigate the driver genes of the similarities between two independent datasets, we determined common core enriched genes; genes make main contribution to significant enrichment result of a gene set. Figures 4.10 and 4.11 show common core enriched genes of six EpiReg groups in Wurmbach and Yildiz datasets. Identification of common core enriched genes revealed high similarity in core enriched genes in these two datasets. Among histone methyltransferase gene sets 25 genes were commonly core enriched in two datasets (25 out of 29 core enriched genes of Wurmbach samples, 86%, and 25 out of 35 genes of Yildiz samples, 71%, were common). The SET domain containing genes set, which is highly similar to HMT gene set had same 23 genes among core enriched genes, 23/26 (89%) and 23/30

(77%) in Wurmbach and Yildiz datasets, respectively. The highest similarity scores were observed in BROMO domain and SANT domain gene sets. All 21 core enriched BROMO domain genes and all 19 SANT domain genes of Yildiz dataset were also core enriched in Wurmbach dataset. Histone chaperone and other modifier gene sets also displayed high similarities in these two datasets (Figure 4.10, Figure 4.11). In addition to that, since these six epigenetic player gene sets also enriched in early HCC samples of the Wurmbach dataset compared to non-tumor dysplastic samples, we also determined core enriched genes of these gene sets in Wurmbach dataset (Figure 4.12).

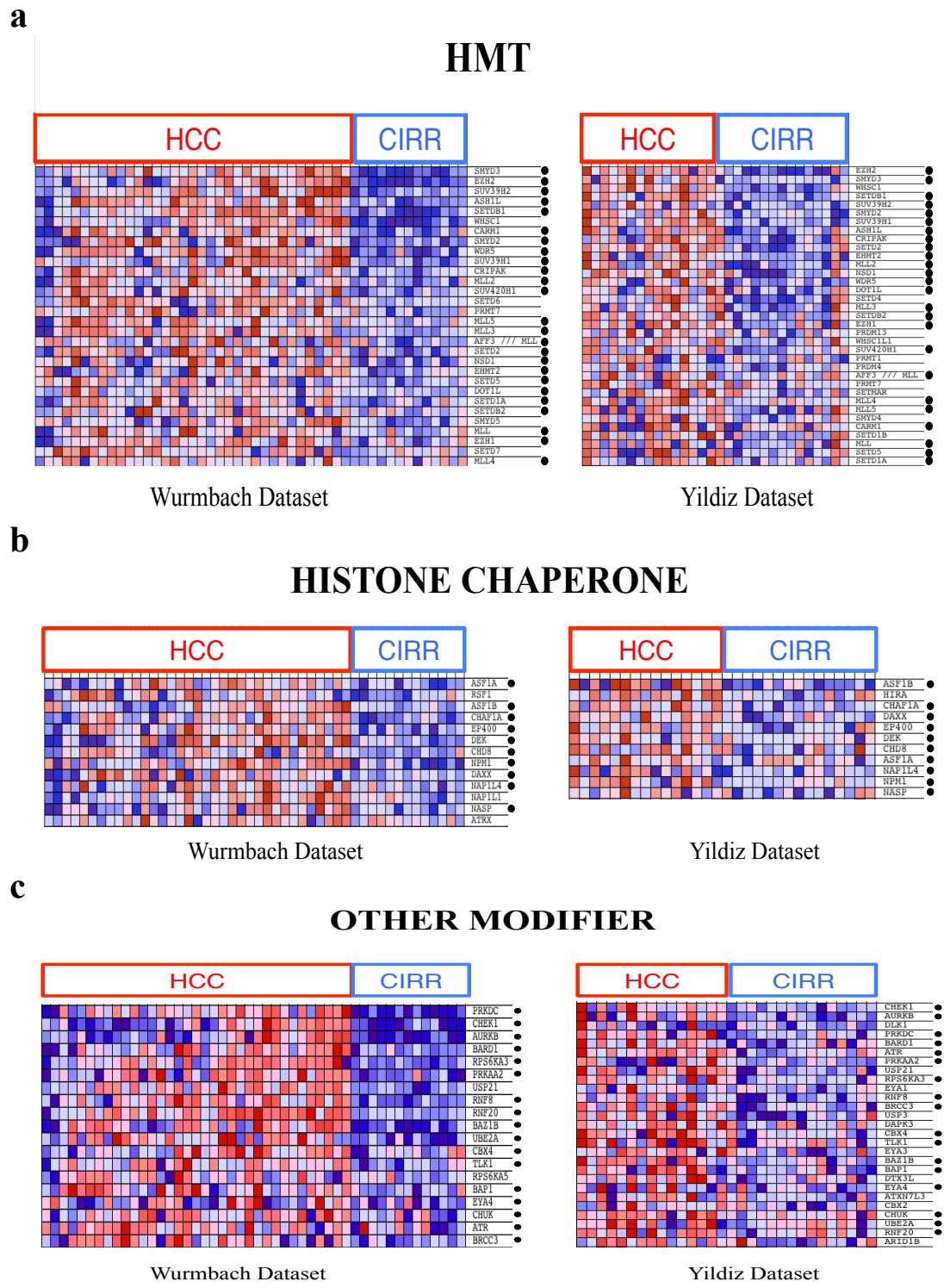
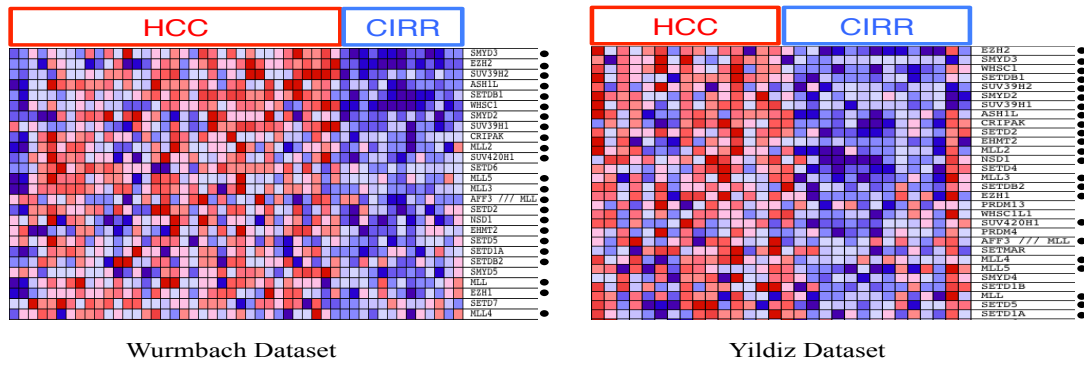


Figure 4.10: Commonly core enriched genes of the three significantly enriched EpiReg group gene sets in Wurmlich and Yildiz datasets: Only core enriched genes of a gene set were included heat maps. Red indicates up-regulation, blue indicate down-regulation of a gene. Black dots indicate common genes in gene sets of the two datasets. HCC: hepatocellular carcinoma, CIRR: cirrhosis.

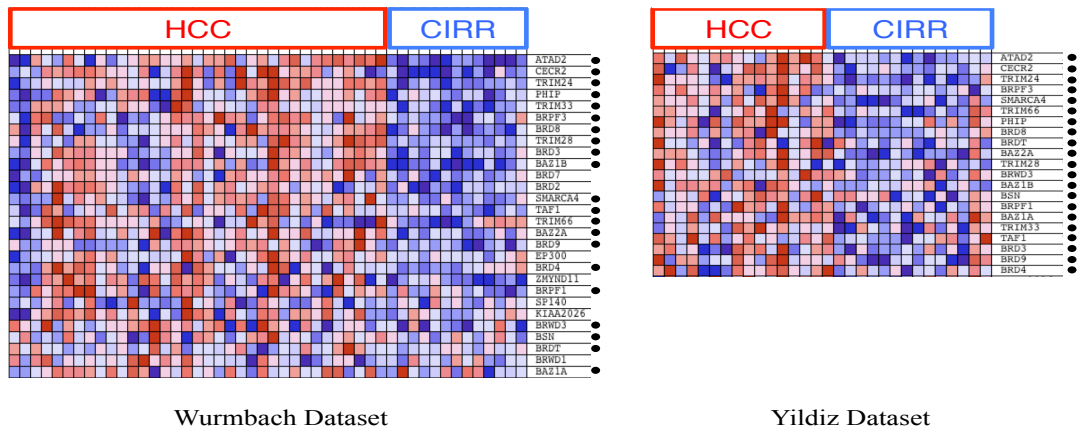
a

SET



b

BROMO



c

SANT

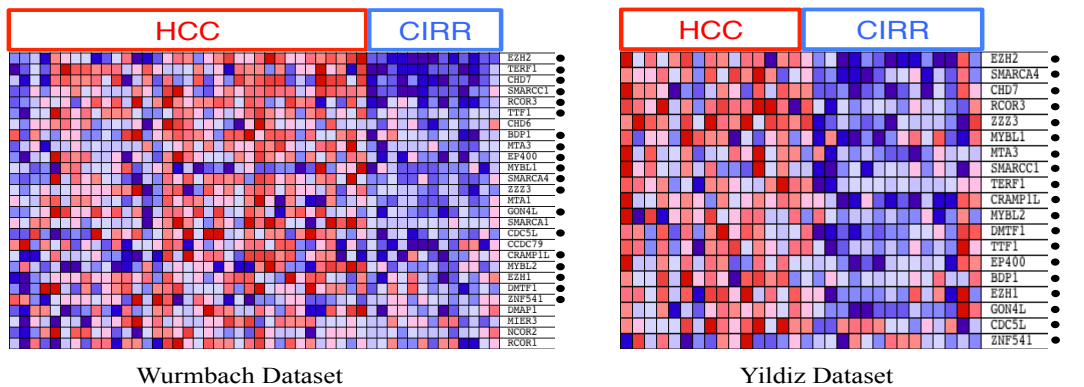


Figure 4.11: Commonly core enriched genes of the three significantly enriched EpiReg domain gene sets in Wurmback and Yildiz datasets: Only core enriched genes of a gene set were included heat maps. Red indicates up-regulation, blue indicate down-regulation of a gene. Black dots indicate common genes in gene sets of the two datasets. HCC: hepatocellular carcinoma, CIRR: cirrhosis.

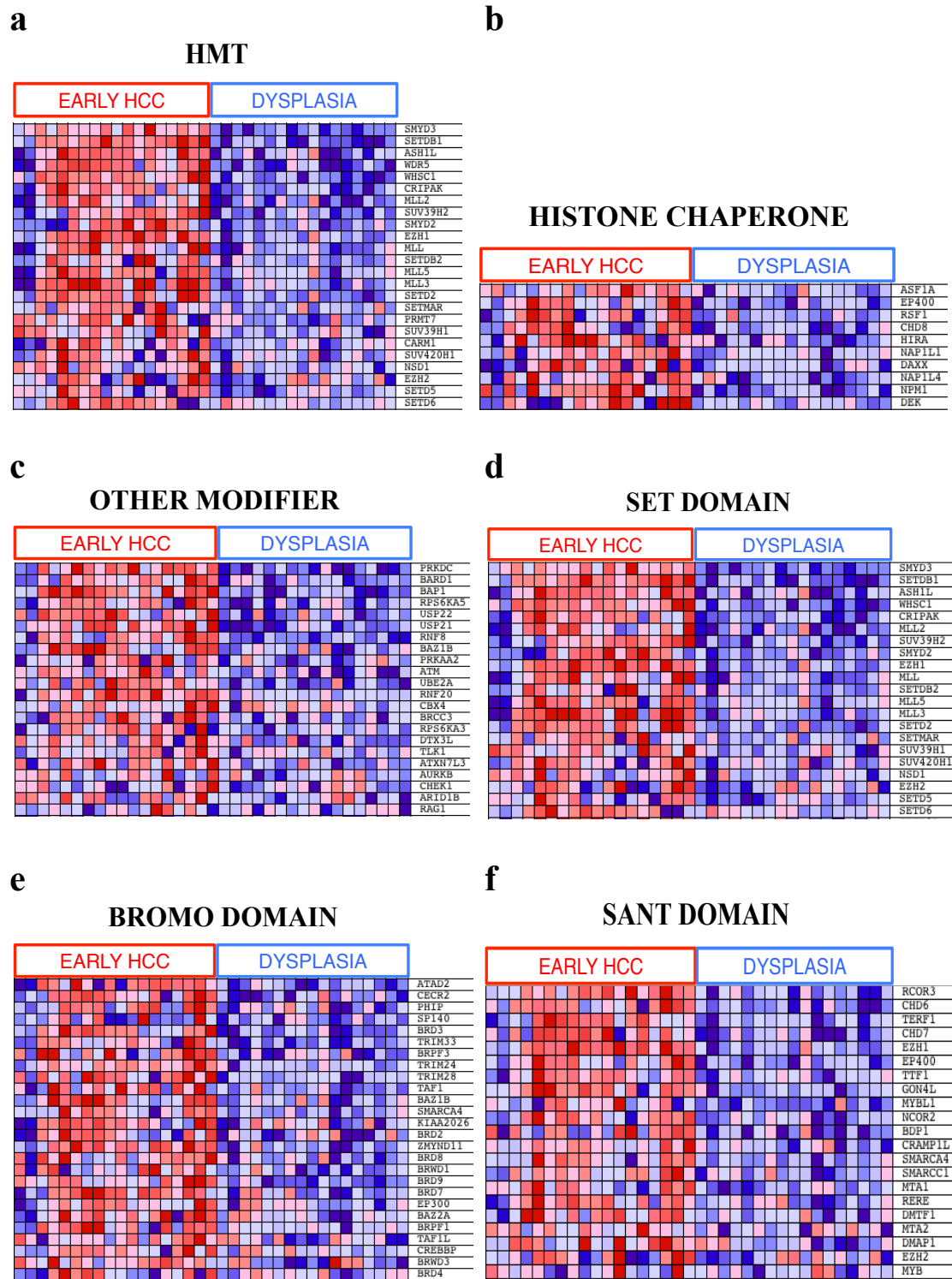


Figure 4.12: Core enriched genes of the six significantly enriched EpiReg group gene sets in early HCC and dysplasia comparison of the Wurmbach dataset: Only core enriched genes of a gene set were included heat maps. Red indicates up-regulation, blue indicate down-regulation of a gene. HCC: hepatocellular carcinoma.

4.3 N-Terminal tail coding sequences of H2A and H3 histone variants have no mutation in HCC

Last year a new epigenetic mechanism in cancer, amino acid substitution leading mutations in N-terminal tail encoding DNA sequences of histone H3 variant H3F3A had been identified in 31% of the pediatric glioblastoma samples [218]. These three somatic mutations (K27M, G34R/G34V) in histone H3 raised a new possibility in the field of molecular oncology that, histone code disrupting mutations could cause cancer.

Before checking whether histone variant encoding DNA sequences are also mutated in HCC, we first determined possible gene expression differences of the histone variants between cirrhosis and HCC samples. Gene expression patterns and consistencies of the histone variants in two independent datasets (Figure 4.13, Figure 4.14) suggested that histone variants could be important players in HCC.

Thus, we investigated possible amino acid substitution causing mutations in histone N-terminal tail coding DNA sequences of seven histone variants (H3F3A, H3F3B, CENPA, H2AFZ, H2AFV, H2AFY, H2AFY2) in HCC patient samples. Analyzes of PCR and sequencing results (from both forward and reverse directions) of 32 HCC samples could not detect consistent difference in any histone variants investigated, except one possible amino acid substitution leading mutation (ACC to TCC, Threonine to Serine) at 31. amino acid of histone H3 variant H3F3B in 31% of the samples investigated with readings from forward direction only (Figure 4.15a).

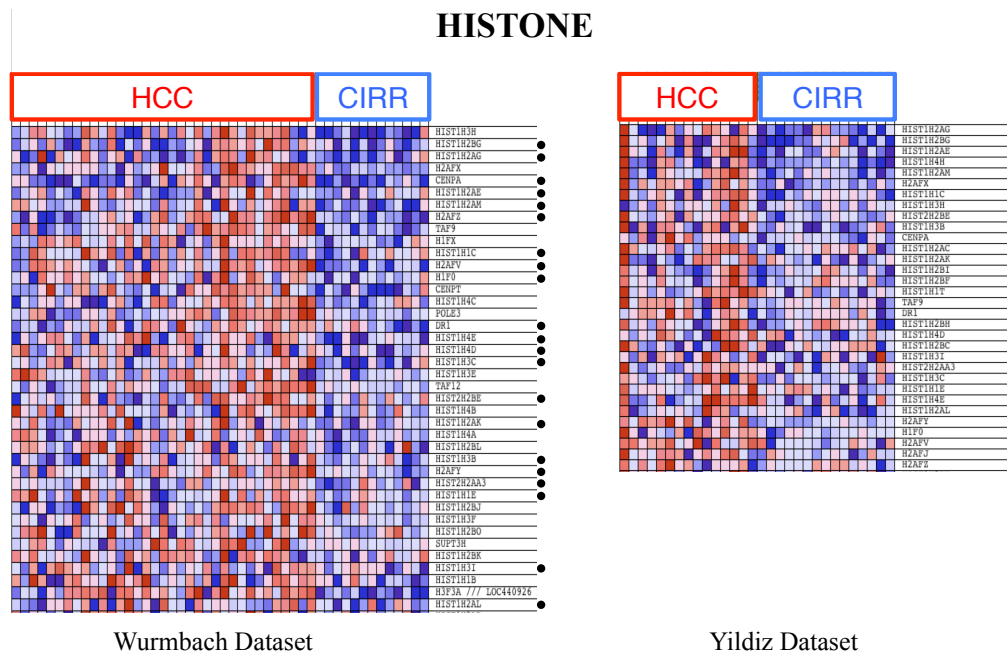
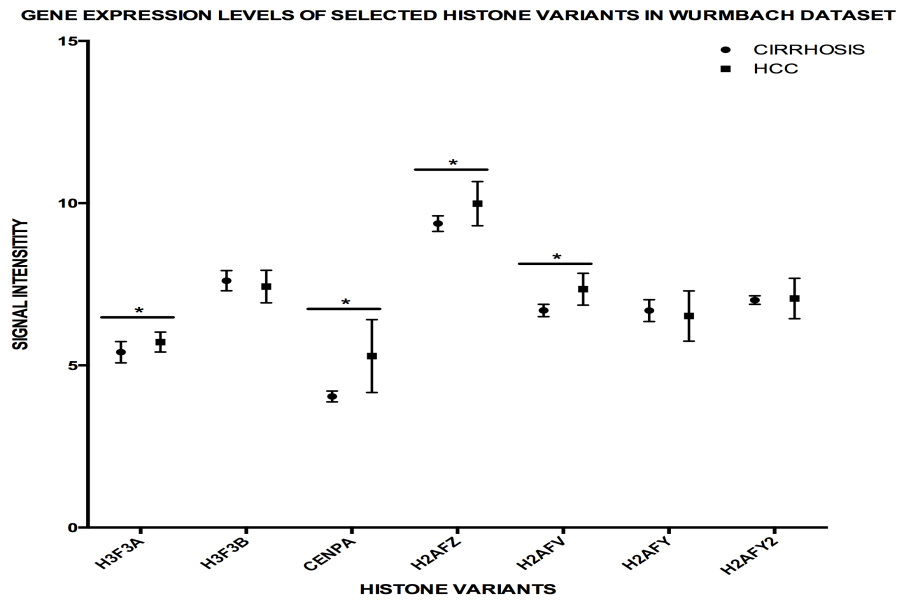


Figure 4.13: Core enriched genes of the Histone EpiReg gene set in Wurbach and Yildiz datasets: Some of the conventional and variant histones were core enriched and transcriptionally up-regulated in both datasets. Red indicates up-regulation, blue indicate down-regulation of a gene. Black dots indicate common genes in gene sets of the two datasets. HCC: hepatocellular carcinoma, CIRR: cirrhosis.

To validate this finding we determined two restriction enzymes (MboII, and EarI), which give different products from possible mutant and wild type (wt) samples with restriction enzyme digestion. However, restriction enzyme digestion experiments indicated that nucleotide differences determined via Sanger sequencing experiments were results of a consistent reading error occur in one reading direction (Figure 4.15b). In conclusion, we could not determine any amino acid substitution leading mutation in protein histone N-terminal tail region coding genomic DNA sequences of 7 histone variants in HCC samples investigated, as other researchers could not identify for other cancer types [218].

a



b

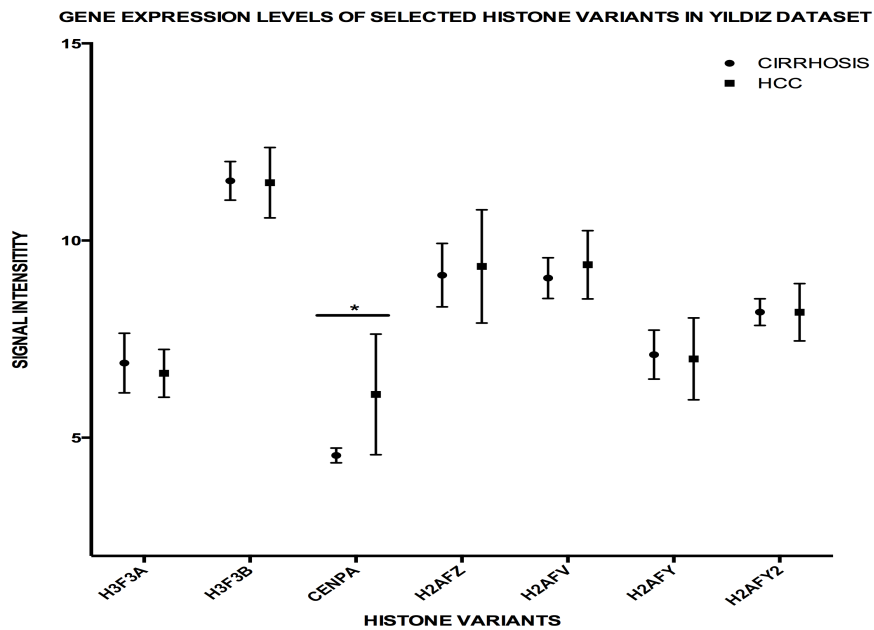
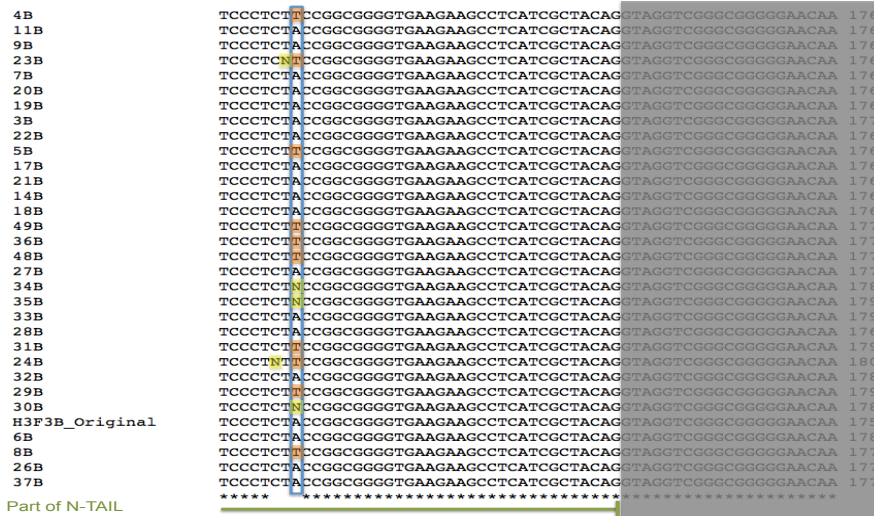


Figure 4.14: Cirrhosis versus HCC gene expression level comparisons of seven histone variants in Wurmbach and Yildiz datasets: Mean microarray gene expression signal intensities of seven histone variants in cirrhosis and HCC samples of the two datasets were calculated and compared. Asterisk indicated significant gene expression difference ($p < 0.05$), determined with the t-test method.

a



b

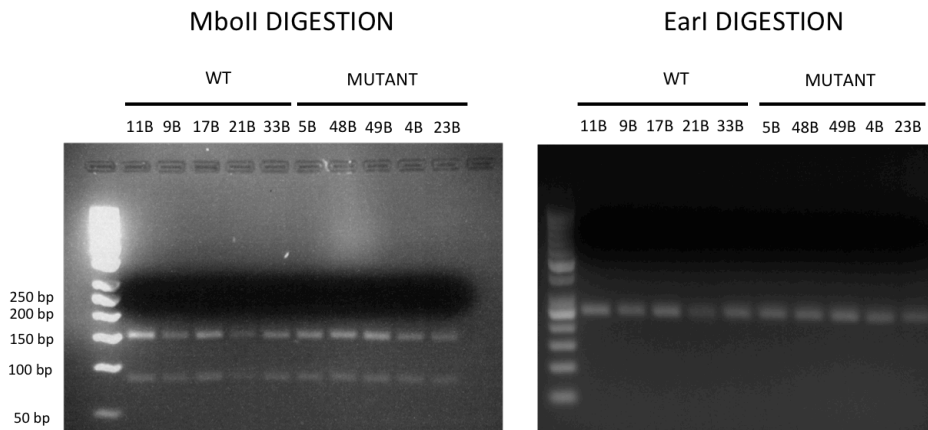


Figure 4.15: A possible amino acid substitution leading mutation in histone N-terminal encoding DNA sequences of Histone H3F3B: a) Multiple sequence alignment of amplified and sequenced region of H3F3B in 32 HCC samples revealed ACC to TCC (Threonine to Serine) mutation at 31. amino acid of histone H3 variant H3F3B in ten samples (31% of the samples) with reading results from forward direction. Green line indicates N-terminal tail encoding sequences. Blue box shows the differing region. Orange box shows possible mutant sequences. Yellow box shows the sequences could not be specified by the Sanger sequencing method, but identified manually. b) Mutation validation experiments by restriction enzymes digestions with selected five possible wild type (wt) and mutant samples did not present any difference. Total PCR product is 329 bas pairs (bp). EarI cuts only mutant and gives 125 bp and 104 bp product. MboII digests both wt and mutant. It gives 146 bp and 83 bp products for wt samples and 112 bp, 83 bp and 34 bp products for mutant samples.

CHAPTER 5

DISCUSSION

5.1 Genome-Wide Transcriptional Reorganization Associated with Senescence-to-Immortality Switch during Human Hepatocellular Carcinogenesis

Hepatocellular carcinogenesis is a multi-step progressive disease as explained in the introduction section [44]. Main steps of the hepatocellular carcinogenesis are transition of the normal liver to fibrotic liver, generation of fatty liver, cirrhosis, dysplastic liver and cancerous liver (mainly hepatocellular carcinoma). Cancerous

liver also progress from early HCC to advanced HCC, or well-differentiated HCC to poorly differentiated HCC [44].

Our current knowledge on hepatocellular carcinogenesis suggests that there are two main events in hepatocellular carcinogenesis: *i*) chronic inflammation, which is triggered by various factors that we know as HCC inducing factors, such as HBV infection, HCV infection, chronic alcohol consumption, and obesity [3, 44]. Briefly, chronic inflammation can be categorized as “initiative” process of molecular mechanisms, which cause hepatocellular carcinogenesis. *ii*) senescence escape and immortalization, which is the important event regulating transition of tumor-free cells to immortalized cancerous cells. Thus, senescence escape can be categorized as “critical” step of hepatocellular carcinogenesis, since non-dividing hepatocytes transform into immortal cancer cells in this step. My Ph.D. studies are sum of an attempt to understand distinct molecular mechanisms altering during senescence escape of hepatocytes, in order to better understand the critical step of the hepatocellular carcinogenesis.

Cellular senescence, considered for a long time to be an *in vitro* phenomenon, emerged in recent years as a critical mechanism that may play key roles in tissue aging as well as in the development of different tumor types [140]. Here, we used a unique *in vitro* hepatocellular senescence model to map senescence-related events associated with *in vivo* HCC development. Our *in vitro* model displayed a gene expression pattern compatible with replicative senescence and TERT-induced cellular immortalization, in conformation of our previously published observations [195]. We were fortunate to find a high number of differentially expressed genes between

senescent and immortal clones that served as an investigational tool to examine senescence-related transcriptional events occurring during hepatocellular carcinogenesis. Based on this, we provide here transcription-based evidence that cirrhosis and HCC represent two opposite cellular phenotypes, senescence and immortality, respectively. One of the major features of this phenotypic opposition was the status of telomere maintenance genes both between senescence and immortality, and cirrhosis and HCC (Figures. 3.1 and 3.2). The activation of TERT and telomere end extension genes in immortal and HCC phenotypes is of particular interest. Accelerated shortening of telomeres associated with a lack of telomerase activity and high cell turnover during chronic hepatitis has been recognized as a hallmark of cirrhosis several years ago [220, 221]. More recently, constitutional “loss-of-function” type of telomerase (*TERT* or *TERC* genes) mutations have been identified as a risk factor for cirrhosis [222, 223]. In contrast to cirrhosis, HCC is known to reactivate TERT expression [224], display high telomerase activity [225] and stabilize telomeres [219], [226]. Based on our present data supported by these earlier reports, we propose that the activation of telomerase activity is a key event for the gain of immortalized phenotype by HCC cells. Supporting this idea very recently, recurrent and activating *TERT* promoter mutations have been reported for HCC cell lines and tissues [116-118], in strong support of our hypothesis. More interestingly, we identified one of the mutations described in these publications, C228T mutation, in parental Huh7 cells and C1 immortal clones, but not in C3 senescent clones (data not shown). In addition to that, we determined that the C228T mutation in promoter of the TERT gene creates a suitable transcription factor binding domain for both (E-twenty six) ETS and (signal transducer and activator of transcription) STAT family proteins (data not shown). Thus, the difference in C228T mutation in immortal and senescent

clones used in my studies may provide an important clue in order to better understand the senescence escape mechanisms during hepatocellular carcinogenesis. However, further studies are needed.

The list of significantly enriched senescence and immortality related gene sets in the C2_ALL list in of *in vitro* and *in vivo* results indicate that eight and three senescence and immortality gene sets were enriched in *in vitro* and *in vivo* datasets, respectively. The significant enrichment results in correct *in vitro* phenotypes (genes found up-regulated in senescent cells or immortal cells by different researchers were also up-regulated or down-regulated our senescent or immortal samples) provided an important reliability to our *in vitro* datasets (Table 4.1; Fig. 4.2).

Considering the specific trait of our *in vitro* samples (senescent and immortal samples), the difference of numbers of enriched gene sets (eight versus three) between two datasets seems quite normal. In addition, two of the three gene sets enriched in the *in vivo* dataset, “TANG_SENESCENCE_TP53_TARGETS_UP” and “REACTOME_EXTENSION_OF_TELOMERES”, were common in two datasets, suggesting promising similarities between senescent and cirrhosis samples, as well as immortal and HCC samples.

The types of the commonly enriched gene sets in two dataset are also quite informative regarding to the mechanisms of cellular senescence and immortalization events of our samples. The “TANG_SENESCENCE_TP53_TARGETS_UP” gene set, containing p53-responsive genes up-regulated during replicative senescence arrest, was enriched in both senescent and cirrhosis samples. Since our senescent Huh7 cells were generated via the replicative senescence process (see materials and

methods), this enrichment result provided a reliability for the transcriptional profile-based analyses we were performing. In addition to that, enrichment of the replicative senescence gene sets in both senescence and cirrhosis samples among different senescence mechanisms (e.g., oncogene induced senescence, PTEN-loss induced senescence, etc.) also suggests that the replicative senescence is the major senescence process in cirrhosis samples during the hepatocellular carcinogenesis. The common enrichment of the gene set called “REACTOME_EXTENSION_OF_TELOMERES”, in immortal and HCC samples of the two datasets also suggests that the active mechanisms of extending the telomere ends are a critical event in HCC samples.

The transition from a senescent state to an immortal state coincided with early HCC lesions while dysplastic lesions remained associated with cirrhosis and normal liver sample groups indicating a non-immortal state (Figure 3.6). This pattern correlates with malignant transformation in other tissues where pre-neoplastic lesions display a senescent state from which neoplastic transformation emerges with a gain of phenotypic and molecular features that are linked to an immortal state [227].

Co-enrichment of a high number of gene sets in cirrhotic tissues and senescent cells as well as in HCCs and immortal cells was highly interesting. This finding further emphasized the biological evidence for a gain of immortal phenotype in human HCC. Among the gene sets co-enriched in HCC and immortal cells, cell cycle and DNA repair gene sets were at the top of the list (Figure 4.4b, Table 4.2).

Up-regulation of cell cycle and DNA repair genes in HCC is already known [202], [228]; and the over-expression of cell cycle genes in immortal cells is expected.

The up-regulation of DNA repair genes may serve as a mechanism to escape from DNA damage-induced senescence arrest by increasing DNA repair capacity of immortal or HCC cells. However, the situation might be more complex, according to the data of differentially up-regulated DNA repair and cell cycle mechanisms and genes in immortal and HCC phenotypes (Figure 4.4, Figure 5.1). Among three single-strand DNA damage repair mechanisms [229] only two of them, base excision repair (BER) and mismatch repair (MMR), were commonly up-regulated in immortal and HCC samples. In a similar vein, among three double strand break repair mechanisms (non-homologous end joining repair, microhomology mediated end joining and homologous recombination repair) [229] only homologous recombination (HR) gene sets were up-regulated commonly in immortal cells and HCC tissue samples (Figure 4.4a, Table 4.2). The list of at least five times commonly core enriched genes among selected common DNA repair and cell cycle gene sets (Figure 4.4b) indicates that despite the similarities in *in vitro* immortal cells and *in vivo* HCC tissue samples, *in vitro* and *in vivo* samples selectively up-regulates transcription of specific genes in certain mechanisms (Figure 5.1). For example, among core enriched DNA damage signal mediators *in vitro* HCC cells selectively up-regulates transcription of the Ataxia telangiectasia and Rad3 related (ATR) gene, whereas *in vivo* HCC cells have selective up-regulation of Ataxia telangiectasia mutated (ATM) gene. Although ATR is mostly associated with repair of single strand DNA breaks and ATM is mostly associated with repair of double strand DNA breaks [230], these transcriptional differences are indicative of a different mechanism; since both single strand and double strand DNA repair mechanisms are commonly active in both *in vitro* and *in vivo* HCC samples. Selective transcriptional differences also occur in DNA damage and cell cycle mechanisms. *In vitro* HCC cells selectively up-regulates gene

expression of certain genes of DNA damage repair mechanisms; whereas certain cell cycle mediator genes are repeatedly up-regulated only in *in vivo* HCC cells (Figure 5.1). Thus, selective repeated transcriptional up-regulation differences of certain DNA damage and cell cycle repair genes in *in vitro* and *in vivo* HCC samples might provide valuable insight information to better understand DNA repair and cell cycle mechanism alterations in HCC.

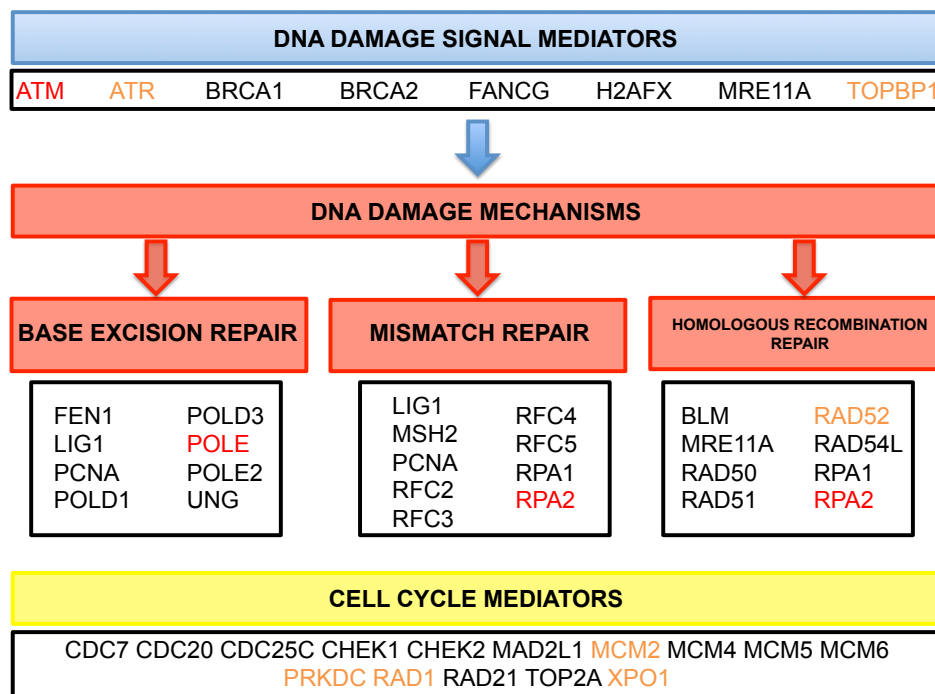


Figure 5.1: Genes core enriched at least five times in different common DNA repair and cell cycle gene sets of immortal or HCC samples: Determined genes were categorized according to their functional groups using their data on KEGG (www.genome.jp/kegg/) and Genecards (genecards.org) databases. Gene symbols in black color indicate core enrichment in both phenotypes. Genes in red indicate a repeatedly core enriched gene only *in vitro* immortal samples. Genes in orange color indicate a repeatedly core enriched gene only in *in vivo* HCC samples.

Another interesting outcome of co-enrichment analysis was the differential association of metabolism regulatory gene sets with cirrhosis/senescence and HCC/immortality phenotypes. Co-enrichment patterns revealed that genes involved in glycolysis as well as those regulating drug, lipid and retinol metabolisms were down-regulated in both immortal cells and HCC tumors. Down-regulation of genes encoding the enzymes necessary for retinoic acid biosynthesis and intracellular retinoid storage in HCC is of particular interest. Retinoic acid, which is the active metabolite of retinoids, regulates a wide range of biological processes including development, differentiation, proliferation, and apoptosis [231]. Normal hepatocytes together with hepatic stellate cells play an indispensable role in the availability of retinoic acid and the storage of dietary retinoids [232]. Deregulated expression of retinoid metabolism genes in HCC is expected to cause a deficit in the synthesis of retinoic acid as well as in the storage of its metabolic precursors (Figure 4.5). Accordingly, reduced retinoid content has been reported for HCC [232-234]. A deficit in cellular retinoic acid levels in HCC cells, due to the expression changes reported here, may cause severe perturbations in a multitude of cellular processes governed by retinoic acid [231] by conferring a survival advantage to immortalized HCC cells. Thus the restoration of retinoic acid availability in HCC cells may adversely affect their survival. In favor of this hypothesis, treatment with a synthetic analog of retinoic acid successfully prevented second primary tumors in post-surgical HCC patients [235]. Thus, a deficit in the availability of endogenous retinoic acid might facilitate malignant transformation and tumor progression.

The most important risk factor for HCC is cirrhosis that is present in 80 to 90% of patients with HCC [3]. The patients with cirrhosis develop HCC with a rate of 1.4–3.3% per year [3]. Therefore, the screening of cirrhotic patients by

ultrasonography of the liver combined with measurement of serum alpha-fetoprotein levels every 6 to 12 months for HCC development is recommended. However, the strength of the evidence supporting the efficacy of surveillance is modest [110]. To overcome the lack of efficacy, molecular HCC diagnosis techniques have been proposed [236]. Previously reported molecular techniques used either candidate genes [237] or genome-wide expression data [202, 224, 238, 239] to discriminate HCC from cirrhosis or dysplasia. None of these molecular tests have yet to enter into surveillance recommendations [236], probably because their prediction strength did not reach the required level and/or they require simultaneous analysis of dozens, even hundreds, of genes. Here, we provide a highly promising hepatocellular immortality signature test for HCC diagnosis. This novel molecular test requires the expression profiles of only 15 genes. Moreover, this is a functional test based on the analysis of senescence- and immortality-associated genes in tissue samples. The test was able to correctly predict 100% of cirrhosis cases. Twenty percent of HCCs displayed a borderline gene expression pattern, so that the classifier was not able to categorize them as HCC or cirrhosis. However, the test was able to predict the remaining HCC patients with 97.5% accuracy.

Literature investigation of the 15 genes hepatocellular immortality signature list had lead us to further analyze ATAD2 gene for several reasons (Table 5.1). We wanted to further analyze a gene up-regulated in HCC and immortal cells. This aim narrowed down our list to five genes (ATAD2, TOP2A, CCNE2, FAM83D and CRNDE). Since CRNDE was a gene encoding a large non-coding RNA, but not a protein [240] we also excluded this gene. Among the remaining four genes TOP2A and CCNE2 genes and their protein products had already been well characterized in HCC [241, 242]. In addition to that, FAM83D was a characterized cytoplasmic,

spindle pole related protein, which could not be directly related to the genome-wide transcriptional alterations during senescence escape processes. Thus, finally we decided to focus on ATAD2 in the 15 genes list, which was up-regulated in HCC, encoded in a well-known amplified genomic region (chromosome 8q24), chromatin remodeling protein domain containing, nucleus protein [http://www.ncbi.nlm.nih.gov/gene/29028].

Table 5.1: Table of 15 genes hepatocellular immortality signature test list: Official gene symbols, either up-regulated in HCC or cirrhosis, encoded from a well-known amplified genomic location, either encoding a protein or not, cellular component of the encoded protein and cellular processes of the encoded protein are listed. N.A: Not available.

SYMBOL	UP IN HCC	AMPLIFIED REGION	PROTEIN CODING	CELLULAR COMPONENT	CELLULAR PROCESS
ATAD2	YES	YES	YES	Nucleus	Regulation of DNA dependent transcription
TOP2A	YES	YES	YES	Nucleus	Mitotic cell cycle, DNA replication, DNA repair
CCNE2	YES	YES	YES	Cytosol	cell cycle checkpoint
FAM83D	YES	YES	YES	Cytoplasm, spindle pole	Cell division, mitosis
CRNDE	YES	NO	NO	N.A.	N.A.
EPCAM	NO	NO	YES	Cell surface	Positive regulation of cell proliferation
TMEM27	NO	NO	YES	Integral to membrane	Proteolysis
TFPI2	NO	YES	YES	Extracellular matrix	Blood coagulation
FOS	NO	NO	YES	Cytosol, nucleus	Inflammatory response, transcription factor activity
NAT2	NO	NO	YES	Cytosol	Xenobiotic metabolic process
GPR128	NO	NO	YES	Plasma membrane	G-protein coupled receptor signaling pathway
CYP39A1	NO	YES	YES	ER membrane	Bile acid metabolic process
FAM134B	NO	YES	YES	Golgi and ER	Sensory perception of pain
SDCBP2	NO	NO	YES	Cytoplasm, plasma membrane	Intracellular signal transduction
MUM1L1	NO	NO	YES	Nucleus	N.A.

One of the hepatocellular immortality signature genes is ATAD2. By using techniques independent of microarray tools, we demonstrated *in vitro* that ATAD2 RNA and protein that are weakly present or not expressed in normal hepatocytes and fibroblasts are highly expressed in HCC cell lines. We also showed that ATAD2 protein levels go down in association with Adriamycin-induced senescence arrest in otherwise immortal Huh7 cells. ATAD2 protein is likely to be a chromatin modifier [214]. Its exact cellular function is unknown, but its overexpression in immortal cells, and in many cancer types [196, 243] is in favor of an essential role in tumor

malignancy. Finally, our preliminary findings suggest that hepatocellular immortality signature genes such as ATAD2 may serve as promising HCC biomarkers.

5.2 Differential Expression of Epigenetic Regulatory Genes During Liver Carcinogenesis

The initial research findings that liver cancer is one of the rare malignancies that can be induced by dietary restriction of methyl donors [244, 245] and high number of transcriptional alterations during senescence escape step of the liver carcinogenesis provided us clues regarding to crucial role of epigenetic mechanisms in liver cancer. Thanks to the increasing interest on the epigenetics research area in recent years, epigenetic changes during liver carcinogenesis have been studied extensively as the other diseases [114, 127, 129, 130]. So far, different deregulated epigenetic mechanisms have been identified in liver cancer including promoter DNA hypermethylation of tumor suppressor genes, hypomethylated conserved DNA elements, roles of several over-expressed and under-expressed noncoding RNAs, over-expressed histone modifying enzymes and mutated chromatin regulators [105]; however still more data are needed to understand epigenetic mechanisms of the liver carcinogenesis.

In order to understand transcriptional changes of epigenetics related genes during hepatocellular carcinogenesis, I started with generating a list of known and putative protein coding epigenetic regulatory (EpiReg) genes and analyzed them using two independent microarray gene expression datasets, one containing samples of five different stages of liver tissue types [202].

Using very stringent criteria (only gene sets significantly enriched in terms of both p value and FDR values in both datasets at the same time were considered as significantly enriched gene sets), we identified six out of 30 significantly deregulated gene sets in two independent cirrhosis and HCC samples containing datasets. Interestingly, all gene sets were enriched in HCC samples, suggesting increased activities of epigenetic mechanisms in cancerous liver samples. Enrichments of both SET domain and TUDOR domain containing protein groups, which recognize specific methylated lysine residues of histones, as well as HMT proteins, which enzymatically catalyze transfer of methyl moieties to lysine residues of histones, suggest increase of histone methylation patterns in HCC cells compared to cirrhotic hepatocytes. Furthermore, transcriptional up-regulation of genes encoding BROMO domain containing proteins, which bind to acetylated histones, SANT domain containing proteins, which bind to unmethylated lysines, and other modifiers, which contains histone ubiquitinases and kinases, as groups in HCC samples also suggest that different histone code modifications increase in liver cancer. In addition to these alterations, significant enrichment of histone chaperones in two datasets might be correlated with increase cell proliferation and increase need of histone deposition in HCC cells.

In order to determine deregulated epigenetic mechanisms during multi-step progression of hepatocellular carcinogenesis, we performed similar pair-wised GSEA experiments using samples of the Wurmbach dataset. These analyzes revealed several results:

- i)* A significant enrichment of EpiReg gene sets does not occur during normal liver to cirrhotic liver transition step of the hepatocellular carcinogenesis.
- ii)* Significant enrichments of epigenetic gene sets start at cirrhosis to dysplasia transition, but with a negative enrichment in more advanced stage. Since these enriched gene sets are methylated lysine binding domain gene sets (Ankyrin repeat, WD40, PWWP proteins) and it is known that heterochromatin formation with increased histone lysine methylation occurs in senescent-cirrhosis cells, significant down-regulations of these proteins might be related to preparation to transcriptional increase in dysplastic cells.
- iii)* The highest number of enrichment occurs during non-tumor to tumor transition (dysplasia to early HCC transition) step of the hepatocellular carcinogenesis. Six of the totally 11 significantly up-regulated genes were also enriched during cirrhosis to HCC transition. These results suggest that, during progression from non-tumor tissue to tumor tissue high number of epigenetic alterations occur in HCC and both dysplasia to HCC transition and cirrhosis to HCC transition (known two possible ways of hepatocellular carcinogenesis) are similar in terms of deregulated epigenetic mechanisms.
- iv)* During progression to curable early HCC step to incurable advanced HCC stage none of the epigenetic regulatory mechanisms are transcriptionally deregulated; suggesting that epigenetic alterations are mostly related to initiation of HCC, but not its progression.

Despite these findings, we could not determine any genetic abnormalities in histone N-terminal tail encoding genomic DNA sequences of HCC samples. The amino acid substitution leading mutations identified in childhood gliomas can be a unique feature of this cancer type, since other researchers also could not determine these mutations in several different cancer types [219]; or the same study should be repeated using hepatoblastoma patient samples, since the mutations were identified in glioblastomas but not in gliomas [218].

5.3 Future perspectives

The work provided here is results of an attempt to determine genome-wide transcriptional alterations based biological differences during cirrhosis to HCC, or senescence escape to immortality, transition step of the hepatocellular carcinogenesis. With this work we provided lists of important biological mechanisms as well as genes that need to be further analyzed, in order to better understand mechanism of senescence escape during hepatocellular carcinogenesis.

In order to better understand the molecular biology of liver carcinogenesis based on my findings, following studies will be quite beneficial:

- i)* Genes in the list of hepatocellular immortality signature test, especially ATAD2 and CRNDE, should be more analyzed with extensive wet-lab experiments.
- ii)* Determined deregulated metabolism pathways both *in vitro* and *in vivo* samples should be further studied. Retinol and lipid metabolisms should be priorities.

- iii) Even though deregulations of DNA repair and cell cycle mechanisms in HCC are already identified, specific mechanisms and selective transcriptional up-regulation of specific genes determined in *in vitro* and *in vivo* HCC samples will be helpful to identify previously unknown molecular mechanisms in terms of DNA repair in HCC.
- iv) Even though the data were not shown here we identified mutational difference in promoter region of TERT loci of senescent and immortal clones, which were used in the experiments described here. A possible scenario of transcriptional activation of the TERT gene in mutant hepatocytes by STAT proteins as a previously unidentified senescence escape molecular mechanism seems quite plausible. Thus, this hypothesis should be investigated with extensive wet-lab experiments.
- v) The predictive accuracy of the 15 gene test should be further tested with new independent and extensive tissue samples, if possible, in order to emphasize the predictive capacity of the test.
- vi) The high number of genes transcriptionally differed in senescent and immortal cells as well as cirrhosis and HCC tissue samples suggest that extensive epigenetic alterations, which are responsible for this result, occur during senescence escape. Results of our comprehensive epigenetic study with the EpiReg gene list were also suggesting this idea. In order to better determine and understand these epigenetic changes bioinformatics data should be further analyzed and supported with wet-lab experiments with use of patient tissue samples.

REFERENCES

1. Zhang DY, Friedman SL. (2012). Fibrosis-dependent mechanisms of hepatocarcinogenesis. *Hepatology*. 56:769-75.
2. Rahimi RS, Rockey DC. (2012). Complications of cirrhosis. *Curr. Opin. Gastroenterol.* 28:223-9.
3. El-Serag HB. (2012). Epidemiology of viral hepatitis and hepatocellular carcinoma. *Gastroenterology*. 142:1264-1273.e1.
4. Schuppan D, Pinzani M. (2012). Anti-fibrotic therapy: lost in translation? *J. Hepatol.* 56. Suppl 1:S66-74.
5. Angulo P. Non Alcoholic Fatty Liver Disease. (2002). *N. Eng. J. Med.* 346:1221-31.
6. Fattovich G, Stroffolini T, Zagni I, Donato F. (2004). Hepatocellular carcinoma in cirrhosis: incidence and risk factors. *Gastroenterology*. 127:S35-50.
7. Beasley RP, Hwang LY, Lin CC, Chien CS. (1981). Hepatocellular carcinoma and hepatitis B virus. A prospective study of 22 707 men in Taiwan. *Lancet*. 2:1129-33.
8. Arzumanyan A, Reis HM, Feitelson MA. (2013). Pathogenic mechanisms in HBV- and HCV-associated hepatocellular carcinoma. *Nat. Rev. Cancer*. 13:123-35.
9. Hussain SP, Schwank J, Staib F, Wang XW, Harris CC. (2007). TP53 mutations and hepatocellular carcinoma: insights into the etiology and pathogenesis of liver cancer. *Oncogene*. 26:2166-76.
10. Guyton, A.C. Textbook of medical physiology. 8th. Ed. Philadelphia: W.B. Saunders Co. (1991). p: 880-888.
11. Bechmann LP, Hannivoort RA, Gerken G, Hotamisligil GS, Trauner M, Canbay A. (2012). The interaction of hepatic lipid and glucose metabolism in liver diseases. *J. Hepatol.* 56:952-64.

12. Cole LK, Vance JE, Vance DE. (2012). Phosphatidylcholine biosynthesis and lipoprotein metabolism. *Biochim. Biophys. Acta.* 1821:754-61.
13. Schuppan D, Kim YO. (2013). Evolving therapies for liver fibrosis. *J Clin Invest.* 123:1887-901.
14. Friedman SL. (2010). Evolving challenges in hepatic fibrosis. *Nat. Rev. Gastroenterol. Hepatol.* 7:425-36.
15. van Zijl F, Mair M, Csiszar A, Schneller D, Zulehner G, Huber H, *et al.* (2009). Hepatic tumor-stroma crosstalk guides epithelial to mesenchymal transition at the tumor edge. *Oncogene.* 28:4022-33.
16. Georges PC, Hui JJ, Gombos Z, McCormick ME, Wang AY, Uemura M, *et al.* (2007). Increased stiffness of the rat liver precedes matrix deposition: implications for fibrosis. *Am. J. Physiol. Gastrointest. Liver Physiol.* 293:G1147-54.
17. Todorovic V, Rifkin DB. (2012). LTBPs, more than just an escort service. *J. Cell. Biochem.* 113:410-8.
18. Golden-Mason L, Madrigal-Estebas L, McGrath E, Conroy MJ, Ryan EJ, Hegarty JE, *et al.* (2008). Altered natural killer cell subset distributions in resolved and persistent hepatitis C virus infection following single source exposure. *Gut.* 57:1121-8.
19. Kawarabayashi N, Seki S, Hatsuse K, Ohkawa T, Koike Y, Aihara T, *et al.* (2000). Decrease of CD56(+)T cells and natural killer cells in cirrhotic livers with hepatitis C may be involved in their susceptibility to hepatocellular carcinoma. *Hepatology.* 32:962-9.
20. Ekstedt M, Franzén LE, Mathiesen UL, Thorelius L, Holmqvist M, Bodemar G, Kechagias S. (2006). Long-term follow-up of patients with NAFLD and elevated liver enzymes. *Hepatology.* 44:865-73.
21. Wang SN, Lee KT, Ker CG. (2010). Leptin in hepatocellular carcinoma. *World J. Gastroenterol.* 16:5801-9.
22. Marchesini G, Bugianesi E, Forlani G, Cerrelli F, Lenzi M, Manini R, *et al.* (2003). Nonalcoholic fatty liver, steatohepatitis, and the metabolic syndrome. *Hepatology.* 37:917-23.
23. Peng CY, Chien RN, Liaw YF. (2012). Hepatitis B virus-related decompensated liver cirrhosis: benefits of antiviral therapy. *J Hepatol.* 57:442-

50.

24. Rahimi RS, Rockey DC. (2012). Complications of cirrhosis. *Curr. Opin. Gastroenterol.* 28:223-9.
25. Roberts LR, Gores GJ. (2005). Hepatocellular carcinoma: molecular pathways and new therapeutic targets. *Semin. Liver Dis.* 25:212-25.
26. Somasundaram A, Venkataraman J. (2012). Antiviral treatment for cirrhosis due to hepatitis C: a review. *Singapore Med. J.* 53:231-5.
27. Venook AP, Papandreou C, Furuse J, de Guevara LL. (2010). The incidence and epidemiology of hepatocellular carcinoma: a global and regional perspective. *Oncologist.* 15 S5-S13.
28. Guidotti LG, Ishikawa T, Hobbs MV, Matzke B, Schreiber R, Chisari FV. (1996). Intracellular inactivation of the hepatitis B virus by cytotoxic T lymphocytes. *Immunity.* 4:25-36.
29. Fallot G, Neuveut C, Buendia MA. (2012). Diverse roles of hepatitis B virus in liver cancer. *Curr. Opin. Virol.* 2:467-73.
30. Ke PY, Chen SS. (2012). Hepatitis C virus and cellular stress response: implications to molecular pathogenesis of liver diseases. *Viruses.* 4:2251-90.
31. Machida K, McNamara G, Cheng KT, Huang J, Wang CH, Comai L, *et al.* (2010). Hepatitis C virus inhibits DNA damage repair through reactive oxygen and nitrogen species and by interfering with the ATM-NBS1/Mre11/Rad50 DNA repair pathway in monocytes and hepatocytes. *J. Immunol.* 185:6985-98.
32. Park SH, Jung JK, Lim JS, Tiwari I, Jang KL. (2011). Hepatitis B virus X protein overcomes all-trans retinoic acid-induced cellular senescence by downregulating levels of p16 and p21 via DNA methylation. *J. Gen. Virol.* 92:1309-17.
33. Lim JS, Park SH, Jang KL. (2012). Hepatitis C virus Core protein overcomes stress-induced premature senescence by down-regulating p16 expression via DNA methylation. *Cancer Lett.* 321:154-61.
34. Zender L, Xue W, Zuber J, Semighini CP, Krasnitz A, Ma B, *et al.* (2008). An oncogenomics-based in vivo RNAi screen identifies tumor suppressors in liver cancer. *Cell.* 135:852-64.
35. Zhang Y, Proenca R, Maffei M, Barone M, Leopold L, Friedman JM. (1994).

- Positional cloning of the mouse obese gene and its human homologue. *Nature*. 372:425-32.
36. Cheung O, Sanyal AJ. (2010). Recent advances in nonalcoholic fatty liver disease. *Curr. Opin. Gastroenterol.* 26:202-8.
 37. Day CP, James OF. (1998). Steatohepatitis: a tale of two "hits"? *Gastroenterology*. 114:842-5.
 38. Browning JD, Horton JD. (2004). Molecular mediators of hepatic steatosis and liver injury. *J. Clin. Invest.* 114:147-52.
 39. Wang SN, Lee KT, Ker CG. (2010). Leptin in hepatocellular carcinoma. *World J. Gastroenterol.* 16:5801-9.
 40. Brooks PJ, Theruvathu JA. (2005). DNA adducts from acetaldehyde: implications for alcohol-related carcinogenesis. *Alcohol*. 35:187-93.
 41. McClain CJ, Hill DB, Song Z, Deaciuc I, Barve S. (2002). Monocyte activation in alcoholic liver disease. *Alcohol*. 27:53-61.
 42. Hoek JB, Pastorino JG. (2002). Ethanol, oxidative stress, and cytokine-induced liver cell injury. *Alcohol*. 27:63-8.
 43. Balasubramaniyan V, Murugaiyan G, Shukla R, Bhonde RR, Nalini N. (2007). Leptin downregulates ethanol-induced secretion of proinflammatory cytokines and growth factor. *Cytokine*. 37:96-100.
 44. Farazi PA, DePinho RA. (2006). Hepatocellular carcinoma pathogenesis: from genes to environment. *Nat. Rev. Cancer*. 6:674-87.
 45. Mínguez B, Tovar V, Chiang D, Villanueva A, Llovet JM. (2009). Pathogenesis of hepatocellular carcinoma and molecular therapies. *Curr. Opin. Gastroenterol.* 25:186-94.
 46. Villanueva A, Newell P, Chiang DY, Friedman SL, Llovet JM. (2007). Genomics and signaling pathways in hepatocellular carcinoma. *Semin. Liver Dis.* 27:55-76.
 47. Grivennikov SI, Karin M. (2010). Dangerous liaisons: STAT3 and NF-kappaB collaboration and crosstalk in cancer. *Cytokine Growth Factor Rev.* 21:11-9.
 48. Bollrath J, Greten FR. (2009). IKK/NF-kappaB and STAT3 pathways: central signalling hubs in inflammation-mediated tumour promotion and metastasis.

EMBO Rep. 10:1314-9.

49. Ghosh S, Karin M. (2002). Missing pieces in the NF-kappaB puzzle. *Cell.* 109:S81-96.
50. Vallabhapurapu S, Karin M. (2009). Regulation and function of NF-kappaB transcription factors in the immune system. *Annu. Rev. Immunol.* 27:693-733.
51. Beg AA, Sha WC, Bronson RT, Ghosh S, Baltimore D. (1995). Embryonic lethality and liver degeneration in mice lacking the RelA component of NF-kappa B. *Nature.* 376:167-70.
52. Doi TS, Marino MW, Takahashi T, Yoshida T, Sakakura T, Old LJ, Obata Y. (1999). Absence of tumor necrosis factor rescues RelA-deficient mice from embryonic lethality. *Proc. Natl. Acad. Sci. U S A.* 96:2994-9.
53. Pham CG, Bubici C, Zazzeroni F, Papa S, Jones J, Alvarez K, *et al.* (2004). Ferritin heavy chain upregulation by NF-kappaB inhibits TNFalpha-induced apoptosis by suppressing reactive oxygen species. *Cell.* 119:529-42.
54. Pikarsky E, Porat RM, Stein I, Abramovitch R, Amit S, Kasem S, *et al.* (2004). NF-kappaB functions as a tumour promoter in inflammation-associated cancer. *Nature.* 431:461-6.
55. Naugler WE, Sakurai T, Kim S, Maeda S, Kim K, Elsharkawy AM, Karin M. (2007). Gender disparity in liver cancer due to sex differences in MyD88-dependent IL-6 production. *Science.* 317:121-4.
56. He G, Yu GY, Temkin V, Ogata H, Kuntzen C, Sakurai T, *et al.* (2010). Hepatocyte IKKbeta/NF-kappaB inhibits tumor promotion and progression by preventing oxidative stress-driven STAT3 activation. *Cancer Cell.* 17:286-97.
57. Takeda K, Akira S. (2000). STAT family of transcription factors in cytokine-mediated biological responses. *Cytokine Growth Factor Rev.* 11:199-207.
58. Hirano T, Ishihara K, Hibi M. (2000). Roles of STAT3 in mediating the cell growth, differentiation and survival signals relayed through the IL-6 family of cytokine receptors. *Oncogene.* 19:2548-56.
59. Ogata H, Kobayashi T, Chinen T, Takaki H, Sanada T, Minoda Y, *et al.* (2006). Deletion of the SOCS3 gene in liver parenchymal cells promotes hepatitis-induced hepatocarcinogenesis. *Gastroenterology.* 131(1):179-93.
60. Rebouissou S, Amessou M, Couchy G, Poussin K, Imbeaud S, Pilati C, *et al.*

- (2009). Frequent in-frame somatic deletions activate gp130 in inflammatory hepatocellular tumours. *Nature*. 457:200-4.
61. Min L, He B, Hui L. (2011). Mitogen-activated protein kinases in hepatocellular carcinoma development. *Semin. Cancer Biol.* 21:10-20.
 62. Hasselblatt P, Rath M, Komnenovic V, Zatloukal K, Wagner EF. (2007). Hepatocyte survival in acute hepatitis is due to c-Jun/AP-1-dependent expression of inducible nitric oxide synthase. *Proc. Natl. Acad. Sci. U S A.* 104:17105-10.
 63. Tournier C, Hess P, Yang DD, Xu J, Turner TK, Nimnual A, *et al.* (2000). Requirement of JNK for stress-induced activation of the cytochrome c-mediated death pathway. *Science*. 288:870-4.
 64. Guo L, Guo Y, Xiao S, Shi X. (2005). Protein kinase p-JNK is correlated with the activation of AP-1 and its associated Jun family proteins in hepatocellular carcinoma. *Life Sci.* 77:1869-78.
 65. Hui L, Zatloukal K, Scheuch H, Stepniak E, Wagner EF. (2008). Proliferation of human HCC cells and chemically induced mouse liver cancers requires JNK1-dependent p21 downregulation. *J. Clin. Invest.* 118:3943-53.
 66. Chang Q, Zhang Y, Beezhold KJ, Bhatia D, Zhao H, Chen J, Castranova V, Shi X, Chen F. (2009). Sustained JNK1 activation is associated with altered histone H3 methylations in human liver cancer. *J. Hepatol.* 50:323-33.
 67. De Smaele E, Zazzeroni F, Papa S, Nguyen DU, Jin R, Jones J, *et al.* (2001). Induction of gadd45beta by NF-kappaB downregulates pro-apoptotic JNK signalling. *Nature*. 414:308-13.
 68. Papa S, Zazzeroni F, Bubici C, Jayawardena S, Alvarez K, Matsuda S, *et al.* (2004). Gadd45 beta mediates the NF-kappa B suppression of JNK signalling by targeting MKK7/JNKK2. *Nat. Cell. Biol.* 6:146-53.
 69. Hirosumi J, Tuncman G, Chang L, Görgün CZ, Uysal KT, Maeda K, *et al.* (2002). A central role for JNK in obesity and insulin resistance. *Nature*. 420:333-6.
 70. Cuenda A, Rousseau S. (2007). p38 MAP-kinases pathway regulation, function and role in human diseases. *Biochim. Biophys. Acta.* 1773:1358-75.
 71. Remy G, Risco AM, Iñesta-Vaquera FA, González-Terán B, Sabio G, Davis RJ, Cuenda A. (2010). Differential activation of p38MAPK isoforms by

MKK6 and MKK3. *Cell Signal.* 22:660-7.

72. Kim S, Kim HY, Lee S, Kim SW, Sohn S, Kim K, Cho H. (2007). Hepatitis B virus x protein induces perinuclear mitochondrial clustering in microtubule- and Dynein-dependent manners. *J. Virol.* 81:1714-26.
73. Spaziani A, Alisi A, Sanna D, Balsano C. (2006). Role of p38 MAPK and RNA-dependent protein kinase (PKR) in hepatitis C virus core-dependent nuclear delocalization of cyclin B1. *J. Biol. Chem.* 281:10983-9.
74. Hui L, Bakiri L, Mairhorfer A, Schweifer N, Haslinger C, Kenner L, *et al.* (2007). p38alpha suppresses normal and cancer cell proliferation by antagonizing the JNK-c-Jun pathway. *Nat. Genet.* 39:741-9.
75. Meloche S, Pouyssegur J. (2007). The ERK1/2 mitogen-activated protein kinase pathway as a master regulator of the G1- to S-phase transition. *Oncogene.* 26:3227-39.
76. Tran SE, Holmstrom TH, Ahonen M, Kahari VM, Eriksson JE. (2001). MAPK/ERK overrides the apoptotic signaling from Fas, TNF, and TRAIL receptors. *J. Biol. Chem.* 276:16484-90.
77. You H, Ding W, Dang H, Jiang Y, Rountree CB. (2011). c-Met represents a potential therapeutic target for personalized treatment in hepatocellular carcinoma. *Hepatology.* 54:879-89.
78. Beer DG, Neveu MJ, Paul DL, Rapp UR, Pitot HC. (1988). Expression of the c-raf protooncogene, gamma-glutamyltranspeptidase, and gap junction protein in rat liver neoplasms. *Cancer Res.* 48:1610-7.
79. Hwang YH, Choi JY, Kim S, Chung ES, Kim T, Koh SS, *et al.* (2004). Over-expression of c-raf-1 proto-oncogene in liver cirrhosis and hepatocellular carcinoma. *Hepatol Res.* 29:113-121.
80. Huynh H, Nguyen TT, Chow KH, Tan PH, Soo KC, Tran E. (2003). Over-expression of the mitogen-activated protein kinase (MAPK) kinase (MEK)-MAPK in hepatocellular carcinoma: its role in tumor progression and apoptosis. *BMC Gastroenterol.* 3:19.
81. Bessard A, Frémin C, Ezan F, Fautrel A, Gailhouste L, Baffet G. (2008). RNAi-mediated ERK2 knockdown inhibits growth of tumor cells in vitro and in vivo. *Oncogene.* 27:5315-25.
82. Gailhouste L, Ezan F, Bessard A, Frémin C, Rageul J, Langouët S, Baffet G.

- (2010). RNAi-mediated MEK1 knock-down prevents ERK1/2 activation and abolishes human hepatocarcinoma growth in vitro and in vivo. *Int. J. Cancer*. 126:1367-77.
83. Henklova P, Vrzal R, Papouskova B, Bednar P, Jancova P, Anzenbacherova E, *et al.* (2008). SB203580, a pharmacological inhibitor of p38 MAP kinase transduction pathway activates ERK and JNK MAP kinases in primary cultures of human hepatocytes. *Eur. J Pharmacol*. 593:16-23.
84. Kudo M. (2011). Signaling pathway and molecular-targeted therapy for hepatocellular carcinoma. *Dig Dis*. 29:289-302.
85. Engelman JA. (2009). Targeting PI3K signalling in cancer: opportunities, challenges and limitations. *Nat. Rev. Cancer*. 9:550-62.
86. Zhou L, Huang Y, Li J, Wang Z. (2010). The mTOR pathway is associated with the poor prognosis of human hepatocellular carcinoma. *Med. Oncol*. 27:255-61.
87. Majumdar A, Curley SA, Wu X, Brown P, Hwang JP, Shetty K, *et al.* (2012). Hepatic stem cells and transforming growth factor β in hepatocellular carcinoma. *Nat. Rev. Gastroenterol. Hepatol*. 9:530-8.
88. Dooley S, ten Dijke P. (2012). TGF- β in progression of liver disease. *Cell Tissue Res*. 347:245-56.
89. Roth S, Michel K, Gressner AM. (1998). (Latent) transforming growth factor beta in liver parenchymal cells, its injury-dependent release, and paracrine effects on rat hepatic stellate cells. *Hepatology*. 27:1003-12.
90. Senturk S, Mumcuoglu M, GURSOY-YUZUGULLU O, CINGOZ B, AKCALI KC, OZTURK M. (2010). Transforming growth factor-beta induces senescence in hepatocellular carcinoma cells and inhibits tumor growth. *Hepatology*. 52:966-74.
91. Nejak-Bowen KN, Monga SP. (2011). Beta-catenin signaling, liver regeneration and hepatocellular cancer: sorting the good from the bad. *Semin. Cancer Biol*. 21:44-58.
92. Giles RH, van Es JH, Clevers H. (2003). Caught up in a Wnt storm: Wnt signaling in cancer. *Biochim. Biophys. Acta*. 1653:1-24.
93. Austinat M, Dunsch R, Wittekind C, Tannapfel A, Gebhardt R, Gaunitz F. (2008). Correlation between beta-catenin mutations and expression of Wnt-

- signaling target genes in hepatocellular carcinoma. *Mol. Cancer*. 18;7:21.
94. Fujie H, Moriya K, Shintani Y, Tsutsumi T, Takayama T, Makuuchi M, Kimura S, Koike K. (2001). Frequent beta-catenin aberration in human hepatocellular carcinoma. *Hepatol. Res*. 20:39-51.
 95. Kim YD, Park CH, Kim HS, Choi SK, Rew JS, Kim DY, *et al.* (2008). Genetic alterations of Wnt signaling pathway-associated genes in hepatocellular carcinoma. *J. Gastroenterol. Hepatol*. 23:110-8.
 96. Suzuki M, Shiraha H, Fujikawa T, Takaoka N, Ueda N, Nakanishi Y, *et al.* (2005). Des-gamma-carboxy prothrombin is a potential autologous growth factor for hepatocellular carcinoma. *J. Biol. Chem*. 280:6409-15.
 97. Gao J, Inagaki Y, Song P, Qu X, Kokudo N, Tang W. (2012). Targeting c-Met as a promising strategy for the treatment of hepatocellular carcinoma. *Pharmacol. Res*. 65:23-30.
 98. Suzuki K, Hayashi N, Yamada Y, Yoshihara H, Miyamoto Y, Ito Y, *et al.* (1994). Expression of the c-met protooncogene in human hepatocellular carcinoma. *Hepatology*. 20:1231-6.
 99. Ueki T, Fujimoto J, Suzuki T, Yamamoto H, Okamoto E. (1997). Expression of hepatocyte growth factor and its receptor c-met proto-oncogene in hepatocellular carcinoma. *Hepatology*. 25:862-6.
 100. Ke AW, Shi GM, Zhou J, Wu FZ, Ding ZB, Hu MY, *et al.* (2009). Role of overexpression of CD151 and/or c-Met in predicting prognosis of hepatocellular carcinoma. *Hepatology*. 49:491-503.
 101. Wang ZL, Liang P, Dong BW, Yu XL, Yu de J. (2008). Prognostic factors and recurrence of small hepatocellular carcinoma after hepatic resection or microwave ablation: a retrospective study. *J. Gastrointest. Surg*. 12:327-37.
 102. Kaposi-Novák P. (2009). Comparative genomic classification of human hepatocellular carcinoma. *Magy. Onkol*. 53:61-7.
 103. Whittaker S, Marais R, Zhu AX. (2010). The role of signaling pathways in the development and treatment of hepatocellular carcinoma. *Oncogene*. 29:4989-5005.
 104. Buckley AF, Burgart LJ, Sahai V, Kakar S. (2008). Epidermal growth factor receptor expression and gene copy number in conventional hepatocellular carcinoma. *Am. J. Clin. Pathol*. 129:245-51.

105. Finn RS, Zhu AX. (2009). Targeting angiogenesis in hepatocellular carcinoma: focus on VEGF and bevacizumab. *Expert Rev. Anticancer Ther.* 9:503-9.
106. Hoshida Y, Toffanin S, Lachenmayer A, Villanueva A, Minguez B, Llovet JM. (2010). Molecular classification and novel targets in hepatocellular carcinoma: recent advancements. *Semin. Liver Dis.* 30:35-51.
107. Han ZG. (2012). Functional genomic studies: insights into the pathogenesis of liver cancer. *Annu Rev. Genomics Hum. Genet.* 13:171-205.
108. Ozen C, Yildiz G, Dagcan AT, Cevik D, Ors A, Keles U, *et al.* (2013). Genetics and epigenetics of liver cancer. *N. Biotechnol.* 30:381-4.
109. Schlaeger C, Longerich T, Schiller C, Bewerunge P, Mehrabi A, Toedt G, *et al.* (2008). Etiology-dependent molecular mechanisms in human hepatocarcinogenesis. *Hepatology.* 47:511-20.
110. El-Serag HB. (2011). Hepatocellular carcinoma. *N. Engl. J. Med.* 365:1118-27.
111. Bressac B, Galvin KM, Liang TJ, Isselbacher KJ, Wands JR, Ozturk M. (1990). Abnormal structure and expression of p53 gene in human hepatocellular carcinoma. *Proc. Natl. Acad. Sci. U S A.* 87:1973-7.
112. de La Coste A, Romagnolo B, Billuart P, Renard CA, Buendia MA, Soubrane O, *et al.* (1998). Somatic mutations of the beta-catenin gene are frequent in mouse and human hepatocellular carcinomas. *Proc. Natl. Acad. Sci. U S A.* 95:8847-51.
113. Park WS, Dong SM, Kim SY, Na EY, Shin MS, Pi JH, *et al.* (1999). Somatic mutations in the kinase domain of the Met/hepatocyte growth factor receptor gene in childhood hepatocellular carcinomas. *Cancer Res.* 59:307-10.
114. Guichard C, Amaddeo G, Imbeaud S, Ladeiro Y, Pelletier L, Maad IB, *et al.* (2012). Integrated analysis of somatic mutations and focal copy number changes identifies key genes and pathways in hepatocellular carcinoma. *Nat Genet.* 44:694-8.
115. Fujimoto A, Totoki Y, Abe T, Boroevich KA, Hosoda F, Nguyen HH, *et al.* (2012). Whole-genome sequencing of liver cancers identifies etiological influences on mutation patterns and recurrent mutations in chromatin regulators. *Nat. Genet.* 44:760-4.

116. Horn S, Figl A, Rachakonda PS, Fischer C, Sucker A, Gast A, *et al.* (2013). TERT promoter mutations in familial and sporadic melanoma. *Science*. 339:959-61.
117. Huang FW, Hodis E, Xu MJ, Kryukov GV, Chin L, Garraway LA. (2013). Highly recurrent TERT promoter mutations in human melanoma. *Science*. 339:957-9.
118. Killela PJ, Reitman ZJ, Jiao Y, Bettegowda C, Agrawal N, Diaz LA Jr, *et al.* (2013). TERT promoter mutations occur frequently in gliomas and a subset of tumors derived from cells with low rates of self-renewal. *Proc. Natl. Acad. Sci. U S A*. 110:6021-6.
119. Liu WR, Shi YH, Peng YF, Fan J. (2012). Epigenetics of hepatocellular carcinoma: a new horizon. *Chin. Med J.(Engl)*. 125:2349-60.
120. Franchini DM, Schmitz KM, Petersen-Mahrt SK. (2012). 5-Methylcytosine DNA demethylation: more than losing a methyl group. *Annu. Rev. Genet.* 46:419-41.
121. Mandrekar P. (2011). Epigenetic regulation in alcoholic liver disease. *World J. Gastroenterol.* 17:2456-64.
122. Choi MS, Shim YH, Hwa JY, Lee SK, Ro JY, Kim JS, Yu E. (2003). Expression of DNA methyltransferases in multistep hepatocarcinogenesis. *Hum. Pathol.* 34:11-7.
123. Saito Y, Kanai Y, Sakamoto M, Saito H, Ishii H, Hirohashi S. (2001). Expression of mRNA for DNA methyltransferases and methyl-CpG-binding proteins and DNA methylation status on CpG islands and pericentromeric satellite regions during human hepatocarcinogenesis. *Hepatology*. 33:561-8.
124. Lu SC, Huang ZZ, Yang H, Mato JM, Avila MA, Tsukamoto H. (2000). Changes in methionine adenosyltransferase and S-adenosylmethionine homeostasis in alcoholic rat liver. *Am. J. Physiol. Gastrointest. Liver Physiol.* 279:G178-85.
125. Saito Y, Hibino S, Saito H. (2013). Alterations of epigenetics and microRNA in hepatocellular carcinoma. *Hepatol Res*. [Epub ahead of print].
126. Zhou J, Yu L, Gao X, Hu J, Wang J, Dai Z, *et al.* (2011). Plasma microRNA panel to diagnose hepatitis B virus-related hepatocellular carcinoma. *J. Clin. Oncol.* 29:4781-8.

127. Herceg Z, Paliwal A. (2011). Epigenetic mechanisms in hepatocellular carcinoma: how environmental factors influence the epigenome. *Mutat. Res.* 727:55-61.
128. Cai MY, Hou JH, Rao HL, Luo RZ, Li M, Pei XQ, *et al.* (2012). High expression of H3K27me3 in human hepatocellular carcinomas correlates closely with vascular invasion and predicts worse prognosis in patients. *Mol. Med.* 17:12-20.
129. Sasaki M, Ikeda H, Itatsu K, Yamaguchi J, Sawada S, Minato H, *et al.* (2008). The overexpression of polycomb group proteins Bmi1 and EZH2 is associated with the progression and aggressive biological behavior of hepatocellular carcinoma. *Lab. Invest.* 88:873-82.
130. Cheng AS, Lau SS, Chen Y, Kondo Y, Li MS, Feng H, *et al.* (2011). EZH2-mediated concordant repression of Wnt antagonists promotes β -catenin-dependent hepatocarcinogenesis. *Cancer Res.* 71:4028-39.
131. Au SL, Wong CC, Lee JM, Fan DN, Tsang FH, Ng IO, Wong CM. (2012). Enhancer of zeste homolog 2 epigenetically silences multiple tumor suppressor microRNAs to promote liver cancer metastasis. *Hepatology.* 56:622-31.
132. Yang L, He J, Chen L, Wang G. (2009). Hepatitis B virus X protein upregulates expression of SMYD3 and C-MYC in HepG2 cells. *Med. Oncol.* 26:445-51.
133. Osawa T, Muramatsu M, Wang F, Tsuchida R, Kodama T, Minami T, Shibuya M. (2011). Increased expression of histone demethylase JHDM1D under nutrient starvation suppresses tumor growth via down-regulating angiogenesis. *Proc. Natl. Acad. Sci. U S A.* 108:20725-9.
134. Wu LM, Yang Z, Zhou L, Zhang F, Xie HY, Feng XW, *et al.* (2010). Identification of histone deacetylase 3 as a biomarker for tumor recurrence following liver transplantation in HBV-associated hepatocellular carcinoma. *PLoS One.* 5:e14460.
135. Choi HN, Bae JS, Jamiyandorj U, Noh SJ, Park HS, Jang KY, *et al.* (2011). Expression and role of SIRT1 in hepatocellular carcinoma. *Oncol. Rep.* 26:503-10.
136. Boyarchuk E, Montes de Oca R, Almouzni G. (2011). Cell cycle dynamics of histone variants at the centromere, a model for chromosomal landmarks.

Curr. Opin. Cell Biol. 23:266-76.

137. Li Y, Zhu Z, Zhang S, Yu D, Yu H, Liu L, *et al.* (2011). ShRNA-targeted centromere protein A inhibits hepatocellular carcinoma growth. *PLoS One.* 6:e17794.
138. Rappa F, Greco A, Podrini C, Cappello F, Foti M, Bourgoin L, *et al.* (2013). Immunopositivity for histone macroH2A1 isoforms marks steatosis-associated hepatocellular carcinoma. *PLoS One.* 8:e54458.
139. Itahana K, Campisi J, Dimri GP. (2007). Methods to detect biomarkers of cellular senescence: the senescence-associated beta-galactosidase assay. *Methods Mol. Biol.* 371:21-31.
140. Kuilman T, Michaloglou C, Mooi WJ, Peeper DS. (2010). The essence of senescence. *Genes. Dev.* 24:2463-79.
141. Campisi J, d'Adda di Fagagna F. (2007). Cellular senescence: when bad things happen to good cells. *Nat. Rev. Mol. Cell Biol.* 8:729-40.
142. Pazolli E, Stewart SA. (2008). Senescence: the good the bad and the dysfunctional. *Curr. Opin. Genet. Dev.* 18:42-7.
143. Maicher A, Kastner L, Luke B. (2012). Telomeres and disease: enter TERRA. *RNA Biol.* 9:843-9.
144. Epel E. (2012). How "reversible" is telomeric aging? *Cancer Prev. Res. (Phila).* 5:1163-8.
145. Palm W, de Lange T. (2008). How shelterin protects mammalian telomeres. *Annu. Rev. Genet.* 42:301-34.
146. Hug N, Lingner J. (2006). Telomere length homeostasis. *Chromosoma.* 115:413-25.
147. Greider CW. (1990). Telomeres, telomerase and senescence. *Bioessays.* 12:363-9.
148. Bodnar AG, Ouellette M, Frolkis M, Holt SE, Chiu CP, Morin GB, *et al.* (1998). Extension of life-span by introduction of telomerase into normal human cells. *Science.* 279:349-52.
149. d'Adda di Fagagna F, Reaper PM, Clay-Farrace L, Fiegler H, Carr P, Von Zglinicki T, *et al.* (2003). A DNA damage checkpoint response in telomere-

- initiated senescence. *Nature*. 426:194-8.
150. Kiyono T, Foster SA, Koop JI, McDougall JK, Galloway DA, Klingelutz AJ. (1998). Both Rb/p16INK4a inactivation and telomerase activity are required to immortalize human epithelial cells. *Nature*. 396:84-8.
 151. Serrano M, Lin AW, McCurrach ME, Beach D, Lowe SW. (1997). Oncogenic ras provokes premature cell senescence associated with accumulation of p53 and p16INK4a. *Cell*. 88:593-602.
 152. Di Micco R, Fumagalli M, d'Adda di Fagagna F. (2007). Breaking news: high-speed race ends in arrest--how oncogenes induce senescence. *Trends Cell Biol*. 17:529-36.
 153. Dhomen N, Reis-Filho JS, da Rocha Dias S, Hayward R, Savage K, Delmas V, Larue L, Pritchard C, Marais R. (2009). Oncogenic Braf induces melanocyte senescence and melanoma in mice. *Cancer Cell*. 15:294-303.
 154. Zhu J, Woods D, McMahon M, Bishop JM. (1998). Senescence of human fibroblasts induced by oncogenic Raf. *Genes Dev*. 12:2997-3007.
 155. Dankort D, Filenova E, Collado M, Serrano M, Jones K, McMahon M. (2007). A new mouse model to explore the initiation, progression, and therapy of BRAFV600E-induced lung tumors. *Genes Dev*. 21:379-84.
 156. Chan CH, Gao Y, Moten A, Lin HK. (2001). Novel ARF/p53-independent senescence pathways in cancer repression. *J Mol Med (Berl)*. 89:857-67.
 157. Kiyono T, Foster SA, Koop JI, McDougall JK, Galloway DA, Klingelutz AJ. (1998). Both Rb/p16INK4a inactivation and telomerase activity are required to immortalize human epithelial cells. *Nature*. 396:84-8.
 158. Giacinti C, Giordano A. (2006). RB and cell cycle progression. *Oncogene*. 25:5220-7.
 159. Alimonti A, Nardella C, Chen Z, Clohessy JG, Carracedo A, Trotman LC, *et al*. (2010). A novel type of cellular senescence that can be enhanced in mouse models and human tumor xenografts to suppress prostate tumorigenesis. *J Clin Invest*. 120:681-93.
 160. Nardella C, Carracedo A, Alimonti A, Hobbs RM, Clohessy JG, Chen Z, *et al*. (2009). Differential requirement of mTOR in postmitotic tissues and tumorigenesis. *Sci Signal*. 2:ra2.

161. Song MS, Carracedo A, Salmena L, Song SJ, Egia A, Malumbres M, Pandolfi PP. (2011). Nuclear PTEN regulates the APC-CDH1 tumor-suppressive complex in a phosphatase-independent manner. *Cell*. 144:187-99.
162. Kodama R, Kato M, Furuta S, Ueno S, Zhang Y, Matsuno K, *et al.* (2013). ROS-generating oxidases Nox1 and Nox4 contribute to oncogenic Ras-induced premature senescence. *Genes Cells*. 18:32-41.
163. Jung MS, Yun J, Chae HD, Kim JM, Kim SC, Choi TS, Shin DY. (2001). p53 and its homologues, p63 and p73, induce a replicative senescence through inactivation of NF-Y transcription factor. *Oncogene*. 20:5818-25.
164. Guo X, Keyes WM, Papazoglu C, Zuber J, Li W, Lowe SW, *et al.* (2009). TAp63 induces senescence and suppresses tumorigenesis in vivo. *Nat. Cell Biol*. 11:1451-7.
165. Young AP, Schlisio S, Minamishima YA, Zhang Q, Li L, Grisanzio C, *et al.* (2008). VHL loss actuates a HIF-independent senescence programme mediated by Rb and p400. *Nat. Cell Biol*. 10:361-9.
166. Lin HK, Chen Z, Wang G, Nardella C, Lee SW, Chan CH, *et al.* (2010). Skp2 targeting suppresses tumorigenesis by Arf-p53-independent cellular senescence. *Nature*. 464:374-9.
167. Krizhanovsky V, Yon M, Dickins RA, Hearn S, Simon J, Miething C, *et al.* (2008). Senescence of activated stellate cells limits liver fibrosis. *Cell*. 134:657-67.
168. Ramakrishna G, Anwar T, Angara RK, Chatterjee N, Kiran S, Singh S. (2012). Role of cellular senescence in hepatic wound healing and carcinogenesis. *Eur. J. Cell Biol*. 91:739-47.
169. Ozturk M, Arslan-Ergul A, Bagislar S, Senturk S, Yuzugullu H. (2009). Senescence and immortality in hepatocellular carcinoma. *Cancer Lett*. 286:103-13.
170. Kang TW, Yevsa T, Woller N, Hoenicke L, Wuestefeld T, Dauch D, *et al.* (2011). Senescence surveillance of pre-malignant hepatocytes limits liver cancer development. *Nature*. 479:547-51.
171. Rochette PJ, Brash DE. (2008). Progressive apoptosis resistance prior to senescence and control by the anti-apoptotic protein BCL-xL. *Mech. Ageing Dev*. 129:207-14.

172. Seluanov A, Gorbunova V, Falcovitz A, Sigal A, Milyavsky M, Zurer I, *et al.* (2001). Change of the death pathway in senescent human fibroblasts in response to DNA damage is caused by an inability to stabilize p53. *Mol. Cell Biol.* 21:1552-64.
173. Wang E. (1995). Senescent human fibroblasts resist programmed cell death, and failure to suppress bcl2 is involved. *Cancer Res.* 55:2284-92.
174. Simboeck E, Ribeiro JD, Teichmann S, Di Croce L. (2011). Epigenetics and senescence: learning from the INK4-ARF locus. *Biochem. Pharmacol.* 82:1361-70.
175. Cosentino C, Mostoslavsky R. (2013). Metabolism, longevity and epigenetics. *Cell Mol. Life Sci.* 70:1525-41.
176. O'Sullivan RJ, Kubicek S, Schreiber SL, Karlseder J. (2010). Reduced histone biosynthesis and chromatin changes arising from a damage signal at telomeres. *Nat. Struct. Mol. Biol.* 17:1218-25.
177. Zhang R, Poustovoitov MV, Ye X, Santos HA, Chen W, Daganzo SM, *et al.* (2005). Formation of MacroH2A-containing senescence-associated heterochromatin foci and senescence driven by ASF1a and HIRA. *Dev. Cell.* 8:19-30.
178. Kosar M, Bartkova J, Hubackova S, Hodny Z, Lukas J, Bartek J. (2011). Senescence-associated heterochromatin foci are dispensable for cellular senescence, occur in a cell type- and insult-dependent manner and follow expression of p16(ink4a). *Cell Cycle.* 10:457-68.
179. Freund A, Orjalo AV, Desprez PY, Campisi J. (2010). Inflammatory networks during cellular senescence: causes and consequences. *Trends Mol. Med.* 16:238-46.
180. Kuilman T, Peeper DS. (2009). Senescence-messaging secretome: SMS-ing cellular stress. *Nat. Rev. Cancer.* 9:81-94.
181. Chambers SM, Shaw CA, Gatz C, Fisk CJ, Donehower LA, Goodell MA. (2007). Aging hematopoietic stem cells decline in function and exhibit epigenetic dysregulation. *PLoS Biol.* 5:e201.
182. Chuang JY, Hung JJ. (2011). Overexpression of HDAC1 induces cellular senescence by Sp1/PP2A/pRb pathway. *Biochem. Biophys. Res. Commun.* 407:587-92.

183. Willis-Martinez D, Richards HW, Timchenko NA, Medrano EE. (2010). Role of HDAC1 in senescence, aging, and cancer. *Exp. Gerontol.* 45:279-85.
184. Fusco S, Maulucci G, Pani G. (2012). Sirt1: def-eating senescence? *Cell Cycle.* 11:4135-46.
185. Sasaki T, Maier B, Bartke A, Scrable H. (2006). Progressive loss of SIRT1 with cell cycle withdrawal. *Aging Cell.* 5:413-22.
186. Qiang L, Lin HV, Kim-Muller JY, Welch CL, Gu W, Accili D. (2011). Proatherogenic abnormalities of lipid metabolism in SirT1 transgenic mice are mediated through Creb deacetylation. *Cell Metab.* 14:758-67.
187. Tazawa H, Tsuchiya N, Izumiya M, Nakagama H. (2007). Tumor-suppressive miR-34a induces senescence-like growth arrest through modulation of the E2F pathway in human colon cancer cells. *Proc. Natl. Acad. Sci. U S A.* 104:15472-7.
188. Kumamoto K, Spillare EA, Fujita K, Horikawa I, Yamashita T, Appella E, *et al.* (2008). Nutlin-3a activates p53 to both down-regulate inhibitor of growth 2 and up-regulate mir-34a, mir-34b, and mir-34c expression, and induce senescence. *Cancer Res.* 68:3193-203.
189. Hermeking H. (2010). The miR-34 family in cancer and apoptosis. *Cell Death Differ.* 17:193-9.
190. Boominathan L. (2010). The tumor suppressors p53, p63, and p73 are regulators of microRNA processing complex. *PLoS One.* 5:e10615.
191. Knouf EC, Garg K, Arroyo JD, Correa Y, Sarkar D, Parkin RK, *et al.* (2012). An integrative genomic approach identifies p73 and p63 as activators of miR-200 microRNA family transcription. *Nucleic Acids Res.* 40:499-510.
192. Chang TC, Zeitels LR, Hwang HW, Chivukula RR, Wentzel EA, Dews M, *et al.* (2009). Lin-28B transactivation is necessary for Myc-mediated let-7 repression and proliferation. *Proc. Natl. Acad. Sci. U S A.* 106:3384-9.
193. Hong L, Lai M, Chen M, Xie C, Liao R, Kang YJ, *et al.* (2010). The miR-17-92 cluster of microRNAs confers tumorigenicity by inhibiting oncogene-induced senescence. *Cancer Res.* 70:8547-57.
194. Binet R, Ythier D, Robles AI, Collado M, Larrieu D, Fonti C, *et al.* (2009). WNT16B is a new marker of cellular senescence that regulates p53 activity

and the phosphoinositide 3-kinase/AKT pathway. *Cancer Res.* 69:9183-91.

195. Ozturk N, Erdal E, Mumcuoglu M, Akcali KC, Yalcin O, Senturk S, *et al.* (2006). Reprogramming of replicative senescence in hepatocellular carcinoma-derived cells. *Proc. Natl. Acad. Sci. U S A.* 103:2178-83.
196. Caron C, Lestrat C, Marsal S, Escoffier E, Curtet S, Virolle V, *et al.* (2010). Functional characterization of ATAD2 as a new cancer/testis factor and a predictor of poor prognosis in breast and lung cancers. *Oncogene.* 29:5171-81.
197. Gursoy-Yuzugullu O, Yuzugullu H, Yilmaz M, Ozturk M. (2011). Aflatoxin genotoxicity is associated with a defective DNA damage response bypassing p53 activation. *Liver Int.* 31:561-71.
198. Subramanian A, Tamayo P, Mootha VK, Mukherjee S, Ebert BL, Gillette MA, *et al.* (2005). Gene set enrichment analysis: a knowledge-based approach for interpreting genome-wide expression profiles. *Proc. Natl. Acad. Sci. U S A.* 102:15545-50.
199. de Hoon MJ, Imoto S, Nolan J, Miyano S. (2004). Open source clustering software. *Bioinformatics.* 20:1453-4.
200. Saldanha AJ. (2004). Java Treeview--extensible visualization of microarray data. *Bioinformatics.* 20:3246-8.
201. Tibshirani R, Hastie T, Narasimhan B, Chu G. (2002). Diagnosis of multiple cancer types by shrunken centroids of gene expression. *Proc. Natl. Acad. Sci. U S A.* 99:6567-72.
202. Wurmbach E, Chen YB, Khitrov G, Zhang W, Roayaie S, Schwartz M, *et al.* (2007). Genome-wide molecular profiles of HCV-induced dysplasia and hepatocellular carcinoma. *Hepatology.* 45:938-47.
203. Hoshida Y. (2010). Nearest template prediction: a single-sample-based flexible class prediction with confidence assessment. *PLoS One.* 5(11):e15543.
204. Deng YB, Nagae G, Midorikawa Y, Yagi K, Tsutsumi S, Yamamoto S, *et al.* (2010). Identification of genes preferentially methylated in hepatitis C virus-related hepatocellular carcinoma. *Cancer Sci.* 101:1501-10.
205. Arrowsmith CH, Bountra C, Fish PV, Lee K, Schapira M. (2012). Epigenetic protein families: a new frontier for drug discovery. *Nat. Rev. Drug Discov.*

11: 384–400.

206. Yun M, Wu J, Workman JL, Li B. (2011) Readers of histone modifications. *Cell Res.* 21: 564–578.
207. Acun T, Terzioğlu-Kara E, Konu O, Ozturk M, Yakicier MC. (2010). Mdm2 Snp309 G allele displays high frequency and inverse correlation with somatic P53 mutations in hepatocellular carcinoma. *Mutat. Res.* 684:106-8.
208. Fridman AL, Tainsky MA. (2008). Critical pathways in cellular senescence and immortalization revealed by gene expression profiling. *Oncogene.* 27:5975-87.
209. Tang X, Milyavsky M, Goldfinger N, Rotter V. (2007). Amyloid-beta precursor-like protein APLP1 is a novel p53 transcriptional target gene that augments neuroblastoma cell death upon genotoxic stress. *Oncogene.* 26:7302-12.
210. Chang YE, Laimins LA. (2000). Microarray analysis identifies interferon-inducible genes and Stat-1 as major transcriptional targets of human papillomavirus type 31. *J. Virol.* 74:4174-82.
211. Kang SK, Putnam L, Dufour J, Ylostalo J, Jung JS, Bunnell BA. (2004). Expression of telomerase extends the lifespan and enhances osteogenic differentiation of adipose tissue-derived stromal cells. *Stem Cells.* 22:1356-72.
212. Smith LL, Collier HA, Roberts JM. (2003). Telomerase modulates expression of growth-controlling genes and enhances cell proliferation. *Nat. Cell Biol.* 5:474-9.
213. Yildiz G, Arslan-Ergul A, Bagislar S, Konu O, Yuzugullu H, Gursoy-Yuzugullu O, *et al.* (2013). Genome-wide transcriptional reorganization associated with senescence-to-immortality switch during human hepatocellular carcinogenesis. *PLoS One.* 8:e64016.
214. Zou JX, Revenko AS, Li LB, Gemo AT, Chen HW. (2007). ANCCA, an estrogen-regulated AAA+ ATPase coactivator for ERalpha, is required for coregulator occupancy and chromatin modification. *Proc. Natl. Acad. Sci. U S A.* 104:18067-72.
215. Fujiwara Y, Monden M, Mori T, Nakamura Y, Emi M. (1993). Frequent multiplication of the long arm of chromosome 8 in hepatocellular carcinoma. *Cancer Res.* 53:857-60.

216. Beroukhi R, Mermel CH, Porter D, Wei G, Raychaudhuri S, Donovan J, *et al.* (2010). The landscape of somatic copy-number alteration across human cancers. *Nature*. 463:899-905.
217. Yuzugullu Haluk. August, 2010. Genetic and epigenetic targets in liver cancer. Ph.D. thesis submitted to Bilkent University.
218. Schwartzenuber J, Korshunov A, Liu XY, Jones DT, Pfaff E, Jacob K, *et al.* (2012). Driver mutations in histone H3.3 and chromatin remodeling genes in paediatric glioblastoma. *Nature*. 482:226-31.
219. Je EM, Yoo NJ, Kim YJ, Kim MS, Lee SH. (2013). Somatic mutation of H3F3A, a chromatin remodeling gene, is rare in acute leukemias and non-Hodgkin lymphoma. *Eur J. Haematol.* 90:169-70.
220. Wiemann SU, Satyanarayana A, Tsahuridu M, Tillmann HL, Zender L, Klempnauer J, *et al.* (2002). Hepatocyte telomere shortening and senescence are general markers of human liver cirrhosis. *FASEB J.* 16:935-42.
221. Kitada T, Seki S, Kawakita N, Kuroki T, Monna T. (1995). Telomere shortening in chronic liver diseases. *Biochem. Biophys. Res. Commun.* 211:33-9.
222. Hartmann D, Srivastava U, Thaler M, Kleinhans KN, N'kontchou G, Scheffold A, *et al.* (2011). Telomerase gene mutations are associated with cirrhosis formation. *Hepatology*. 53:1608-17.
223. Calado RT, Brudno J, Mehta P, Kovacs JJ, Wu C, Zago MA, *et al.* (2011). Constitutional telomerase mutations are genetic risk factors for cirrhosis. *Hepatology*. 53:1600-7.
224. Llovet JM, Chen Y, Wurmbach E, Roayaie S, Fiel MI, Schwartz M, *et al.* (2006). A molecular signature to discriminate dysplastic nodules from early hepatocellular carcinoma in HCV cirrhosis. *Gastroenterology*. 131:1758-67.
225. Kojima H, Yokosuka O, Imazeki F, Saisho H, Omata M. (1997). Telomerase activity and telomere length in hepatocellular carcinoma and chronic liver disease. *Gastroenterology*. 112:493-500.
226. Urabe Y, Nouse K, Higashi T, Nakatsukasa H, Hino N, Ashida K, *et al.* (1996). Telomere length in human liver diseases. *Liver*. 16:293-7.
227. Collado M, Serrano M. (2010). Senescence in tumours: evidence from mice

- and humans. *Nat. Rev. Cancer*. 10:51-7.
228. Xu XR, Huang J, Xu ZG, Qian BZ, Zhu ZD, Yan Q, *et al.* (2001). Insight into hepatocellular carcinogenesis at transcriptome level by comparing gene expression profiles of hepatocellular carcinoma with those of corresponding noncancerous liver. *Proc. Natl. Acad. Sci. U S A*. 98:15089-94.
229. Bruce Alberts, Alexander Johnson, Julian Lewis, Martin Raff, Keith Roberts, and Peter Walter. (2008). *Molecular biology of the cell*. 5th edition. Garland Science. ISBN: 978-0-8153-4105-5.
230. Smith J, Tho LM, Xu N, Gillespie DA. (2010). The ATM-Chk2 and ATR-Chk1 pathways in DNA damage signaling and cancer. *Adv. Cancer Res*. 108:73-112.
231. Bushue N, Wan YJ. (2010). Retinoid pathway and cancer therapeutics. *Adv. Drug Deliv. Rev*. 62:1285-98.
232. Shirakami Y, Lee SA, Clugston RD, Blaner WS. (2012). Hepatic metabolism of retinoids and disease associations. *Biochim. Biophys. Acta*. 21:124-36.
233. Adachi S, Moriwaki H, Muto Y, Yamada Y, Fukutomi Y, Shimazaki M, *et al.* (1991). Reduced retinoid content in hepatocellular carcinoma with special reference to alcohol consumption. *Hepatology*. 14:776-80.
234. Clemente C, Elba S, Buongiorno G, Berloco P, Guerra V, Di Leo A. (2002). Serum retinol and risk of hepatocellular carcinoma in patients with child-Pugh class A cirrhosis. *Cancer Lett*. 2002 178:123-9.
235. Takai K, Okuno M, Yasuda I, Matsushima-Nishiwaki R, Uematsu T, Tsurumi H, *et al.* (2005). Prevention of second primary tumors by an acyclic retinoid in patients with hepatocellular carcinoma. Updated analysis of the long-term follow-up data. *Intervirology*. 48:39-45.
236. Villanueva A, Minguez B, Forner A, Reig M, Llovet JM. (2010). Hepatocellular carcinoma: novel molecular approaches for diagnosis, prognosis, and therapy. *Annu. Rev. Med*. 61:317-28.
237. Paradis V, Bièche I, Dargère D, Laurendeau I, Laurent C, Bioulac Sage P, *et al.* (2003). Molecular profiling of hepatocellular carcinomas (HCC) using a large-scale real-time RT-PCR approach: determination of a molecular diagnostic index. *Am. J. Pathol*. 163:733-41.
238. Nam SW, Park JY, Ramasamy A, Shevade S, Islam A, Long PM, *et al.*

- (2005). Molecular changes from dysplastic nodule to hepatocellular carcinoma through gene expression profiling. *Hepatology*. 42:809-18.
239. Kim JW, Ye Q, Forgues M, Chen Y, Budhu A, Sime J, *et al.* (2004). Cancer-associated molecular signature in the tissue samples of patients with cirrhosis. *Hepatology*. 39:518-27.
240. Ellis BC, Molloy PL, Graham LD. (2012). CRNDE: A Long Non-Coding RNA Involved in Cancer, Neurobiology, and DEvelopment. *Front. Genet.* 3:270.
241. Wong N, Yeo W, Wong WL, Wong NL, Chan KY, Mo FK, *et al.* (2009). TOP2A overexpression in hepatocellular carcinoma correlates with early age onset, shorter patients survival and chemoresistance. *Int. J. Cancer*. 124:644-52.
242. Qin LX, Tang ZY. (2002). The prognostic molecular markers in hepatocellular carcinoma. *World J. Gastroenterol.* 8:385-92.
243. Ciró M, Prosperini E, Quarto M, Grazini U, Walfridsson J, McBlane F, *et al.* (2009). ATAD2 is a novel cofactor for MYC, overexpressed and amplified in aggressive tumors. *Cancer Res*. 69:8491-8.
244. Poirier LA. (1986). The role of methionine in carcinogenesis in vivo. *Adv. Exp. Med. Biol.* 206: 269–282.
245. Zeisel SH, Da Costa KA, Albright CD, Shin OH. (1995). Choline and hepatocarcinogenesis in the rat. *Adv. Exp. Med. Biol.* 375: 65–74.

APPENDIX


REUSE PERMISSIONS OF THE FIGURES:

Permission for reuse of Figure 1.2

JOURNAL OF CLINICAL INVESTIGATION. ONLINE

Billing Status: N/A

Order detail ID: 63875002
ISSN: 1558-8238
Publication Type: e-Journal
Volume:
Issue:
Start page:
Publisher: AMERICAN SOCIETY FOR CLINICAL INVESTIGATION

Permission Status:  **Granted**
Permission type: Republish or display content
Type of use: Republish in a thesis/dissertation
Order License Id: 3200650814924

[Hide details](#)

Requestor type	Academic institution
Format	Print, Electronic
Portion	image/photo
Number of images/photos requested	2
Title or numeric reference of the portion(s)	Figures 1 and 2
Title of the article or chapter the portion is from	Evolving therapies for liver fibrosis
Editor of portion(s)	N/A
Author of portion(s)	Detlef Schuppan and Yong Ook Kim
Volume of serial or monograph	123
Issue, if republishing an article from a serial	5
Page range of portion	1888, 1889
Publication date of portion	May 2013
Rights for	Main product
Duration of use	Life of current and all

Permission for reuse of Figure 1.3

RightLink Printable License

8/11/13 1:30 PM

NATURE PUBLISHING GROUP LICENSE TERMS AND CONDITIONS

Aug 11, 2013

This is a License Agreement between Gokhan YILDIZ ("You") and Nature Publishing Group ("Nature Publishing Group") provided by Copyright Clearance Center ("CCC"). The license consists of your order details, the terms and conditions provided by Nature Publishing Group, and the payment terms and conditions.

All payments must be made in full to CCC. For payment instructions, please see information listed at the bottom of this form.

License Number	3200651325520
License date	Aug 02, 2013
Licensed content publisher	Nature Publishing Group
Licensed content publication	Nature Reviews Cancer
Licensed content title	Hepatocellular carcinoma pathogenesis: from genes to environment
Licensed content author	Paraskevi A. Farazi, Ronald A. DePinho
Licensed content date	Sep 1, 2006
Volume number	6
Issue number	9
Type of Use	reuse in a thesis/dissertation
Requestor type	academic/educational
Format	print and electronic
Portion	figures/tables/illustrations
Number of figures/tables/illustrations	2
High-res required	no
Figures	Figures 1 and 2
Author of this NPG article	no
Your reference number	
Title of your thesis / dissertation	Roles of Senescence Escape and Epigenetic Modifications in Liver Cancer
Expected completion date	Aug 2013
Estimated size (number of pages)	200
Total	0.00 USD
Terms and Conditions	Terms and Conditions for Permissions

Nature Publishing Group hereby grants you a non-exclusive license to reproduce this

<https://i100.copyright.com/CustomerAdmin/RF.jsp?ref=327489cb-c225-496d-b80d-f1184b05170d>

Page 1 of 3

Permission for reuse of Figure 1.4

RightLink Printable License

8/11/13 2:01 PM

NATURE PUBLISHING GROUP LICENSE TERMS AND CONDITIONS

Aug 11, 2013

This is a License Agreement between Gokhan YILDIZ ("You") and Nature Publishing Group ("Nature Publishing Group") provided by Copyright Clearance Center ("CCC"). The license consists of your order details, the terms and conditions provided by Nature Publishing Group, and the payment terms and conditions.

All payments must be made in full to CCC. For payment instructions, please see information listed at the bottom of this form.

License Number	3205880059936
License date	Aug 11, 2013
Licensed content publisher	Nature Publishing Group
Licensed content publication	Nature Reviews Cancer
Licensed content title	Pro-senescence therapy for cancer treatment
Licensed content author	Caterina Nardella, John G. Clohessy, Andrea Allimonti, Pier Paolo Pandolfi
Licensed content date	Jun 24, 2011
Volume number	11
Issue number	7
Type of Use	reuse in a thesis/dissertation
Requestor type	academic/educational
Format	print and electronic
Portion	figures/tables/illustrations
Number of figures/tables/illustrations	1
High-res required	no
Figures	Figure 1
Author of this NPG article	no
Your reference number	
Title of your thesis / dissertation	Roles of Senescence Escape and Epigenetic Modifications in Liver Cancer
Expected completion date	Aug 2013
Estimated size (number of pages)	200
Total	0.00 USD
Terms and Conditions	Terms and Conditions for Permissions

<https://i100.copyright.com/CustomerAdmin/RF.jsp?ref=202b0568-1cca-4678-8eac-73ba2079c0cd>

Page 1 of 3

GENES OF EPIGENETIC REGULATORY (EpiReg) GENE SETS

GENES OF ACTRFASE GENE SET:

CSRP2BP	HAT1	CREBBP	MYST3
MYST2	EP300	MYST4	MYST1

GENES OF ANKYRIN_RPT GENE SET:

ANKRD43	TRPC1	ANKRD45	TRPV3
PPP1R16A	ANKRD13C	ASB13	ANKAR
ANKRD27	ANKHD1	CAMTA1	ILK
CDKN2C	SHANK3	ANKRD29	ANKRD9
ACBD6	INVS	ANKRD28	ANKMY2
ANKFN1	NFKBIL1	EHMT1	TNNI3K
CDKN2B	GIT2	YTHDC2	DYSFIP1
CDKN2A	TRPC6	ANKS3	TRPV6
BARD1	DGKZ	ASB12	NUDT12
TP53BP2	ASB7	TRPC3	GLS
BCOR	TNKS2	HECTD1	ANKRD55
ANKRD16	ANKRD18A	CDKN2D	ANK1
HACE1	ANKRD40	IBTK	NFKBIA
ASB9	MIB2	ANKRD13A	ASB1
ANKRD32	ASB6	ASB14	TRPC7
RAI14	ANKRD7	ANKRD33	ANKRD1
ANKRD39	FEM1B	TEX14	ANKRD42
ANKS1B	ANKRD17	SHANK1	PIK3AP1
ANKRD5	ANKRD2	PPP1R13B	PPP1R13L
ANKRD46	FEM1C	ANKRD13B	CTTNBP2
ANKRD35	MTPN	ABTB1	ANKRD53
MIB1	ANKRD31	ANKDD1A	ANKFY1
TNKS	PPP1R12A	ANKRD30A	USH1G
ANKS6	ASZ1	ASB2	FANK1
GABPB2	ASB17	ANKRD6	TANC2
ANKRA2	BTBD11	ANKRD22	ASB16
ANKIB1	ASB5	UACA	NFKBIE
SNCAIP	TRPV1	NFKBIB	ANKRD37
ANKZF1	ZDHHC17	GIT1	ASB10
ASB8	TRPC5	TRPV2	PPP1R12B
RFXANK	ASB15	RNASEL	ANKRD57
ANKRD50	DGKI	BCORL1	PPP1R16B
ANKRD26	ANKRD11	ASB11	OSBPL1A
PSMD10	PLA2G6	ANKRD24	CASKIN2
ASB4	ABTB2	CASKIN1	BANK1
KIDINS220	ANKRD30B	TRPA1	ANKS4B
ASB3	FEM1A	TRPV5	BCL3
ANKRD49	CLPB	ANKMY1	OSTF1
ANKRD52	ANKRD12	ANKRD10	ANK2
KRIT1	TRPC4	ESPN	NFKBIZ
EHMT2	PPP1R12C	ZDHHC13	TANC1

ANKRD44	TRPV4	GLS2
ANKS1A	ANK3	

GENES OF BROMO GENE SET:

ATAD2	BAZ1B	BRD4	BAZ1A
CECR2	BRD7	ZMYND11	CREBBP
TRIM24	BRD2	BRPF1	TAF1L
PHIP	SMARCA4	SP140	BRD1
TRIM33	TAF1	KIAA2026	BAZ2B
BRPF3	TRIM66	BRWD3	SMARCA2
BRD8	BAZ2A	BSN	SP110
TRIM28	BRD9	BRDT	
BRD3	EP300	BRWD1	

GENES OF CHAPERONE GENE SET:

ASF1A	EP400	DAXX	ATRX
RSF1	DEK	NAP1L4	HIRA
ASF1B	CHD8	NAP1L1	SRCAP
CHAF1A	NPM1	NASP	

GENES OF CHROMO GENE SET:

CBX3	CHD6	CHD1	MORF4L1
SUV39H2	CBX4	CHD2	CHD5
CHD7	CHD8	ARID4A	CBX7
SMARCC1	CBX5	CHD9	CHD3
ARID4B	CBX8	CBX2	MYST1
SUV39H1	CDYL	CBX6	CDYL2
CBX1	CHD4	SMARCC2	

GENES OF CODEREADER GENE SET:

ATAD2	CDKN2B	PHIP	BRD3
UHRF1	CHD7	ANKRD32	PHF20
TDRKH	CDKN2A	TRIM33	SND1
ANKRD43	PHF20L1	RAI14	ANKRD5
CECR2	TP53BP2	ANKRD39	AKAP1
PPP1R16A	SMARCC1	BRPF3	CHD6
RBBP5	RCOR3	PHF6	ANKRD46
TAF5	BCOR	RNF2	ANKRD35
ANKRD27	MORC2	CBX1	PLEKHF2
TERF1	LBR	HGS	MIB1
TRIM24	FOXA1	MSH6	SUPT16H
CDKN2C	ANKRD16	ANKS1B	BDP1
CBX3	SUZ12	BRD8	TNKS
ACBD6	HACE1	TRIM28	MTA3
PHF16	ARID4B	TTF1	ANKS6
ANKFN1	ASB9	PHF14	BRD7

SYTL4	ASB3	MIB2	RERE
PYGO2	ANKRD49	ASB6	TRPC4
GABPB2	BRD9	TCF20	PPP1R12C
ZFYVE26	BRD4	PHF17	ANKRD45
FGD1	ANKRD52	BRWD1	ASB13
ANKRA2	TDRD3	RAG2	CAMTA1
ANKIB1	KRIT1	ANKRD7	PLEKHF1
SNCAIP	ZMYND11	DMAP1	ANKRD29
ANKZF1	PHF3	FEM1B	APBB1
RUFY1	TRPC1	ANKRD17	ANKRD28
BMI1	MTMR4	TDRD10	CHAF1B
HDGF	ANKRD13C	BAZ1A	MYB
HIRIP3	ANKHD1	ANKRD2	PHF21B
MYBL1	PCGF2	FEM1C	YTHDC2
BRD2	TAF5L	ARID4A	ANKS3
ASB8	NFX1	MIER3	ASB12
SMARCA4	RBBP7	NCOR2	DPF1
UHRF2	ZFYVE20	ZFYVE16	CXXC1
SPIRE2	DIDO1	RCOR1	MYRIP
ZZZ3	BRPF1	MTPN	ZFYVE1
MTA1	CCDC79	ANKRD31	TRPC3
MLLT6	CRAMP1L	CHD9	HECTD1
SCML2	RBBP4	PPP1R12A	RNF17
RFXANK	SHANK3	ASZ1	CDKN2D
EED	INVS	ASB17	RING1
ING3	MYBL2	BTBD11	ZCWPW2
ANKRD50	CHD4	ASB5	IBTK
ZFYVE19	MTF2	ING5	INTS12
PHF12	NFKBIL1	TRPV1	ANKRD13A
ANKRD26	CHD1	ZDHHC17	ASB14
TRIM66	SP140	TAF3	TAF1L
MLLT10	GIT2	MIER2	TDRD5
GON4L	CHD2	PHF19	ANKRD33
RIMS2	TRPC6	TRPC5	FOXA3
ZFYVE9	DGKZ	DNAJC1	MORC3
PSMD10	DPF2	MTA2	L3MBTL2
CBX5	DMTF1	ASB15	ZFYVE28
PHF13	SFMBT1	DGKI	STK31
TRIM27	ASB7	ANKRD11	ING4
PHF21A	TNKS2	PLA2G6	ING2
SET	KIAA2026	ABTB2	TEX14
SMARCA1	MUM1	SCMH1	SHANK1
ASB4	ANKRD18A	ANKRD30B	MARCH9
CBX8	ZNF541	TERF2	BRD1
L3MBTL4	RFFL	FEM1A	PPP1R13B
KIDINS220	BRWD3	RNF34	ANKRD13B
EEA1	FYCO1	MORC1	ABTB1
BAZ2A	BSN	CLPB	L3MBTL3
CDC5L	ANKRD40	WDFY1	PHF11
BRCA1	BRDT	ANKRD12	PYGO1

MTMR3	MORF4L1	NFKBIA	ASB10
ANKDD1A	RUFY2	CBX7	PPP1R12B
TDRD7	TRPA1	KIAA1045	ANKRD57
PHF15	SHPRH	ASB1	PPP1R16B
ANKRD30A	HDGFL1	FGD4	OSBPL1A
ASB2	TRPV5	TRPC7	SP110
PHF1	ANKMY1	DPF3	FGD2
ANKRD6	ANKRD10	ANKRD1	CASKIN2
TP53BP1	ESPN	ANKRD42	BANK1
ING1	PHF23	WDFY3	ANKS4B
ANKRD22	BAZ2B	PIK3AP1	BCL3
CBX6	ZCWPW1	PPP1R13L	SPIRE1
SMARCC2	WDFY2	SFMBT2	AIRE
UACA	ZDHHC13	RAI1	MORC4
NFKBIB	TRPV3	CTTNBP2	OSTF1
GIT1	ANKAR	MLPH	SYTL2
MBTD1	ILK	CHD3	SYTL5
NCOR1	ANKRD9	ANKRD53	ANK2
TRPV2	ANKMY2	ANKFY1	NFKBIZ
RNASL	TNNI3K	SMARCA2	FGD3
BCORL1	MIER1	USH1G	TANC1
ASB11	DYSFIP1	SYTL3	HDGFRP3
ANKRD24	CHD5	FANK1	PCLO
RIMS1	RCOR2	TRERF1	ANKRD44
TDRD6	CCDC101	TANC2	ANKS1A
ZFYVE21	PHF10	SMARCA5	TRPV4
RPH3A	TRPV6	ASB16	ANK3
ZFYVE27	NUDT12	NFKBIE	GLS2
CASKIN1	GLS	ANKRD37	MUM1L1
PHF7	ANKRD55	CDYL2	
RPH3AL	ANK1	TDRD9	

GENES OF DNA MTFASE GENE SET:

DNMT3A	DNMT3B	DNMT1	MGMT
--------	--------	-------	------

GENES OF DNADEM GENE SET:

ALKBH2	ALKBH1	ALKBH3	
--------	--------	--------	--

GENES OF DNMT GENE SET:

DNMT3A	DNMT1	DNMT3L	
DNMT3B	MGMT		

GENES OF HAT GENE SET:

CSRP2BP	TAF1	CDYL	MYST3
MYST2	HAT1	CREBBP	MYST1
METTL8	EP300	MYST4	

GENES OF HDAC GENE SET:

HDAC4	SIRT4	SIRT2	SIRT5
SIRT1	HDAC1	HDAC11	HDAC6
HDAC5	HDAC8	SIRT6	HDAC9
HDAC2	HDAC3	HDAC10	
SIRT7	MGC16025	SIRT3	

GENES OF HDEM GENE SET:

PHF8	MINA	JMJD1C	UTY
HSPBAP1	JARID2	PHF2	JMJD5
JMJD4	HIF1AN	HR	

GENES OF HIS_DEACETYLSE GENE SET:

HDAC4	SIRT4	SIRT2	SIRT5
SIRT1	HDAC1	HDAC11	HDAC6
HDAC5	HDAC8	SIRT6	HDAC9
HDAC2	HDAC3	HDAC10	
SIRT7	MGC16025	SIRT3	

GENES OF HISTONE GENE SET:

HIST1H3H	HIST1H3E	HIST1H2AL	HIST1H2BM
HIST1H2BG	TAF12	HIST1H2AB	HIST1H4G
HIST1H2AG	HIST2H2BE	HIST1H1T	TAF6L
H2AFX	HIST1H4B	HP1BP3	HIST1H3A
CENPA	HIST1H2AK	HIST1H4H	H2BFM
HIST1H2AE	HIST1H4A	H2AFJ	HIST1H1D
HIST1H2AM	HIST1H2BL	HIST1H3G	HIST1H2AI
H2AFZ	HIST1H3B	HIST1H2BI	HIST1H2BN
TAF9	H2AFY	HIST1H4L	HIST3H2A
H1FX	HIST2H2AA3	HIST1H2BF	HIST1H2AJ
HIST1H1C	HIST1H1E	HIST1H2BB	HIST1H2BC
H2AFV	HIST1H2BJ	POLE4	H1FOO
H1F0	HIST1H3F	HIST1H2BH	HIST3H3
CENPT	HIST1H2BO	H2BFS	H1FNT
HIST1H4C	SUPT3H	HILS1	HIST1H2BA
POLE3	HIST1H2BK	H2AFY2	H3F3B
DR1	HIST1H3I	HIST1H4F	HIST1H3J
HIST1H4E	HIST1H1B	HIST1H2BE	
HIST1H4D	H3F3A	HIST1H2AC	
HIST1H3C	LOC440926	HIST1H2BD	

GENES OF HMT GENE SET:

SMYD3	ASH1L	CARM1	SUV39H1
EZH2	SETDB1	SMYD2	CRIPAK
SUV39H2	WHSC1	WDR5	MLL2

SUV420H1	SETDB2	PRDM4	PRDM14
SETD6	SMYD5	WHSC1L1	PRDM11
PRMT7	MLL	EHMT1	PRDM13
MLL5	EZH1	PRDM8	PRMT8
MLL3	SETD7	PRDM16	PRDM5
AFF3 /// MLL	MLL4	SMYD4	PRDM7
SETD2	PRMT5	SUV420H2	PRDM12
NSD1	SETMAR	SETD3	ASH2L
EHMT2	PRMT1	SETD8	PRDM9
SETD5	PRDM15	PRDM2	PRMT6
DOT1L	SETD4	SMYD1	PRDM1
SETD1A	SETD1B	PRDM6	

GENES OF JMJ GENE SET:

PHF8	MINA	JMJD1C	UTY
HSPBAP1	JARID2	PHF2	JMJD5
JMJD4	HIF1AN	HR	

GENES OF MBT GENE SET:

SCML2	SFMBT1	L3MBTL2	MBTD1
L3MBTL4	SCMH1	L3MBTL3	SFMBT2

GENES OF ME CPG DNA BINDING GENE SET:

MBD3	MBD1	MBD4	
MBD5	MBD2		

GENES OF ME CPG DNA BNDGENE SET:

BAZ2A	MBD5	MBD2	MBD4
MBD3	MBD1	BAZ2B	

GENES OF METRFASE GENE SET:

CARM1	DOT1L	PRMT1	PRMT6
SETD6	SETD7	SETD4	
METTL8	MLL4	SETD8	
PRMT7	PRMT5	PRMT8	

GENES OF OTHER GENE SET:

TOP2A	MCM2	HMGA1	KLHDC3
HELLS	CDCA5	MCM7	APTX
NUSAP1	SMC4	ACTL6A	BAT3
OIP5	NCAPH	TMPO	SMARCD1
TIPIN	TIMELESS	ARID2	RCC1
POLA1	ITGB3BP	SYCP3	BNIP3

RAN	TNP1	MYCN	PAM
TLK2	CTCFL	ZFP57	MAF
SUPT4H1	ARID1A	HMG1	NAP1L3
RBL1	SMARCE1	NAP1L2	JUNB
ACIN1	TOP2B	JUND	
UPF1	ATF7IP	RB1	
FOXC1	NPM2	RBL2	

GENES OF OTHERMODIFIER GENE SET:

PRKDC	TLK1	EYA3	RNF168
CHEK1	RPS6KA5	DAPK3	PIM1
AURKB	BAP1	HLCS	EYA1
BARD1	EYA4	CBX2	ITGB1
RPS6KA3	CHUK	USP16	ATXN7
PRKAA2	ATR	RPS6KA4	MYSM1
USP21	BRCC3	RNF40	MAP3K12
RNF8	USP22	RAG1	EYA2
RNF20	GSG2	DTX3L	DLK1
BAZ1B	ATXN7L3	ARID1B	ZFAND6
UBE2A	USP3	HUWE1	JAK2
CBX4	UBE2B	ATM	

GENES OF PHD GENE SET:

UHRF1	SYTL4	NSD1	ZFYVE16
TRIM24	PYGO2	ZMYND11	ING5
PHF16	ZFYVE26	PHF3	TAF3
ASH1L	FGD1	MTMR4	PHF19
DNMT3A	ANKIB1	PCGF2	RNF34
PHF20L1	RUFY1	NFX1	WDFY1
BARD1	BMI1	ZFYVE20	USP16
WHSC1	MLL5	DIDO1	PLEKHF1
DNMT3B	UHRF2	BRPF1	WHSC1L1
PHF8	SPIRE2	CHD4	RNF40
TRIM33	MLLT6	MTF2	PHF21B
BRPF3	AFF3 /// MLL	SP140	RAG1
PHF6	ING3	USP22	DPF1
RNF8	ZFYVE19	MLL	CXXC1
RNF2	PHF12	ATRX	DTX3L
HGS	TRIM66	DPF2	MYRIP
TRIM28	MLLT10	MLL4	ZFYVE1
RNF20	RIMS2	RFLL	RNF17
PHF14	ZFYVE9	FYCO1	RING1
PHF20	PHF13	MIB2	INTS12
RSF1	TRIM27	USP3	ZFYVE28
MLL2	PHF21A	TCF20	PHF2
BAZ1B	EEA1	PHF17	ING4
PLEKHF2	BAZ2A	RAG2	RNF168
MIB1	BRCA1	BAZ1A	ING2

MARCH9	RPH3A	DNMT3L	OSBPL1A
BRD1	ZFYVE27	MYST3	SP110
PHF11	PHF7	KIAA1045	FGD2
PYGO1	RPH3AL	FGD4	HDAC6
MTMR3	RUFY2	DPF3	SPIRE1
PHF15	SHPRH	WDFY3	AIRE
PHF1	PHF23	RAI1	SYTL2
ING1	BAZ2B	MLPH	SYTL5
RIMS1	WDFY2	CHD3	FGD3
MYST4	CHD5	ANKFY1	PCLO
ZFYVE21	PHF10	SYTL3	

GENES OF PWWP GENE SET:

DNMT3A	HDGF	MUM1	ZCWPW1
DNMT3B	ZMYND11	ZCWPW2	HDGFRP3
BRPF3	BRPF1	BRD1	MUM1L1
MSH6	MBD5	HDGFL1	

GENES OF SANT GENE SET:

EZH2	SMARCA4	ZNF541	SRCAP
TERF1	ZZZ3	DMAP1	SMARCC2
CHD7	MTA1	MIER3	NCOR1
SMARCC1	GON4L	NCOR2	MYSM1
RCOR3	SMARCA1	RCOR1	MIER1
TTF1	CDC5L	MIER2	RCOR2
CHD6	CCDC79	DNAJC1	SMARCA2
BDP1	CRAMP1L	MTA2	TRERF1
MTA3	MYBL2	TERF2	SMARCA5
EP400	EZH1	RERE	
MYBL1	DMTF1	MYB	

GENES OF SET GENE SET:

SMYD3	MLL3	SETMAR	PRDM2
EZH2	AFF3 /// MLL	PRDM15	SMYD1
SUV39H2	SETD2	SETD4	PRDM6
ASH1L	NSD1	SETD1B	PRDM14
SETDB1	EHMT2	PRDM4	PRDM11
WHSC1	SETD5	WHSC1L1	PRDM13
SMYD2	SETD1A	EHMT1	PRDM5
SUV39H1	SETDB2	PRDM8	PRDM7
CRIPAK	SMYD5	PRDM16	PRDM12
MLL2	MLL	SMYD4	PRDM9
SUV420H1	EZH1	SUV420H2	PRDM1
SETD6	SETD7	SETD3	
MLL5	MLL4	SETD8	

GENES OF TUDOR GENE SET:

TDRKH	SND1	ARID4A	TDRD7
PHF20L1	AKAP1	PHF19	PHF1
LBR	TDRD3	RNF17	TP53BP1
ARID4B	MTF2	TDRD5	TDRD6
PHF20	TDRD10	STK31	TDRD9

GENES OF WD40 GENE SET:

RBBP5	EED	BRWD3	HIRA
TAF5	TAF5L	BRWD1	WDFY2
WDR5	RBBP7	WDFY1	WDFY3
PHIP	RBBP4	CHAF1B	

GENES OF ZNF_CW GENE SET:

MORC2
MORC1
ZCWPW2
MORC3
ZCWPW1
MORC4

PUBLICATIONS

1. **Yildiz G**, Arslan-Ergul A, Bagislar S, Konu O, Yuzugullu H, Gursoy-Yuzugullu O, *et al.* (2013). Genome-wide transcriptional reorganization associated with senescence-to-immortality switch during human hepatocellular carcinogenesis. *PLoS One*. 8:e64016.
2. Ozen C, **Yildiz G**, Dagcan AT, Cevik D, Ors A, Keles U, *et al.* (2013). Genetics and epigenetics of liver cancer. *N. Biotechnol.* 30:381-4.

Genome-Wide Transcriptional Reorganization Associated with Senescence-to-Immortality Switch during Human Hepatocellular Carcinogenesis

Gokhan Yildiz^{1,2,9}, Ayca Arslan-Ergul^{1,9}, Sevgi Bagislar^{1,2,9}, Ozlen Konu¹, Haluk Yuzugullu^{1,2}, Ozge Gursoy-Yuzugullu^{1,2}, Nuri Ozturk¹, Cigdem Ozen¹, Hilal Ozdag³, Esra Erdal⁴, Sedat Karademir⁵, Ozgul Sagol⁶, Dilsa Mizrak⁷, Hakan Bozkaya⁷, Hakki Gokhan Ilk⁸, Ozlem Ilk⁹, Biter Bilen¹, Rengul Cetin-Atalay¹, Nejat Akar³, Mehmet Ozturk^{1,2*}

1 BilGen Genetics and Biotechnology Center, Department of Molecular Biology and Genetics, Bilkent University, Ankara, Turkey, **2** INSERM - Université Joseph Fourier, CRI U823, Grenoble, France, **3** Biotechnology Institute, Ankara University, Ankara, Turkey, **4** Department of Medical Biology, Dokuz Eylul University Medical School, Izmir, Turkey, **5** Department of Surgery, Dokuz Eylul University Medical School, Izmir, Turkey, **6** Department of Pathology, Dokuz Eylul University Medical School, Izmir, Turkey, **7** Department of Gastroenterology, Ankara University, Ankara, Turkey, **8** Department of Electronic Engineering, Ankara University, Ankara, Turkey, **9** Department of Statistics, Middle East Technical University, Ankara, Turkey

Abstract

Senescence is a permanent proliferation arrest in response to cell stress such as DNA damage. It contributes strongly to tissue aging and serves as a major barrier against tumor development. Most tumor cells are believed to bypass the senescence barrier (become “immortal”) by inactivating growth control genes such as *TP53* and *CDKN2A*. They also reactivate telomerase reverse transcriptase. Senescence-to-immortality transition is accompanied by major phenotypic and biochemical changes mediated by genome-wide transcriptional modifications. This appears to happen during hepatocellular carcinoma (HCC) development in patients with liver cirrhosis, however, the accompanying transcriptional changes are virtually unknown. We investigated genome-wide transcriptional changes related to the senescence-to-immortality switch during hepatocellular carcinogenesis. Initially, we performed transcriptome analysis of senescent and immortal clones of Huh7 HCC cell line, and identified genes with significant differential expression to establish a senescence-related gene list. Through the analysis of senescence-related gene expression in different liver tissues we showed that cirrhosis and HCC display expression patterns compatible with senescent and immortal phenotypes, respectively; dysplasia being a transitional state. Gene set enrichment analysis revealed that cirrhosis/senescence-associated genes were preferentially expressed in non-tumor tissues, less malignant tumors, and differentiated or senescent cells. In contrast, HCC/immortality genes were up-regulated in tumor tissues, or more malignant tumors and progenitor cells. In HCC tumors and immortal cells genes involved in DNA repair, cell cycle, telomere extension and branched chain amino acid metabolism were up-regulated, whereas genes involved in cell signaling, as well as in drug, lipid, retinoid and glycolytic metabolism were down-regulated. Based on these distinctive gene expression features we developed a 15-gene hepatocellular immortality signature test that discriminated HCC from cirrhosis with high accuracy. Our findings demonstrate that senescence bypass plays a central role in hepatocellular carcinogenesis engendering systematic changes in the transcription of genes regulating DNA repair, proliferation, differentiation and metabolism.

Citation: Yildiz G, Arslan-Ergul A, Bagislar S, Konu O, Yuzugullu H, et al. (2013) Genome-Wide Transcriptional Reorganization Associated with Senescence-to-Immortality Switch during Human Hepatocellular Carcinogenesis. PLoS ONE 8(5): e64016. doi:10.1371/journal.pone.0064016

Editor: Birke Bartosch, Inserm, U1052, UMR 5286, France

Received: February 11, 2013; **Accepted:** April 7, 2013; **Published:** May 15, 2013

Copyright: © 2013 Yildiz et al. This is an open-access article distributed under the terms of the Creative Commons Attribution License, which permits unrestricted use, distribution, and reproduction in any medium, provided the original author and source are credited.

Funding: This study was supported by grants from TÜBİTAK (104S045, 106S151, 109S191, 111T558) with additional support from State Planning Office (DPT-Kaniltek Project), Turkish Academy of Sciences, Institut National de Cancer and La Ligue Nationale Contre le Cancer in France (Equipe labellisée). G.Y. was supported by TÜBİTAK (BİDEB-2211 and BİDEB-2214) and EMBO fellowships. The funders had no role in study design, data collection and analysis, decision to publish, or preparation of the manuscript.

Competing Interests: The authors have declared that no competing interests exist.

* E-mail: ozturk@fen.bilkent.edu.tr

These authors contributed equally to this work.

Introduction

Cellular senescence, a permanent loss of proliferative capacity despite continued viability and metabolic activity, is a critical feature of mammalian cells. It serves as a potent anti-tumor mechanism but it may also contribute to tissue aging [1,2,3]. This process was initially described in the form of replicative senescence [4], or telomere-dependent senescence, that has later been

characterized as a DNA damage checkpoint response to the loss of telomere integrity, because of progressive shrinkage of the telomere DNA during cell replication [5]. Subsequently, telomere-independent or premature forms of senescence have been discovered. Thus, not only telomere attrition but also oncogene activation [6], tumor suppressor gene inactivation, as well as exposure to DNA-damaging agents can trigger senescence responses [1]. Cellular processes leading to a senescence-type of

cell proliferation arrest are mediated mainly by p53 and p16^{INK4A}-Rb signal transduction cascades [1,7,8]. Senescence response can be delayed or bypassed by experimental activation of telomerase reverse transcriptase (TERT), and/or inactivation of p53 and p16^{INK4A}-Rb pathways. This leads cells to an immortal state with unlimited proliferation capacity [9]. Cells in pre-senescent, senescent and immortal states display highly divergent transcription patterns allowing them to exhibit distinct phenotypic and biochemical features [10,11,12].

Human tumors frequently exhibit TERT activation and inactivation of p53 and p16^{INK4A}-Rb-mediated senescence control pathways leading on the postulation that gain of cellular immortality is one of their common features [13]. Hepatocellular carcinoma (HCC) cells are also believed to acquire immortality, particularly in patients with liver cirrhosis known to exhibit a senescent phenotype [14,15]. Telomerase deficiency in mice accelerates the development of experimentally induced cirrhosis [16] and compromises liver regeneration [17]. The inactivation of *c-myc* or reactivation of p53 in murine HCC cells induces premature senescence leading to tumor regression [18,19]. These findings infer that *c-myc* activation and p53 inactivation may serve as a means to overcome senescence control, at least in murine HCC tumors. Human liver cells do not express the TERT enzyme and exhibit moderate telomere shortening during aging, yet senescence markers usually remain negative in old liver tissues. During chronic hepatitis, the development of cirrhosis is associated with accelerated telomere shortening. Moreover, cirrhotic tissues exhibit strong senescence-associated β -galactosidase (SA- β -Gal) activity, suggesting that most hepatocytes in a cirrhotic liver display a senescent phenotype [20,21,22,23]. In most human HCC tumors TERT expression is positive, telomerase activity is high and telomere length is short, but stabilized. However, a subset of HCC tumors display high SA- β -Gal activity suggestive of senescence arrest [14,20,24,25,26]. Thus, it appears that human HCC cells, as opposed to cirrhotic hepatocytes, acquire an immortal phenotype, although this has not yet been fully demonstrated. In favor of this suggestion, the genes encoding p53 and p16^{INK4A}, two major players in senescence control, are known to be inactivated by mutation and/or epigenetic silencing in nearly 50% of HCCs [15]. However, several important questions remain unanswered with regard to the relevance of senescence escape or immortality in human HCC. Among others, (i) a comprehensive list of genes associated with hepatocellular senescence and immortality is lacking; (ii) the cellular processes associated with senescence-related changes in cirrhosis and HCC are not well-documented; (iii) the timing of senescence-to-immortality transition during HCC development is unknown; and (iv) the potential value of senescence-related gene signatures for the diagnosis and/or prognosis of HCC has not yet been assessed. A better understanding of these mechanisms could contribute significantly to the discovery of novel molecular targets for diagnosis and treatment of cirrhosis and HCC diseases, which account for more than 500,000 deaths each year [27].

Here, we applied an integrative functional genomics approach to explore the impact of senescence-related genes in liver cirrhosis and HCC. We first generated genome-wide expression profiles of *in vitro* hepatocellular senescence and immortality using a unique senescence model based on the reprogramming of replicative senescence in HCC-derived Huh7 cells [28]. By combined analysis of *in vitro*, *in vivo* and *in silico* data, we provide a comprehensive list of genes and cellular processes associated with hepatocellular senescence and gain of cellular immortality in humans. We also report on a robust 15-gene hepatocellular immortality signature test that can efficiently differentiate HCC from cirrhosis.

Materials and Methods

Huh7 Clones

The establishment and culture conditions of senescence-programmed C3 and G12, and immortal C1 and G11 clones have been described previously [28]. Briefly, HCC-derived Huh7 cells were transfected with pcDNA3.1 (Invitrogen) or pEGFP-N2 (Clontech) vectors to obtain C1 and C3, and G11 and G12 clones, respectively. Following transfection, single cell-derived colonies were selected by G-418 sulfate (500 μ g/ml; Gibco) treatment under low-density clonogenic conditions. Senescence-programmed C3 and G12 clones proliferated stably until population doubling 80 (PD80) and PD90, respectively. Then, they entered senescence arrest as manifested by characteristic morphological changes, abundant SA- β -Gal staining and <5% 5-bromo-2'-deoxyuridine (BrdU) positivity after mitotic stimulation. Immortal C1 and G11 clones proliferated stably beyond PD140. For genome-wide expression studies described here, senescence-arrested C3 and G12 clones and immortal C1 and G11 clones were plated in triplicate onto 15-cm diameter petri dishes, left in culture for three days and collected for RNA extraction.

Other Cells and Cell Lines

Freshly isolated human hepatocytes were obtained commercially (hNHEPSTM- Human Hepatocytes, Lonza Group, Basel, Switzerland). Origin and culture conditions of HCC cell lines Huh7, HepG2, Hep3B, Hep40, PLC/PRF/5, SNU-387, SNU-398, SNU-423, SNU-449, SNU-475, FOCUS, Mahlavu and SK-Hep-1 were previously described [29]. The fibrolamellar HCC FLC4 cell line was provided by E. Galun (Hadassah, Israel) and cultivated as described for other HCC cell lines. MRC-5 human embryonic lung fibroblast cells (at PD45) were provided by R. Pedoux (Grenoble, France) and maintained in culture as previously described [30].

Patients and Samples

Liver cirrhosis and HCC samples were collected from two medical centers in Turkey. Tissue samples were snap frozen in liquid nitrogen and stored at -80°C until use. Frozen tissues were cut into 20 μ m thick slices, and scraped into microtubes for RNA extraction. Two 6 μ m tissue slices were also cut for pathological examination.

Ethics Statement

Clinical tissue sample collection was performed in accordance with a study protocol pre-approved by Ethical Committees of Ankara and Dokuz Eylul Universities, following written consent from each patient.

RNA Extraction

Total RNA from cell lines and tissues was extracted using total RNA isolation kit (Promega, Madison, USA) and NucleoSpin RNA II Kit (MN Macherey-Nagel), respectively. DNase digestion was performed following kit instructions. Cell line and tissue RNA samples were analysed using Agilent Bioanalyzer.

Genome-wide Gene Expression Profiling

Affymetrix platform with GeneChip Human Genome U133 Plus 2.0 arrays were used for microarray analysis of both cell and tissue RNA samples, following manufacturer instructions. GeneChip Operating Software (Affymetrix) was used to collect and store the microarray data. CEL files were uploaded to RMAExpress software to assess the quality of the arrays at the image level

(<http://rmaexpress.bmbolstad.com>). Quality assessment of the Affymetrix datasets was performed using affyPLM (<http://www.bioconductor.org>). NUSE and RLE plots were drawn and outliers with high deviation from the average probe intensity value were excluded from further analyses. The microarray data reported in this paper have been deposited in the Gene Expression Omnibus (GEO) database under accession numbers of GSE17546 (Huh7 clones) and GSE17548 (cirrhosis and HCC tumor samples). All cell line clones, 15 cirrhosis and 15 HCC tumor samples passed RNA quality control (RNA Integrity Number, RIN>6.5) and microarray quality control tests. RMA normalization and class comparison analyses were performed using BRB-ArrayTools developed by Dr. Richard Simon and BRB-ArrayTools Development Team (<http://linus.nci.nih.gov/BRB-ArrayTools.html>; Version 4.2.0).

Other Microarray Datasets

Two independent microarray datasets (GSE6764 and GSE19665) were downloaded from Gene Expression Omnibus (GEO) database (<http://www.ncbi.nlm.nih.gov/geo>) and analyzed by BRB Array tools after normalization with RMA.

Gene Set Enrichment Analysis

Gene set enrichment analyses (GSEA) were performed using GSEA program of the Broad Institute [31]. For comparing *in vitro* and *in vivo* GSEA profiles based on “C2_ALL” curated gene list, a custom Matlab[®] routine was applied to extract commonly enriched gene sets. Pearson’s correlation coefficients were calculated using Matlab[®] and Fisher’s exact test performed using VassarStats (Vassarstats.net).

Cluster Analysis

Cluster 3.0 software [32] was used to assess unsupervised clustering of datasets. First, data were adjusted by centering genes and arrays separately based on mean values, and then the average linkage clustering was applied to genes and arrays using a correlation (uncentered) similarity metric. Cluster files were visualized by Java Treeview [33].

Generation and Validation of a Senescence-based Genomic Classifier

A senescence-based genomic classifier associated with differential diagnosis of HCC from cirrhosis was generated in BRB Array Tools by Prediction Analysis of Microarrays [34] using data reported by Wurmbach et al. [35] as a “training set”. The resulting classifier was tested using the nearest template prediction (NTP) method [36] on a validation set constructed by combining data reported here for Turkish patients with data from Deng et al. [37] for Japanese patients. Nearest template prediction was performed using NTP module [36] of GenePattern program (<http://www.broadinstitute.org/cancer/software/genepattern/>) using default parameters of the module. The final image was generated using HeatMapImage module of the GenePattern and the output of the NTP.

ATAD2 Expression Analysis by Quantitative PCR and Western Blot Analyses

ATAD2, one of the 15 genes identified as a senescence-based genomic classifier set was further analyzed for immortality-associated over-expression in 14 HCC cell lines, as compared to freshly isolated human hepatocytes and MRC-5 human embryonic lung fibroblast cells (PD44) at RNA and protein levels. ATAD2 RNA expression was compared by quantitative real-time

PCR as previously described [38], using a specific primer pair (forward: 5'-AGG CTC ATT GGA AAA ACC T-3'; reverse: 5'-CCT GCG GAA GAT AAT CGG TA-3'). GAPDH was tested as a housekeeping control gene using the following primers: forward: 5'-GGC TGA GAA CGG GAA GCT TGT CAT-3'; reverse: 5'-CAG CCT TCT CCA TGG TGG TGA AGA-3'. The relative expression of ATAD2 RNA in cell lines was calculated as compared to that of normal hepatocytes. ATAD2 protein expression was compared by western blot analysis of cell lysates, as described previously [38], except that an anti-ATAD2 rabbit polyclonal antibody (Sigma; cat. no: HPA019860) was used at 1:500 dilution as the primary antibody. Anti-calnexin rabbit polyclonal antibody (Sigma; cat. no: C4731) was used at 1:10000 dilution for the loading control. The specificity of anti-ATAD2 antibody was validated by western blot analysis in Hep3B cells after transfection with ATAD2-siRNA1 described by Caron et al. [39]. For comparative analysis of ATAD2 protein expression between immortal and senescent cells, senescence was induced in Huh7 cells by Adriamycin (0.1 μ M) treatment for three days as previously described [40]. Briefly, Adriamycin- and DMSO vehicle control-treated cells were maintained in culture for three days. After confirming the senescence induction by morphological examination and SA- β -Gal staining, cell lysates were subjected to western blot analysis.

Results

Study Design

In order to analyze the participation of senescence-related genes in human liver diseases, we designed a study protocol, as outlined in Fig. 1. First, we generated genome-wide expression profiles of Huh7 cell-line derived isogenic clones, as well as cirrhosis and HCC tissues. The isogenic Huh7 clones that we used differed from each other by their entry into replicative senescence arrest (at PD80 to PD90) or lack of it (beyond PD150), resulting in a major shift in tumorigenicity [28]. Next, we subjected *in vitro* and *in vivo* gene expression data to gene set enrichment analysis (GSEA) to identify and compare functional groups of genes associated with senescence *versus* immortality, and cirrhosis *versus* HCC. Furthermore, we integrated our *in vitro* data with publicly available *in vivo* data for a senescence-based comparison of progressive liver lesions associated with hepatitis C virus (HCV)-induced HCC, and established a senescence-based gene signature test for differential diagnosis of HCC.

Gene Expression Profiles of Hepatocellular Senescence *in vitro*

We profiled four independently established Huh7 clones, subdivided into senescent and immortal phenotypes (i.e., two clones from each phenotype) using gene expression analysis with pangenomic 54 K Affymetrix microarrays. Three independent biological replicates from each clone were used so that a total of 12 gene chips were performed. Hierarchical clustering of expression values of the top 50 down- and up-regulated genes of each phenotype segregated cell samples based on phenotypic assignment, which suggested a common transcriptional consequence of a switch between senescent and immortal fates (Fig. 2a). Next we calculated GSEA enrichment scores [31] for six senescent cell samples against six immortal cell samples using all curated gene sets (“C2_All”) available at molecular signature database (MSigDB; www.broadinstitute.org/gsea/). Based on significant nominal P values ($P < 0.05$), senescent and immortal phenotypes were enriched in 598 and 113 gene sets, respectively (Data S1).

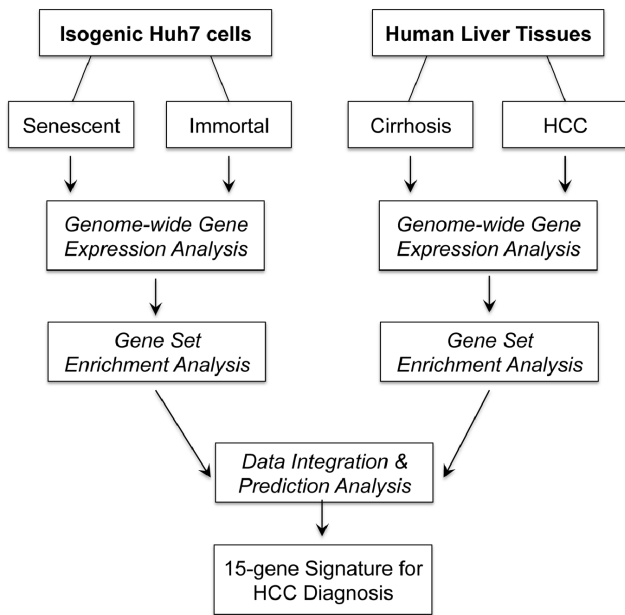


Figure 1. Flow chart summarizing the study design. We analyzed genome-wide gene expression in isogenic Huh7 clones with senescent and immortal phenotypes, as well as in cirrhotic tissues and HCC tumors. Both sets of data were subjected to GSEA using “C2-All” curated gene sets (“C2-All”) of molecular signature database (MSigDB; www.broadinstitute.org/gsea/). In order to assess senescence- and immortality-related gene expression changes during hepatocellular carcinogenesis, genes differentially expressed in the model of cellular senescence and immortality were identified and the evolution of their expression profiles in pre-neoplastic and neoplastic liver lesions were examined. Finally, a 15-gene senescence-based signature was generated using a training set of cirrhosis and HCC samples, and validated using independently generated test datasets. doi:10.1371/journal.pone.0064016.g001

Enriched gene sets included those participating in senescence- and immortality-related cellular processes and pathways, providing evidence for transcriptional validation of senescent and immortal phenotypes of Huh7 clones (Figs. 2b–e). As shown in Fig. 2b, senescent Huh7 cells were enriched in gene sets that are commonly up-regulated in senescent cells (“FRIDMAN_SENES-CENCE_UP”) [10]. In addition, p53-responsive genes up-regulated during replicative senescence arrest (“TANG_SENES-CENCE_TP53_TARGETS_UP”) [41], as well as genes down-regulated during immortalization in general (“FRIDMAN_IM-MORTALIZATION_DN”) [10], and by human papillomavirus 31 (“CHANG_IMMORTALIZED_BY_HPV_DN”) [42], were also up-regulated in senescent Huh7 clones. Interestingly, four enriched gene sets were connected directly with either TERT or telomeres (Fig. 2c–e). Genes down-regulated by TERT-mediated immortalization (“KANG_IMMORTALIZED_BY_TERT_DN”) [43], as well as TERT-repressed target genes (“SMITH_TERT_TARGETS_DN”) [44], were enriched in senescent Huh7 clones (Fig. 2c). Furthermore, genes involved in telomere end packaging (“REACTOME_PACKAGING_OF_TELOMERE_ENDS”; www.reactome.org) were up-regulated in senescent Huh7 clones (Fig. 2d), while genes involved in telomere extension (“REACTOME_EXTENSION_OF_TELOMERES”; www.reactome.org) were enriched in immortal Huh7 clones (Fig. 2e).

Association of Cirrhosis and Hepatocellular Carcinoma with Senescent and Immortal Phenotypes Respectively

According to the protocol described in Fig. 1, next we performed global gene expression analysis of 30 liver tissues, including 15 cirrhosis and 15 HCC samples. All HCC samples used in this study were obtained from cirrhotic patients (Table S1). Hierarchical clustering with 50 most up- and down-regulated genes were identified by GSEA-segregated tissue samples according to their clinical phenotypes (Fig. 3a). Gene set enrichment analysis of this *in vivo* data set using “C2-All” gene sets determined that cirrhosis and HCC phenotypes are associated with 161 and 189 enriched gene sets, respectively (nominal P values < 0.05; Data S1). Among those gene sets, several were connected to senescence- and immortality-related events. For example, cirrhosis was enriched in p53-responsive genes up-regulated during replicative senescence arrest (“TANG_SENES-CENCE_TP53_TARGETS_UP”) [41] (Fig. 3b). In contrast, HCC was enriched in p53-responsive genes down-regulated during replicative senescence arrest (“TANG_SENES-CENCE_TP53_TARGETS_DN”) [41] (Fig. 3c-top). Hepatocellular carcinoma tumors were also enriched in the expression of genes involved in telomere extension (“REACTOME_EXTENSION_OF_TELOMERES”; www.reactome.org) (Fig. 3c-down).

Senescence-related Gene Networks in Cirrhosis and Hepatocellular Carcinoma

The comparison of cell line and tissue enrichment scores based on commonly enriched gene lists (Data S1) revealed a striking correlation between senescence and cirrhosis ($P < 10^{-115}$; $r = 0.35$), as well as, between immortality and HCC ($P = 8 \times 10^{-114}$; $r = 0.72$). This finding suggested that many functional gene clusters overexpressed in cirrhosis and HCC were directly related to the senescent and immortal phenotypes, respectively. To further investigate this interesting correlation, we selected gene sets that are co-enriched in four groups of biological samples (i.e. senescent cells, immortal cells, cirrhotic tissues and HCCs) with a nominal P-value less than 0.05. As shown in Fig. 4a, 34 of 74 common gene sets (46%) were co-enriched in senescent cells and cirrhotic tissues, whereas 39 (53%) were co-enriched in immortal cells and HCCs (Two-tailed Fisher exact test, $P = 2.6 \times 10^{-20}$). Pearson correlation values of co-enrichment scores were also significant ($r = 0.97$, $P = 2 \times 10^{-43}$; Data S1). Gene sets up-regulated in cirrhosis/senescence group were also up-regulated in non-tumor tissues as opposed to those with tumors (four gene sets), or in less malignant tumors *versus* more malignant tumors (11 gene sets). In contrast, genes up-regulated in HCC/immortality group were associated with tumors as opposed to non-tumor tissues (four out of five gene sets), or in more malignant tumors as compared to less malignant tumors (four gene sets). The HCC/immortality state was characterized by an up-regulation of genes involved in DNA repair (13 gene sets), cell cycle (seven gene sets), progenitor state (two gene sets), telomere extension, DNA methylation and branched chain amino acid metabolism. In contrast, genes involved in cell signaling (six gene sets), lipid metabolism (four gene sets), drug metabolism, retinol metabolism and glycolysis were down-regulated (Fig. 4b).

Detailed analysis of genes involved in retinoid metabolism [45,46] revealed that the expression of several genes encoding critical enzymes catalyzing the synthesis of retinoic acid (the active form of retinoids) was down-regulated in HCC tumors as compared to cirrhotic liver tissue. There was also down-regulated expression of genes involved in the storage of retinoids in tumors. Down-regulated genes included two members of retinol dehydro-

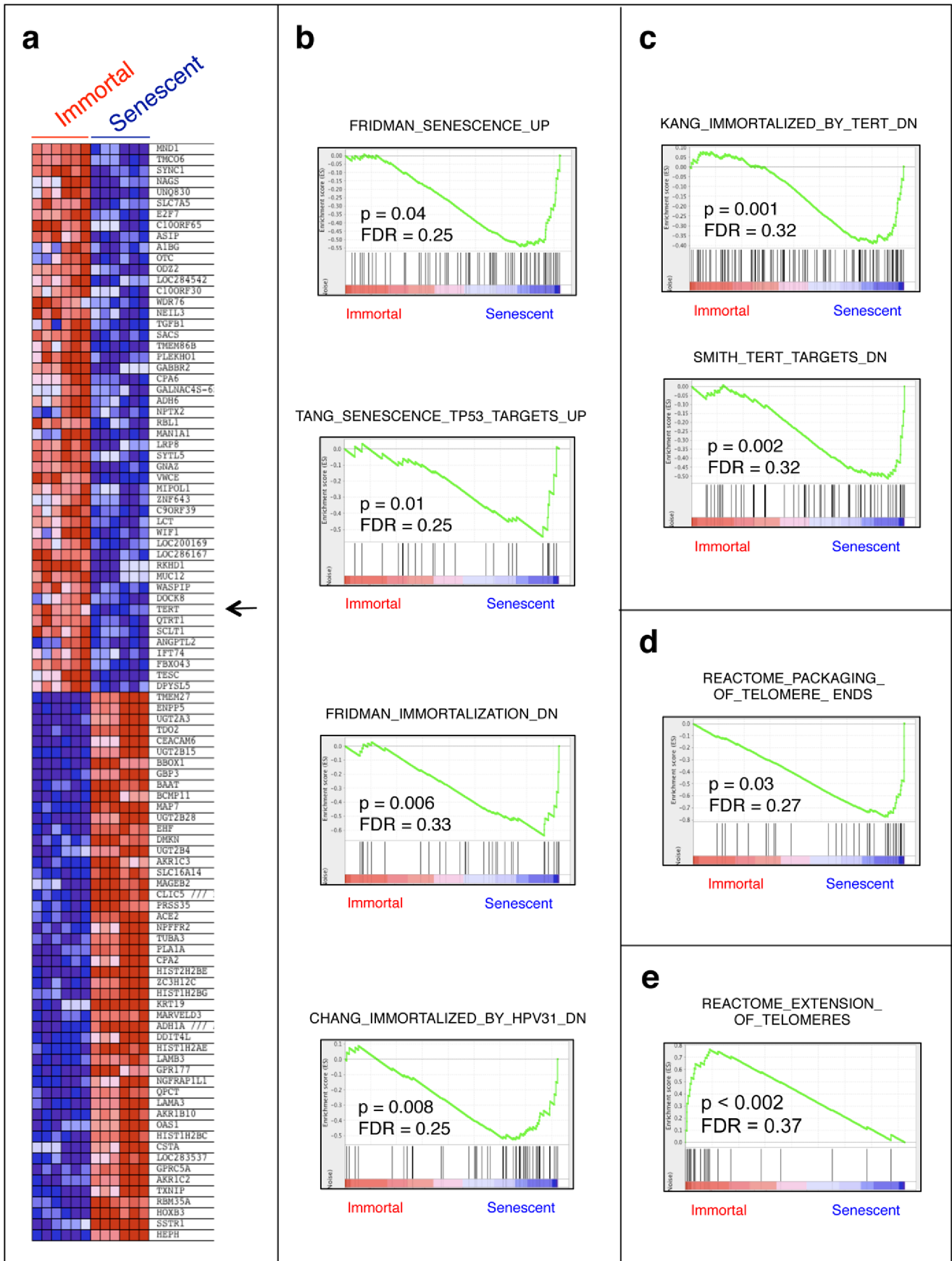


Figure 2. Gene expression profile analysis by gene set enrichment analysis assay (GSEA) established that senescent and immortal Huh7 clones displayed differential expression of previously identified senescence- and immortality-associated gene sets respectively, as well as those regulating telomere maintenance. (a) Heat map representation of the top 100 deregulated genes in immortal Huh7 clones (Immortal) versus senescent Huh7 (Senescent) clones. Red: up-regulated; blue: down-regulated; arrow indicates TERT gene whose expression is down-regulated in senescent clones. Previously identified gene sets (available at molecular signature database (MSigDB; www.broadinstitute.org/gsea/) were screened to identify those that are differentially enriched in senescent or immortal Huh7 clones by the analysis of their relative expression levels using GSEA method. (b) Gene set enrichment plots showing the up-regulated expression of two previously known senescence-associated gene sets in senescent Huh7 clones, including genes that are commonly up-regulated in senescent cells ("FRIDMAN_SENESCENCE_UP") [10] and p53-responsive genes up-regulated during replicative senescence arrest ("TANG_SENESCENCE_TP53_TARGETS_UP") [41]. In addition, genes known to be down-regulated during immortalization in general ("FRIDMAN_IMMORTALIZATION_DN") [10], and by human papillomavirus 31 ("CHANG_IMMORTALIZED_BY_HPVDN") [42] were also up-regulated in senescent Huh7 clones. (c) Genes known to be down-regulated by TERT-mediated immortalization ("KANG_IMMORTALIZED_BY_TERT_DN") [43] and TERT-repressed target genes ("SMITH_TERT_TARGETS_DN") [44] were also enriched in senescent Huh7 clones. (d) Genes involved in telomere end packaging ("REACTOME_PACKAGING_OF_TELOMERE_ENDS"; www.reactome.org) were upregulated in senescent Huh7 clones. (e) In contrast, genes involved in telomere extension ("REACTOME_EXTENSION_OF_TELOMERES"; www.reactome.org) were enriched in immortal Huh7 clones. Enrichment scores (ES) are shown on the y-axis. Positive and negative ES indicate enrichment in immortal and senescent Huh7 clones, respectively. X-axis bars represent individual genes of the indicated gene sets. FDR: False discovery rate, p: nominal p-value. Three biological replicates from each clone were analyzed for genome-wide gene expression using Affymetrix 54 K microarrays and normalized data were used for gene set enrichment analysis (GSEA). doi:10.1371/journal.pone.0064016.g002

genes, four members of alcohol dehydrogenases, NADP(H)-dependent retinol dehydrogenase/reductase (*DHRS4*) and β -carotene 15,15'-monooxygenase 1 (*BCMO1*), which are all involved in the synthesis of retinal, the immediate precursor of retinoic acid. Two genes involved in the synthesis of storage retinyl esters, namely lecithin:retinol acyltransferase (*LRAT*) and patatin-like phospholipase-4 (*PNPLA4*) were also down-regulated in HCC cells (Fig. 5).

A Senescence-to-immortality Switch between Dysplasia and Hepatocellular Carcinoma

Hepatocellular carcinogenesis is a multi-step process that is usually manifested by progressive histological changes in the liver from the cirrhosis stage to dysplasia followed by HCC [47]. Based on close association of cirrhosis with senescence and that of HCC with immortality, we hypothesized that the relative expression of senescence- and immortality-associated genes in different liver lesions may serve as a powerful means to dissect the timing of transition from a senescent state to an immortal phenotype during hepatocellular carcinogenesis. With this aim, we first generated a list of "senescence-related genes" by comparing differential gene expression between senescent and immortal Huh7 clones. Then, we analyzed the expression patterns of these "senescence-related genes" in a spectrum of hepatic lesions representing different steps of HCC development. The list of senescence-related genes was established by class comparison analysis of *in vitro* gene expression data. Multivariate permutation tests identified 1220 genes represented by 1813 probe sets with statistically significant expression changes between senescent and immortal clones (P -values $< 10^{-7}$; fold-changes between senescent and immortal clones: > 2.0). The selected probe sets were then tested against a publicly available gene expression dataset for tissues at different histological stages of HCC development in HCV patients [35]. The tissue set was composed of 10 normal liver samples, 13 cirrhotic tissues, 17 dysplastic lesions (originally described low- and high-grade dysplasia cases combined), 17 early HCCs (originally described very early and early HCC cases combined) and 18 advanced HCCs (originally described advanced and very advanced cases combined). Unsupervised clustering analysis applied to compare these hepatic tissue samples ($n = 75$ in total) generated two major clusters. Cluster 1 grouped together 39 out of the 40 non-HCC samples (97.5%) and 1 out of the 35 (3%) HCC samples. Conversely, cluster 2 was composed of 34 out of the 35 HCCs (97%) and one of 40 (2.5%) of the non-HCC samples (Fig. 6). Dysplastic lesions together with a subset of cirrhosis tissues formed a homogenous subgroup under cluster 1, while normal liver

samples shared similarities with either cirrhotic or dysplastic tissue. HCC samples formed several minor clusters, with a tendency of early and advanced tumors to form distinct sub-clusters. The most interesting finding of this analysis was the clustering of dysplastic liver lesions together with cirrhosis samples that are in a senescent-like state rather than with HCC samples assigned to an immortal-like state.

Fifteen-gene Hepatocellular Immortality Signature for Diagnosis of Hepatocellular Carcinoma

Based on remarkable clustering of tumor and non-tumor tissues by the 1220 senescence-related genes, we then asked whether we could select a smaller subset for discrimination of HCC from cirrhosis. We used expression data from 35 HCC and 13 cirrhosis samples from Wurmbach et al. [35] as a "training set". A PAM analysis using "nearest shrunken centroid method" [34] identified 18 classifiers, composed of six immortality-associated probe sets (representing five genes) up-regulated in HCC tissues, ten senescence-associated probe sets up-regulated in cirrhosis samples, and two senescence-associated probe sets up-regulated in HCC (Fig. 7a). Fisher's exact test demonstrated a strong association of cirrhosis with senescence and HCC with immortal phenotypes ($P = 0.0015$). Then, we selected ten "cirrhosis- and senescence-associated" and five "HCC- and immortality-associated" genes (16 probe sets in total) to construct a "hepatocellular immortality signature set" (Table S2). Next, we tested the diagnostic value of the signature genes using a "test set" composed of 45 tissue samples, including 30 Turkish patient samples reported here and 15 Japanese patient samples with publicly available expression data [37]. Based on Nearest Template Prediction method [36], the signature set was able to predict 100% (20/20) of cirrhotic tissues with high confidence ($FDR < 0.05$). Five of 25 HCC samples (20%) were unpredictable ($FDR > 0.05$). Of the remaining 20 HCC samples, 19 (95%) were predicted correctly (Fig. 7b). Overall, the signature set provided high confidence prediction ($FDR < 0.05$) in 89% (40/45) of patients with 97.5% (39/40) accuracy.

Association of ATAD2 RNA and Protein Expressions with HCC and Cellular Immortality

The *ATAD2*, one of the fifteen hepatocellular immortality signature genes, was of particular interest warranting further investigation. The *ATAD2* gene is mapped to chromosome 8q24 and codes for a predicted protein of 1,391 amino acids that contains a double AAA ATPase domain and a bromodomain [48].

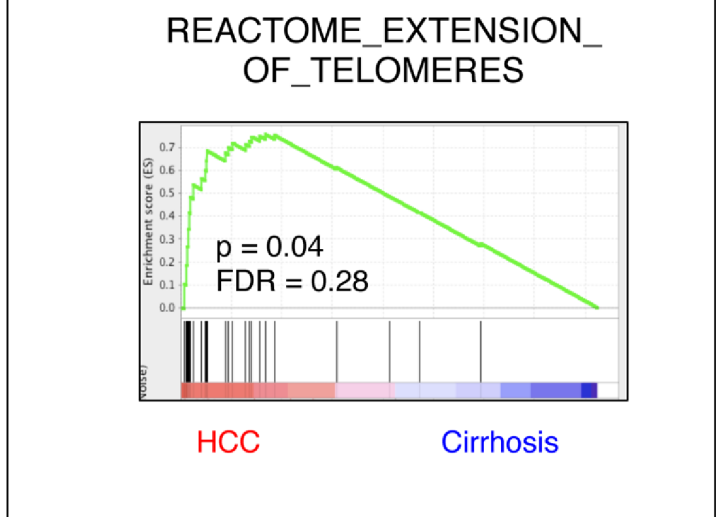
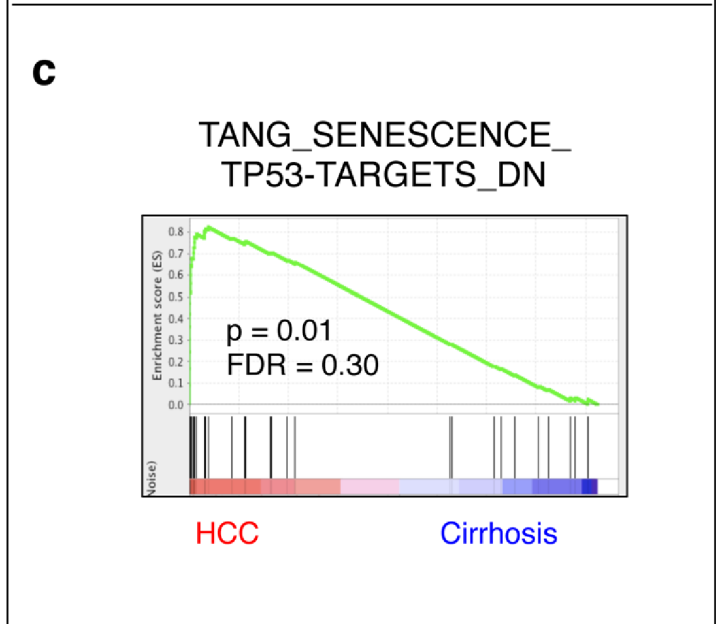
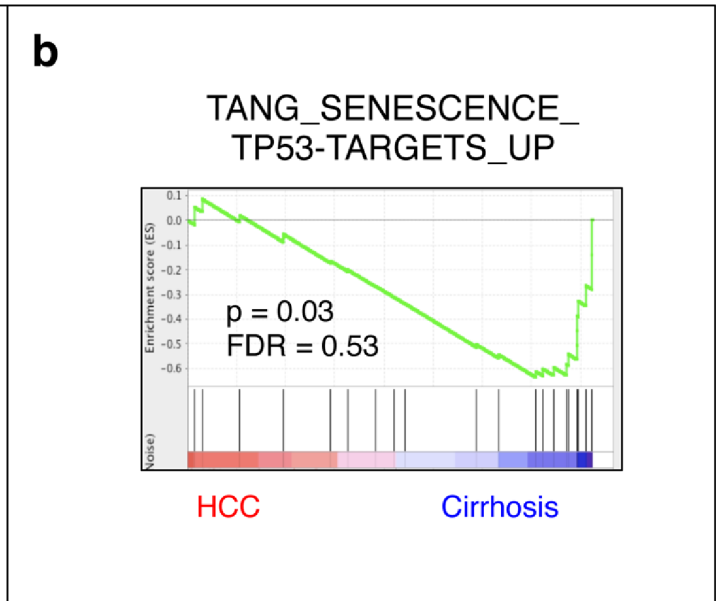
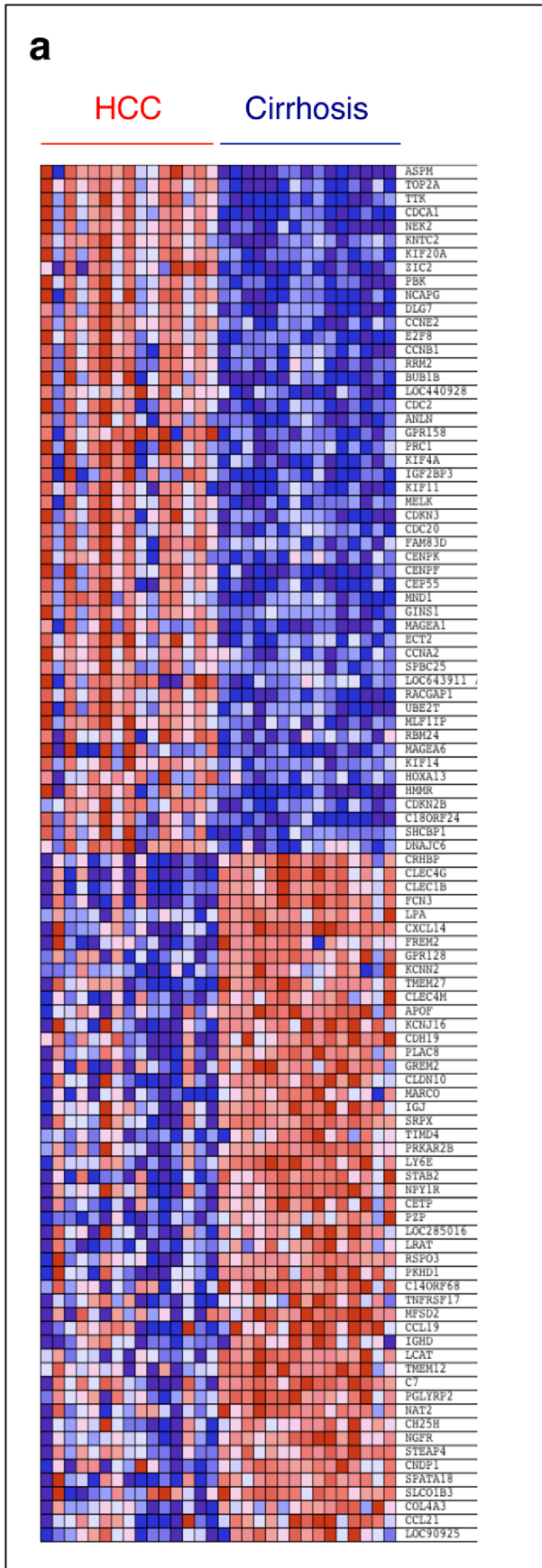


Figure 3. Gene expression profile analysis by gene set enrichment analysis (GSEA) revealed the overexpression of senescence-upregulated genes in cirrhosis, but over-expression of senescence-downregulated genes and telomere extension genes in HCC tissues. (a) Heat map representation of the top 100 deregulated genes in hepatocellular carcinoma (HCC) versus cirrhosis samples. Red: up-regulated; blue: down-regulated. Previously identified gene sets (available at molecular signature database (MSigDB; www.broadinstitute.org/gsea/)) were screened to identify those that are up-regulated in cirrhosis or HCC tissues by the analysis of their relative expression levels using GSEA method. (b) Enrichment plot of p53-responsive genes up-regulated during replicative senescence arrest ("TANG_SENESCENCE_TP53_TARGETS_UP") [41] showing over-expression in cirrhosis. (b) In contrast, p53-responsive genes down-regulated during replicative senescence arrest ("TANG_SENESCENCE_TP53_TARGETS_DN") [41] and those involved in telomere extension ("REACTOME_EXTENSION_OF_TELOMERES"; www.reactome.org) were overexpressed in HCC tumors. Enrichment scores (ES) are shown on the y-axis. Positive and negative ES indicate enrichment in HCC and cirrhosis samples, respectively. X-axis bars represent individual genes of the indicated gene sets. FDR: False discovery rate, p: nominal p-value. Fifteen cirrhosis and fifteen HCC samples were analyzed for genome-wide gene expression using Affymetrix 54 K microarrays and normalized data were used for gene set enrichment analysis (GSEA). doi:10.1371/journal.pone.0064016.g003

The 8q24 locus displays frequent copy number gains in HCC [49], and many other cancers [50]. Therefore, we selected ATAD2 as a representative of our hepatocellular immortality signature to validate its immortality- and HCC-associated expression by additional experiments (Fig. 8). Freshly isolated normal adult

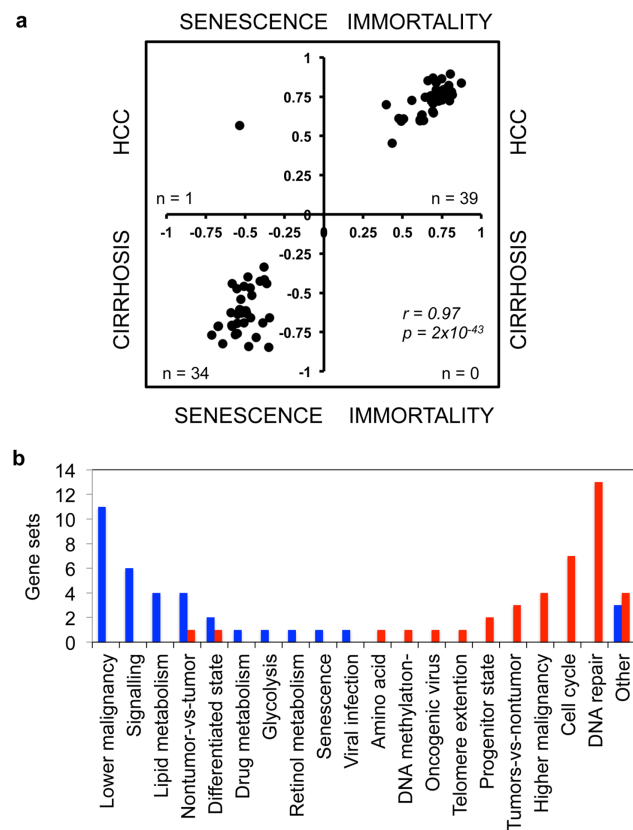


Figure 4. Comparative analysis of gene sets enriched in Huh7 clones and diseased liver tissues associated cirrhosis with senescence and HCC with immortality phenotypes, respectively. (a) This analysis revealed also that cirrhosis/senescence- and HCC/immortality-associated gene sets implicated distinct biological features specific to each phenotype (b). (a) Scatter plot compares enrichment scores of 74 gene sets commonly enriched in Huh7 clones (senescent or immortal) and diseased liver tissues (cirrhosis or HCC) with a P value less than 0.05. Thirty-nine gene sets (53%) were significantly enriched in both HCC and immortal samples whereas 34 (46%) gene sets were significantly enriched in both cirrhosis and senescent samples (correlation value $r = 0.97$, $p = 2 \times 10^{-43}$). Only one gene set (1%) was enriched in both HCC and senescent clones. (b) Distribution of biological features defined by different gene sets in cirrhosis/senescence (blue columns) and HCC/immortality (red columns) phenotypes, respectively. doi:10.1371/journal.pone.0064016.g004

human hepatocytes and MRC-5 normal human fetal lung fibroblasts (at PD44) were used as non-immortal control cells that enter replicative senescence at around PD65 [30]. When compared to normal hepatocytes, most HCC cell lines ($n = 12/14$; 86%) displayed between two- and 20-fold higher ATAD2 mRNA expression. ATAD2 expression was less in MRC-5 cells than hepatocytes (Fig. 8a). In order to further investigate ATAD2 expression, we tested its protein levels using a polyclonal rabbit anti-ATAD2 antibody that recognized a single major band in Hep3B HCC cells (Fig. 8b line Hep3B). The knock-down of ATAD2 by siRNA1 [39] in these cells resulted in the loss of an anti-ATAD2 immunoreactive band (Fig. 8b line Hep3B-si), demonstrating the specificity of this antibody. ATAD2 protein was undetectable in normal hepatocytes, but highly abundant in six out of nine HCC cell lines, and easily detectable in the remaining three (Fig. 8b). In order to further investigate immortality-associated expression of ATAD2 in HCC cells, we induced senescence arrest in Huh7 cells by 0.1 μ M Adriamycin treatment (Fig. 8c) as previously described [40], and compared ATAD2 expression between Adriamycin-treated and control Huh7 cells by western blot assay. We observed a drop in the levels of ATAD2 proteins in senescence-arrested cells, as compared to immortal Huh7 cells (Fig. 8d).

Discussion

Cellular senescence, considered for a long time to be an *in vitro* phenomenon, emerged in recent years as a critical mechanism that may play key roles in tissue aging as well as in the development of different tumor types [1]. Here, we used a unique *in vitro* hepatocellular senescence model to map senescence-related events associated with *in vivo* HCC development. Our *in vitro* model displayed a gene expression pattern compatible with replicative senescence and TERT-induced cellular immortalization, in conformation of our previously published observations [28]. We were fortunate to find a high number of differentially expressed genes between senescent and immortal clones that served as an investigational tool to examine senescence-related transcriptional events occurring during hepatocellular carcinogenesis. Based on this, we provide here transcription-based evidence that cirrhosis and HCC represent two opposite cellular phenotypes, senescence and immortality, respectively. One of the major features of this phenotypic opposition was the status of telomere maintenance genes both between senescence and immortality, and cirrhosis and HCC (Figs. 2, 3). The activation of TERT and telomere end extension genes in immortal and HCC phenotypes is of particular interest. Accelerated shortening of telomeres associated with a lack of telomerase activity and high cell turnover during chronic hepatitis has been recognized as a hallmark of cirrhosis several years ago [16,21,51]. More recently, constitutional "loss-of-function" type of telomerase (*TERT* or *TERC* genes) mutations have been identified as a risk factor for cirrhosis [52,53]. In

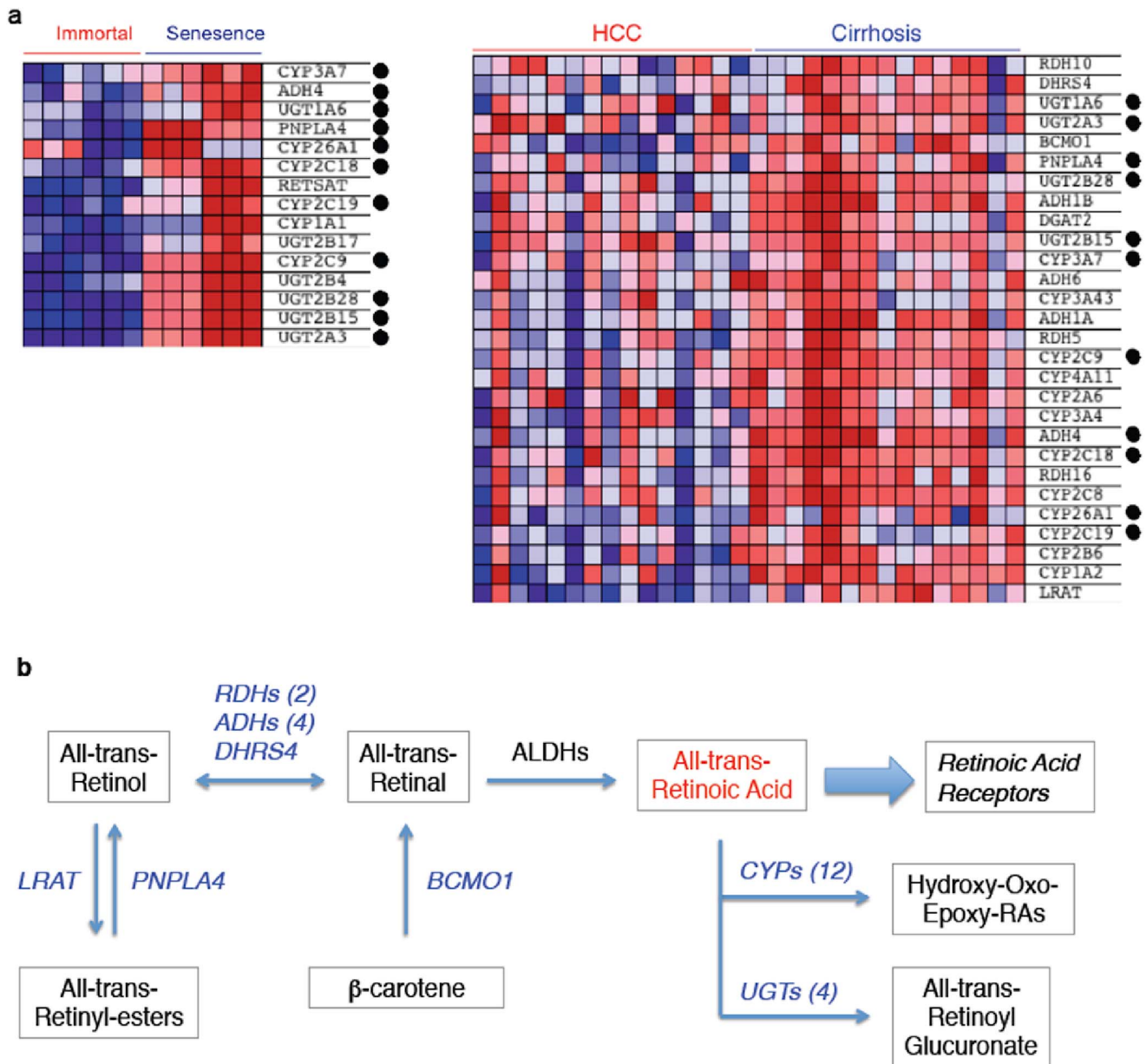


Figure 5. Comparative analysis of core enriched gene sets in Huh7 clones (senescent versus immortal) and diseased liver tissues (cirrhosis versus HCC) indicated that retinoid metabolism genes (“KEGG_RETINOL_METABOLISM”) undergo systematic changes in immortal cells and HCC, when compared to senescent cells and cirrhosis, respectively. (a) Heat map of core enriched retinoid metabolism genes in Huh7 clones (left) and diseased liver tissues (right). Red: up-regulated; blue: down-regulated. Genes commonly deregulated in both Huh7 clones and diseased liver tissues are indicated with a dot. (b) A simplified view of retinoid metabolism. Enzyme-encoding genes down-regulated in HCC are shown in blue. LRAT: lecithin retinol acetyl transferase, PNPLA4: patatin-like phospholipase domain containing-4, RDHs: retinol dehydrogenases; ADHs: alcohol dehydrogenases; DHRSA4: dehydrogenase/reductase (SDR family) member-4; BCMO1: beta-carotene 15,15'-monooxygenase-1; CYPs: Cytochrome P-450 family proteins; UGTs: UDP glucuronosyltransferases.
doi:10.1371/journal.pone.0064016.g005

contrast to cirrhosis, HCC is known to reactivate *TERT* expression [54], display high telomerase activity [24] and stabilize telomeres [24,55]. Based on our present data supported by these earlier reports, we propose that the activation of telomerase activity is a key event for the gain of immortalized phenotype by HCC cells. While working on this manuscript, recurrent and activating *TERT* promoter mutations have been reported for HCC cell lines [56], in strong support of our hypothesis.

The transition from a senescent state to an immortal state coincided with early HCC lesions while dysplastic lesions

remained associated with cirrhosis and normal liver sample groups indicating a non-immortal state. This pattern correlates with malignant transformation in other tissues where pre-neoplastic lesions display a senescent state from which neoplastic transformation emerges with a gain of phenotypic and molecular features that are linked to an immortal state [57].

Co-enrichment of a high number of gene sets in cirrhotic tissues and senescent cells as well as in HCCs and immortal cells was highly interesting. This finding further emphasized the biological evidence for a gain of immortal phenotype in human HCC. Among the gene sets

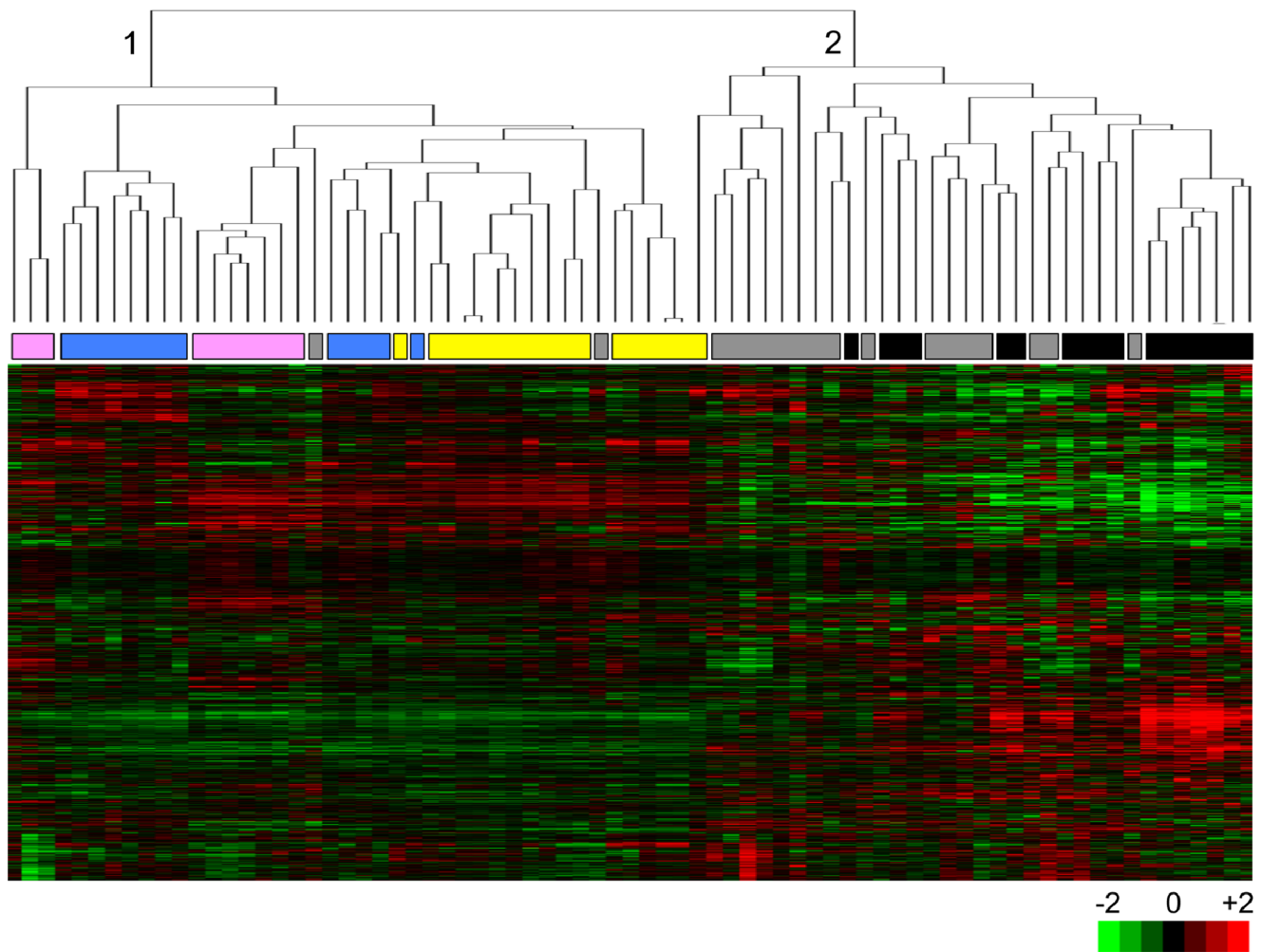


Figure 6. Hierarchical clustering of 75 non-malignant and malignant liver tissue samples using 1813 senescence-associated gene probe sets. Hepatocellular carcinoma and non-tumor liver tissues formed two distinct clusters (1 and 2) with the exception of one dysplasia and two early HCC samples. The rows and columns represent genes and samples, respectively on the cluster map. Tissue samples are normal liver (pink), cirrhosis (blue), dysplasia (yellow), early HCC (gray), and advanced HCC (black). Red: over-expressed, green: under-expressed probe set in the heat map.

doi:10.1371/journal.pone.0064016.g006

co-enriched in HCC and immortal cells, cell cycle and DNA repair gene sets were at the top of the list (Fig. 4b). Up-regulation of cell cycle and DNA repair genes in HCC is already known [35,58]; and the overexpression of cell cycle genes in immortal cells is expected. The up-regulation of DNA repair genes may serve as a mechanism to escape from DNA damage-induced senescence arrest by increasing DNA repair capacity of immortal or HCC cells.

Another interesting outcome of co-enrichment analysis was the differential association of metabolism regulatory gene sets with cirrhosis/senescence and HCC/immortality phenotypes. Co-enrichment patterns revealed that genes involved in glycolysis as well as those regulating drug, lipid and retinol metabolisms were down-regulated in both immortal cells and HCC tumors. Down-regulation of genes encoding the enzymes necessary for retinoic acid biosynthesis and intracellular retinoic storage in HCC is of particular interest. Retinoic acid, which is the active metabolite of retinoids, regulates a wide range of biological processes including development, differentiation, proliferation, and apoptosis [59]. Normal hepatocytes together with hepatic stellate cells play an indispensable role in the availability of retinoic acid and the storage of dietary retinoids [46]. Deregulated expression of

retinoid metabolism genes in HCC is expected to cause a deficit in the synthesis of retinoic acid as well as in the storage of its metabolic precursors (Fig. 5). Accordingly, reduced retinoid content has been reported for HCC [46,60,61]. A deficit in cellular retinoic acid levels in HCC cells, due to the expression changes reported here, may cause severe perturbations in a multitude of cellular processes governed by retinoic acid [59] by conferring a survival advantage to immortalized HCC cells. Thus the restoration of retinoic acid availability in HCC cells may adversely affect their survival. In favor of this hypothesis, treatment with a synthetic analog of retinoic acid successfully prevented second primary tumors in post-surgical HCC patients [62]. Thus, a deficit in the availability of endogenous retinoic acid might facilitate malignant transformation and tumor progression.

The most important risk factor for HCC is cirrhosis that is present in 80 to 90% of patients with HCC. The patients with cirrhosis develop HCC with a rate of 1.4–3.3% per year [27]. Therefore, the screening of cirrhotic patients by ultrasonography of the liver combined with measurement of serum alpha-fetoprotein levels every 6 to 12 months for HCC development is recommended. However, the strength of the evidence supporting

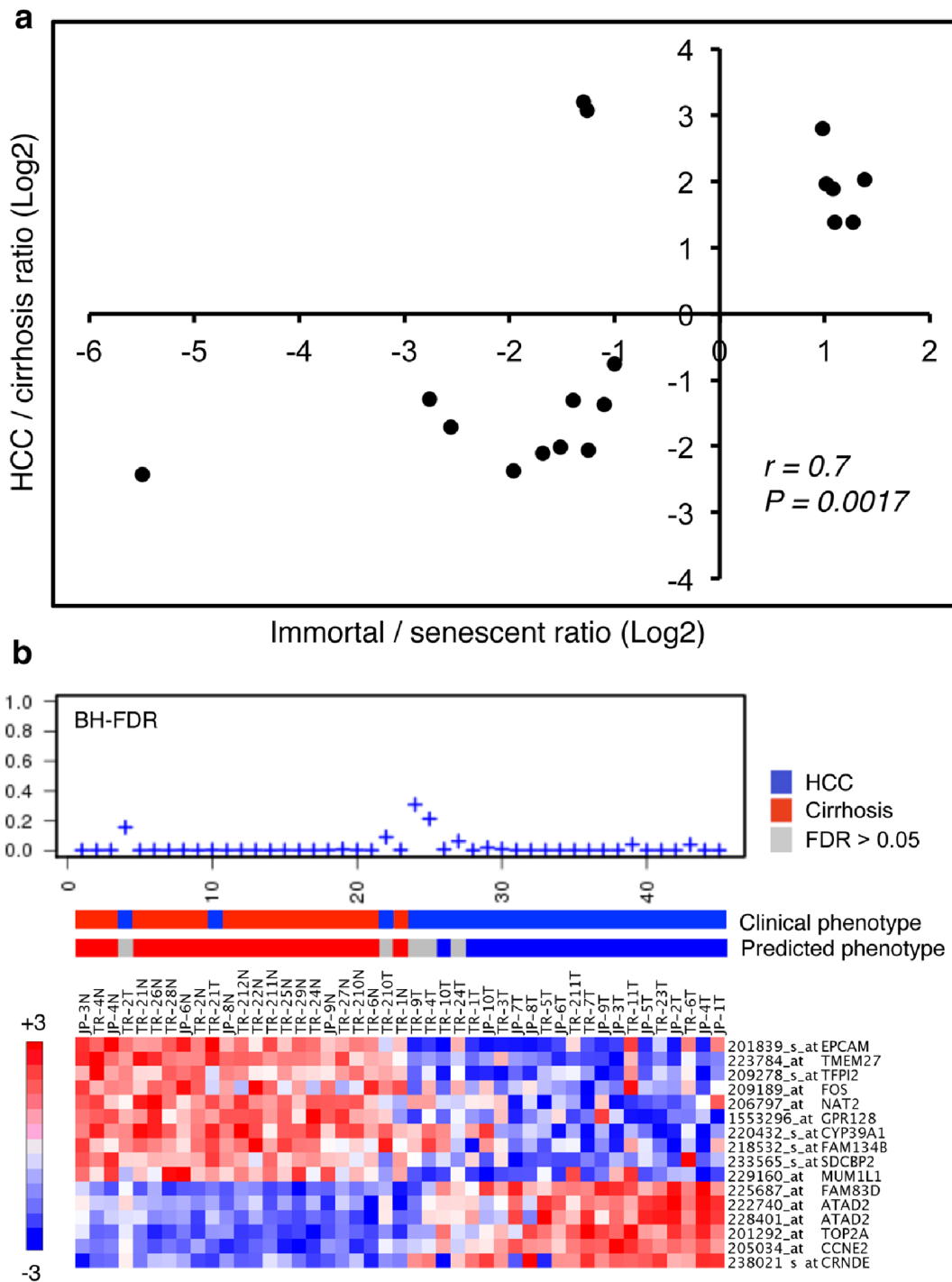


Figure 7. Generation and validation of a senescence-based gene classifier for differential diagnosis of cirrhosis and HCC. (a) Scatter plot graphic compares relative expression levels (Log2 ratios) of 18 classifier probe sets representing 17 genes in Huh7 clones (immortal versus senescent) and diseased liver tissues (HCC versus cirrhosis). Expression ratios of classifier genes showed a linear correlation (correlation value $r = 0.7$, $p = 0.0017$) with ratios observed in Huh7 clones (immortal/senescent) and diseased liver tissues (HCC/cirrhosis). The classifier set was identified by PAM analysis of 1813 senescence-associated probe sets using a training tissue set composed of cirrhosis ($n = 13$) and HCC ($n = 35$) samples described by Wurmbach et al. [35]. Two probe sets which did not show expression patterns compatible with our *in vivo* senescence model were discarded to define a final signature set composed of 16 probe sets representing 15 genes. (b) Validation of molecular prediction of HCC and cirrhosis by 15-classifier gene set. Using the nearest template prediction method [36], we compared expression levels of sixteen probe sets representing 15 classifier genes in a test tissue set composed of 20 cirrhosis and 25 HCC samples originating from Turkish (TR) patients described in this report, and Japanese (JP) patients described elsewhere [37]. BH FDR (Benjamini-Hochberg false discovery rates) values (top), clinical versus predicted phenotypes (middle) and heatmaps of classifier gene expression levels (bottom) are shown. The test provided a diagnostic result for 40 out of 45 samples (89%) with 97.5% (39/40) accuracy.
doi:10.1371/journal.pone.0064016.g007

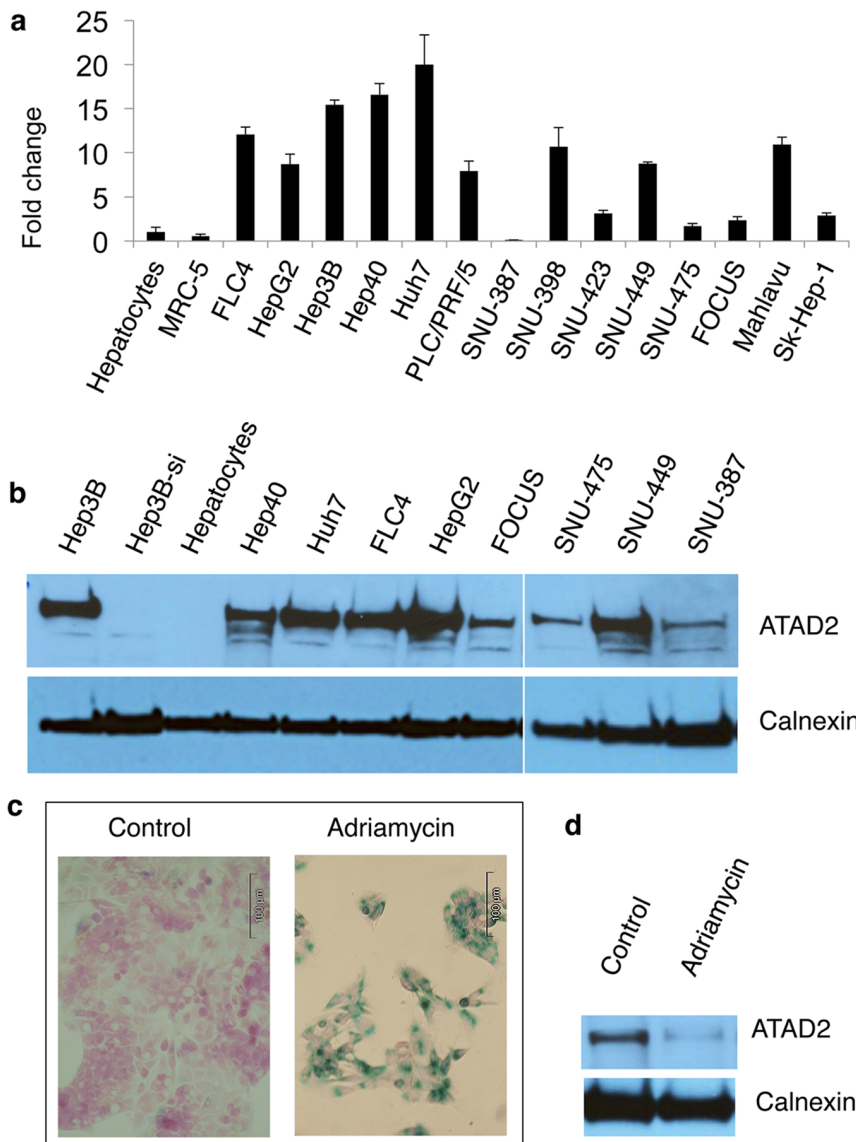


Figure 8. Association of ATAD2 RNA and protein expressions with HCC and cellular immortality. (a) Amplified expression of ATAD2 RNA in HCC cell lines, as compared to normal hepatocytes and MRC-5 fibroblasts. Total RNAs were extracted from freshly isolated adult human hepatocytes (Hepatocytes), MRC-5 human embryonic lung fibroblast cells (PD44) and 14 HCC cell lines; reverse transcribed into cDNA; and ATAD2 RNA was quantified by quantitative real-time PCR using specific primers. ATAD2 expression values for each sample were normalized with housekeeping gene GAPDH RNA values. Relative expression of ATAD2 in MRC-5 and HCC cell lines was expressed in reference to its expression in hepatocytes. Averages of three measurements. Error bars: SD. (b) Amplified expression of ATAD2 protein in HCC cells, as compared to normal hepatocytes. Total proteins were extracted from freshly isolated adult human hepatocytes (Hepatocytes), untreated (Hep3B) and ATAD2 siRNA1-treated (Hep3B-si) Hep3B and eight other HCC cell lines, and ATAD2 protein levels were tested by western blot analysis using a specific anti-ATAD2 antibody (ATAD2). Western blot analysis of calnexin protein from the same blots was used for loading control (Calnexin). (c, d) Comparative analysis by western blotting demonstrated that ATAD2 protein is overexpressed in immortal Huh7 cells as compared to senescence-arrested Huh7 cells. (c) Huh7 cells were treated with Adriamycin (0.1 μ M) or DMSO (Control) for three days and subjected to senescence assay by SA- β -Gal staining (blue). Cells were counterstained with fast red (red). (d) Total protein was extracted from control and Adriamycin-treated Huh7 cells, and ATAD2 and Calnexin proteins were tested as described in (b). doi:10.1371/journal.pone.0064016.g008

the efficacy of surveillance is modest [63]. To overcome the lack of efficacy, molecular HCC diagnosis techniques have been proposed [64]. Previously reported molecular techniques used either candidate genes [65] or genome-wide expression data [35,54,66,67] to discriminate HCC from cirrhosis or dysplasia. None of these molecular tests have yet to enter into surveillance recommendations [64], probably because their prediction strength did not reach the required level and/or they require simultaneous

analysis of dozens, even hundreds, of genes. Here, we provide a highly promising hepatocellular immortality signature test for HCC diagnosis. This novel molecular test requires the expression profiles of only 15 genes. Moreover, this is a functional test based on the analysis of senescence- and immortality-associated genes in tissue samples. The test was able to correctly predict 100% of cirrhosis cases. Twenty percent of HCCs displayed a borderline gene expression pattern, so that the classifier was not able to

categorize them as HCC or cirrhosis. However, the test was able to predict the remaining HCC patients with 97.5% accuracy.

One of the hepatocellular immortality signature genes is ATAD2. By using techniques independent of microarray tools, we demonstrated *in vitro* that ATAD2 RNA and protein that are weakly present or not expressed in normal hepatocytes and fibroblasts are highly expressed in HCC cell lines. We also showed that ATAD2 protein levels go down in association with Adriamycin-induced senescence arrest in otherwise immortal Huh7 cells. ATAD2 protein is likely to be a chromatin modifier [48]. Its exact cellular function is unknown, but its overexpression in immortal cells, and in many cancer types [39,68] is in favor of an essential role in tumor malignancy. Finally, our preliminary findings suggest that hepatocellular immortality signature genes such as ATAD2 may serve as promising HCC biomarkers.

Supporting Information

Table S1 Patient demographic data, diagnosis and disease etiology of clinical samples used for gene signature validation test.
(XLSX)

References

- Kuilman T, Michaloglou C, Mooi WJ, Peeper DS (2010) The essence of senescence. *Genes & development* 24: 2463–2479.
- Collado M, Blasco MA, Serrano M (2007) Cellular senescence in cancer and aging. *Cell* 130: 223–233.
- Adams PD (2009) Healing and hurting: molecular mechanisms, functions, and pathologies of cellular senescence. *Molecular cell* 36: 2–14.
- Hayflick L, Moorhead PS (1961) The serial cultivation of human diploid cell strains. *Experimental cell research* 25: 585–621.
- d'Adda di Fagnana F, Reaper PM, Clay-Farrace L, Fiegler H, Carr P, et al. (2003) A DNA damage checkpoint response in telomere-initiated senescence. *Nature* 426: 194–198.
- Serrano M, Lin AW, McCurrach ME, Beach D, Lowe SW (1997) Oncogenic ras provokes premature cell senescence associated with accumulation of p53 and p16INK4a. *Cell* 88: 593–602.
- Grimes A, Chandra SB (2009) Significance of cellular senescence in aging and cancer. *Cancer research and treatment: official journal of Korean Cancer Association* 41: 187–195.
- Lanigan F, Geraghty JG, Bracken AP (2011) Transcriptional regulation of cellular senescence. *Oncogene* 30: 2901–2911.
- Hahn WC, Counter CM, Lundberg AS, Beijersbergen RL, Brooks MW, et al. (1999) Creation of human tumour cells with defined genetic elements. *Nature* 400: 464–468.
- Fridman AL, Tainsky MA (2008) Critical pathways in cellular senescence and immortalization revealed by gene expression profiling. *Oncogene* 27: 5975–5987.
- Shelton DN, Chang E, Whittier PS, Choi D, Funk WD (1999) Microarray analysis of replicative senescence. *Current biology: CB* 9: 939–945.
- Zhang H, Pan KH, Cohen SN (2003) Senescence-specific gene expression fingerprints reveal cell-type-dependent physical clustering of up-regulated chromosomal loci. *Proceedings of the National Academy of Sciences of the United States of America* 100: 3251–3256.
- Hanahan D, Weinberg RA (2011) Hallmarks of cancer: the next generation. *Cell* 144: 646–674.
- Rudolph KL, Hartmann D, Opitz OG (2009) Telomere dysfunction and DNA damage checkpoints in diseases and cancer of the gastrointestinal tract. *Gastroenterology* 137: 754–762.
- Ozturk M, Arslan-Ergul A, Bagislar S, Senturk S, Yuzugullu H (2009) Senescence and immortality in hepatocellular carcinoma. *Cancer letters* 286: 103–113.
- Rudolph KL, Chang S, Millard M, Schreiber-Agus N, DePinho RA (2000) Inhibition of experimental liver cirrhosis in mice by telomerase gene delivery. *Science* 287: 1253–1258.
- Satyanarayana A, Wiemann SU, Buer J, Lauber J, Dittmar KE, et al. (2003) Telomere shortening impairs organ regeneration by inhibiting cell cycle re-entry of a subpopulation of cells. *EMBO J* 22: 4003–4013.
- Xue W, Zender L, Miething C, Dickins RA, Hernandez E, et al. (2007) Senescence and tumour clearance is triggered by p53 restoration in murine liver carcinomas. *Nature* 445: 656–660.
- Wu CH, van Riggelen J, Yetil A, Fan AC, Bachireddy P, et al. (2007) Cellular senescence is an important mechanism of tumor regression upon c-Myc inactivation. *Proc Natl Acad Sci U S A* 104: 13028–13033.
- Paradis V, Youssef N, Dargere D, Ba N, Bonvoust F, et al. (2001) Replicative senescence in normal liver, chronic hepatitis C, and hepatocellular carcinomas. *Hum Pathol* 32: 327–332.
- Wiemann SU, Satyanarayana A, Tshuridid M, Tillmann HL, Zender L, et al. (2002) Hepatocyte telomere shortening and senescence are general markers of human liver cirrhosis. *FASEB J* 16: 935–942.
- Brunt EM, Walsh SN, Hayashi PH, Labundy J, Di Bisceglie AM (2007) Hepatocyte senescence in end-stage chronic liver disease: a study of cyclin-dependent kinase inhibitor p21 in liver biopsies as a marker for progression to hepatocellular carcinoma. *Liver Int* 27: 662–671.
- Hoare M, Das T, Alexander G (2010) Ageing, telomeres, senescence, and liver injury. *Journal of hepatology* 53: 950–961.
- Kojima H, Yokosuka O, Imazeki F, Saisho H, Omata M (1997) Telomerase activity and telomere length in hepatocellular carcinoma and chronic liver disease. *Gastroenterology* 112: 493–500.
- Plentz RR, Caselitz M, Bleck JS, Gebel M, Flemming P, et al. (2004) Hepatocellular telomere shortening correlates with chromosomal instability and the development of human hepatoma. *Hepatology* 40: 80–86.
- Plentz RR, Park YN, Lechel A, Kim H, Nellessen F, et al. (2007) Telomere shortening and inactivation of cell cycle checkpoints characterize human hepatocarcinogenesis. *Hepatology* 45: 968–976.
- El-Serag HB, Rudolph KL (2007) Hepatocellular carcinoma: epidemiology and molecular carcinogenesis. *Gastroenterology* 132: 2557–2576.
- Ozturk N, Erdal E, Mumcuoglu M, Akcali KC, Yalcin O, et al. (2006) Reprogramming of replicative senescence in hepatocellular carcinoma-derived cells. *Proc Natl Acad Sci U S A* 103: 2178–2183.
- Yuzugullu H, Benhaj K, Ozturk N, Senturk S, Celik E, et al. (2009) Canonical Wnt signaling is antagonized by noncanonical Wnt5a in hepatocellular carcinoma cells. *Molecular cancer* 8: 90.
- Binet R, Ythier D, Robles AI, Collado M, Larrieu D, et al. (2009) WNT16B is a new marker of cellular senescence that regulates p53 activity and the phosphoinositide 3-kinase/AKT pathway. *Cancer research* 69: 9183–9191.
- Subramanian A, Tamayo P, Mootha VK, Mukherjee S, Ebert BL, et al. (2005) Gene set enrichment analysis: a knowledge-based approach for interpreting genome-wide expression profiles. *Proceedings of the National Academy of Sciences of the United States of America* 102: 15545–15550.
- de Hoon MJ, Imoto S, Nolan J, Miyano S (2004) Open source clustering software. *Bioinformatics* 20: 1453–1454.
- Saldanha AJ (2004) Java Treeview—extensible visualization of microarray data. *Bioinformatics* 20: 3246–3248.
- Tibshirani R, Hastie T, Narasimhan B, Chu G (2002) Diagnosis of multiple cancer types by shrunken centroids of gene expression. *Proceedings of the National Academy of Sciences of the United States of America* 99: 6567–6572.
- Wurmbach E, Chen YB, Khitrov G, Zhang W, Roayaie S, et al. (2007) Genome-wide molecular profiles of HCV-induced dysplasia and hepatocellular carcinoma. *Hepatology* 45: 938–947.
- Hoshida Y (2010) Nearest template prediction: a single-sample-based flexible class prediction with confidence assessment. *PLoS one* 5: e15543.
- Deng YB, Nagae G, Midorikawa Y, Yagi K, Tsutsumi S, et al. (2010) Identification of genes preferentially methylated in hepatitis C virus-related hepatocellular carcinoma. *Cancer science* 101: 1501–1510.

Table S2 Microarray gene expression data and literature review of 15 classifier genes.
(XLSX)

Data S1 Gene Set Enrichment Analysis (GSEA) results of gene expression data from Huh7 clones (immortal and senescent) and diseased liver tissues (cirrhosis and HCC). “C2_All” curated gene sets of the MSig Database were analyzed. Commonly enriched gene sets in senescent/cirrhosis, immortal/cirrhosis, immortal/HCC, senescent/HCC groups are provided. The final worksheet summarizes 74 gene sets with significant co-enrichment ($P < 0.05$) in both Huh7 clones and diseased liver tissues.
(XLSX)

Author Contributions

Conceived and designed the experiments: MO. Performed the experiments: GY AAE SB HY OGY NO CO HO. Analyzed the data: GY AAE SB OK HY OGY OI HGI MO. Contributed reagents/materials/analysis tools: EE SK OS DM HB BB RCA NA. Wrote the paper: MO GY AAE SB OK.

38. Senturk S, Mumcuoglu M, Gursoy-Yuzugullu O, Cingoz B, Akcali KC, et al. (2010) Transforming growth factor-beta induces senescence in hepatocellular carcinoma cells and inhibits tumor growth. *Hepatology* 52: 966–974.
39. Caron C, Lestrat C, Marsal S, Escoffier E, Curtet S, et al. (2010) Functional characterization of ATAD2 as a new cancer/testis factor and a predictor of poor prognosis in breast and lung cancers. *Oncogene* 29: 5171–5181.
40. Gursoy-Yuzugullu O, Yuzugullu H, Yilmaz M, Ozturk M (2011) Aflatoxin genotoxicity is associated with a defective DNA damage response bypassing p53 activation. *Liver international: official journal of the International Association for the Study of the Liver* 31: 561–571.
41. Tang X, Milyavsky M, Goldfinger N, Rotter V (2007) Amyloid-beta precursor-like protein APLP1 is a novel p53 transcriptional target gene that augments neuroblastoma cell death upon genotoxic stress. *Oncogene* 26: 7302–7312.
42. Chang YE, Laimins LA (2000) Microarray analysis identifies interferon-inducible genes and Stat-1 as major transcriptional targets of human papillomavirus type 31. *Journal of virology* 74: 4174–4182.
43. Kang SK, Putnam L, Dufour J, Ylostalo J, Jung JS, et al. (2004) Expression of telomerase extends the lifespan and enhances osteogenic differentiation of adipose tissue-derived stromal cells. *Stem cells* 22: 1356–1372.
44. Smith LL, Collier HA, Roberts JM (2003) Telomerase modulates expression of growth-controlling genes and enhances cell proliferation. *Nature cell biology* 5: 474–479.
45. D'Ambrosio DN, Clugston RD, Blaner WS (2011) Vitamin A metabolism: an update. *Nutrients* 3: 63–103.
46. Shirakami Y, Lee SA, Clugston RD, Blaner WS (2012) Hepatic metabolism of retinoids and disease associations. *Biochimica et biophysica acta* 1821: 124–136.
47. Farazi PA, DePinho RA (2006) Hepatocellular carcinoma pathogenesis: from genes to environment. *Nat Rev Cancer* 6: 674–687.
48. Zou JX, Revenko AS, Li LB, Gemo AT, Chen HW (2007) ANCCA, an estrogen-regulated AAA+ ATPase coactivator for ERalpha, is required for coregulator occupancy and chromatin modification. *Proceedings of the National Academy of Sciences of the United States of America* 104: 18067–18072.
49. Fujiwara Y, Monden M, Mori T, Nakamura Y, Emi M (1993) Frequent multiplication of the long arm of chromosome 8 in hepatocellular carcinoma. *Cancer research* 53: 857–860.
50. Beroukhi R, Mermel CH, Porter D, Wei G, Raychaudhuri S, et al. (2010) The landscape of somatic copy-number alteration across human cancers. *Nature* 463: 899–905.
51. Kitada T, Seki S, Kawakita N, Kuroki T, Monna T (1995) Telomere shortening in chronic liver diseases. *Biochemical and biophysical research communications* 211: 33–39.
52. Hartmann D, Srivastava U, Thaler M, Kleinhans KN, N'Kontchou G, et al. (2011) Telomerase gene mutations are associated with cirrhosis formation. *Hepatology* 53: 1608–1617.
53. Calado RT, Brudno J, Mehta P, Kovacs JJ, Wu C, et al. (2011) Constitutional telomerase mutations are genetic risk factors for cirrhosis. *Hepatology* 53: 1600–1607.
54. Llovet JM, Chen Y, Wurbach E, Roayaie S, Fiel MI, et al. (2006) A molecular signature to discriminate dysplastic nodules from early hepatocellular carcinoma in HCV cirrhosis. *Gastroenterology* 131: 1758–1767.
55. Urabe Y, Nouse K, Higashi T, Nakatsukasa H, Hino N, et al. (1996) Telomere length in human liver diseases. *Liver* 16: 293–297.
56. Huang FW, Hodis E, Xu MJ, Kryukov GV, Chin L, et al. (2013) Highly recurrent TERT promoter mutations in human melanoma. *Science* 339: 957–959.
57. Collado M, Serrano M (2010) Senescence in tumours: evidence from mice and humans. *Nature reviews Cancer* 10: 51–57.
58. Xu XR, Huang J, Xu ZG, Qian BZ, Zhu ZD, et al. (2001) Insight into hepatocellular carcinogenesis at transcriptome level by comparing gene expression profiles of hepatocellular carcinoma with those of corresponding noncancerous liver. *Proceedings of the National Academy of Sciences of the United States of America* 98: 15089–15094.
59. Bushue N, Wan YJ (2010) Retinoid pathway and cancer therapeutics. *Advanced drug delivery reviews* 62: 1285–1298.
60. Adachi S, Moriwaki H, Muto Y, Yamada Y, Fukutomi Y, et al. (1991) Reduced retinoid content in hepatocellular carcinoma with special reference to alcohol consumption. *Hepatology* 14: 776–780.
61. Clemente C, Elba S, Buongiorno G, Berloco P, Guerra V, et al. (2002) Serum retinol and risk of hepatocellular carcinoma in patients with child-Pugh class A cirrhosis. *Cancer letters* 178: 123–129.
62. Muto Y, Moriwaki H, Saito A (1999) Prevention of second primary tumors by an acyclic retinoid in patients with hepatocellular carcinoma. *The New England journal of medicine* 340: 1046–1047.
63. El-Serag HB (2011) Hepatocellular carcinoma. *The New England journal of medicine* 365: 1118–1127.
64. Villanueva A, Minguez B, Forner A, Reig M, Llovet JM (2010) Hepatocellular carcinoma: novel molecular approaches for diagnosis, prognosis, and therapy. *Annual review of medicine* 61: 317–328.
65. Paradis V, Bieche I, Dargere D, Laurendeau I, Laurent C, et al. (2003) Molecular profiling of hepatocellular carcinomas (HCC) using a large-scale real-time RT-PCR approach: determination of a molecular diagnostic index. *The American journal of pathology* 163: 733–741.
66. Nam SW, Park JY, Ramasamy A, Shevade S, Islam A, et al. (2005) Molecular changes from dysplastic nodule to hepatocellular carcinoma through gene expression profiling. *Hepatology* 42: 809–818.
67. Kim JW, Ye Q, Forgues M, Chen Y, Budhu A, et al. (2004) Cancer-associated molecular signature in the tissue samples of patients with cirrhosis. *Hepatology* 39: 518–527.
68. Ciro M, Prosperini E, Quarto M, Grazini U, Walfridsson J, et al. (2009) ATAD2 is a novel cofactor for MYC, overexpressed and amplified in aggressive tumors. *Cancer research* 69: 8491–8498.



Genetics and epigenetics of liver cancer

Cigdem Ozen¹, Gokhan Yildiz^{1,2}, Alper Tunga Dagcan¹, Dilek Cevik^{1,2}, Aysegul Ors^{1,2}, Umur Keles¹, Hande Topel¹ and Mehmet Ozturk^{1,2}

¹ Bilkent University, BilGen Genetics and Biotechnology Center, Department of Molecular Biology and Genetics, 06800 Ankara, Turkey

² Université Joseph Fourier – Grenoble 1, INSERM Institut Albert Bonniot, U823, Site Santé-BP 170, 38042 Grenoble Cedex 9, France

Hepatocellular carcinoma (HCC) represents a major form of primary liver cancer in adults. Chronic infections with hepatitis B (HBV) and C (HCV) viruses and alcohol abuse are the major factors leading to HCC. This deadly cancer affects more than 500,000 people worldwide and it is quite resistant to conventional chemo- and radiotherapy. Genetic and epigenetic studies on HCC may help to understand better its mechanisms and provide new tools for early diagnosis and therapy. Recent literature on whole genome analysis of HCC indicated a high number of mutated genes in addition to well-known genes such as *TP53*, *CTNNB1*, *AXIN1* and *CDKN2A*, but their frequencies are much lower. Apart from *CTNNB1* mutations, most of the other mutations appear to result in loss-of-function. Thus, HCC-associated mutations cannot be easily targeted for therapy. Epigenetic aberrations that appear to occur quite frequently may serve as new targets. Global DNA hypomethylation, promoter methylation, aberrant expression of non-coding RNAs and dysregulated expression of other epigenetic regulatory genes such as *EZH2* are the best-known epigenetic abnormalities. Future research in this direction may help to identify novel biomarkers and therapeutic targets for HCC.

Introduction

The most frequent primary liver cancers are hepatocellular carcinoma (HCC) and cholangiocarcinoma in adults, and hepatoblastoma in children. More than 80% of liver tumours are HCCs [1]. This review will focus primarily on HCC, one of the most frequent cancers worldwide with more than 500,000 new cases observed each year. Almost the same number of deaths is observed because of this cancer could not be easily treated. The most efficient treatment for HCC is liver transplantation, provided that it is detected early enough. Surgical removal and chemo-embolisation of tumour nodules are other alternatives. These tumours are usually resistant to chemo- or radiotherapy [1–3]. Targeted therapy of HCC is in its infancy. The only clinically relevant drug is a kinase inhibitor, Sorafenib, has only a modest effect on patient survival [4].

The aetiology of HCC is well known. Chronic liver injury associated primarily with hepatitis B (HBV) and C (HCV) virus infection

constitutes the most important cause of HCC. Other factors, such as alcohol abuse and dietary exposure to aflatoxins, are also established causes, but their contribution to the disease aetiology is much less than the contributions of viral agents. The unprecedented increase in obesity rates in both developed and developing countries is a rising concern for HCC risk that may account for the unexpected increase in HCC incidence in the Western world [1].

Molecular mechanisms of hepatocellular carcinogenesis remain ill-defined, mainly due to disease heterogeneity. The heterogeneity of agents that cause chronic liver injury (HBV, HCV, aflatoxins and alcohol) and the ways they interact with the host DNA and epigenetic players are the most probable parameters contributing to HCC heterogeneity.

Chromosomal aberrations and hepatitis B virus integration into the host genome

Chromosomal aberrations such as deletions and copy number gains are frequent in HCC. Initial studies identified that HCC

Corresponding author: Ozturk, M. (ozturk@fen.bilkent.edu.tr)

harbours multiple chromosomal abnormalities, predominantly losses, with increased chromosomal instability in tumours associated with HBV infection. Common alterations include gain of chromosomes 1q, 8q and 17q, and loss of 4q [5]. Recently, data from whole genome analysis techniques showed that chromosomes 1q, 5, 6p, 7, 8q, 17q and 20 display chromosomal gains, while 1p, 4q, 6q, 8p, 13q, 16, 17p and 21 exhibit losses in HCC [6].

In addition, HBV DNA is often integrated into the host genome in patients with HBV-related HCCs [7]. This integration may have *cis* and *trans* effects. Viral DNA integration into or near gene sequences may alter gene expression as well as gene integrity. In addition, integrated viral DNA may encode wild-type or truncated viral proteins acting in *trans* on the host genome, either by deregulating gene expression or by interacting with host proteins [8]. Recently reported whole genome studies indicated that the viral integration is associated with breakpoints within the HBV genome that primarily localised to the downstream region of the *HBX* gene. HBV genome integration was observed within or upstream of the *TERT* (telomerase reverse transcriptase) gene in four HBV-related HCCs. However, HBV integration sites within the same or different tumours did not show specific patterns, suggesting that the virus does not target specific host sequences. [9]. Based on these findings, it is highly probable that landscape changes in the structural integrity of chromosomes, as well as random but multiple integrations of HBV genomes into host genomes, cause high levels of instability in the chromosomal integrity of HCC. Some of these aberrations may hit crucial genes such as *TERT*, which may directly contribute to tumour development by inappropriate activation or inactivation of the genes themselves. In addition, the integration of viral enhancer sequences in the vicinity of crucial genes may lead to aberrant gene expression in HCC.

Gene mutations

Since the discovery of *TP53* as the first mutated gene in HCC over 20 years ago [10] and until very recently, only four genes were known to display frequent alterations in liver cancers. While *TP53*, *CTNNB1* (encoding β -catenin) and *AXIN1* genes usually display point mutations and small deletions, *CDKN2A* (encoding p16^{INK4a}) undergoes homozygous deletions and epigenetic silencing [11,12].

During the past two years, the first reports of whole-genome or exome sequencing data for HCC have appeared [6,9,13]. This is the beginning of a new era of HCC genetics, because of the fact that these new techniques will allow the visualisation of the mutational landscape of HCC. Figure 1 shows a summary of primary findings gathered by ourselves from two recently published reports [6,9]. Each study first analysed a small set of tumours ($n = 20\text{--}25$) for a genome-wide search of somatically mutated genes; significantly mutated genes were then further tested for mutations using a larger set of tumours ($n > 100$).

A close examination of the data of Fig. 1 indicates that *TP53* and *CTNNB1* represent the two most frequently mutated genes. A second group of genes (*AXIN1* and *ARID1A*) was found to present less frequent mutations, but still present in more than 10% of HCC samples studied. The third group is the largest with 22 genes displaying recurrent mutations in less than 10% of tumours. Guichard et al. [6] reported that Wnt/ β -catenin, p53, PI3K/Ras signalling, oxidative, endoplasmic reticulum stress pathways and chromatin remodelling were frequently affected by these mutations.

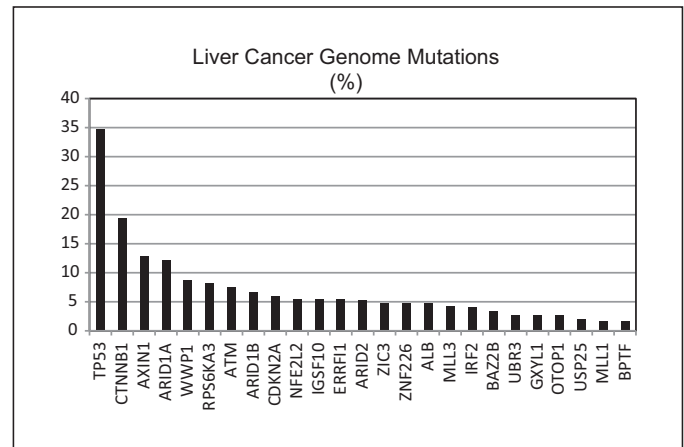


FIGURE 1

Most frequently mutated genes in hepatocellular carcinoma.

Whole genome sequencing allowed the detection of recurrent somatic mutations in several genes annotated as associated with chromatin regulation, such as *ARID1A*, *ARID1B*, *ARID2*, *MLL*, *MLL3*, *BAZ2B*, *BRD8*, *BPTF*, *BRE* and *HIST1H4B*. Notably, 14 out of the 27 tumours (52%) had either somatic point mutations or indels in at least one of these chromatin regulators. In both sets of experiments (whole genome sequencing and the validation sets), the number of indels in chromatin regulator genes was significantly higher than those in genes belonging to the other categories. This suggests that loss-of-function mutations are enriched in these chromatin-regulator genes in HCC genomes [9].

As shown in Table 1, the frequent mutations that identified so far in HCC are likely to result in loss of function with the notable exception of *CTNNB1* mutations. It will be interesting to study why loss of function rather than gain of function of crucial genes is associated with HCC. By contrast, this pattern of mutation does not offer a broad spectrum of therapeutic intervention applications. Cancer cells can easily be targeted by blocking genes that are aberrantly overactive in these cells. The restoration of a lost gene activity to achieve a therapeutic intervention is difficult to achieve. Thus, although the genome-wide analyses have been very helpful in establishing the list of a large set of mutated genes in HCC, this will most probably serve diagnostic needs while the chance of their therapeutic use is more limited.

Epigenetic deregulation

Epigenetic regulation of gene expression involves DNA methylation, post-translational histone modifications, chromatin changes and non-coding RNAs that are often affected in cancer cells [14,15]. The role of epigenetic deregulation in HCC is being increasingly recognised [16]. In addition to changes in DNA methylation, microRNA expression, mutations affecting epigenetic regulatory genes have recently been discovered in HCC [6,9,13].

HCC cells display global hypomethylation as well as promoter hypermethylation of a large set of genes [17]. Promoter hypermethylation appears to affect mainly tumour suppressor and anti-proliferative genes resulting in downregulation of gene expression (Fig. 2). Aberrations in microRNA expression have also been observed with several of them being linked to metabolic and phenotypic changes in HCC cells [14,18–20].

TABLE 1
Most frequent gene mutations in hepatocellular carcinoma are predicted to lead to a loss-of-function

Genes	% mutation rates	Protein function	Known/expected outcome
<i>TP53</i>	35	DNA damage response, other	Loss-of-function
<i>CTNNB1</i>	19	Positive regulator of Wnt signalling	Gain-of-function
<i>AXIN1</i>	13	Negative regulator of Wnt signalling	Loss-of-function
<i>ARID1A</i>	12	Chromatin remodelling	Loss-of-function
<i>WWP1</i>	9	E3 ubiquitin ligase	Loss-of-function?
<i>RPS6KA3</i>	8	Ribosomal protein S6 kinase	?
<i>ATM</i>	8	DNA damage response	Loss-of-function?
<i>ARID1B</i>	7	Chromatin remodelling	Loss-of-function?
<i>CDKN2A</i>	6	Positive regulator of senescence	Loss-of-function
<i>NFE2L2</i>	5	Redox homeostasis?	?
<i>IGSF10</i>	5	?	Loss-of-function
<i>ERRFI1</i>	5	EGFR/ERB2 kinase inhibitor	Loss-of-function
<i>ARID2</i>	5	Chromatin remodelling	Loss-of-function?

Several genes encoding epigenetic regulatory proteins are involved in hepatocellular malignancy. The *EZH2* (*KMT6*) encodes the catalytic component of the Polycomb Repressive Complex 2 (*PRC2*), creating the transcriptionally repressive H2K27Me3 histone mark which results in transcriptional silencing [21]. *EZH2* is over-expressed in HCC and mostly associated with the progression and aggressive biological behaviour of HCC [22,23]. *EZH2* protein silences Wnt pathway antagonists and constitutively activates Wnt/ β -catenin signalling causing cell proliferation in HCC cells [24]. *EZH2* also exerts a prometastatic function through epigenetic silencing of multiple tumour suppressor miRNAs including miR-139-5p, miR-125b, miR-101, let-7c and miR-200b [25]. Yang et al. identified an lncRNA called lncRNA-HEIH (High Expression in HCC) that associates with *EZH2* to repress *EZH2* target genes such

as p16^{Ink4a} and p21^{Cip1} in HBV-related HCC [26]. BMI1 is another *PRC2* member overexpressed in HCC. Effendi et al. determined that BMI1 is upregulated in early and well-differentiated HCC and this expression correlates with ABCB1 expression [27].

Expression of histone deacetylases (*HDACs*) is deregulated in different cancers [28], and some of them are also deregulated in HCC. *HDACs*-1, -2 and -3 are over-expressed in HCC [29,30]. *LC3B-II*-induced inactivation of *HDAC1* caused regression of HCC cell proliferation and triggered caspase independent autophagy. p21^{Cip1} and p27^{Kip1} were selectively induced while cyclin D1 and *CDK2* were suppressed by inactivation of *HDAC1*. As a result, *HDAC1* inactivation resulted in hypophosphorylation of pRb in the G1/S checkpoint to inactivate *E2F/DP1* transcriptional activity. Also, p21^(WAF1/Cip1) transcriptional activity was suppressed by

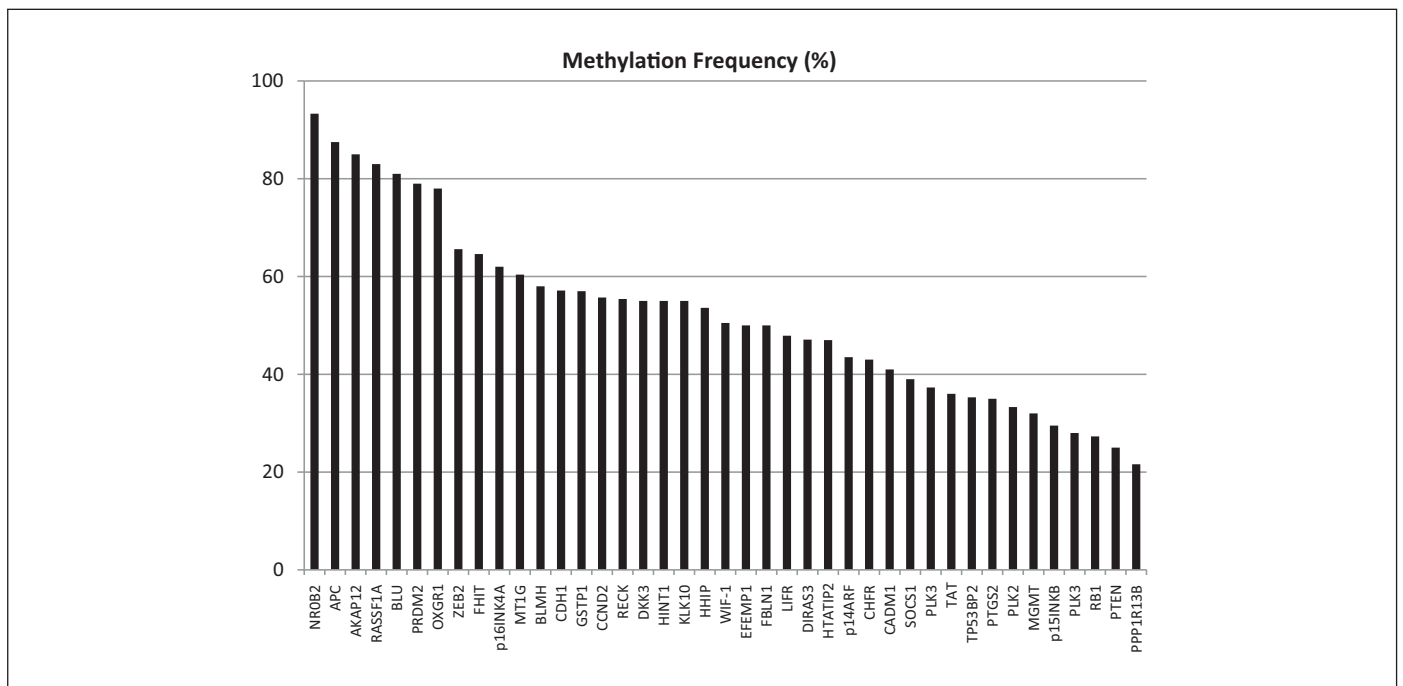


FIGURE 2
The frequency of promoter methylation in hepatocellular carcinoma.

HDAC1 by interaction with an Sp1-binding site in the p21^(WAF1/Cip1) promoter [31]. HDAC4 also suppresses the promoter activity of miR-200a and its expression and interacts with Sp1 in the miR-200a promoter to attenuate histone H3 acetylation levels. miR-200a represses HDAC4 expression through targeting the 3'-untranslated region of messenger RNA of HDAC4. In this respect, miR-200a has an ability to induce its own transcription and increase the levels of histone H3 acetylation at its promoter. Furthermore, miR-200a induces up-regulation of the levels of total acetyl-histone H3 and histone H3 acetylation in the p21^{Cip1} promoter [32].

DNA methylating enzymes *DNMT1*, *DNMT3A* and *DNMT3B* are over-expressed in HCC compared to noncancerous liver samples [33,34]. Finally, *CENPA* expression was found to be significantly elevated in HCC tissues, and a positive correlation exists between CENP-A expression and HBx COOH mutations in HCC tissues. HBx mutant increases the expression of *CENPA* mRNA [35].

Future perspectives

Recent advances in genome sequencing technologies will change radically our capabilities for fine mapping of hepatocellular cancer genomes. It is expected that patient tumours will be fully analysed in a short time at a moderate cost. Therefore, the genomic and

epigenomic status of the patient's own tumour will be a crucial element for decision making in terms of disease prognosis, therapeutic choices and prediction of patient survival. However, most of the known mutations observed in HCC are associated with a loss of function. Apparently, targetable genes found in other cancers such as growth factor receptors and intracellular protein kinases are not mutated at significant levels in HCC. Therefore, we need to find other targets for the treatment of liver cancers. Epigenetic characterisation of HCC has allowed the discovery of many epigenetic players in this disease. However, these studies are far from being complete. The rarity of targetable mutations in HCC justifies a systematic study of epigenetic changes to identify new targets for the therapy of this disease.

Acknowledgements

The research study is supported by grants from TÜBİTAK (109S191 and 111T558) with additional support from State Planning Office (DPT-KANİLTEK Project), Turkish Academy of Sciences, Institut National de Cancer and La Ligue Nationale Contre le Cancer in France (Equipe labélisée). C.O., G.Y. and D.C. received fellowships from Turkish Academy of Sciences (C.O.), TÜBİTAK (G.Y., D.C.) and EMBO (G.Y.).

References

- [1] El-Serag HB. Hepatocellular carcinoma. *New England Journal of Medicine* 2011;365:1118–27.
- [2] El-Serag HB. Epidemiology of viral hepatitis and hepatocellular carcinoma. *Gastroenterology* 2012;142:1264–1273.e1.
- [3] El-Serag HB, Marrero JA, Rudolph L, Reddy KR. Diagnosis and treatment of hepatocellular carcinoma. *Gastroenterology* 2008;134:1752–63.
- [4] Forner A, Llovet JM, Bruix J. Hepatocellular carcinoma. *Lancet* 2012;379:1245–55.
- [5] Buendia MA. Genetic alterations in hepatoblastoma and hepatocellular carcinoma: common and distinctive aspects. *Medical and Pediatric Oncology* 2002;39:530–5.
- [6] Guichard C, Amaddeo G, Imbeaud S, Ladeiro Y, Pelletier L, Maad IB, et al. Integrated analysis of somatic mutations and focal copy-number changes identifies key genes and pathways in hepatocellular carcinoma. *Nature Genetics* 2012;44:694–8.
- [7] Brechot C, Pourcel C, Louise A, Rain B, Tiollais P. Presence of integrated hepatitis B virus DNA sequences in cellular DNA of human hepatocellular carcinoma. *Nature* 1980;286:533–5.
- [8] Brechot C, Gozuacik D, Murakami Y, Paterlini-Brechot P. Molecular bases for the development of hepatitis B virus (HBV)-related hepatocellular carcinoma (HCC). *Seminars in Cell Biology* 2000;10:211–31.
- [9] Fujimoto A, Totoki Y, Abe T, Borojevich KA, Hosoda F, Nguyen HH, et al. Whole-genome sequencing of liver cancers identifies etiological influences on mutation patterns and recurrent mutations in chromatin regulators. *Nature Genetics* 2012;44:760–4.
- [10] Bressan B, Galvin KM, Liang TJ, et al. Abnormal structure and expression of p53 gene in human hepatocellular carcinoma. *Proceedings of the National Academy of Sciences of the United States of America* 1990;87:1973–7.
- [11] Ozturk M. Genetic aspects of hepatocellular carcinogenesis. *Seminars in Liver Disease* 1999;19:235–42.
- [12] Ozturk M, Arslan-Ergul A, Bagislar S, Senturk S, Yuzugullu H. Senescence and immortality in hepatocellular carcinoma. *Cancer Letters* 2009;286:103–13.
- [13] Huang J, Deng Q, Wang Q, Li KY, Dai JH, Li N, et al. Exome sequencing of hepatitis B virus-associated hepatocellular carcinoma. *Nature Genetics* 2012;44:1117–21.
- [14] Sandoval J, Esteller M. Cancer epigenomics: beyond genomics. *Current Opinion in Genetics and Development* 2012;22:50–5.
- [15] Rodriguez-Paredes M, Esteller M. Cancer epigenetics reaches mainstream oncology. *Nature Medicine* 2011;17:330–9.
- [16] Pogribny IP, Rusyn I. Role of epigenetic aberrations in the development and progression of human hepatocellular carcinoma. *Cancer Letters* 2012 [Epub ahead of print].
- [17] Sceusi EL, Loose DS, Wray CJ. Clinical implications of DNA methylation in hepatocellular carcinoma. *HPB (Oxford)* 2011;13:369–76.
- [18] Burchard J, Zhang C, Liu AM, Poon RT, Lee NP, Wong KF, et al. microRNA-122 as a regulator of mitochondrial metabolic gene network in hepatocellular carcinoma. *Molecular Systems Biology* 2010;6:402.
- [19] Lachenmayer A, Alsinet C, Savic R, Cabellos L, Toffanin S, Hoshida Y, et al. Wnt-pathway activation in two molecular classes of hepatocellular carcinoma and experimental modulation by sorafenib. *Clinical Cancer Research* 2012;18:4997–5007.
- [20] Murakami Y, Yasuda T, Saigo K, Urashima T, Toyoda H, Okanou T, et al. Comprehensive analysis of microRNA expression patterns in hepatocellular carcinoma and non-tumorous tissues. *Oncogene* 2006;25:2537–45.
- [21] Cao R, Wang L, Wang H, Xia L, Xia L, Erdjument-Bromage H, Tempst P, et al. Role of histone H3 lysine 27 methylation in Polycomb-group silencing. *Science* 2002;298:1039–43.
- [22] Cai MY, Tong ZT, Zheng F, Liao YJ, Wang Y, Rao HL, et al. EZH2 protein: a promising immunomarker for the detection of hepatocellular carcinomas in liver needle biopsies. *Gut* 2011;60:967–76.
- [23] Sasaki M, Ikeda H, Itatsu K, Yamaguchi J, Sawada S, Minato H, et al. The overexpression of polycomb group proteins Bmi1 and EZH2 is associated with the progression and aggressive biological behavior of hepatocellular carcinoma. *Laboratory Investigation* 2008;88:873–82.
- [24] Cheng AS, Lau SS, Chen Y, Kondo Y, Li MS, Feng H, et al. EZH2-mediated concordant repression of Wnt antagonists promotes beta-catenin-dependent hepatocarcinogenesis. *Cancer Research* 2011;71:4028–39.
- [25] Au SL, Wong CC, Lee JM, Fan DN, Tsang FH, Ng IO, et al. Enhancer of zeste homolog 2 epigenetically silences multiple tumour suppressor microRNAs to promote liver cancer metastasis. *Hepatology* 2012;56:622–31.
- [26] Yang F, Zhang L, Huo XS, Yuan JH, Xu D, Yuan SX, et al. Long noncoding RNA high expression in hepatocellular carcinoma facilitates tumour growth through enhancer of zeste homolog 2 in humans. *Hepatology* 2011;54:1679–89.
- [27] Effendi K, Mori T, Komuta M, Masugi Y, Du W, Sakamoto M. Bmi-1 gene is upregulated in early-stage hepatocellular carcinoma and correlates with ATP-binding cassette transporter B1 expression. *Cancer Science* 2010;101:666–72.
- [28] Weichert W. HDAC expression and clinical prognosis in human malignancies. *Cancer Letters* 2009;280:168–76.
- [29] Wu LM, Yang Z, Zhou L, Zhang F, Xie HY, Feng XW, et al. Identification of histone deacetylase 3 as a biomarker for tumour recurrence following liver transplantation in HBV-associated hepatocellular carcinoma. *PLoS ONE* 2010;5:e14460.
- [30] Quint K, Agaimy A, Di Fazio P, Montalbano R, Steindorf C, Jung R, et al. Clinical significance of histone deacetylases 1, 2, 3, and 7: HDAC2 is an independent predictor of survival in HCC. *Virchows Archiv* 2011;459:129–39.
- [31] Xie HJ, Noh JH, Kim JK, Jung KH, Eun JW, Bae HJ, et al. HDAC1 inactivation induces mitotic defect and caspase-independent autophagic cell death in liver cancer. *PLoS ONE* 2012;7:e34265.
- [32] Yuan JH, Yang F, Chen BF, Lu Z, Huo XS, Zhou WP, et al. The histone deacetylase 4/SP1/microRNA-200a regulatory network contributes to aberrant histone acetylation in hepatocellular carcinoma. *Hepatology* 2011;54:2025–35.
- [33] Choi MS, Shim YH, Hwa JY, Lee SK, Ro JY, Kim JS, et al. Expression of DNA methyltransferases in multistep hepatocarcinogenesis. *Human Pathology* 2003;34:11–7.
- [34] Saito Y, Kanai Y, Sakamoto M, Saito H, Ishii H, Hirohashi S. Expression of mRNA for DNA methyltransferases and methyl-CpG-binding proteins and DNA methylation status on CpG islands and pericentromeric satellite regions during human hepatocarcinogenesis. *Hepatology* 2001;33:561–8.
- [35] Li Y, Zhu Z, Zhang S, Yu D, Yu H, Liu L, et al. ShRNA-targeted centromere protein A inhibits hepatocellular carcinoma growth. *PLoS ONE* 2011;6:e17794.